frontiers | Research Topics

Immunonutrition: bridging precision nutrition and modern medicine

Edited by
Sofia Viana, Helena Sá, Francisco José Pérez-Cano and Jani Almeida

Published in
Frontiers in Nutrition
Frontiers in Immunology

ISSN 1664-8714
ISBN 978-2-8325-6843-9
DOI 10.3389/978-2-8325-6843-9

Generative AI statement
Any alternative text (Alt text) provided alongside figures in the articles in this ebook has been generated by Frontiers with the support of artificial intelligence and reasonable efforts have been made to ensure accuracy, including review by the authors wherever possible. If you identify any issues, please contact us.

About Frontiers

Frontiers is more than just an open access publisher of scholarly articles: it is a pioneering approach to the world of academia, radically improving the way scholarly research is managed. The grand vision of Frontiers is a world where all people have an equal opportunity to seek, share and generate knowledge. Frontiers provides immediate and permanent online open access to all its publications, but this alone is not enough to realize our grand goals.

Frontiers journal series

The Frontiers journal series is a multi-tier and interdisciplinary set of open-access, online journals, promising a paradigm shift from the current review, selection and dissemination processes in academic publishing. All Frontiers journals are driven by researchers for researchers; therefore, they constitute a service to the scholarly community. At the same time, the *Frontiers journal series* operates on a revolutionary invention, the tiered publishing system, initially addressing specific communities of scholars, and gradually climbing up to broader public understanding, thus serving the interests of the lay society, too.

Dedication to quality

Each Frontiers article is a landmark of the highest quality, thanks to genuinely collaborative interactions between authors and review editors, who include some of the world's best academicians. Research must be certified by peers before entering a stream of knowledge that may eventually reach the public - and shape society; therefore, Frontiers only applies the most rigorous and unbiased reviews. Frontiers revolutionizes research publishing by freely delivering the most outstanding research, evaluated with no bias from both the academic and social point of view. By applying the most advanced information technologies, Frontiers is catapulting scholarly publishing into a new generation.

What are Frontiers Research Topics?

Frontiers Research Topics are very popular trademarks of the *Frontiers journals series*: they are collections of at least ten articles, all centered on a particular subject. With their unique mix of varied contributions from Original Research to Review Articles, Frontiers Research Topics unify the most influential researchers, the latest key findings and historical advances in a hot research area.

Find out more on how to host your own Frontiers Research Topic or contribute to one as an author by contacting the Frontiers editorial office: frontiersin.org/about/contact

Immunonutrition: bridging precision nutrition and modern medicine

Topic editors

Sofia Viana — University of Coimbra, Portugal
Helena Sá — Unidade Local de Saúde de Coimbra, Portugal
Francisco José Pérez-Cano — University of Barcelona, Spain
Jani Almeida — University of Coimbra, Portugal

Citation

Viana, S., Sá, H., Pérez-Cano, F. J., Almeida, J., eds. (2025). *Immunonutrition: bridging precision nutrition and modern medicine*. Lausanne: Frontiers Media SA. doi: 10.3389/978-2-8325-6843-9

Table of contents

frontiers | Frontiers in Nutrition

TYPE Editorial
PUBLISHED 29 August 2025
DOI 10.3389/fnut.2025.1685397

OPEN ACCESS

EDITED AND REVIEWED BY
Willem Van Eden,
Utrecht University, Netherlands

*CORRESPONDENCE
Sofia Viana
✉ sofia_viana@estescoimbra.pt

RECEIVED 13 August 2025
ACCEPTED 15 August 2025
PUBLISHED 29 August 2025

CITATION
Almeida J, Sá H, Pérez-Cano FJ and Viana S (2025) Editorial: Immunonutrition: bridging precision nutrition and modern medicine. *Front. Nutr.* 12:1685397.
doi: 10.3389/fnut.2025.1685397

Editorial: Immunonutrition: bridging precision nutrition and modern medicine

Jani Almeida[1], Helena Sá[2], Francisco José Pérez-Cano[3,4] and Sofia Viana[5]*

[1]Laboratory of Immunology and Oncology, Center for Neurosciences and Cell Biology (CNC), University of Coimbra, Coimbra, Portugal, [2]Nephrology Department, Centro Hospitalar e Universitário de Coimbra, ULS Coimbra, Coimbra, Portugal, [3]Physiology Section, Department of Biochemistry and Physiology, Faculty of Pharmacy and Food Science, University of Barcelona, Barcelona, Spain, [4]Nutrition and Food Safety Research Institute (INSA-UB), Santa Coloma de Gramenet, Spain, [5]Faculty of Medicine, Institute of Pharmacology and Experimental Therapeutics, University of Coimbra, Coimbra, Portugal

KEYWORDS

immunonutrition, natural bioactive compounds, nutritional indices, clinical interventions, pre-clinical models

Editorial on the Research Topic
Immunonutrition: bridging precision nutrition and modern medicine

Inflammation imposes substantial metabolic demands and depletes critical nutrient reserves, often impairing immune function. While adequate nutrition is foundational to immune homeostasis, the targeted use of supraphysiological doses of immunomodulatory nutrients to redirect immune responses toward tolerance or resolution of inflammation remains an evolving frontier. Immunonutrition, a key domain within precision nutrition, encompasses bioactive compounds—nutrients and non-nutrients—such as amino acids, fatty acids, nucleotides, vitamins, minerals, polyphenols, glucans, and an expanding repertoire of pre-, pro-, sym-, and post-biotics. Its clinical applications span early-life immune development, cancer and infection management, modulation of autoimmunity and allergies, and attenuation of immunosenescence and inflamm-aging in chronic diseases. Despite the advances propelled by multi-omics research, critical gaps remain in mechanistic understanding, immune–nutrient interactions, synergy of bioactives within the food, biomarker identification, and the safety profile of immunonutrients, including nutrient–drug interactions. The nine contributions to this Research Topic advance immunonutrition across domains ranging from epidemiology and theoretical modeling to clinical intervention, illustrating the field's maturation and translational promise.

Four epidemiological studies based on NHANES datasets explore the predictive utility of composite nutritional–inflammatory indices. Ma et al. demonstrated that a higher Magnesium Depletion Score (MDS) independently predicted increased incidence and mortality from osteoarthritis, including cardiovascular mortality. These findings underscore magnesium as a modifiable immunonutrient in inflammation-driven degenerative disease. In patients with COPD, Yao et al. found a non-linear association between the Advanced Lung Cancer Inflammation Index (ALI) and mortality, with protective effects up to a threshold (~88–90), beyond which benefits declined. This

U-shaped relationship highlights the nuanced role of nutritional and inflammatory balance in chronic respiratory disease outcomes. Xiao et al. introduced the Dietary Index for Gut Microbiota (DI-GM) and found it inversely associated with chronic kidney disease. Higher scores, driven by intake of fiber, whole grains, and coffee, were particularly protective in women, emphasizing the importance of sex-specific immunonutrition and the gut–immune–renal axis. Xu et al. evaluated the Dietary Inflammatory Index (DII) in over 43,000 adults and found that a higher score was independently associated with increased risk of coronary heart disease. These effects were mediated by metabolic and lipid-related pathways including BMI, triglyceride-glucose index, and HDL levels. Notably, the association was stronger in younger individuals, women, and those with otherwise low cardiovascular risk, suggesting that dietary inflammation may disproportionately affect populations traditionally considered at low-risk. Key dietary components included carbohydrates, vitamin C, and iron. Collectively, these studies validate composite dietary indices as both predictors and potential indicators of immune-mediated disease risk, while reinforcing the gut–immune–metabolic interface as a pivotal therapeutic axis.

Mechanistic innovation in immunonutrition is reflected in contributions that provide both conceptual and experimental tools. Ramal-Sanchez et al. developed a tri-cellular *in vitro* intestinal model incorporating enterocytes, goblet cells, and immune cells to simulate the human gut epithelium. Using this model, they evaluated the immunomodulatory effects of broccoli digesta and observed suppression of inflammatory cytokines (IL-6, TNF-α, IL-8, IL-18) alongside upregulation of tight junction proteins (ZO-1), supporting the model's utility for functional screening of food-derived immunonutrients. LeGrand et al. proposed the conceptual framework of "immune stressing," in which effector immune cells impose metabolic stress, via glucose deprivation, ROS generation, and lactate accumulation, on pathogens. This resource-restriction model reframes nutritional immunity as an active metabolic strategy that targets the fragility of proliferating pathogens while sparing host cells. It extends the classic paradigm of micronutrient withholding and offers new avenues for understanding host–pathogen dynamics.

Three intervention studies further illustrate the translational potential and limitations of immunonutrition. Singh et al. conducted a longitudinal pediatric study to assess the neutropenic diet in children undergoing chemotherapy. Despite moderate adherence, the diet did not reduce febrile neutropenia, infections, or mortality. Socioeconomic status influenced compliance, and the findings suggest that restrictive dietary practices may not be necessary in this population. Instead, emphasis should shift toward food safety and hygiene. Qin et al., using a murine model of peritonitis, demonstrated that retinoic acid (RA) enhanced peritoneal macrophage phagocytosis, promoted recruitment of small peritoneal macrophages, and upregulated adhesion and migration gene expression. Encapsulation of RA in ZIF-8 nanoparticles sustained these effects, highlighting a promising strategy for precision-targeted immunonutrition, though further validation is needed for model specificity and delivery system stability. In a 90-day clinical pilot trial, Perlmutter et al. evaluated a polyphenol-rich Tartary buckwheat supplement in healthy adults. The intervention directionally influenced CpG methylation patterns across biological aging clocks (PCPhenoAge, PCGrimAge, OmicAge) and correlated with shifts in immune cell composition, particularly markers of immunosenescence. Pathway analyses highlighted ceramide kinase and immune regulatory networks, supporting polyphenols as modulators of epigenetic aging via immune-related mechanisms.

Several converging insights emerge across these contributions. Composite indices such as MDS, ALI, DI-GM, and DII show dual utility as biomarkers for disease risk and as intervention targets. Mechanistic innovation, through both modeling and conceptual frameworks, expands our understanding of how nutrients shape immune responses. Clinical interventions underscore both the promise of targeted strategies—such as polyphenols and RA nanoparticles—and the limitations of traditional approaches like exclusionary diets. Sex and life stage repeatedly emerge as key modifiers of nutritional immunity, highlighting the need for personalization. Multi-omics and systems-level analyses offer powerful tools for biomarker discovery and may help accelerate clinical translation. Nonetheless, persistent challenges include the cross-sectional design of most epidemiological studies, limited sample sizes in clinical trials, and the need for further refinement and validation of mechanistic models in human systems.

This Research Topic presents a cohesive body of work that advances immunonutrition from theory and mechanism to intervention and epidemiology. Through the development of nutritional indices, modeling of host–pathogen metabolic interactions, and testing of food-derived bioactives, these studies underscore the transformative potential of immunonutrition in modern medicine. Future efforts should prioritize longitudinal, multi-omic, and personalized approaches to fully integrate immunonutrition into evidence-based clinical practice. The editors thank all authors and reviewers for their contributions and invite continued interdisciplinary collaboration to propel the field forward.

Author contributions

JA: Formal analysis, Investigation, Validation, Writing – original draft, Writing – review & editing. HS: Conceptualization, Formal analysis, Investigation, Validation, Writing – original draft, Writing – review & editing. FP-C: Conceptualization, Formal analysis, Supervision, Validation, Writing – original draft, Writing – review & editing. SV: Conceptualization, Data curation, Formal analysis, Investigation, Methodology, Project administration, Supervision, Validation, Writing – original draft, Writing – review & editing.

Conflict of interest

The authors declare that the research was conducted in the absence of any commercial or financial relationships that could be construed as a potential conflict of interest.

Generative AI statement

The author(s) declare that no Gen AI was used in the creation of this manuscript.

Any alternative text (alt text) provided alongside figures in this article has been generated by Frontiers with the support of artificial intelligence and reasonable efforts have been made to ensure accuracy, including review by the authors wherever possible. If you identify any issues, please contact us.

Publisher's note

frontiers | Frontiers in Nutrition

TYPE Original Research
PUBLISHED 18 November 2024
DOI 10.3389/fnut.2024.1474597

OPEN ACCESS

EDITED BY
Sofia Viana,
University of Coimbra, Portugal

REVIEWED BY
Ana Luísa De Sousa-Coelho,
Algarve Biomedical Center Research Institute (ABC-RI), Portugal
Sara Nunes,
University of Coimbra, Portugal

*CORRESPONDENCE
Austin Perlmutter
austinperlmutter@bigboldhealth.com
Varun B. Dwaraka
varun@trudiagnostic.com

RECEIVED 01 August 2024
ACCEPTED 15 October 2024
PUBLISHED 18 November 2024

CITATION
Perlmutter A, Bland JS, Chandra A, Malani SS, Smith R, Mendez TL and Dwaraka VB (2024) The impact of a polyphenol-rich supplement on epigenetic and cellular markers of immune age: a pilot clinical study.
Front. Nutr. 11:1474597.
doi: 10.3389/fnut.2024.1474597

The impact of a polyphenol-rich supplement on epigenetic and cellular markers of immune age: a pilot clinical study

Austin Perlmutter[1]*, Jeffrey S. Bland[1], Arti Chandra[1], Sonia S. Malani[1], Ryan Smith[2], Tavis L. Mendez[2] and Varun B. Dwaraka[2]*

[1]Big Bold Health PBC, Bainbridge Island, WA, United States, [2]TruDiagnostic Inc., Lexington, KY, United States

Age-related alterations in immune function are believed to increase risk for a host of age-related diseases leading to premature death and disability. Programming of the immune system by diet, lifestyle, and environmental factors occurs across the lifespan and influences both makeup and function of the immune system, including immunometabolism. This programming is believed to act in large part through epigenetic modification. Among dietary components that affect this process, polyphenols may play an outsized role. Polyphenols are a widely distributed group of plant nutrients consumed by humans. Certain foods possess distinctive and relatively higher levels of these compounds. One such food is Tartary buckwheat (*fagopyrum tataricum*), an ancient seed historically prized for its health benefits. It is suggested that the specific composition of polyphenols found in foods like Tartary buckwheat may lead to a unique impact on immunometabolic physiological pathways that could be interrogated through epigenetic analyses. The objective of this study was to investigate the epigenetic effects on peripheral immune cells in healthy individuals of a standardized polyphenol concentrate based on naturally occurring nutrients in Tartary buckwheat. This pilot clinical trial tested the effects of consuming 90 days of this concentrate in 50 healthy male (40%) and female (60%) participants aged 18–85 years using epigenetic age clocks and deconvolution methods. Analysis revealed significant intervention-related changes in multiple epigenetic age clocks and immune markers as well as population-wide alterations in gene ontology (GO) pathways related to longevity and immunity. This study provides previously unidentified insights into the immune, longevity and epigenetic effects of consumption of polyphenol-rich plants and generates additional support for health interventions built around historically consumed plants like Tartary buckwheat while offering compelling opportunities for additional research.

Clinical trial registration: ClinicalTrials.gov, Identifier: NCT05234203.

KEYWORDS

diet and nutrition, epigenetic clocks, aging, immunity, polyphenols, epigenome-wide association study, Tartary buckwheat, food-is-medicine

1 Introduction

In the last century, in high-income countries, national life expectancy has steadily risen. Concurrent with a longer lifespan, there has been a rapid rise in the prevalence of chronic conditions including cardiovascular diseases, diabetes, cancers, chronic respiratory diseases (e.g., asthma and chronic obstructive pulmonary disease) (1). These represent significant contributors to morbidity and mortality as well as unsustainable increases in healthcare costs. Thus, increasing the number of healthy years lived (i.e., health span) remains a challenge despite the increase in lifespan.

Biological age is described as a local or organismal rate of cellular aging and has emerged as a superior predictor risk for disease, mortality, and morbidity when compared to chronological age. Biological aging is most often measured through evaluation of epigenetic markers, most commonly methylation of the cytosine-guanine (CpG) islands in DNA. Biological aging and epigenetic aging are often used interchangeably. Notably, many epigenetic testing approaches utilize DNA from peripheral immune cells, which allows for simultaneous assessment of immune-related epigenetic markers that change with age. Algorithms using epigenetic methylation data such as GrimAge (2), PhenoAge (3), and DunedinPace (4) have been applied to the determination of biological age of immune cells (5). It has been found that a higher biological age of the immune system represents a significant risk factor for all-cause mortality and reduction in longevity (6–8).

Shifts in immune cell subsets, cytokines, and functions are seen in chronic disease states ranging from cardiovascular disease to dementia. In addition, research has progressively focused on the role of the immune system in the aging process itself. Pharmaceutical and non-pharmaceutical approaches have been proposed as potential avenues for ameliorating the putative damage from immune aging (i.e., immunosenescence). The combined measurement of epigenetic aging metrics and immune-specific measurements may, therefore, provide considerable insights into one's risk for disease and disability.

A state of relative immunosenescence (age-related changes in immune system makeup and function) may contribute to chronic disease via the generation of senescent cells– cells outside the cell replicative cycle due to stress or other insults (9). While senescence appears to play a key role in tumor suppression, senescent cells can nonetheless remain metabolically active and produce and secrete a wide range of immunologically active molecules, including inflammatory mediators. The development of senescent cells that produce inflammatory mediators has been termed the senescence-associated secretory phenotype (SASP) and is thought to contribute to the higher levels of inflammation that are often seen with advancing chronological and biological age.

Research on interventions to slow the rate of biological aging, including targeting pathways of immunosenescence has primarily been conducted in cell and animal models. Several recent studies have examined the effect of lifestyle and pharmaceutical interventions on biological aging in humans as well. For example, associations between nutritional intervention, or diet and lifestyle, with epigenetic aging have been reported (10, 11). Food-related molecules have been proposed to play an outsized protective role in slowing or potentially reversing epigenetic aging. Among the best-studied health-promoting dietary nutrients are polyphenols, non-caloric plant-derived compounds which have a wide variety of proposed effects in humans. Indeed, consumption of a polyphenol-rich beverage was found to correlate with epigenetic changes in immune cells of dyslipidemic humans in a recent study (12). A recent randomized controlled trial (13) additionally demonstrated epigenetic effects linked to consumption of a polyphenol-enriched Mediterranean diet proposed to have effects on the immune response.

Several lines of research have more explicitly examined slowing or reversing immunosenescence. Here again, polyphenols have been proposed to play a potential role, and in numerous cell and animal studies polyphenols, including quercetin and curcumin, have been implicated in the reversal of various markers of immunosenescence (14, 15).

Polyphenols are a large family of molecules naturally occurring in plants characterized by the presence of multiple phenolic hydroxyl groups providing putative antioxidant potential. Diets high in polyphenols, especially the Mediterranean diet, have been linked to a variety of positive health outcomes. These include lower rates of degenerative diseases like atherosclerosis, as well as improved metabolic function (16, 17). One of the central mechanisms proposed to account for some of these benefits is the effect of polyphenols on immune function and, specifically, in decreasing excessive inflammation. Additionally, it has been postulated that these molecules may exert a positive influence on the gut microbiome by acting as prebiotics, which support healthy microbial communities (18).

While a wide range of polyphenols have been studied in preclinical and clinical trials for their effects on human health, a smaller number have been implicated for potential benefit to both epigenetic age and immunological health. This group includes the molecules quercetin and fisetin. Quercetin occurs naturally in many plants, including red onions, capers, teas, and cruciferous vegetables. Fisetin is found in fruits such as strawberries, kiwis and apples, vegetables like onions and tomatoes, and nuts.

Most research on polyphenols has followed a pharmaceutical-like model, focusing on the isolated effects of individual polyphenols on specific outcomes. However, it is notable that naturally occurring polyphenols are delivered alongside a complex mixture of minerals, vitamins, fiber and other non-caloric plant nutrients (phytochemicals). It is suggested that the benefits of polyphenols may be synergistic when consumed alongside these other plant food components (19, 20). Therefore, naturally occurring combinations of polyphenols and other phytochemicals may be more ideally suited to exert beneficial biological effects than the same molecules consumed in isolation.

1.1 Potential mechanism of actions of polyphenols in regulating immunity through epigenetics

Polyphenols are best understood as antioxidants primarily on the merit of *in vitro* studies and chemical structure. It is a widespread belief that the principal health benefit of polyphenol consumption stems from this antioxidant ability. While it is now recognized that oxidative stress (and subsequent antioxidant neutralization) may directly impact epigenetic regulation, including within immune cells, additional mechanisms of polyphenol-induced cellular effects are now being characterized (21). Polyphenols are poorly absorbed in the human GI tract, allowing most dietary polyphenols to reach the large

intestine intact, where they are acted upon by the diverse microbes of the gut microbiome (21). Here, polyphenols may be modified by microbial metabolism to generate new metabolites and other bioactive compounds that may impact epigenetic regulation. For example, consumption of polyphenols may induce gut microbes to increase production of short-chain fatty acids [e.g., β-hydroxybutyrate (BHB)] which are known epigenetic regulators as well as immune modulators. Polyphenols are additionally acted on by various phase I biotransformation enzymes present in the GI tract prior to absorption, as well as phase II enzymes present in enterocytes and hepatocytes (22). Within circulation, polyphenols and metabolites can bind to immune cells. Polyphenols may modulate epigenetics by way of DNA methylation, histone modification and miRNA expression (23). This has been quantified using epigenetic methylation analysis of immune cell composition with well-respected machine learning algorithms.

1.2 Potential metabolic, longevity, and immune pathway effects of polyphenols

Several cellular pathways have been identified as putative drivers of the health impacts of polyphenols within the last decade. From a metabolic perspective, polyphenols have been proposed to act on ceramide production and downstream effects. Ceramides are bioactive lipid species within the sphingolipid class involved in cell-signaling, and their production is known to be regulated by nutritional intervention (24), including preclinical data suggesting a direct impact of polyphenols. Other work suggests an effect of polyphenols on the ubiquitin-proteasome system (UPS), a key cell pathway involved in protein degradation and metabolic function (25). Polyphenols may also exert effects on the Janus kinase-signal transducer and activator of transcription (JAK–STAT) pathway (26), with implications for immunity, metabolism and longevity (27, 28). In addition, the effect of polyphenols on mechanistic target of rapamycin (mTOR) and 5′-Adenosine monophosphate activated protein kinase (AMPK) pathways (29) represents an area of overlap between these three domains.

One challenge in determining the relative contribution of individual pathways to the health-promoting effects of polyphenols is that much of the existing research has focused on the effect of polyphenolic intervention in *in vitro* data looking at specific pathways identified *a priori*, especially antioxidant potential. Thus, a study designed to examine a full spectrum of potential pathway effects of polyphenol and phytochemical interventions in humans presents a unique opportunity to better understand influences of these molecules across disparate biological systems.

1.3 Tartary buckwheat

Tartary buckwheat is a buckwheat cultivar used for thousands of years for its medicinal and food properties. It is known to contain phytochemicals that include the polyphenols rutin, quercetin, luteolin and hesperidin, as well as nutrients such as d-chiro-inositol, a cyclic polyol clinically studied for its effects on human metabolism (30–32).

Dietary interventions with Tartary buckwheat have been independently studied and shown to have positive effects on human physiology related to immune function and metabolism (33, 34). The sum of this research suggests that consumption of phytonutrients found in Tartary buckwheat may positively affect human immune function and epigenetic expression, potentially through shared pathways.

With specific regard to the polyphenol content of Tartary buckwheat, it is notable that the seed contains up to 2.42% flavonoid polyphenolic content by weight (35), compared to a significantly lower content in wheat 0.84% (36). Tartary buckwheat is also the most concentrated food source of rutin, a flavonol glycoside polyphenol which demonstrates primarily preclinical efficacy in modulating metabolic and immune pathways (37, 38).

The relatively high and unique polyphenol content of Tartary buckwheat makes it an ideal candidate for further investigation as a health-promoting food, as well as examination of the value of its representative nutrient profile. The supplement used in this trial contains potentially epigenetically- and immunologically- active polyphenols, as well as additional phytochemicals included to better mirror the suite of biologically active phytochemicals naturally occurring in Tartary buckwheat.

We hypothesize that consumption of a polyphenol concentrate based on the makeup of Tartary buckwheat over 90 days will lead to significant changes in the epigenetic methylation patterns and immune cell phenotypes in healthy adults, as measured by epigenetic age clocks and immune markers, potentially contributing to enhanced immune function and longevity-related physiological pathways.

2 Materials and methods

2.1 Ethical approval and study design

The Institute of Cellular and Regenerative Medicine Institutional Review Board granted approval for all procedures involving humans in this study. This study is registered on ClinicalTrials.gov under the registration number NCT05234203.

2.2 Participant recruitment and eligibility

50 generally healthy (defined as the absence of exclusion criteria below) men and women between the ages of 18 and 85 years (inclusive) with body mass index (BMI) <40 kg/m^2 were enrolled in the study. This age range was selected to capture a diverse range of adult participants while avoiding the potential for outlier variability introduced at extremes of aging, and to capture the population most likely to be taking a nutritional supplement. Participants were required to have an established primary care provider and active health insurance; be able to read, write, and speak English fluently; and be able to comply with the protocol instructions including performing the in-home venous blood draw using a Tasso device. Investors or immediate family members possessing investment in Big Bold Health were excluded from the study.

Women who were pregnant and/or lactating and individuals on jobs requiring night shift work were excluded. Exclusion criteria also included history (prior 2 years) or presence of cancer, except for non-melanoma skin cancer; known history of blood dyscrasias including coagulopathy or use of prescription anticoagulants;

10.3389/fnut.2024.1474597

TABLE 1 Composition of HTB Rejuvenate.

Component	Amount per Serving (2 capsules)	Amount per day (4 capsules)
Himalayan Tartary buckwheat (HTB) flour	95 mg	190 mg
D-chiro inositol (DCI/D-chiro-inositol)	150 mg	300 mg
2-hydroxybenzylamine (2-HOBA)	13 mg	26 mg
Hydroxymethylbutyrate (HMB)	69 mg	138 mg
Chlorophyllin	7.5 mg	15 mg
Polyphenols*	579 mg	1,158 mg
Vitamin C	20 mg	40 mg
Calcium	30 mg	60 mg

*Polyphenols delivered in one serving (2 capsules) included 330 mg quercetin, 83 mg rutin, 83 mg hesperidin, and 83 mg luteolin.

diagnosis of a transient ischemic attack (within 6 months); presence of clinically significant acute or unstable cardiovascular or cerebrovascular disease, psychiatric disorder, alcohol or chemical dependence; immune-related conditions (e.g., hepatitis C, HIV, or active infection within the previous 4 weeks) or other illness that in the opinion of the Clinical Investigator would render a participant unsuitable to participate in the study. In addition, those with known allergy to any of the components of the test product, those consuming known prescription immunomodulating products (e.g., oral glucocorticoids, TNF-α inhibitors) or concentrated polyphenolic supplements within 1 month the baseline visit. Concentrated polyphenolic substances that were specifically excluded prior to, and during the study were quercetin, rutin, luteolin, epigallocatechin gallate (EGCG), resveratrol, curcumin, fisetin, berberine, soy isoflavones (genistein, daidzein, and glycitein), hesperidin, and ellagic acid.

2.3 Study objectives

The primary objective of this exploratory clinical trial was to evaluate the effect of consuming a polyphenol-rich supplement largely based around the phytochemical composition of Tartary buckwheat (HTB Rejuvenate) for 90 days on epigenetically-measured immune age. The duration of the study period was chosen based on previous polyphenol intervention trials (39, 40) and is generally in line with duration of diet-based polyphenol interventional research (41, 42). Additionally, it was determined that this period would allow for multiple rounds of immune cell turnover as the average lifespan of the majority of peripherally-measured immune cells falls in this range (e.g., the majority of circulating immune cells are neutrophils, with a lifespan of less than 5 days, B cell lifespan average is 52 days) (43).

The secondary objective was to assess the effects of HTB Rejuvenate on peripheral leukocyte immune profiles after 90 days, as well as on GO pathways. Tertiary objectives included capture and review of descriptive clinical observations using a General Health Questionnaire (GHQ). Safety was also assessed via reports of adverse events (AEs).

2.4 Study product

The study product was a polyphenol-rich supplement (HTB Rejuvenate) that is commercially available and produced under Good Manufacturing Practices (GMP). The HTB Rejuvenate supplement delivered 579 mg of polyphenols per serving (2 capsules), which is within the studied ranges of polyphenol intake consumed through diet (44).

The study product is a concentrated version of naturally occurring phytonutrients in Tartary buckwheat that contains rutin, quercetin, luteolin, hesperidin as well as d-chiro-inositol (Table 1). 2-hydroxybenzylamine (2-HOBA) is an antioxidant phytochemical also isolated from Tartary buckwheat. Hydroxymethylbutyrate (HMB) was also included in the study product as this is a naturally-occurring byproduct of leucine metabolism linked to improvement in age-related metrics including muscle loss (45). Tartary buckwheat is particularly enriched in leucine (46). Test product was consumed at 4 capsules per day, taken as 2 capsules twice per day close to 12 h apart. Specifically, participants were counseled to consume 2 capsules in the morning (between 6 and 10 am) and 2 capsules in the evening (between 6 and 10 pm) with food.

2.5 Analysis populations

A review of compliance and protocol deviations was conducted prior to data analysis, and those participants whose data is included for analysis populations is summarized in Appendix 1. Based on the completion of the blood sampling for the epigenetic tests, the modified intent to treat (ITT) population, which includes all participants who completed both baseline and final labs, was composed of $n = 47$. One participant withdrew consent at visit 2, and two participants who did not complete the final blood draw were excluded from the ITT population because the outcome required both tests for analysis. In addition to removal of the two individuals who were excluded from the ITT, the per-protocol (PP) population excluded seven other participants, including two for use of excluded medications/supplements, four for low study supplement compliance, and one for both inclusion of an excluded medication/supplement and low compliance. The final analyzed population therefore included 40 people.

2.6 Demographics

The demographics obtained during screening/baseline clinical interviews for the ITT and PP populations are provided in Table 2. Participants in the PP population, which was the primary population for the laboratory analyses, were 54 y (SD, 11 y) old with BMI of 24.2 kg/m^2 (SD, 3.3 kg/m^2). A total of 14 participants had documented cases of COVID during the study (See Appendix 1).

TABLE 2 Characteristics of participants.

Characteristic	Units	ITT	PP
Population Number	*N*	47	40
Age	y (±SD)	54 (±11)[‡]	54 (±11)[§]
Sex	% Female	60	62.5
Weight (self-report)†	kg	70.3 (±15.7)[‡]	69.2 (±14.7)[§]
Height (self-report)†	cm	166.7 (±11.1)[‡]	166.5 (±11.2)[§]
BMI	kg/m^2	24.6 (±3.5)	24.2 (±3.3)

BMI, body mass index; cm, centimeter; ITT, intent-to-treat; kg, kilogram; m, meter; *N*, subject number; PP, per protocol; SD, standard deviation; y, years. *The ITT data excluded the two participants who did not complete final lab tests. †Self-reported weight and height data were converted to metric units for reporting purposes. ‡The ITT population had no data for 3 participants for age, and 11 participants for weight and height. All participants had reported BMI data. §The PP population had no data for 3 participants for age, and 7 participants for weight and height. All participants had reported BMI data.

2.7 Study design

This was a virtual, single-arm open-label prospective pilot clinical trial comparing epigenetic and immune assays in participants prior to and after 90 days of supplementation with the polyphenol-rich HTB Rejuvenate supplement. The study included a screening/baseline visit (Visit 1, Day −15), communication for starting product (Visit 2, Day 0), 24-h check-in after product start (Visit 3, Day 1), and three follow-up visits (Visit 4, Day 30. Visit 5, Day 60; Visit 6, Day 90). In addition, participants were contacted by phone approximately 30 to 90 d after completing the study and when laboratory results were available. Study details are provided in the Study tracking table (Table 3).

Participants were pre-screened using an on-line questionnaire and those meeting criteria were provided a detailed study description and the electronic Informed Consent. Interested individuals attended a TeleVisit (Visit 1, Day −15) with the Clinical Investigator, during which it was confirmed that they met all the inclusion and none of the exclusion criteria. Eligible participants who voluntarily signed the Informed Consent were then provided the baseline GHQ electronically and sent the Tasso blood draw device and instructions to obtain an in-home blood sample for the baseline epigenetic testing. Participants were also sent two bottles of study product (120 capsules/bottle) and instructions for starting consumption after baseline data were obtained (Visit 2, Day 0), and scheduling the 24-h call (Visit 3, Day 1). Participants were instructed not to make substantial changes to diet and lifestyle (e.g., dietary and physical activity programs, new supplements) during study period unless explicitly recommended by their treating medical provider.

At Visit 3, participants were asked about adverse events (AEs), product consumption start date was confirmed, and participants were reminded of the study instructions, including not consuming polyphenol supplements and maintaining habitual diet and lifestyle during the study. Mid-study check-in visits were conducted by phone call with the Research Associate at Visit 4 (Day 30) and Visit 5 (Day 60), during which participants were queried for compliance, AEs, and changes to concomitant medications/supplements and habitual diet and lifestyle. In addition, participants were sent the GHQ electronically and queried on completing the questionnaire. Bottles of study product (30 capsules) were sent after Visit 4 and Visit 5.

Prior to the end-of-study visit (Visit 6, Day 90), participants were sent the link to the final GHQ as well as a Tasso blood draw kit. At Visit 6, participants attended a TeleVisit with the Clinical Investigator for the final review, which included study product consumption compliance, completion of the final GHQ, AEs, maintenance of habitual diet and lifestyle, and any changes to concomitant medications and supplements. Confirmation that the final blood was obtained before participants discontinued the study product.

2.8 Clinical and anthropometric information

Relevant medical history was reviewed by the Clinical Investigator prior to signing the Informed Consent. Anthropometric information included self-reported height and weight, with the date when the participant last weighed themselves documented, and BMI was calculated. Participants were questioned on medication and supplement use at Visit 1 (Day −15) and asked about changes to medication and supplement use, as well as diet and lifestyle at Visits 4, 5, and 6 (Days 30, 60, and 90).

2.9 General health questionnaire (GHQ)

Participants were asked to complete an electronic GHQ (Appendix 2) at baseline and 30-d, 60-d, and 90-d after the start of test product consumption which allowed for collection of subjective data. The GHQ included questions on general health over the previous 4 weeks with answers scored on a 5-point balanced Likert scale. The Likert scale varied randomly from lowest to highest score for questions 3, 4, 7, 9, 11, 12, 13, and 15, and from highest to lowest score for questions 1, 2, 5, 6, 8, 10, and 14 to decrease order-effects. In addition, leading and subjective language were avoided in the question design. The individual health categories included: 1: General Health: questions 1, 2, and 13, score range 3 to 15 points. 2: Gastrointestinal (GI): questions 3 and 4, score range 2 to 10 points. 3: Energy & Mood: questions 5, 10, 11, 12, 14, and 15, score range 6 to 30 points. 4: Allergy & Skin: questions 6, 7, 8, and 9, score range 4 to 20 points.

2.10 Compliance

Participants were provided a paper study log (a basic printable tracking document) with the initial product shipment that included a tracking form for documenting the consumption of 2 capsules of study product in the morning and 2 capsules in the evening every day, as well as a section for daily notes for unusual symptoms, illness and reasons for missed product consumption. The study log was not collected but provided to aid participants in answering queries at the relevant visits. Compliance was obtained during Visits 4, 5, and 6 by query and documented as % consumed over the previous 4 weeks from data on the study logs, as verbally provided by participants.

2.11 Epigenetic age biomarkers

Blood samples were obtained by participants at baseline and after 90 days of starting the trial using the in-home Tasso device and shipped

TABLE 3 Study tracking table.

	Screening/ Baseline	Start product	24-h check-in	Mid-study check-in	Mid-study check-in	End of study
Visit	1	2	3	4	5	6
Day[1]	−15	0	1	30	60	90
TeleVisit	X					X
Phone/email visit[1]		X	X	X	X	
Informed consent[2]	X					
Inclusion/exclusion criteria[3]	X					
Pregnancy verbal screen[3]	X					
Consume test product[4]		X				
Compliance check[5]			X	X	X	X
General Health Questionnaire (GHQ)[6]	X			X	X	X
TruDiagnostic Questionnaire[7]	X					X
Blood collection/ Epigenetics Test[8]	X					X
Adverse events (AEs)[9]			X	X	X	X

[1]A window of +14 d was allowed between Visit 1 and 2. An email communication was provided prior to Visit 2 instructing participants to start product within 7-d (Visit 2, Day 0). Visits 3, 4, 5, and 7 were conducted by phone call with the Research Associate, and Visits 1 and 6 conducted by TeleVisit with the Clinical Investigator. A window of +24 h was allowed for Visit 3, anchored to product start (Visit 2, Day 0). A window of ±5 days was allowed between Visits 4 and 5, anchored to Visit 2 (Day 0). A window of +10 d was allowed for Visit 6, anchored to Visit 2 (Day 0).
[2]HIPAA, Health Insurance Portability and Accountability Act authorization for disclosure of protected health information and Informed Consents. Signed documents authorize the use and disclosure of the subject's Protected Health Information by the Investigator and by those persons who need that information for the purposes of the study.
[3]Inclusion Exclusion Criteria were reviewed at study initiation for eligibility, and at end of study for possible changes and deviations from the study. Inclusion/exclusion review included verbal assessment for pregnancy for all women age < 60 y.
[4]Eligible participants were shipped study products after confirmation of eligibility and agreement to participate (Visit 1). Study product was labeled "FOR RESEARCH USE ONLY" and participants were sent an email when confirmation of shipping was obtained. Participants were instructed to begin product consumption within 7 d and schedule the 24-h follow-up call. The first day of product consumption was documented and defined as study Day 0.
[5]Participants were verbally queried about compliance at Visits 4, 5, and 6. Participants were provided a paper Study Log to allow for self-monitoring of daily product consumption and documentation of clinical experiences and AEs as an aid.
[6]The General Health Questionnaire (GHQ) was sent to participants electronically via the clinical database module prior to Visit 1 (Day −15), Visit 4 (Day 30), Visit 5 (Day 60), and Visit 6 (Day 90), and follow-up queries on completion were made at the subsequent study visits.
[7]The TruDiagnostic intake questionnaire, which contains questions on health history, diet and lifestyle, was provided at baseline (Visit 1, Day 0), and a follow-up brief questionnaire was obtained at the final blood sampling, Visit 6, Day 90.
[8]Epigenetics testing was conducted at baseline (Visit 1, Day 0) and end of product consumption (Visit 6, Day 90). Blood was obtained in the home by participants using the Tasso device and sent to the TruDiagnostic laboratory, where it was analyzed by epigenetic testing.
[9]AEs were obtained by open-ended questioning at Visit 3 (24 h),Visit 4 (30 d), Visit 5 (60 d) and Visit 6 (90 d) and assessed for severity and relationship to product by the Clinical Investigator. The study log included questions for participants to provide daily observations and aid in response to the questions at the subsequent visits.

to the TruDiagnostic laboratory directly. Overall, we analyzed blood samples from 47 adults from an initial sample set of 50 individuals using an Illumina EPICv1 epigenetic panel that analyzed DNA methylation at 850,000 CpG sites prior to and after 90 days of an intervention with a polyphenol-rich supplement designed to mimic major bioactive nutrients found in the plant Tartary buckwheat. Beta values were extracted from IDAT files using the minfi pipeline, and outlier samples were identified using the ENmix R package (47, 48). Final analysis included data from 40 people who successfully completed the study. All analyses were conducted using the R programming environment.

Epigenetic clocks were derived from processed beta values including the OMICmAge clock (49), PhenoAge clock (3) and GrimAge version 1 (2). To ensure high reproducibility, the principal component versions of these clocks were used as outlined by Higgins-Chen et al. (50). The clocks were calculated using a custom R script available on GitHub. Additionally, DunedinPACE was computed using a specific script available on GitHub (4).[1] Epigenetic assessment was conducted using Wilcoxon-rank sum test performed by evaluators blinded to participant identifying information. For all epigenetic statistical tests, epigenetic measures were converted from raw outputs to epigenetic age acceleration (EAA), which is defined as the residual calculated between the epigenetic age measurement and chronological age. To account for batch effects, the variation calculated from the first three principal components of the control probes were added as fixed effects to the EAA estimation.

Immune assessments were obtained via deconvolution algorithms of the epigenetic data, which quantitatively approximate immune cell subsets including CD4+ T cells, CD8+ T cells, granulocytes, natural

1 https://github.com/danbelsky/DunedinPACE

killer cells, monocytes, eosinophils, and neutrophils using the Epidish package (51).

2.12 Differential methylation analysis

Differential methylation analysis was carried out utilizing processed beta values. The Limma package was employed for three distinct comparisons, identifying differentially methylated loci (DMLs) within the individuals during the trial from baseline to the final timepoint collection (day 90). Multivariate linear models incorporated fixed effects including beadchip, five immune cell percentages (CD4T naive, CD4T memory, CD8T naive, CD8T memory, B naive, B memory, eosinophils, T regulatory, natural killer (NK), and neutrophils (Neu)), the third and fourth three principal components of technical probes, and the Study ID for the individual. Q-Q plots and lambda values were utilized to assess *p*-value inflation or deflation across the methylome (52); the final lambda value of was 0.96 suggesting the Epigenome-Wide Analysis (EWAS) model did not show inflation or deflation. DMLs were identified with an unadjusted *p*-value significance threshold of <0.001. Functional annotation of DMLs was conducted using the GREAT pipeline to identify significant gene ontology terms, as implemented in the rGREAT R package (53).

2.13 Safety assessments

Participants were asked about AEs by open-ended questions at Visit 3 (24-h), Visit 4 (Day 30), Visit 5 (Day 60), and Visit 6 (Day 90). The Clinical Investigator reviewed the reports, obtaining follow-up information from participants as needed, and categorized by severity and relationship to study products based upon FDA criteria (detailed in the Study Protocol).

2.14 Statistics

As this was a pilot study, sample size was estimated based on previous analyses with epigenetic studies to require a minimum of $n = 30$. A total of 50 participants were enrolled to account for attrition and non-compliance. Populations for statistical analysis were predefined based on inclusion and exclusion criteria (see below). For epigenetic analysis, we used DNA methylation to compare baseline measures against final measures across the entire study population for OMICmAge PhenoAge, GrimAge and DunedinPACE groups. Subgroup and sensitivity analyses were also performed for each of these subpopulations using +1 and −1 standard deviations from the mean and within/inclusive of 1 standard deviation of the mean and those testing positive to COVID-19 during the study, as accelerated epigenetic aging in the context of COVID-19 has been documented (54). Demographics and analysis of the General Health Questionnaire (GHQ) were conducted in Excel (Microsoft, version 2211) and presented as descriptive statistics. In all epigenetic analyses, the statistical significance was established using a $p < 0.05$ threshold.

3 Results

3.1 Participant disposition

Fifty-seven individuals were screened on-line and scheduled for an initial visit to assess eligibility. Of these, $n = 50$ individuals attended the on-line screening visit and met eligibility criteria, and $n = 7$ did not meet eligibility criteria, as follows:

- Involved in another trial, $n = 2$
- Lactating, $n = 1$
- On excluded high dose polyphenolic supplements, $n = 1$
- BMI outside accepted range (<40 kg/m^2), $n = 1$
- Did not show up for screening, $n = 1$
- Did not want name associated with the DNA results in the database $n = 1$

Of the $n = 50$ enrolled in the study, 47 completed labwork. One participant withdrew consent at Visit 2. In addition, final lab analyses were not obtained from two participants ($n = 2$) and these were considered early terminations (ET) at Visit 6 for purposes of analyses. The participant disposition is summarized in Figure 1.

3.2 Epigenome-wide analysis identifies CpGs related with intake of Tartary buckwheat extract

To investigate the overall epigenetic impact of the standardized polyphenol concentrate upon the cohort, we conducted an epigenome-wide analysis (EWAS) analysis to identify CpGs which showed significant differential methylation between the two visits. To ensure that the EWAS model was not overfit and thus limit false positives, we first tested for inflation by identifying variables which accounted for overfitting. To this end, we estimated the coefficient of overfitting (lambda) at 0.96, which indicated that the EWAS model selected did not show significant overfitting within the data (Supplementary File 2). From the indicated model, we identified 887 Differentially Methylated Loci (DMLs) across the EPIC/850 K data (unadjusted *p*-value <0.001). Among these, 336 CpG sites were hypermethylated at the conclusion of the study (Visit 6), while 551 loci were hypomethylated. The full list of these CpGs is listed in Supplementary File 2. The results of the analysis are further represented in the following Manhattan (Figure 2) and Volcano plots (Figure 3) to allow for visual representation of data. The Manhattan plot is used to identify chromosomal locations of the DMLs and to observe whether DMLs were spatially distributed in clusters or across the genome, whereas the Volcano plot allows for visualization of direction of methylation change (e.g., hyper- vs. hypo-methylation).

3.3 Gene ontology pathways

To link the methylation results to biological processes, enrichment analyses using the GREAT software were conducted on CpGs based on the direction of methylation and used to identify gene ontology (GO) pathways. Hypermethylated CpGs at the conclusion of the study were significantly associated with a total of 15 GO-BP (Biological

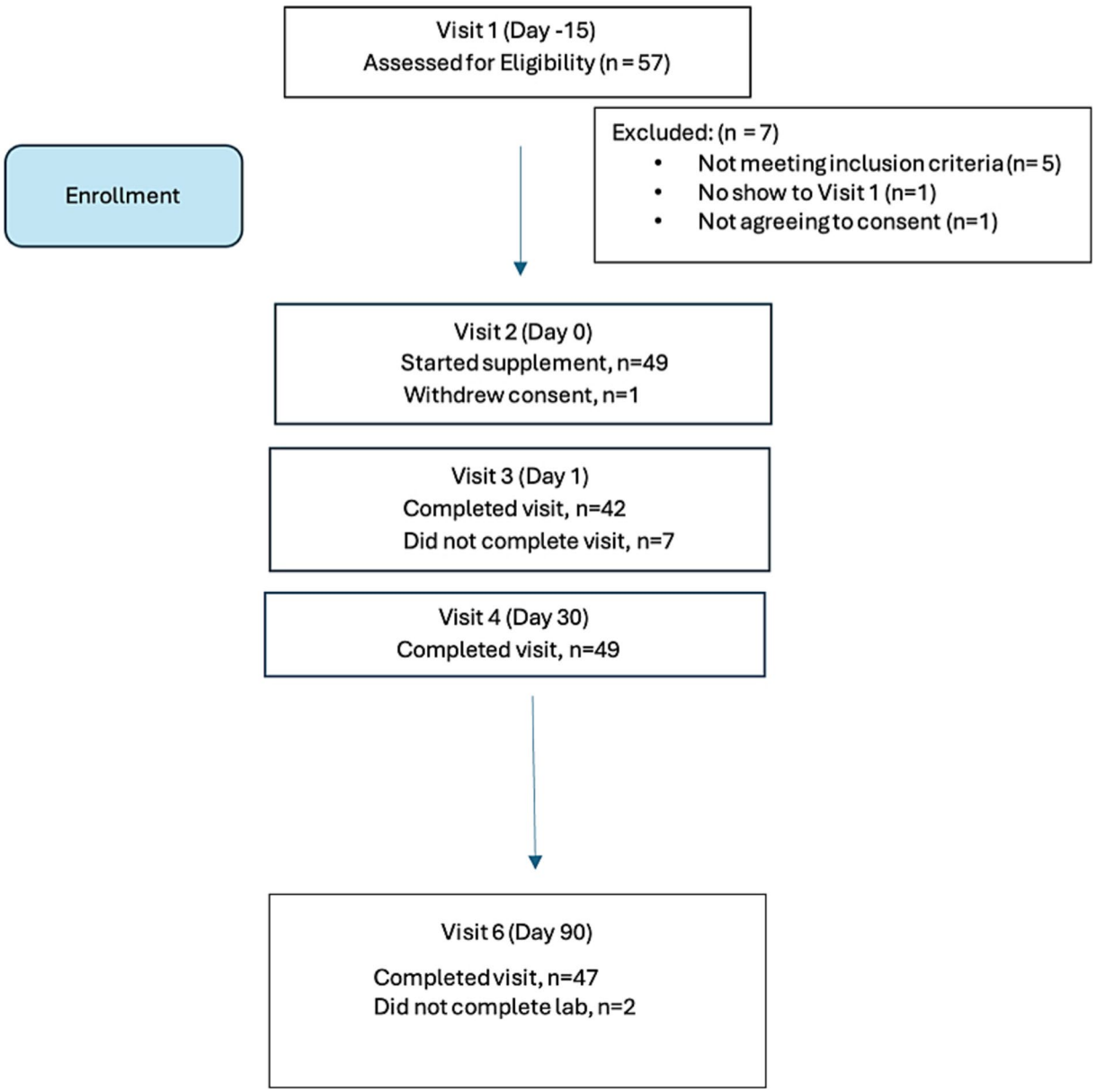

FIGURE 1
Participant disposition chart.

processes) terms, 4 GO-MF (molecular function), and 3 GO-CC (Cellular component) (Supplementary File 3) terms. The top 15 terms for each GO category are shown in Figure 4, which included a diverse group of pathways including ceramide kinase activity, COP9 signalosome activity, labyrinthine layer morphogenesis, and neurofilament activity.

A similar analysis was performed on the hypomethylated DMLs identified in the analysis, which revealed greater significant GO terms compared to the hypermethylated DMLs (Supplementary File 3). Among the hypomethylated DMLs, 124 GO-BP terms, 6 GO-MF terms, and 4 GO-CC terms. The top 15 for each category are reported in Figure 5 which includes the activation of processes that regulate photoreceptor cell differentiation and ventral spinal cord interneuron specification. In addition, we also observed higher enrichment of processes associated with Notch binding.

3.4 Comparison to published dietary DML data

To better interrogate whether the above results might represent changes seen in more comprehensive dietary intervention, and whether the study supplement mimicked the effects of a plant-based diet, we compared our data to the results from (73), which examined DMLs across a vegan intervention and omnivore (control) intervention using a Venn diagram of DMLs across the three groups (Figure 6).

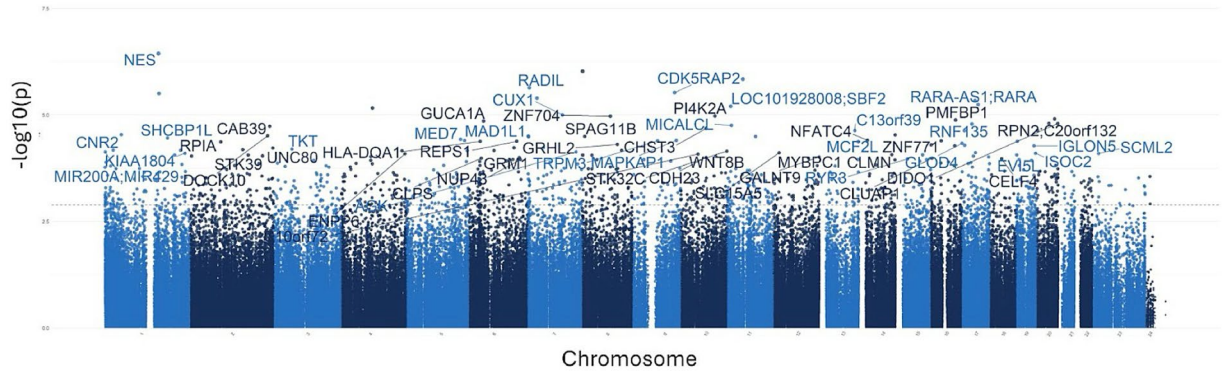

FIGURE 2
Manhattan plots for the epigenome-wide association study (EWAS). The above plot depicts genes associated with CpG sites identified in the analysis. Each dot on the plot represents a CpG site, with its vertical position corresponding to the negative logarithm (base 10) of the unadjusted *p*-value for DNA methylation association, with a significance threshold set at $p = 0.001$. The x-axis shows genomic positions organized by chromosomes, with color-coded dots indicating specific chromosomes; different shades of blue are used to demarcate separate chromosomes. The prominently peaked dots represent CpG sites that surpass the genome-wide significance threshold, indicating significant associations.

The one CpG shared among the current analysis with the Omnivore analysis is cg05093714 (Gene ID: LINC01095) which is significantly higher in the vegan cohort compared to the omnivore cohort at 8 weeks. However, all other CpGs are specific to the Tartary buckwheat cohort identified here. No overlap is observed between the Vegan or Omnivore diet, suggesting different pathways are involved.

3.5 Study supplement use impacts changes in epigenetic age

To determine the response to the study supplement on biological age, we quantified and performed analysis on a host of biological age metrics using DNA methylation. Aging clocks used included the second generation multi-omic informed OMICmAge, the third generation DunedinPACE (PACE) and principal component (PC) based second generation PhenoAge and GrimAge clocks. We additionally utilized epigenetic age acceleration (EAA), a marker of the difference between expected rate of aging based on chronological and biological aging. Remarkable findings included: 1. A slowing of epigenetic age acceleration in people with a PCPhenoAge 1SD Higher than the mean ($p = 0.031$) 2. An increase in epigenetic age acceleration in people with a PCGrimAge 1SD Lower than the mean ($p = 0.031$) 3. An increase in epigenetic age acceleration in people with a OMICmAge 1SD lower than the mean ($p = 0.031$). Note that similar *p* values are a result of a wilcoxon-rank sum test which utilizes a rank-based estimate used against smaller *n* values. We stratified sample groups by subsets one standard deviation higher than the mean, one standard deviation lower than the mean, and within/including one standard deviation (−1 to +1) of the mean to better understand the degree to which starting epigenetic state impacts outcome, and as epigenetic changes seen in the context of dietary modification are typically more subtle. The full results of this analysis are represented in Table 4.

It is important to note the heterogeneity of individual results measured using age-related algorithms across the 90-day study period. An individual's epigenetic response to environmental factors and interventions may be significantly influenced by their pre-existing epigenetic status as well as a host of other factors known to impact epigenetic expression (e.g., gut microbiome composition, immune cell makeup, baseline exercise and dietary regimen). To this end, we'd expect diversity in epigenetic age-related outcomes across participants. This can be visualized in Figure 7 using data on the 40 study participants included in the final analysis. Positive slopes represent increased epigenetic age acceleration and negative slopes represent decreased epigenetic age acceleration across the 90-day study period.

3.6 Deconvoluted immune cell analysis

Alterations in immune cell makeup and function have been studied in references to both dietary change and specific nutrient augmentation. We used deconvolution methods to determine immune cell population changes over the duration of the study period to explore the effects of study supplementation on immune cell parameters across different biological age algorithms and within subsets of study participants. The PhenoAge algorithm has been independently validated to correlate with multiple markers of immunosenescence which are serologically determined (3). These include populations of T cells, B cells and granulocytes. To this end, we chose to apply the deconvolution methods to PCPhenoAge subgroupings. These can be reviewed in Table 5.

3.7 Analysis of GHQ results

The GHQ data were reviewed for completeness prior to analysis. Results were obtained for all 49 participants for the baseline and 90-d questionnaires. However, 10 datapoints were missing from the 30-d questionnaires and five datapoints were missing in the 60-d data set.

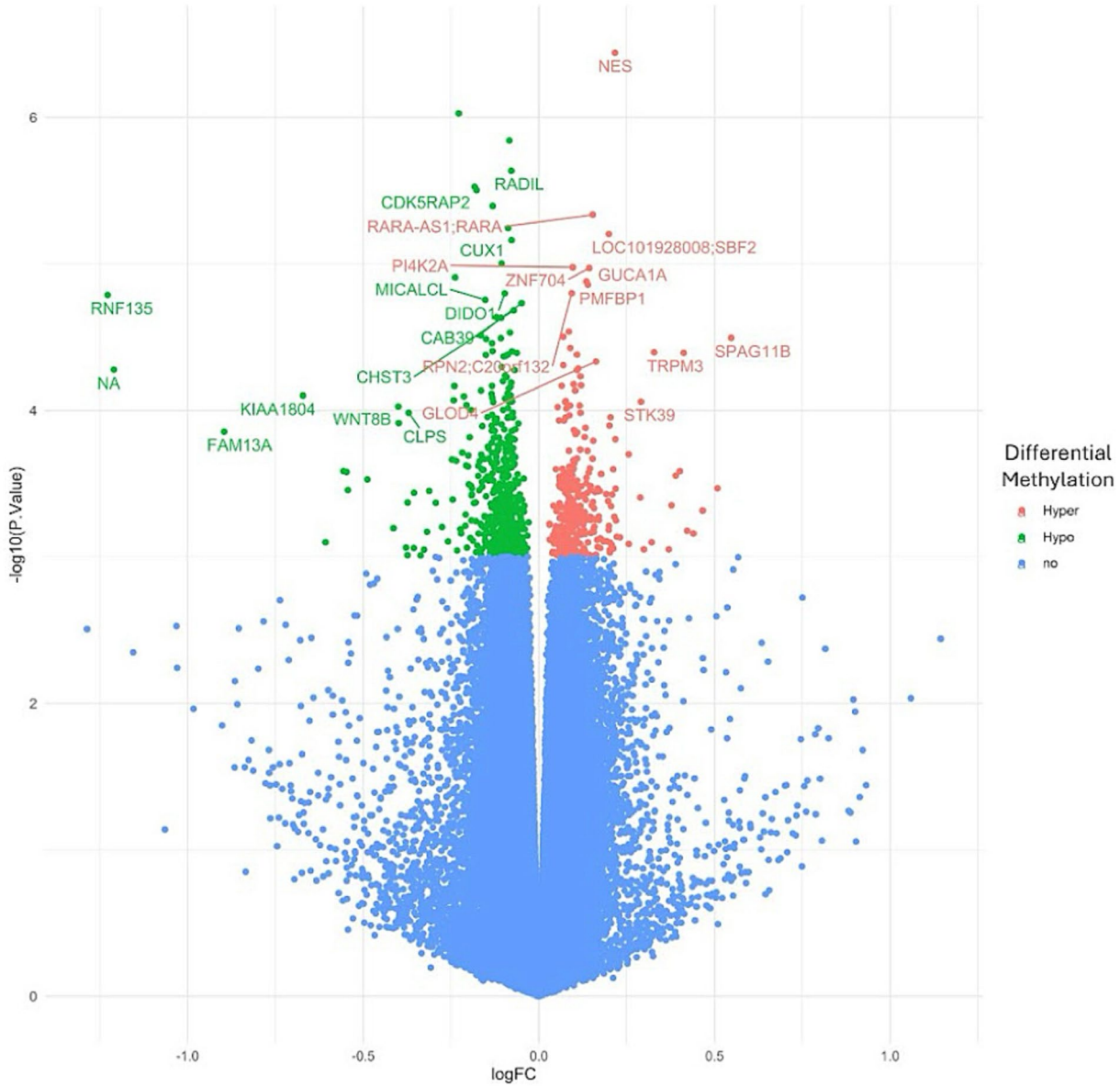

FIGURE 3
Volcano plot for epigenome-wide association study and enrichment analysis. An epigenome-wide association study and enrichment analysis was conducted to compare pre- and post-intervention data (90 days after starting the study supplement). The Volcano plot illustrates differentially methylated loci (DMLs) identified in the pre- vs. post-intervention comparison. Each dot represents a CpG site, with its vertical position indicating the negative logarithm (base 10) of the unadjusted *p*-value for DNA methylation association. The x-axis shows the relative log fold change (logFC) of the m-values between the two timepoints. Negative values indicate CpGs with decreased methylation among study participants (green), while positive values indicate increased methylation (red).

Given this was the first virtual study with this questionnaire, learnings on how easy it was to obtain the data, as well as whether participants were consistent in reporting on the questionnaire was of use. As shown in Table 6, the time between questionnaires ranged widely.

In addition, two participants indicated taking the baseline GHQ after the start of supplement which meant the true baselines were not available for these individuals. Therefore, their data were removed from further analysis of the GHQ. Two participants began supplements that could directly affect the data and were also removed. Therefore, a total of $N = 36$ responses were reviewed for the GHQ. Summary statistics from these respondents are provided in Appendix 3.

The GHQ was provided to participants to gauge for the potential presence of changes in subjective health-related symptoms and metrics. However, these metrics were largely unchanged when analyzing the population across the study period. In general, the population began the study in very good health by self-report. Overall, few changes were noted in any category, however, the population began with middle to high ratings in all areas of health. Therefore, changes in health were not likely to be observed in this population.

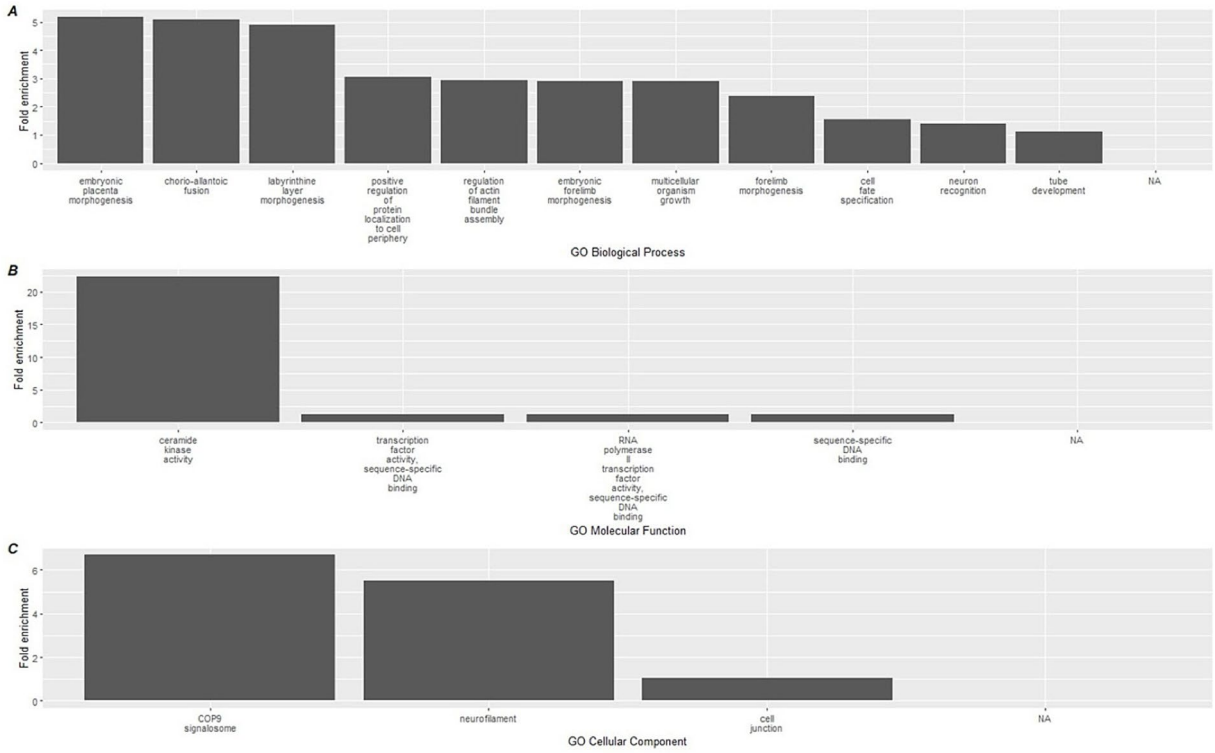

FIGURE 4
Top 15 significant gene ontology terms associated with hypermethylated DMLs using GREAT. Gene ontology databases are reported for **(A)** GO-BP, **(B)** GO-MF, and **(C)** GO-CC. Biological associations shown are gene ontology (GO) terms for Biological Processes (BP), Molecular Function (MF), and cellular components (CC).

4 Discussion

4.1 General discussion

Dietary interventions for modulating health have been well-documented for millennia. In the last hundred years, we have increasingly understood that food represents a complex mixture of caloric and non-caloric components capable of impacting physiology through myriad pathways. In this context, polyphenols have emerged as potential modifiers of human health, including immune health and longevity. However, beyond antioxidant effects, the specifics of *how* polyphenols and foods containing high levels of polyphenols and other phytochemicals impact health have remained relatively poorly interrogated.

Recent publications suggest the role of a polyphenol-rich diet in modulating epigenetics through direct gene methylation and through differential transcription of genes related to epigenetic regulation (13). Individual studies have especially highlighted the role of flavonoid polyphenols in their action on epigenetics. For example, a 2018 trial in cells taken from type 2 diabetic patients found significant changes in histone acetylation after six months of supplementation with resveratrol (74), while a 2013 study found multiple epigenetic alterations associated with cocoa supplementation for two weeks in participants with metabolic dysfunction (75). With roughly 88% of American adults possessing at least one characteristic of metabolic dysfunction, this nevertheless maintains relevance for most of the population (76). Coffee consumption (a top source of dietary polyphenols) has additionally been associated with alterations in methylation across CpG sites (77), which interestingly was only found in peripheral immune cells (as opposed to saliva-derived cellular epigenetic analysis).

In this 90-day study, we provide some of the first clinical evidence suggesting that combinations of polyphenols and phytonutrients occurring naturally in Tartary buckwheat may have multiple effects on markers of longevity and immune system makeup.

By comparing participant's epigenetic analyses before and after the 90-day intervention period, we were able to observe statistically significant changes in rate of aging as measured by the PCPhenoAge and PCGrimmAge and OmicAge algorithms in subgroups experiencing higher and lower rates of aging, respectively. This suggests the potential for the combination of nutrients administered to exert an effect on aging parameters in immune cells.

4.2 Discussion of results

In analysis of immune cell subtypes using deconvolution methods, we hypothesized the potential for immunosenescence-related immune cell changes. Therefore, we ran the deconvolution methods against subset-specific data in Table 5 above for the PCPhenoAge evaluation. Notable here were significant increases in CD4 T memory cells (PCPhenoAge – 1SD Higher) and CD8 T memory cells (PCPhenoAge – 1SD Higher), significant decreases in

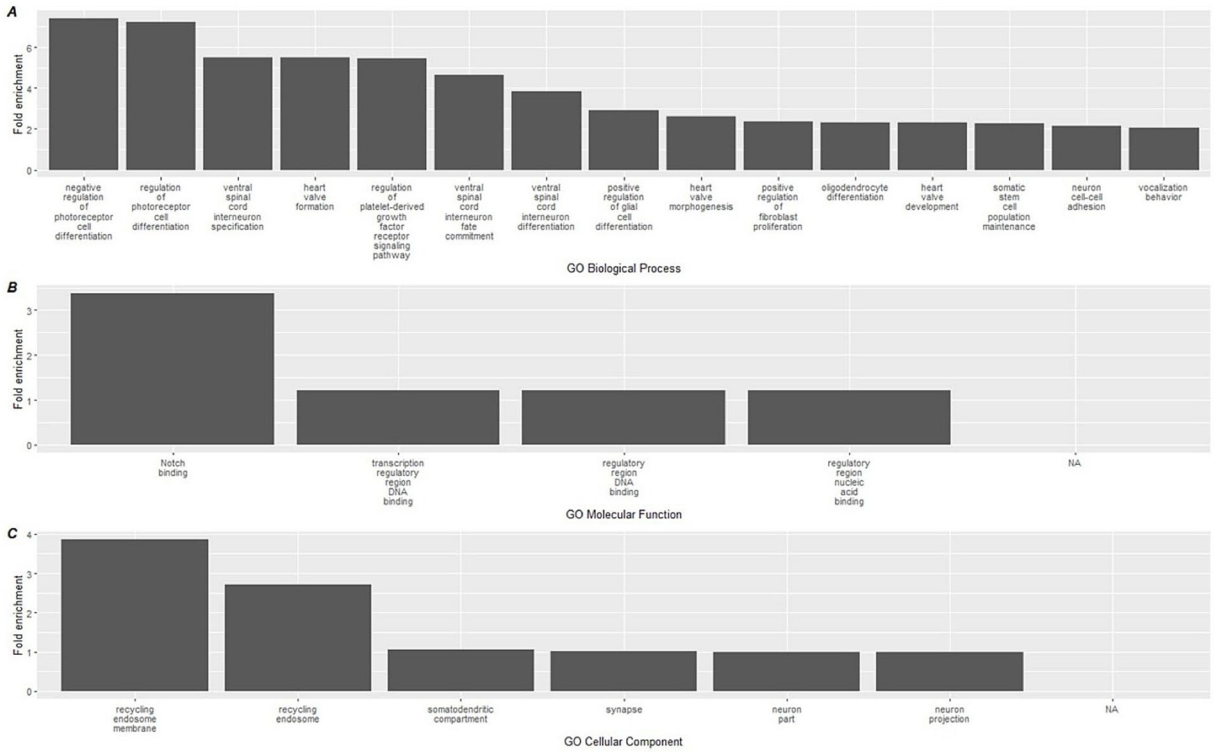

FIGURE 5
Top 15 significant gene ontology terms associated with hypomethylated DMLs using GREAT. Gene ontology databases are reported for **(A)** GO-BP, **(B)** GO-MF, and **(C)** GO-CC. Biological associations shown are gene ontology (GO) terms for Biological Processes (BP), Molecular Function (MF), and cellular components (CC).

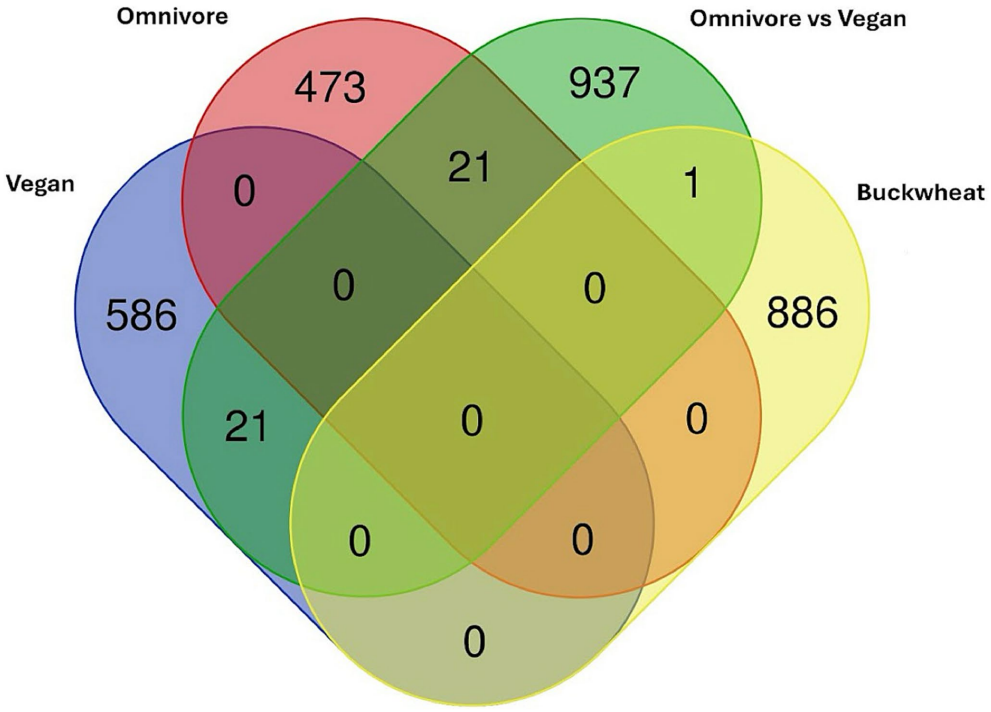

FIGURE 6
Venn diagram of DMLs identified between the comparisons in (73) plotted against DMLs from the Tartary buckwheat supplement intervention.

TABLE 4 Investigation of epigenetic age measures based on subsets one standard deviation higher than the mean, one standard deviation lower than the mean, and within or equal to one standard deviation (−1 to +1) of the mean for multiple epigenetic aging algorithms.

	Mean – Test 1	SD – Test 1	Mean – Test 2	Mean – SD Test 2	*N*	Wilcoxon (*p*-value)
OMICmAge EAA – 1SD Higher	5.686	1.176	4.185	2.904	7	0.380
OMICmAge – 1SD Higher	61.290	10.649	59.940	11.844	7	---
OMICmAge EAA – 1SD Lower	*−4.969*	*1.037*	*−3.718*	*1.851*	*7*	*0.031*
OMICmAge – 1SD Lower	48.032	5.557	49.404	5.709	7	---
OMICmAge EAA – Within 1SD	−0.291	1.906	−0.031	3.120	26	0.860
OMICmAge – Within 1SD	54.785	7.201	55.268	7.538	26	---
OMICmAge EAA – All	−0.063	3.604	0.062	3.699	40	0.740
OMICmAge – All	54.741	8.439	55.059	8.548	40	---
PCPhenoAge EAA – 1SD Higher	*8.065*	*2.163*	*4.262*	*2.294*	*6*	*0.031*
PCPhenoAge – 1SD Higher	51.004	4.785	47.456	6.345	6	---
PCPhenoAge EAA – 1SD Lower	−9.300	2.886	−5.790	4.221	7	0.078
PCPhenoAge – 1SD Lower	36.754	11.490	40.537	11.347	7	---
PCPhenoAge EAA – Within 1SD	−0.087	2.435	0.166	4.132	27	0.360
PCPhenoAge – Within 1SD	48.759	10.207	49.251	10.601	27	---
PCPhenoAge EAA – All	−0.476	5.580	−0.262	4.854	40	0.690
PCPhenoAge – All	46.995	10.778	47.457	10.522	40	---
PCGrimAge EAA – 1SD Higher	2.960	0.822	2.177	1.455	8	0.200
PCGrimAge – 1SD Higher	63.209	11.339	62.561	11.717	8	---
PCGrimAge EAA – 1SD Lower	*−3.759*	*0.554*	*−1.333*	*0.536*	*6*	*0.031*
PCGrimAge – 1SD Lower	57.527	12.238	60.078	12.357	6	---
PCGrimAge EAA – Within 1SD	−0.407	1.165	−0.336	2.166	26	0.670
PCGrimAge – Within 1SD	61.605	7.425	61.855	7.860	26	---
PCGrimAge EAA – All	−0.236	2.248	0.017	2.178	40	0.320
PCGrimAge – All	61.314	8.979	61.730	9.187	40	---
PACE – 1SD Higher	1.007	0.050	0.976	0.071	8	0.250
PACE – 1SD Lower	0.710	0.033	0.699	0.090	7	0.690
PACE – Within 1SD	0.841	0.050	0.866	0.079	25	0.110
PACE – All	0.851	0.104	0.859	0.116	40	0.610

Italicized terms meet statistical significance at a *p*-value of 0.05 or less.

B naive cells (PCPhenoAge – 1SD Lower) and significant decreases in Natural Killer cells (PCPhenoAge – Within 1 SD). While the PCPhenoAge 1SD higher population saw a decrease in speed of epigenetic age progression, this group also demonstrated an increase in CD4T and CD8T memory cells. Conversely, those starting the study at a lower overall epigenetic age score saw a decrease in naive B cells. These alterations in adaptive immune cells speak to potential effects on immune phenotypes over a 90-day interventional window. Additional and more comprehensive profiling of immune cell and cytokine alterations linked to Tartary buckwheat nutrient intake may better characterize the immune effects of dietary consumption of this seed, including on immunosenescence-related pathways.

Using genome-wide EWAS analysis comparing blood samples from the start and end of the study period, we identified 887 differentially methylated CPG sites at a p value of <0.001 with 336 hypermethylated and 551 hypomethylated sites controlled for potential overfitting. These differentially methylated sites were then analyzed using the GREAT software to identify GO pathways.

When we mapped CpG methylation against known biological processes using the GREAT software, a total of 22 pathways were linked to hypermethylated CpGs, while 134 were linked to hypomethylated CpGs. On review of these processes, the most highly enriched changes in biological pathways occurred within the hypermethylated CpG sites, where the largest fold enrichment (22x) was linked to ceramide kinase activity. We additionally found a 6.7-fold enhancement in COP9 activity. Among the hypomethylated biological processes, the largest enrichment changes were seen with negative and positive regulation of photoreceptor cell differentiation (7.41 and 7.21-fold, respectively). While of lower overall effect magnitude, it is also notable in the context of immunity that positive regulation of glial cell maturation was among the top 10 most pronounced findings, at a 2.9x fold-enrichment. These relatively large effects, in contrast with the immune cell deconvolution results, suggest that the more pronounced impact of the dietary supplementation occurred on upstream immune-related biological pathways measurable through epigenetics. The complete list of GREAT software identified GO pathways can be found in Supplementary File 3.

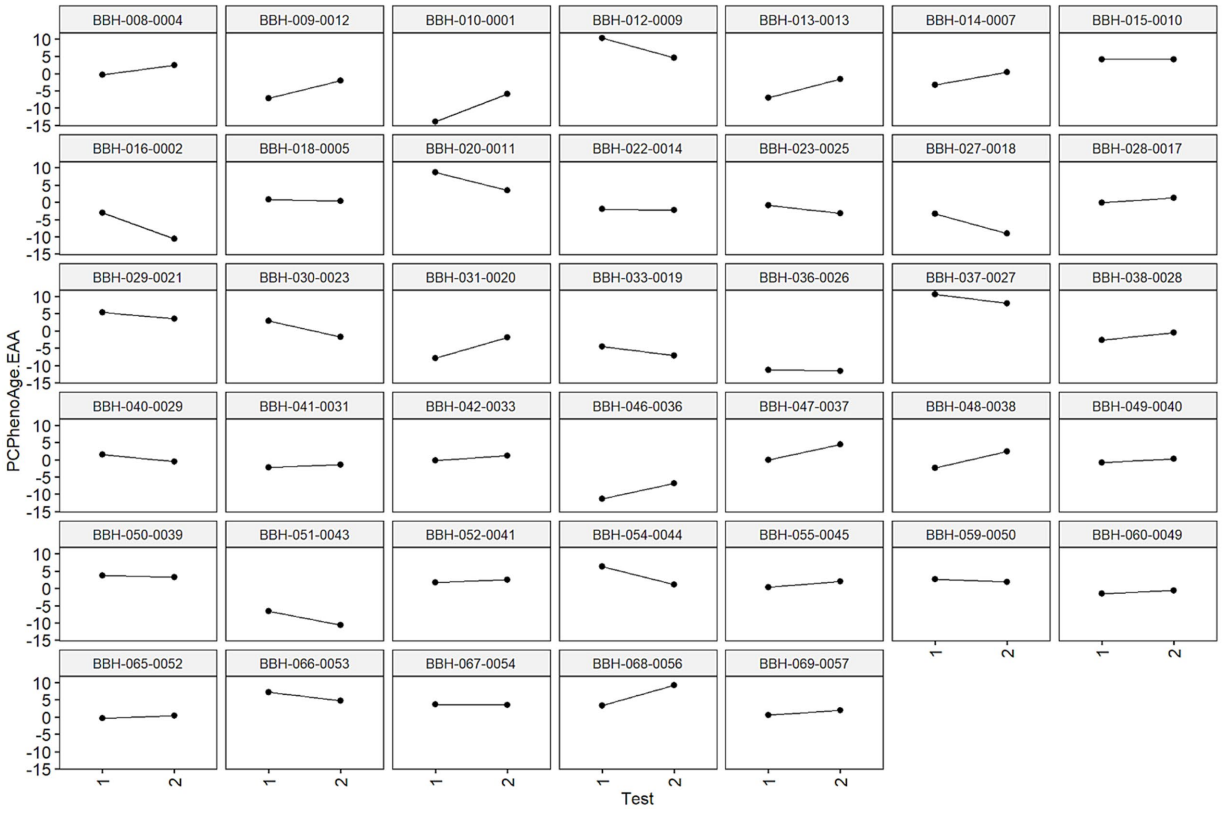

FIGURE 7
Visual representation of individual epigenetic age accelerations (PCPhenoAge used as example). Each graph is faceted by each individual's de-identified ID provided during the trial. Individual slopes calculated as changes in signify changes in epigenetic age metrics during this window (positive slopes represent increased epigenetic age acceleration, negative slopes represent decreased epigenetic age acceleration). These results may speak to individual differences in epigenetic sensitivity to environmental inputs, in this case dietary modification.

4.3 Review of hypermethylated pathways

The single largest fold enrichment pathway in the hypermethylated analysis (and across all GO pathways) was related to ceramide kinase regulation. Ceramides, bioactive lipids found in plasma membranes, regulate numerous cellular processes, such as cell cycle and immunity, by acting as second messengers (55, 56). Elevated circulating ceramide levels are linked to cardiometabolic and immunological dysfunction, often triggered by dietary factors. For instance, palmitic acid raises ceramide levels, whereas polyunsaturated fats lower them (57).

Ceramide kinase (CERK) converts ceramide to ceramide-1-phosphate (C1P), an important regulator of inflammation and immune responses, with context-dependent pro- or anti-inflammatory effects (58). CERK promotes mast cell degranulation (59) and contributes to cellular senescence, a key factor in aging and inflammation. Inhibiting CERK reduces senescent cell burden, while C1P enhances cell survival (60, 78).

Polyphenols like rutin have been shown to modulate the ceramide pathway, reducing ceramide levels in preclinical models (61). Additionally, adherence to the Mediterranean diet is associated with lower ceramide levels in humans (62). A network pharmacology study identified RAF1, a protein involved in cellular proliferation, as a target of Tartary buckwheat, with ceramide-linked phosphorylation playing a role (63, 64). These findings suggest that Tartary buckwheat may influence immune function, longevity, and epigenetic outcomes by inhibiting the ceramide kinase pathway.

Regarding COP9, this is a conserved protein complex composed of 9 subunits found across eukaryotic cells, and well described in plants and animals. In plants, the COP9 signalosome regulates gene expression and resilience to abiotic stress. COP9 is an established cell-cycle regulator through impacts on ubiquitination and transcriptional modification (65). Genes associated with the COP9 signalosome are linked to regulation of senescence (66). The COP9 signalosome has more recently been implicated in the modulation of neuroinflammation including effects on microglial cells and appears to play a key role in maturation of the autophagosome (67, 68) It has previously been shown that curcumin polyphenols are capable of impacting COP9 (69).

4.4 Review of hypomethylated pathways

A relatively higher number of hypomethylated GO pathways were identified by the GREAT software. These diverse biological pathways share a common theme of regulating cell differentiation and development. For example, some of the highest fold change effects occurred in processes governing photoreceptor cell

TABLE 5 Representation of changes in deconvoluted immune cell subsets using epigenetic age accelerations for PCPhenoAge.

	Week 0	Week 8	Wilcoxon – *p*-value	Clock comparison
CD4Tmem	0.096	0.095	0.934	PCPhenoAge – Within
CD8Tmem	0.053	0.052	0.427	PCPhenoAge – Within
CD4Tnv	0.073	0.077	0.117	PCPhenoAge – Within
CD8Tnv	0.034	0.032	0.178	PCPhenoAge – Within
Bmem	0.020	0.019	0.645	PCPhenoAge – Within
Bnv	0.042	0.040	0.470	PCPhenoAge – Within
Treg	0.008	0.009	0.427	PCPhenoAge – Within
Baso	0.019	0.018	0.594	PCPhenoAge – Within
Eos	0.012	0.009	0.786	PCPhenoAge – Within
NK	**0.060**	**0.052**	**0.046**	**PCPhenoAge – Within**
Neu	0.521	0.540	0.441	PCPhenoAge – Within
Mono	0.063	0.057	0.220	PCPhenoAge – Within
CD4Tmem	0.105	0.087	0.156	PCPhenoAge – 1SD Lower
CD8Tmem	0.059	0.045	0.219	PCPhenoAge – 1SD Lower
CD4Tnv	0.143	0.118	0.109	PCPhenoAge – 1SD Lower
CD8Tnv	0.055	0.039	0.078	PCPhenoAge – 1SD Lower
Bmem	0.019	0.017	0.297	PCPhenoAge – 1SD Lower
Bnv	**0.067**	**0.055**	**0.031**	**PCPhenoAge – 1SD Lower**
Treg	0.013	0.011	0.469	PCPhenoAge – 1SD Lower
Baso	0.018	0.014	0.016	PCPhenoAge – 1SD Lower
Eos	0.007	0.003	0.402	PCPhenoAge – 1SD Lower
NK	0.063	0.057	0.469	PCPhenoAge – 1SD Lower
Neu	0.398	0.512	0.109	PCPhenoAge – 1SD Lower
Mono	0.052	0.042	0.375	PCPhenoAge – 1SD Lower
CD4Tmem	**0.071**	**0.107**	**0.031**	**PCPhenoAge – 1SD Higher**
CD8Tmem	**0.037**	**0.055**	**0.031**	**PCPhenoAge – 1SD Higher**
CD4Tnv	0.044	0.063	0.063	PCPhenoAge – 1SD Higher
CD8Tnv	0.034	0.042	0.156	PCPhenoAge – 1SD Higher
Bmem	0.014	0.020	0.031	PCPhenoAge – 1SD Higher
Bnv	0.032	0.039	0.156	PCPhenoAge – 1SD Higher
Treg	0.007	0.005	0.438	PCPhenoAge – 1SD Higher
Baso	0.014	0.019	0.156	PCPhenoAge – 1SD Higher
Eos	0.002	0.007	0.201	PCPhenoAge – 1SD Higher
NK	0.029	0.043	0.063	PCPhenoAge – 1SD Higher
Neu	0.654	0.548	0.063	PCPhenoAge – 1SD Higher
Mono	0.061	0.051	0.563	PCPhenoAge – 1SD Higher

Bolded rows indicate a significant *p* value.

differentiation, ventral spinal cord interneuron specification, oligodendrocyte and generally glial cell differentiation, highlighting mechanisms of neural development and functionality. Of note, polyphenols have been shown in preclinical work to have effects on both neurons and on glial cells (70, 71). Additionally, pathways such as heart valve formation, morphogenesis, and prostate gland epithelium morphogenesis emphasize the precise orchestration of cellular proliferation and specialization necessary for organogenesis. Regulation of signaling pathways, like those involving platelet-derived growth factors or the Wnt signaling pathway, further underscores the delicate balance of activation and inhibition required to maintain tissue homeostasis, control cell fate, and prevent aberrant growth or differentiation. Collectively, these pathways underscore influences on the interplay of various signals that guide the formation, specialization, and maintenance of cells across different biological systems.

TABLE 6 Time between GHQ responses.

GHQ Timepoint	# Participant responses	Days from baseline GHQ			
		Theoretical	Median	Min	Max
Baseline	49	n/a	n/a	n/a	n/a
Day 30	39	30	37	−4	75
Day 30*	37	30	39	18	75
Day 60	44	60	73	53	111
Day 90	49	90	101	67	138

GHQ, General Health Questionnaire; n/a, not applicable. *Two participants indicated taking the 30-d GHQ before consuming the product, resulting in minus days. The data in this line shows median min and max days from baseline when these individuals were removed from the analysis.

4.5 Changes across diverse immune and longevity pathways suggest specific role for Tartary buckwheat in "Food is Medicine" discussion

Suboptimal diet has been clearly established as a major risk factor for global death and disability (72). However, recommendations around dietary modification are largely generalized (e.g., eat more fruits, vegetables and whole grains). While this may help at a population level in preventing disease, there has also been a call to understand whether certain foods and nutrients (beyond total calories, macro and micronutrients) may serve to provide an outsized benefit in the health of the individual. As immune-mediated or related conditions are among the most common chronic diseases, dietary interventions targeting immune dysfunction represent an important part of the conversation of "food is medicine."

Data from this pilot study helps provide a more nuanced understanding of how combinations of naturally occurring phytochemicals might induce beneficial effects on humans through activation of biological pathways involved in immune modulation and immune aging. Compared to pharmaceuticals operating with high potency effects on receptors, the biological impact of naturally occurring nutrients like polyphenols at levels similar to what has typically been found in diets of long-lived populations around the world is expected to be more gradual in onset and less pronounced in effect. Here, we provide preliminary data demonstrating the impact of select phytochemicals from Tartary buckwheat in effecting changes across biological pathways involved in health and disease.

4.6 Limitations

As this was a pilot study and did not include a placebo arm, it is possible that some of the effect seen over the 90-day period was a representation of background epigenetic change due to environmental variables. Additionally, this trial did not study dose associations with epigenetics as only one dose of the study supplement was delivered over the course of the study period. While participants were asked not to make any overt changes to their dietary plan or to start any new supplements that might influence the effect of the study supplement, this was a free-living study and therefore participants were not closely monitored. Similarly, variability in lifestyle and related factor (e.g., sleep quality, exercise frequency, stress) were not controlled for in this study and therefore may have contributed to some of the epigenetic changes observed. Finally, this was a relatively small study, with 40 participants included in the final analysis.

4.7 Future research considerations

As this was a pilot study, only one dose of polyphenol-rich supplement was studied. However, a future investigation would be benefited by testing the relative immune and epigenetic associations seen with higher and lower doses of polyphenols, as well as testing use of these molecules over a shorter and longer timespan. Additionally, it is known that the host microbiome may play a significant role in polyphenol metabolism, and that it may modulate the influence of polyphenols on the gastrointestinal immune system. To this end, future research that examines correlations between the microbiome and the effects of polyphenol supplementation on immune and epigenetic parameters is worthy of consideration. While this study benefited from deconvolution algorithms that allowed us to examine the effects of intervention across various immune cell subtypes, a deeper immunophenotyping using flow cytometry techniques could allow for interrogation of whether polyphenol-related effects were specific to leukocyte subsets and resultant cytokine production. This degree of precision would aid future efforts to tailor nutritional intervention to individuals.

5 Conclusion

In this study, we present novel data indicating the potential for phytochemical nutrients found within Tartary buckwheat to act on multiple metrics of epigenetic immune age, immune cells and related cellular pathways. The polyphenol-rich supplement designed around key bioactive nutrients naturally occurring in Tartary buckwheat appeared to directionally influence CpG methylation patterns in subsets of participants with higher and lower rates of biological aging as measured by the PCPhenoAge, PCGrimAge and OmicAge aging algorithms. These changes were correlated with changes in peripheral immune cell patterns as measured by the PCPhenoAge aging algorithm which is known to be sensitive to changes associated with immunosenescence. Changes in GO pathways additionally suggest the potential for effects on multiple immune and cellular regulatory mechanisms, especially those related to ceramide kinase. These results suggest that polyphenols and associated bioactive nutrients naturally occurring in Tartary buckwheat may significantly influence epigenetic age measurements

that may be driven by or reflected in changes in the immune system and associated pathways.

In the context of the larger intersections between the fields of nutrition and healthy aging, this research provides additional support for uncovering pathway-specific and precision nutritional interventions. The detailed analysis generated by epigenetic analysis permits a more comprehensive demonstration of which biological systems may be most modulated by individual or combinations of nutrients naturally occurring in food or supplements, with in this case, a specific focus on Tartary buckwheat. Moving forward, a deeper understanding of potential nutritional targets within an individual's epigenetic analysis prior to intervention will aid researchers and clinicians in accurately matching nutritional needs with dietary plans and diet adjuncts including supplements.

Data availability statement

The data that support the findings of this study are not publicly available due to protection of patient data in accordance to maintaining HIPAA compliance. However, the corresponding authors can provide the data upon reasonable request after signing a Data Use Agreement. Once signed, corresponding authors will provide a protected link to AWS cloud storage to download raw data.

Ethics statement

The studies involving humans were approved by the Institute of Cellular and Regenerative Medicine Institutional Review Board. The studies were conducted in accordance with the local legislation and institutional requirements. The participants provided their written informed consent to participate in this study.

Author contributions

AP: Writing – review & editing, Writing – original draft, Supervision, Software, Project administration, Methodology, Investigation, Formal analysis, Data curation, Conceptualization. JB: Writing – review & editing, Writing – original draft, Methodology, Funding acquisition, Conceptualization. AC: Writing – review & editing, Supervision, Investigation. SM: Writing – review & editing, Supervision, Project administration, Investigation. RS: Writing – review & editing, Resources, Methodology, Conceptualization. TM: Writing – review & editing, Software, Formal analysis, Data curation. VD: Writing – review & editing, Writing – original draft, Visualization, Software, Methodology, Investigation, Formal analysis, Data curation, Conceptualization.

Funding

The author(s) declare that financial support was received for the research, authorship, and/or publication of this article. This research was funded by Big Bold Health, PBC.

Acknowledgments

Special thanks to DeAnn Liska for guidance in developing the study design and assistance in reporting the clinical data. Additionally, we appreciate the contributions of Sierra Stromberg and Gillian Martin in participant follow up and data management, as well as Annie Prestrud in coordinating data collection. Open AI's ChatGPT version 4.0 was used for ideation around conciseness and clarity of the text.

Conflict of interest

JSB and AP are employees of Big Bold Health. RS, VBD, and TLM are employees of TruDiagnostic. SM and AC are consultants to Big Bold Health.

Publisher's note

All claims expressed in this article are solely those of the authors and do not necessarily represent those of their affiliated organizations, or those of the publisher, the editors and the reviewers. Any product that may be evaluated in this article, or claim that may be made by its manufacturer, is not guaranteed or endorsed by the publisher.

Supplementary material

The Supplementary material for this article can be found online at: https://www.frontiersin.org/articles/10.3389/fnut.2024.1474597/full#supplementary-material

References

1. Kontis V, Bennett JE, Mathers CD, Li G, Foreman K, Ezzati M. Future life expectancy in 35 industrialised countries: projections with a Bayesian model ensemble. *Lancet*. (2017) 389:1323–35. doi: 10.1016/S0140-6736(16)32381-9

2. Lu AT, Quach A, Wilson JG, Reiner AP, Aviv A, Raj K, et al. DNA methylation GrimAge strongly predicts lifespan and healthspan. *Aging*. (2019) 11:303–27. doi: 10.18632/aging.101684

3. Levine ME, Lu AT, Quach A, Chen BH, Assimes TL, Bandinelli S, et al. An epigenetic biomarker of aging for lifespan and healthspan. *Aging*. (2018) 10:573–91. doi: 10.18632/aging.101414

4. Belsky DW, Caspi A, Corcoran DL, Sugden K, Poulton R, Arseneault L, et al. DunedinPACE, a DNA methylation biomarker of the pace of aging. *eLife*. (2022) 11:e73420. doi: 10.7554/eLife.73420

5. Ray D, Yung R. Immune senescence, epigenetics and autoimmunity. *Clin Immunol*. (2018) 196:59–63. doi: 10.1016/j.clim.2018.04.002

6. Ahuja SK, Manoharan MS, Lee GC, McKinnon LR, Meunier JA, Steri M, et al. Immune resilience despite inflammatory stress promotes longevity and favorable health outcomes including resistance to infection. *Nat Commun*. (2023) 14:3286. doi: 10.1038/s41467-023-38238-6

7. Karagiannis TT, Dowrey TW, Villacorta-Martin C, Montano M, Reed E, Belkina AC, et al. Multi-modal profiling of peripheral blood cells across the human lifespan reveals distinct immune cell signatures of aging and longevity. *EBioMedicine*. (2023) 90:104514. doi: 10.1016/j.ebiom.2023.104514

8. Nie C, Li Y, Li R, Yan Y, Zhang D, Li T, et al. Distinct biological ages of organs and systems identified from a multi-omics study. *Cell Rep*. (2022) 38:110459. doi: 10.1016/j.celrep.2022.110459

9. Liu Z, Liang Q, Ren Y, Guo C, Ge X, Wang L, et al. Immunosenescence: molecular mechanisms and diseases. *Signal Transduct Target Ther*. (2023) 8:200. doi: 10.1038/s41392-023-01451-2

10. Fitzgerald KN, Hodges R, Hanes D, Stack E, Cheishvili D, Szyf M, et al. Potential reversal of epigenetic age using a diet and lifestyle intervention: a pilot randomized clinical trial. *Aging*. (2021) 13:9419–32. doi: 10.18632/aging.202913

11. Gensous N, Garagnani P, Santoro A, Giuliani C, Ostan R, Fabbri C, et al. One-year Mediterranean diet promotes epigenetic rejuvenation with country-and sex-specific effects: a pilot study from the NU-AGE project. *Geroscience*. (2020) 42:687–701. doi: 10.1007/s11357-019-00149-0

12. Stojković L, Zec M, Zivkovic M, Bundalo M, Bošković M, Glibetić M, et al. Polyphenol-rich *Aronia melanocarpa* juice consumption affects LINE-1 DNA methylation in peripheral blood leukocytes in dyslipidemic women. *Front Nutr*. (2021) 8:689055. doi: 10.3389/fnut.2021.689055

13. Hoffmann A, Meir AY, Hagemann T, Czechowski P, Müller L, Engelmann B, et al. A polyphenol-rich green Mediterranean diet enhances epigenetic regulatory potential: the DIRECT PLUS randomized controlled trial. *Metabolism*. (2023) 145:155594. doi: 10.1016/j.metabol.2023.155594

14. Santos JC, Ribeiro ML, Gambero A. The impact of polyphenols-based diet on the inflammatory profile in COVID-19 elderly and obese patients. *Front Physiol*. (2021) 11:612268. doi: 10.3389/fphys.2020.612268

15. Sharma R, Padwad Y. Perspectives of the potential implications of polyphenols in influencing the interrelationship between oxi-inflammatory stress, cellular senescence and immunosenescence during aging. *Trends Food Sci Technol*. (2020) 98:41–52. doi: 10.1016/j.tifs.2020.02.004

16. Amiot MJ, Riva C, Vinet A. Effects of dietary polyphenols on metabolic syndrome features in humans: a systematic review. *Obes Rev*. (2016) 17:573–86. doi: 10.1111/obr.12409

17. Bahramsoltani R, Ebrahimi F, Farzaei MH, Baratpourmoghaddam A, Ahmadi P, Rostamiasrabadi P, et al. Dietary polyphenols for atherosclerosis: a comprehensive review and future perspectives. *Crit Rev Food Sci Nutr*. (2019) 59:114–32. doi: 10.1080/10408398.2017.1360244

18. Sharma R, Padwad Y. Plant-polyphenols based second-generation synbiotics: emerging concepts, challenges, and opportunities. *Nutrition*. (2020) 77:110785. doi: 10.1016/j.nut.2020.110785

19. da Silveira VM, de Oliveira LM, Mota EF, de Siqueira OL, Gomes-Rochette NF, Nunes-Pinheiro DC, et al. Consumption of rich/enrich phytonutrients food and their relationship with health status of population In: Phytonutrients in food. Sawston: Woodhead Publishing (2020). 67–101.

20. Liu RH. Health benefits of fruit and vegetables are from additive and synergistic combinations of phytochemicals. *Am J Clin Nutr*. (2003) 78:517S–20S. doi: 10.1093/ajcn/78.3.517S

21. Borsoi FT, Neri-Numa IA, de Oliveira WQ, de Araújo FF, Pastore GM. Dietary polyphenols and their relationship to the modulation of non-communicable chronic diseases and epigenetic mechanisms: a mini-review. *Food Chem*. (2023) 6:100155. doi: 10.1016/j.fochms.2022.100155

22. Zhang Y, Yu W, Zhang L, Wang M, Chang W. The interaction of polyphenols and the gut microbiota in neurodegenerative diseases. *Nutrients*. (2022) 14:5373. doi: 10.3390/nu14245373

23. Marangoni K, Dorneles G, da Silva DM, Pinto LP, Rossoni C, Fernandes SA. Diet as an epigenetic factor in inflammatory bowel disease. *World J Gastroenterol*. (2023) 29:5618–29. doi: 10.3748/wjg.v29.i41.5618

24. Kim E, Jeon S. The impact of phytochemicals in obesity-related metabolic diseases: focus on ceramide metabolism. *Nutrients*. (2023) 15:703. doi: 10.3390/nu15030703

25. Gu W, Wu G, Chen G, Meng X, Xie Z, Cai S. Polyphenols alleviate metabolic disorders: the role of ubiquitin-proteasome system. *Front Nutr*. (2024) 11:1445080. doi: 10.3389/fnut.2024.1445080

26. Yin Q, Wang L, Yu H, Chen D, Zhu W, Sun C. Pharmacological effects of polyphenol phytochemicals on the JAK-STAT signaling pathway. *Front Pharmacol*. (2021) 12:716672. doi: 10.3389/fphar.2021.716672

27. Chen M, Xiao L, Dai G, Lu P, Zhang Y, Li Y, et al. Inhibition of JAK-STAT signaling pathway alleviates age-related phenotypes in tendon stem/progenitor cells. *Front Cell Dev Biol*. (2021) 9:650250. doi: 10.3389/fcell.2021.650250

28. Dodington DW, Desai HR, Woo M. JAK/STAT–emerging players in metabolism. *Trends Endocrinol Metabol*. (2018) 29:55–65. doi: 10.1016/j.tem.2017.11.001

29. Xu W, Luo Y, Yin J, Huang M, Luo F. Targeting AMPK signaling by polyphenols: a novel strategy for tackling aging. *Food Funct*. (2023) 14:56–73. doi: 10.1039/D2FO02688K

30. Caputo M, Bona E, Leone I, Samà MT, Nuzzo A, Ferrero A, et al. Inositols and metabolic disorders: from farm to bedside. *J Tradit Complement Med*. (2020) 10:252–9. doi: 10.1016/j.jtcme.2020.03.005

31. Dziedzic K, Górecka D, Szwengiel A, Sulewska H, Kreft I, Gujska E, et al. The content of dietary fibre and polyphenols in morphological parts of buckwheat (*Fagopyrum tataricum*). *Plant Foods Hum Nutr*. (2018) 73:82–8. doi: 10.1007/s11130-018-0659-0

32. Huda MN, Lu S, Jahan T, Ding M, Jha R, Zhang K, et al. Treasure from garden: bioactive compounds of buckwheat. *Food Chem*. (2021) 335:127653. doi: 10.1016/j.foodchem.2020.127653

33. Nishimura M, Ohkawara T, Sato Y, Satoh H, Suzuki T, Ishiguro K, et al. Effectiveness of rutin-rich Tartary buckwheat (*Fagopyrum tataricum* Gaertn.)'Manten-Kirari'in body weight reduction related to its antioxidant properties: a randomised, double-blind, placebo-controlled study. *J Funct Foods*. (2016) 26:460–9. doi: 10.1016/j.jff.2016.08.004

34. Wieslander G, Fabjan N, Vogrincic M, Kreft I, Janson C, Spetz-Nyström U, et al. Eating buckwheat cookies is associated with the reduction in serum levels of myeloperoxidase and cholesterol: a double blind crossover study in day-care Centre staffs. *Tohoku J Exp Med*. (2011) 225:123–30. doi: 10.1620/tjem.225.123

35. Noda T, Ishiguro K, Suzuki T, Morishita T. Tartary buckwheat bran: a review of its chemical composition, processing methods and food uses. *Plan Theory*. (2023) 12:1965. doi: 10.3390/plants12101965

36. Hithamani G, Srinivasan K. Bioaccessibility of polyphenols from wheat (*Triticum aestivum*), sorghum (*Sorghum bicolor*), green gram (*Vigna radiata*), and chickpea (*Cicer arietinum*) as influenced by domestic food processing. *J Agric Food Chem*. (2014) 62:11170–9. doi: 10.1021/jf503450u

37. Muvhulawa N, Dludla PV, Ziqubu K, Mthembu SX, Mthiyane F, Nkambule BB, et al. Rutin ameliorates inflammation and improves metabolic function: a comprehensive analysis of scientific literature. *Pharmacol Res*. (2022) 178:106163. doi: 10.1016/j.phrs.2022.106163

38. Wang L, Zhao J, Mao Y, Liu L, Li C, Wu H, et al. Tartary buckwheat rutin: accumulation, metabolic pathways, regulation mechanisms, and biofortification strategies. *Plant Physiol Biochem*. (2024) 208:108503. doi: 10.1016/j.plaphy.2024.108503

39. Anton SD, Ebner N, Dzierzewski JM, Zlatar ZZ, Gurka MJ, Dotson VM, et al. Effects of 90 days of resveratrol supplementation on cognitive function in elders: a pilot study. *J Altern Complement Med*. (2018) 24:725–32. doi: 10.1089/acm.2017.0398

40. Mathrani A, Yip W, Sequeira-Bisson IR, Barnett D, Stevenson O, Taylor MW, et al. Effect of a 12-week polyphenol rutin intervention on markers of pancreatic β-cell function and gut microbiota in adults with overweight without diabetes. *Nutrients*. (2023) 15:3360. doi: 10.3390/nu15153360

41. Noad RL, Rooney C, McCall D, Young IS, McCance D, McKinley MC, et al. Beneficial effect of a polyphenol-rich diet on cardiovascular risk: a randomised control trial. *Heart*. (2016) 102:1371–9. doi: 10.1136/heartjnl-2015-309218

42. Tjelle TE, Holtung L, Bøhn SK, Aaby K, Thoresen M, Wiik SÅ, et al. Polyphenol-rich juices reduce blood pressure measures in a randomised controlled trial in high normal and hypertensive volunteers. *Br J Nutr*. (2015) 114:1054–63. doi: 10.1017/S0007114515000562

43. Borghans JA, Tesselaar K, de Boer RJ. Current best estimates for the average lifespans of mouse and human leukocytes: reviewing two decades of deuterium-labeling experiments. *Immunol Rev*. (2018) 285:233–48. doi: 10.1111/imr.12693

44. del Bo' C, Bernardi S, Marino M, Porrini M, Tucci M, Guglielmetti S, et al. Systematic review on polyphenol intake and health outcomes: is there sufficient evidence to define a health-promoting polyphenol-rich dietary pattern? *Nutrients*. (2019) 11:1355. doi: 10.3390/nu11061355

45. Engelen MP, Deutz NE. Is β-hydroxy β-methylbutyrate an effective anabolic agent to improve outcome in older diseased populations? *Curr Opin Clin Nutr Metabolic Care*. (2018) 21:207–13. doi: 10.1097/MCO.0000000000000459

46. Dong Y, Wang N, Wang S, Wang J, Peng W. A review: the nutrition components, active substances and flavonoid accumulation of Tartary buckwheat sprouts and innovative physical technology for seeds germinating. *Front Nutr*. (2023) 10:1168361. doi: 10.3389/fnut.2023.1168361

47. Aryee MJ, Jaffe AE, Corrada-Bravo H, Ladd-Acosta C, Feinberg AP, Hansen KD, et al. Minfi: a flexible and comprehensive Bioconductor package for the analysis of Infinium DNA methylation microarrays. *Bioinformatics*. (2014) 30:1363–9. doi: 10.1093/bioinformatics/btu049

48. Xu Z, Niu L, Li L, Taylor JA. ENmix: a novel background correction method for Illumina HumanMethylation450 BeadChip. *Nucleic Acids Res*. (2016) 44:e20. doi: 10.1093/nar/gkv907

49. Chen Q, Dwaraka VB, Carreras-Gallo N, Mendez K, Chen Y, Begum S, et al. OMICmAge: an integrative multi-omics approach to quantify biological age with electronic medical records. *bioRxiv*. (2023). doi: 10.1101/2023.10.16.562114

50. Higgins-Chen AT, Thrush KL, Wang Y, Minteer CJ, Kuo PL, Wang M, et al. A computational solution for bolstering reliability of epigenetic clocks: implications for clinical trials and longitudinal tracking. *Nature Aging*. (2022) 2:644–61. doi: 10.1038/s43587-022-00248-2

51. Luo Q, Dwaraka VB, Chen Q, Tong H, Zhu T, Seale K, et al. A meta-analysis of immune-cell fractions at high resolution reveals novel associations with common phenotypes and health outcomes. *Genome Med*. (2023) 15:59. doi: 10.1186/s13073-023-01211-5

52. Guintivano J, Shabalin AA, Chan RF, Rubinow DR, Sullivan PF, Meltzer-Brody S, et al. Test-statistic inflation in methylome-wide association studies. *Epigenetics*. (2020) 15:1163–6. doi: 10.1080/15592294.2020.1758382

53. Gu Z, Hübschmann D. rGREAT: an R/bioconductor package for functional enrichment on genomic regions. *Bioinformatics*. (2023) 39:745. doi: 10.1093/bioinformatics/btac745

54. Cao X, Li W, Wang T, Ran D, Davalos V, Planas-Serra L, et al. Accelerated biological aging in COVID-19 patients. *Nat Commun*. (2022) 13:2135. doi: 10.1038/s41467-022-29801-8

55. Albeituni S, Stiban J. Roles of ceramides and other sphingolipids in immune cell function and inflammation. *Adv Exp Med Biol*. (2019):169–91. doi: 10.1007/978-3-030-21735-8_15

56. Hilvo M, Vasile VC, Donato LJ, Hurme R, Laaksonen R. Ceramides and ceramide scores: clinical applications for cardiometabolic risk stratification. *Front Endocrinol*. (2020) 11:570628. doi: 10.3389/fendo.2020.570628

57. Rosqvist F, Kullberg J, Ståhlman M, Cedernaes J, Heurling K, Johansson HE, et al. Overeating saturated fat promotes fatty liver and ceramides compared with polyunsaturated fat: a randomized trial. *J Clin Endocrinol Metabol*. (2019) 104:6207–19. doi: 10.1210/jc.2019-00160

58. Al-Rashed F, Ahmad Z, Snider AJ, Thomas R, Kochumon S, Melhem M, et al. Ceramide kinase regulates TNF-α-induced immune responses in human monocytic cells. *Sci Rep*. (2021) 11:8259. doi: 10.1038/s41598-021-87795-7

59. Vaquer CC, Suhaiman L, Pavarotti MA, Arias RJ, Pacheco Guiñazú AB, De Blas GA, et al. The pair ceramide 1-phosphate/ceramide kinase regulates intracellular calcium and progesterone-induced human sperm acrosomal exocytosis. *Front Cell Dev Biol*. (2023) 11:1148831. doi: 10.3389/fcell.2023.1148831

60. Millner A, Running L, Colon-Rosa N, Aga DS, Frasor J, Atilla-Gokcumen GE. Ceramide-1-phosphate is involved in therapy-induced senescence. *ACS Chem Biol*. (2022) 17:822–8. doi: 10.1021/acschembio.2c00216

61. Ma JQ, Liu CM, Yang W. Protective effect of rutin against carbon tetrachloride-induced oxidative stress, inflammation and apoptosis in mouse kidney associated with the ceramide, MAPKs, p53 and calpain activities. *Chem Biol Interact*. (2018) 286:26–33. doi: 10.1016/j.cbi.2018.03.003

62. Yang F, Chen G. The nutritional functions of dietary sphingomyelin and its applications in food. *Front Nutr*. (2022) 9:1002574. doi: 10.3389/fnut.2022.1002574

63. Lu CL, Zheng Q, Shen Q, Song C, Zhang ZM. Uncovering the relationship and mechanisms of Tartary buckwheat (*Fagopyrum tataricum*) and type II diabetes, hypertension, and hyperlipidemia using a network pharmacology approach. *PeerJ*. (2017) 5:e4042. doi: 10.7717/peerj.4042

64. Yao B, Zhang Y, Delikat S, Mathias S, Basu S, Kolesnick R. Phosphorylation of Raf by ceramide-activated protein kinase. *Nature*. (1995) 378:307–10. doi: 10.1038/378307a0

65. Doronkin S, Djagaeva I, Beckendorf SK. The COP9 signalosome promotes degradation of cyclin E during early Drosophila oogenesis. *Dev Cell*. (2003) 4:699–710. doi: 10.1016/S1534-5807(03)00121-7

66. Leal JF, Fominaya J, Cascón A, Guijarro MV, Blanco-Aparicio C, Lleonart M, et al. Cellular senescence bypass screen identifies new putative tumor suppressor genes. *Oncogene*. (2008) 27:1961–70. doi: 10.1038/sj.onc.1210846

67. Su H, Li F, Ranek MJ, Wei N, Wang X. COP9 signalosome regulates autophagosome maturation. *Circulation*. (2011) 124:2117–28. doi: 10.1161/CIRCULATIONAHA.111.048934

68. Tian Y, Milic J, Monasor LS, Chakraborty R, Wang S, Yuan Y, et al. The COP9 signalosome reduces neuroinflammation and attenuates ischemic neuronal stress in organotypic brain slice culture model. *Cell Mol Life Sci*. (2023) 80:262. doi: 10.1007/s00018-023-04911-8

69. Lim SO, Li CW, Xia W, Cha JH, Chan LC, Wu Y, et al. Deubiquitination and stabilization of PD-L1 by CSN5. *Cancer Cell*. (2016) 30:925–39. doi: 10.1016/j.ccell.2016.10.010

70. Arias-Sánchez RA, Torner L, Fenton NB. Polyphenols and neurodegenerative diseases: potential effects and mechanisms of neuroprotection. *Molecules*. (2023) 28:5415. doi: 10.3390/molecules28145415

71. Carecho R, Carregosa D, Ratilal BO, Figueira I, Ávila-Gálvez MA, Dos Santos CN, et al. Dietary (poly) phenols in traumatic brain injury. *Int J Mol Sci*. (2023) 24:8908. doi: 10.3390/ijms24108908

72. Afshin A, Sur PJ, Fay KA, Cornaby L, Ferrara G, Salama JS, et al. Health effects of dietary risks in 195 countries, 1990–2017: a systematic analysis for the global burden of disease study 2017. *Lancet*. (2019) 393:1958–72. doi: 10.1016/S0140-6736(19)30041-8

73. Dwaraka, VB, Aronica, L, Carreras-Gallo, N, Robinson, JL, Hennings, T, Carter, MM, et al Unveiling the epigenetic impact of vegan vs. omnivorous diets on aging: insights from the Twins Nutrition Study (TwiNS). *BMC medicine*. (2024) 22:301. doi: 10.1186/s12916-024-03513-w

74. Bo, S, Togliatto, G, Gambino, R, Ponzo, V, Lombardo, G, Rosato, R, et al Impact of sirtuin-1 expression on H3K56 acetylation and oxidative stress: a double-blind randomized controlled trial with resveratrol supplementation. *Acta diabetologica*. (2018) 55:331–40. doi: 10.1007/s00592-017-1097-4

75. Crescenti, A, Sola, R, Valls, RM, Caimari, A, DelBas, JM, Anguera, A, et al Cocoa consumption alters the global DNA methylation of peripheral leukocytes in humans with cardiovascular disease risk factors: a randomized controlled trial. *PloS one*. (2013) 8:e65744. doi: 10.1371/journal.pone.0065744

76. Araújo, J, Cai, J, Stevens, J. Prevalence of optimal metabolic health in American adults: National Health and Nutrition Examination Survey 2009–2016. *Metabolic syndrome and related disorders*. (2019) 17, 46–52. doi: 10.1089/met.2018.0105

77. Chuang, YH, Quach, A, Absher, D, Assimes, T, Horvath, S, Ritz, B. Coffee consumption is associated with DNA methylation levels of human blood. *European Journal of Human Genetics*. (2017) 25:608–16. doi: 10.1038/ejhg.2016.175

78. Gómez-Muñoz, A. Ceramide 1-phosphate/ceramide, a switch between life and death. *Biochimica et Biophysica Acta (BBA)-Biomembranes*. (2006) 1758:2049–56. doi: 10.1016/j.bbamem.2006.05.011

frontiers | Frontiers in Immunology

TYPE Original Research
PUBLISHED 05 February 2025
DOI 10.3389/fimmu.2025.1545261

OPEN ACCESS

EDITED BY
Francisco José Pérez-Cano,
University of Barcelona, Spain

REVIEWED BY
Francesca Danesi,
University of Bologna, Italy
Karla Rio-Aige,
University of Barcelona, Spain

*CORRESPONDENCE
Mauro Serafini
mserafini@unite.it

RECEIVED 14 December 2024
ACCEPTED 20 January 2025
PUBLISHED 05 February 2025

CITATION
Ramal-Sanchez M, Bravo-Trippetta C, D'Antonio V, Corvaglia E, Kämpfer AAM, Schins RPF, Serafini M and Angelino D (2025) Development and assessment of an intestinal tri-cellular model to investigate the pro/anti-inflammatory potential of digested foods. *Front. Immunol.* 16:1545261. doi: 10.3389/fimmu.2025.1545261

Development and assessment of an intestinal tri-cellular model to investigate the pro/anti-inflammatory potential of digested foods

Marina Ramal-Sanchez[1], Chiara Bravo-Trippetta[1], Veronica D'Antonio[1], Elena Corvaglia[1], Angela A. M. Kämpfer[2], Roel P. F. Schins[2], Mauro Serafini[1]* and Donato Angelino[1]

[1]Functional Foods and Stress Prevention Laboratory, Department of Biosciences and Technology for Food, Agriculture and Environment, University of Teramo, Teramo, Italy, [2]IUF – Leibniz Research Institute for Environmental Medicine, Düsseldorf, Germany

Introduction: Immunonutrition, defined as the potential of foods, nutrients and dietary patterns to modulate the immune system activity, has been proposed as a strategy to enhance the immune response in both metabolic and immune-mediated diseases. However, the anti-/pro-inflammatory role of foods and diets is far to be fully ascertained, and thus there is a continued needed for appropriate in vitro cell-culture models to investigate the role of foods in modulating cell-mediated inflammatory processes. This study aims to develop and test an in vitro tri-culture model, simulating the complexity of the intestinal tract and its multiple cell interactions.

Methods: To achieve this, the intestinal epithelial barrier was established by co-culturing human Caco-2 enterocyte-like and HT29-MTX-E12 mucus producing goblet-like colon cells, then adding human monocyte THP-1 cells to the basolateral compartment. The integrity and stability of the epithelial barrier were monitored and the inflammatory response of the model was assessed using various stressors at different concentrations, both individually and in combination (phorbol-12- myristate-13-acetate or PMA, and lipopolysaccharide or LPS), in terms of cytokines production. To test the model, different concentrations of *in vitro* digested broccoli (BD) were added to the apical section of the model.

Results: Supernatants from the basolateral compartment were collected and analyzed for cytokines production (IL-6, TNF-α, IL-12p70, IL-18 and IL-8) using automated ELISA (ELLA). Additionally, ZO-1 protein from the tight junctions of epithelial cells was analyzed by flow cytometry. The results indicated that 100 nM PMA added to the whole model for 20 h was the best stressor to simulate a mild-inflammatory status of the gut. Following treatment with BD, IL-6, TNF-α, IL-8 and IL-18 were significantly reduced compared to the control group, while ZO-1 expression increased at the lowest BD concentration.

Conclusions: These findings confirm the feasibility of the model for assessing the effects of food digesta on specific cytokines and permeability markers,

representing a valuable strategy for investigating the role of foods in modulating the inflammatory response. The results obtained may support dietary strategies aimed at promoting wellbeing and preventing inflammatory-related metabolic diseases.

KEYWORDS

immunonutrition, cytokines, nutrition, gut, IBD, tri-culture, advanced cellular model, inflammation

1 Introduction

Over the past few decades, lifestyle factors as smoking/drinking habits, physical inactivity and the adherence to unbalanced dietary patterns – characterized by a high intake of foods rich in (saturated) fats, sugars, salt and a low intake of foods source of fiber and plant-based proteins – has led to an increased incidence of chronic metabolic diseases such as obesity, diabetes and cardiovascular diseases (CVDs), and relative deaths (1, 2). These pathologies are all characterized by a common disruption of the immune system, known as meta-inflammation, defined as a "chronic, low-grade systemic inflammation and differing from the acute inflammatory response typical of the innate immune system" (3).

Among the chronic inflammatory intestinal disorders, Crohn's disease (CD) and ulcerative colitis (UC) are the major representatives of inflammatory bowel diseases (IBDs) (4). While the causes are still unknown, a combination of genetic, immunological and environmental factors may be the triggers of the excessive and abnormal immune response, leading to a wide variety of symptoms and a low quality of life for the patient (5). The initiation of the immune response in CD and UC patients is characterized by an increased migration of monocytes into areas of inflammation, which differentiate then into a pro-inflammatory macrophage phenotype (M1), releasing pro-inflammatory cytokines that amplify the immune response and attract additional cellular and humoral components of the immune system (6, 7). Notably, a strong correlation has been demonstrated between obesity and IBDs (8, 9). While low-grade inflammation is present in obese individuals even without other pathological conditions, a persistent metabolic inflammation has been associated with the development of comorbidities, such as IBDs, type 2 diabetes (T2D) or CVDs (10, 11).

Diet plays an important role in modulating cytokines-induced stress associated with the raising of inflammatory chronic conditions. Specific macronutrients from the unbalanced dietary patterns have been proposed as fuel for the inflammatory response in the gut, perturbing not only the innate immunity but also the gut microbial profile and metabolism (4). In contrast, dietary patterns characterized with a high intake of fruit, vegetables, legumes, whole grain products, and low consumption of animal-based products has been associated with lower levels of chronic inflammation (12–15). Scientific research focused on human studies has shown a protective role for a high intake of plant foods and inflammatory markers of inflammation, as C-reactive protein, interleukin 6 (IL-6) and tumor necrosis factor alpha (TNF-α) (13).

In order to unravel the potential of various food items in modulating the inflammatory response, several *in vitro* gut-mimicking models have been proposed. To date, literature suggests that the most frequently used model is represented by a single-cell culture, mainly represented by the enterocyte or colonocyte (16, 17). However, it represents a simplistic strategy, restricted to the study of preliminary tests on specific situations and well-known mechanisms, omitting the interaction with immune cells and their key participation in inflammatory and immune processes (18). In an effort to solve this issue, a two-cells approach including intestinal and immune cells has been proposed as a valuable alternative (19–22). Nevertheless, the intestinal tract is a complex environment characterized by many interactions among different cells with specific features, underlining the need for using an *in vitro* model able to resemble the human intestine and the interactions between the main participating cells as much as possible, but simple enough to exclude the variability related to the single individual characteristics.

Recently, a more complex culture model composed of three cell lines (tri-culture model or 3C henceforth) has been developed to *in vitro* simulate the physiological inflammatory processes occurring *in vivo* at gut level, within limits (23–26). This tri-culture model is composed by epithelial cells from i) Cao-2, an immortalized human colon carcinoma cell line; ii) HT29-MTX-E12, a human colon intestinal cell clone able to produce mucus; and iii) the monocyte cell line THP-1, isolated from the peripheral blood of a patient affected by acute monocytic leukemia and widely used in immunology research. 3C model can be assembled by co-culturing epithelial cells both in the apical part of the insert and THP-1 in the basolateral compartment, without physical interaction among the cells, or in an inverted position, by culturing epithelial cells in the basolateral surface of the insert and the THP-1 cells in the apical part, allowing a direct interaction among the cell lines. 3C has been already used for different research purposes, as for the screening and evaluation of therapeutic drugs for IBD treatment (23), or to screen potential anti-inflammatory compounds in the context of intestinal inflammation, inducing a mild inflammatory status after lipopolysaccharide (LPS) addition

(25). Kämpfer and collaborators compared the potential toxicity of different engineered nanomaterials (ENMs) on monocultures of Caco-2 and HT29-MTX-E12 cells and on the 3C model including THP-1 cells, confirming that 3C model represent a more adequate strategy to address advanced and multifaceted research questions (24). The same model but in an inverted orientation was used by Busch and colleagues to elucidate intestinal effects of low-density polymeric particles from environmental pollution, finding effects that previously were absent in the non-inverted model (27).

Last but not least, the majority of the approaches have tested foods just with water/organic solvent extraction processes, without undergoing a process of digestion, as happens in "real-life" conditions (28–30). This approach might have led to unreliable results due to the biochemical and/or metabolic transformation that occur during cooking and/or digestion. To overcome this problem, in the development of our model the tested food extracts were subjected to *in vitro* digestion.

The aim of this study is to develop and optimize a tri-culture *in vitro* cellular model, including intestinal and immune cells and simulating a mild-inflammatory status, to assess the pro/anti-inflammatory role of digested foods. To accomplish the aim, the model setting-up has been subdivided into different steps: a) establishment and assessment of the intestinal epithelial barrier composed by Caco-2 and HT29-MTX-E12 cells; b) selection of the baseline inflammatory conditions in the immune component of the model (THP-1 cells); c) tri-culture model assembly and evaluation; d) selection of the baseline inflammatory conditions in the tri-culture model, including an anti-inflammatory drug and the final cytokine pattern; e) analysis of the anti/pro-inflammatory response testing a food digesta on the inflamed tri-culture model; f) quantification of cell lysis by measuring LDH release; and g) evaluation of ZO-1 protein expression on the intestinal epithelial barrier.

2 Materials and methods

2.1 Chemicals

Unless otherwise stated, chemicals were acquired from Sigma-Aldrich (Saint Louis, MO, USA).

2.2 Intestinal epithelial cells co-culture and maintaining

Caco-2 cells (cat. no. 09042001-1VL, ECACC) and HT29-MTX-E12 cells (ECACC, 12040401) were cultured in DMEM cell culture medium supplemented with 10% FBS, 1% penicillin/streptomycin and 1% non-essential amino acids (NEAAs), maintained at 37 °C, 5% CO_2, humified atmosphere. Caco-2 and HT29-MTX-E12 cells were regularly split at ~80% confluence and used at passages 10–30 after thawing for co-culture experiments.

For intestinal epithelial cells co-culture, cells were seeded on Transwell inserts (1 μm pore size; Falcon, Sacco S.r.L., Cadorago, Como, Italy) at a density of $1.66*10^5$ cells per well in a ratio 9:1 (Caco-2:HT29-MTX-E12) and maintained up to 21 days, renewing the medium on Monday, Wednesday and Friday. On the apical (AP) side, cells were cultured in DMEM, whereas the medium in the basolateral (BL) compartment was progressively changed to RPMI-based THP-1 medium without β-mercaptoethanol.

2.3 Trans-epithelial electrical resistance monitoring

To monitor the intestinal barrier integrity and stability, trans-epithelial electrical resistance (TEER) measurements were performed at 7, 14 and 21 days after the beginning of the co-culture using the volt-ohm meter Millicell® ERS-2 (Electrical Resistance System, Merck Millipore). The resistance has been then calculated and expressed as Ohm per cm^2 filter surface, following the equation:

$$\text{Resivity}(\Omega \quad cm^2) = (\text{Ohm2} - \text{Ohm1})^* A$$

where Ohm1 is the blank resistance, Ohm2 the insert resistance and A the surface area of the insert.

2.4 Immune cells culture and stimulation

THP-1 (ATCC, TIB-202) cells were cultured in RPMI 1640-based cell culture medium (containing L-glutamine and 25 mM HEPES) supplemented with 10% FBS, 1% penicillin/streptomycin, 1 nM sodium pyruvate, 0.7% d-glucose and 50 nM β-mercaptoethanol and maintained between $2*10^5$ and $8*10^5$ cells/mL, at 37 °C and 5% CO_2, humified atmosphere.

To stimulate THP-1 differentiation into a pro-inflammatory macrophage phenotype, different concentrations of well-known stressors have been used, in multiple combinations. To that, THP-1 cells have been cultured in 12-well plates ($2*10^5$ cells per well) during 24 hours under culture conditions, adding lipopolysaccharide (LPS) at 100 ng/mL and/or phorbol 12-myristate 13-acetate (PMA) at 50, 75 and 100 nM, added in contemporary (24 hours of inflammation) or consecutively (24h LPS + 24h PMA, reaching a total of 48 h of inflammation). The inflammatory response of the different study groups has been measured in terms of TNF-α and IL-6 production.

2.5 Tri-culture model assembling and stimulation

Tri-culture model has been assembled by transferring the Transwell inserts onto the THP-1 cells, immediately after seeding them in 12-wells plates at a density range of $2*10^5$ cells per well with the different treatments: no treatment (non-differentiated THP-1 cells); LPS (100 ng/mL); PMA (100 nM); PMA + LPS (at the same concentrations and in contemporary). The inflammatory response of the different study groups has been measured in terms of TNF-α and IL-6 production. To decipher the best anti-inflammatory drug

concentration, a dose-concentration analysis of the glucocorticoid prednisolone was performed (5, 1, 0.5 and 0.25 μM). To explore the potential role of the enzymes present in the food digesta (see section 2.6), a digesta with no food was examined as well, at different concentrations (500, 400, 200, 100 and 50 μL per mL of supplemented-DMEM). A schema of the tri-culture model assembling is available in Figure 1.

2.6 Preparation of food digesta and calculation of dry matter concentration

Broccoli digesta (BD) were used as sampling digesta to set the tri-culture model. Specifically, three different cultivars/varieties of the product purchased in local supermarkets/groceries have been washed, steamed for 5 min, then dabbed with paper towel; after mincing, the pool from the different cultivars were considered as unique sample for *in vitro* digestion. Dry matter of samples was determined according to the AOAC gravimetrical method (31).

Digestion protocol referred to the harmonized INFOGEST static *in vitro* digestion procedure, simulating the physiological conditions of the oral, gastric and small intestinal digestion phases *in vitro* (32), with opportune modifications.

The oral phase was carried out by using human saliva collected from healthy volunteers, according to Chen et al. (33). The fresh saliva samples were collected after 2 hours from the last meal. The donors were invited to rinse their mouth with deionized water for at least 30 sec to obtain a neutral environment and then saliva at the first 30 s was discarded. Saliva was collected in the next 5 min each 30 sec, until the needed amount was reached. The collected saliva was immediately centrifuged at 1780 *x g* for 10 min and the supernatant used for the following procedure.

In order to simulate mastication, 4 mL of human saliva was added to 4 g of food sample and then the mixture was grinded with

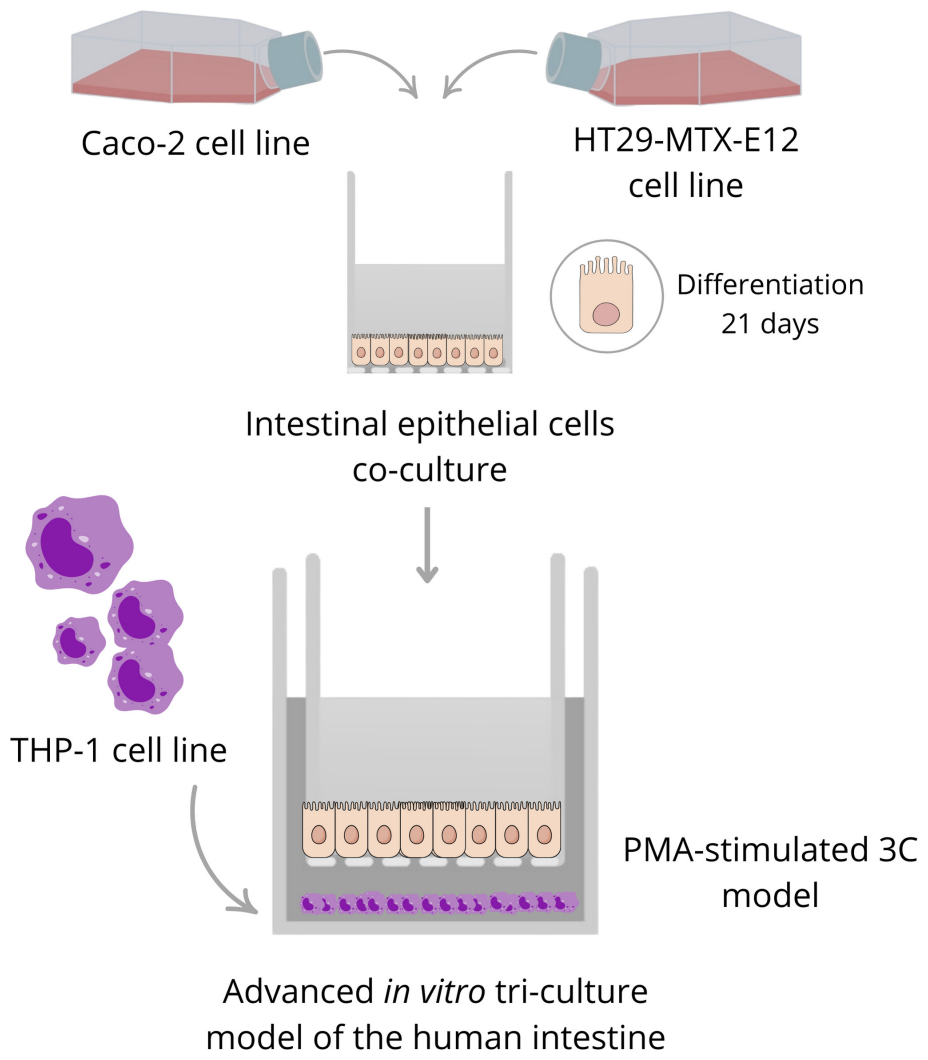

FIGURE 1
Schema of the tri-culture model assembling.

mortar and pestle for 2 min. The gastric phase was started by adding simulated gastric fluid containing 2000 U/mL pepsin in the final volume. The pH was adjusted to 3 and the volume to 16 mL and the mixture was incubated at 37°C for 2 h in a rotating mixer. Then, a solution containing simulated intestinal fluid, containing bile extract (10 mM of bile salts in the final volume) and pancreatin (100 U/mL of trypsin activity in the final volume) was added. The pH was adjusted to 7 and the volume to 32 mL and the mixture was incubated at 37°C for 2 h in a rotating mixer. Digesta were collected, centrifuged at 1780 *x g* and the supernatant was aliquoted and stored at -20°C until cell treatments. For testing, BD were diluted in supplemented-DMEM at different concentrations (400, 200, 100, 50 µL per mL of supplemented-DMEM). A digesta solution with no food (NF), but containing the enzymes and subjected to the standard procedure described, was used as a blank for the experiments evaluating the digesta effects.

2.7 Anti-inflammatory drug selection and digesta enzymes evaluation

To decipher the best anti-inflammatory drug concentration to be used, a dose-concentration analysis using a glucocorticoid was performed. Different concentrations of prednisolone were used: 5, 1, 0.5 and 0.25 µM. In addition, the NF solution at different concentrations (500, 400, 200, 100, 50 µL per mL of supplemented-DMEM) was tested as well in terms of cytokines production. After the stimulation of the model with PMA at 100 nM for 20 hours, treatments were added to the apical part of the model and incubated for 4 hours under culture conditions. Then, the supernatants from the basolateral compartments were recovered and stored at -80°C until the analysis.

2.8 Cytokines analysis by traditional ELISA or ELLA Simple Plex®

To select the final cytokine pattern to be used, the whole 3C model was stimulated with 100 nM PMA during 24 hours (PMA-CTRL) and the supernatants from the basolateral compartment were compared with those from a non-stimulated 3C model (CTRL). Prednisolone and NF digesta were used to evaluate potential cytokines differences, tested on the model as previously described. The supernatants from the basolateral compartments were recovered and stored at -80°C until the analysis.

For the model setting-up and the selection of the cytokine pattern, TNF-α, IL-6, IL-1β, IFN-γ, IL-12p70, IL-23, CCL20, IL-18 and IL-8 cytokines were analyzed using traditional Human Quantikine ELISA kits (Bio-Techne, Minneapolis, MN, USA), following the manufacturer instructions and measuring with the spectrophotometer (Enspire, Perkin Elmer). Once the pattern was identified, for digesta testing, TNF-α, IL-6, IL-12p70, IL-18 and IL-8 cytokines were analyzed using ELLA Simple Plex® automated immunoassay system (ProteinSimple, San Jose, CA, USA), using commercially available customized simple plex kits and according to the manufacturer instructions.

2.9 Evaluation of cell lysis by LDH quantification assay

Cell damage (or necrotic cell death) has been measured by quantifying the enzymatic activity of the lactate dehydrogenase (LDH) released. Briefly, 50 µL of 200 mM TRIS, 50 µL of 50 mM lithium lactate, and 50 µL mix of iodonitrotetrazolium (INT), phenazine methosulfate (PMS), and nicotinamide adenine dinucleotide (NAD) at 1.32 mg/mL, 0.36 mg/mL and 3.44 mg/mL concentrations, respectively, were added to a 96-wells plate. Subsequently, 50 µL of cell-free supernatants have been added to the previous mix and incubated for 5 min at room temperature (RT). As a control of 100% cell lysis, cells exposed to 0.1% Triton X-100 in PBS for 24 h have been used. Optical density has been spectrophotometrically measured (Enspire, Perkin Elmer) at 490 nm. A background control in complete cell culture medium (CCM) was subtracted from the results.

2.10 Analysis of ZO-1 protein expression

To analyze ZO-1 protein expression on the intestinal epithelial barrier, cells were recovered from the inserts using Accutase®, then washed and fixed using a 4% paraformaldehyde (PFA) solution. For flow cytometry analysis, fixed cells were incubated with an anti-ZO-1 antibody produced in rabbit for 1 h, and then with a goat anti-rabbit IgG Alexa Fluo 488 (ThermoFisher Scientific) for 1h. Samples were then analyzed using a CytoFLEX flow cytometer with 488 nm and 638 nm wavelength lasers (B53013) and operated with the CytExpert software (Beckman Coulter, Brea, CA, USA). Events were acquired exciting with the 488 nm laser light and using the band-passes of 525/40 nm for Alexa Fluor 488. Positive events were considered those expressing the protein ZO-1. Flow rate was adjusted to 100 events/sec, acquiring at least 5000 events for each independent sample. Data were extracted and analyzed with CytExpert, considering the fluorescence median from each sample group and comparing every treatment group to the control group. Experiments were performed in biological triplicate.

2.11 Statistical analysis

Statistical analysis was performed on data from at least 3 independent biological and technical experiments. Data were obtained using Graphpad Prism 9.1.0 and expressed as violin or histogram plots. To evaluate the treatment effect, delta value of cytokines was calculated by subtracting the control value to every treatment value. Normality tests (Shapiro-Wilk test for n<50) and outlier identification (ROUT) were carried out for every individual experiment. For cytokines analysis, ANOVA with Dunnett's multiple comparisons or Friedman tests were performed; for the cytokines analysis following BD treatments, one-way ANOVA with

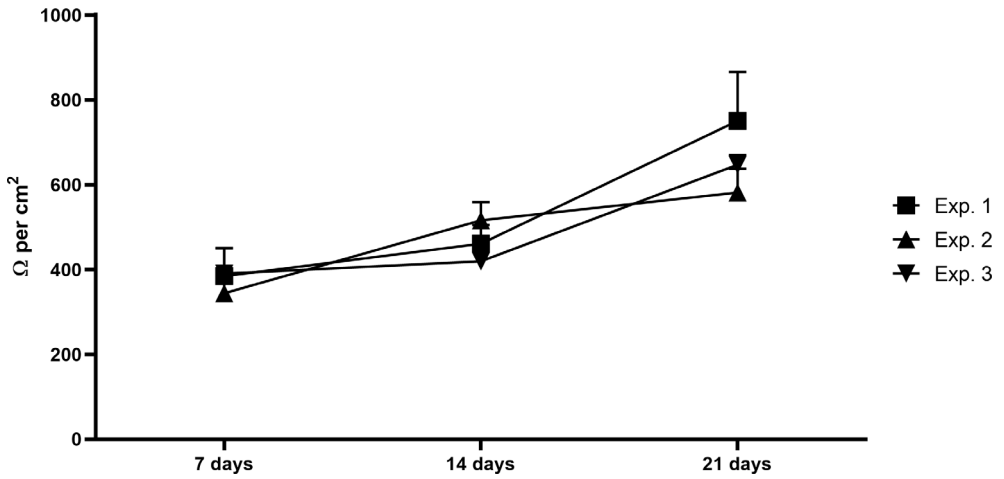

FIGURE 2
Intestinal barrier integrity. Graph shows the TEER values of the intestinal epithelial barrier composed by Caco-2 and HT29-MTX-E12 after 7, 14 and 21 days, confirming the cells growing and differentiation and the barrier stability. Exp, experiment; N= 3 independent experiments; every experiment corresponds to the mean of at least 10 different wells.

Geisser-Greenhouse correction and uncorrected Fisher's LSD was applied (information available for every figure legend).

3 Results

3.1 Establishment and assessment of intestinal epithelial barrier

Intestinal epithelial co-culture has been monitored up to 21 days after the beginning of the co-culture in terms of barrier integrity and stability, confirming the expected cell differentiation and barrier stability along the culture, reaching TEER values of 600-700 Ω per cm^2 at the end of the co-culture (Figure 2).

3.2 Baseline inflammatory conditions in THP-1 cells

Stimulated-THP-1 cells either with LPS (100 ng/mL), PMA (50, 75 or 100 nM) or 100 nM PMA in combination with LPS (100 ng/mL) produced concentrations of TNF-α significantly different

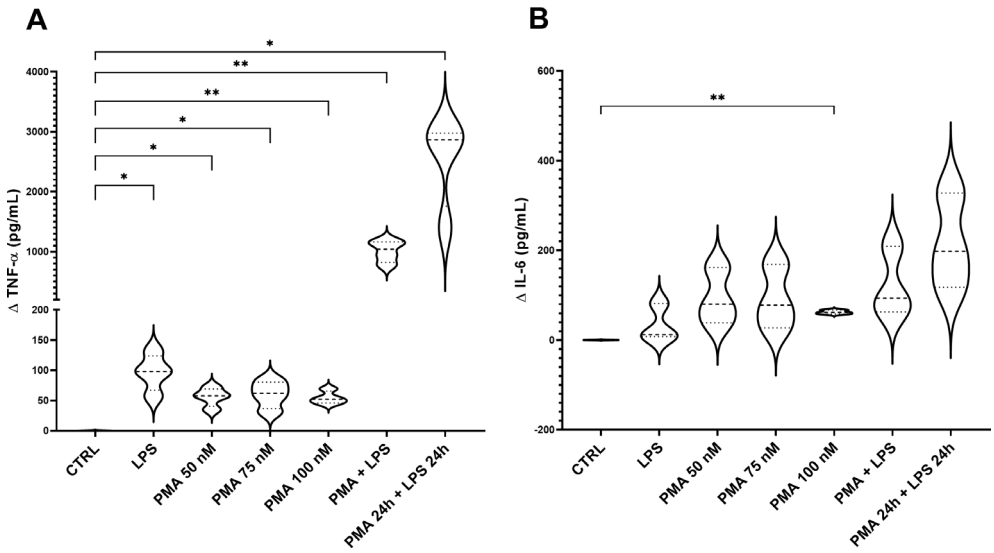

FIGURE 3
Concentration of TNF-α **(A)** and IL-6 **(B)** in the supernatant of stimulated-THP-1. The graph shows the delta values of TNF-α and IL-6 for each experimental group: THP-1 treated with LPS (100 ng/mL), PMA at different concentrations (50, 75, 100 nM), PMA + LPS (100 nM and 100 ng/mL, respectively) and PMA + LPS at the same concentrations but in a consecutive period (24 h + 24 h). CTRL: non-stimulated THP-1; PMA, phorbol-12-myristate-13-acetate; LPS, lipopolysaccharide. N=4. *p<0.05; **p<0.01, with respect to the CTRL group (one-way ANOVA, Dunnett's multiple comparisons test).

compared to the control group, and particularly higher for 100 nM PMA and the combo PMA+LPS (results represented as delta value, Figure 3A). Regarding IL-6, significantly higher concentrations were observed for 100 nM PMA group compared to control (Figure 3B). In conclusion, 100 nM PMA was identified as the best option simulating a mild-inflammatory status.

3.3 Inflammatory conditions in the 3C model

To decipher the best stimulation conditions of the 3C model, once assembled the whole model was treated with PMA (100 nM) or LPS (100 ng/mL), added to the basolateral compartment. Results showed that there was a significant increase in concentrations following both stressor incubations in terms of TNF-α production, especially pronounced for PMA treatment (Figure 4A), compared to control. Regarding IL-6 concentrations, significant results were observed in the LPS group compared to control, showing for the PMA group a not significantly increase in IL-6 production than control, but it is worth reporting the higher variability in the concentration range (Figure 4B).

3.4 Dose-concentration analysis of prednisolone and digesta enzymes evaluation

Among the different studied concentrations of prednisolone (5, 1, 0.5 and 0.25 μM), 1 μM stand out as the best concentration to be used, showing significant results in the reduction of TNF-α compared to control and an absolute reduction of IL-6 compared to control, although not statistically significant. Moreover, values for digesta no-food showed no differences with respect to the control group. Figure 5 shows the data obtained for NF at a specific concentration (100 μL per mL of supplemented-DMEM, as a representation of the concentration range studied (data not shown).

3.5 Selection and screening of the final cytokine pattern

Among the cytokines analyzed, TNF- α, IL-6, IL-12p70, IL-8 and IL-18 showed a significant increase when the model was stimulated with PMA at the selected concentrations, compared to the non-stimulated model. On the contrary, IL-1β, IFN-γ, CCL-20 and IL-23 showed no differences in terms of cytokines production (Figure 6).

3.6 Testing the 3C model in terms of cytokines production with a broccoli digesta

Broccoli digesta (dry-matter 9.67 g/L) were added to the 3C model and the production of TNF-α, IL-6, IL-12p70, IL-18 and IL-8 were assayed. Four concentrations of broccoli digesta were tested: BD4 (3.9 g/L), BD3 (1.9 g/L), BD2 (0.97 g/L) and BD1 (0.49 g/L). Significant differences were shown in TNF-α values with respect to the control group in all the BD concentrations, especially marked for BD4, BD3 and BD2 (Figure 7A), while IL-6 showed a significant reduction with BD4 and BD2 treatments compared to control (Figure 7B). Regarding IL-12p70, no significant differences were found for any food digesta (Figure 7C), while IL-18 showed a decrease with the lowest BD concentration (BD1), compared to the control group (Figure 7D). IL-8 showed a significant reduction with all the BD concentrations, particularly observed with the highest concentration (BD4) (Figure 7E).

3.7 Quantification of cell lysis after treatments by LDH assay

Quantification of cell lysis of intestinal epithelial cells after BD treatments showed similar values to those from the control group (stimulated with PMA but not treated with BD), obtaining a significant reduction in LDH release on BD4 and BD2 groups compared to control (Figure 8).

3.8 Analysis of ZO-1 expression on intestinal epithelial cells following broccoli digesta

ZO-1 protein from the tight junctions was significantly increased on the intestinal epithelial cells by treatment with BD at the lowest concentration (BD1) compared to the control group, with no differences regarding the NF or 1 μM prednisolone treatments and a slight increase for BD4 and BD2 groups (Figure 9).

4 Discussion

In this study we developed and tested a tri-culture *in vitro* model of mild-inflammatory status, that included intestinal and immune cells, and is aimed to study the pro-/anti-inflammatory effects of *in vitro* digested foods. To that, three different cell lines have been contemporary assembled to simulate the physical and biochemical interactions naturally occurring *in vivo* between enterocyte-like cells that constitute the intestinal barrier, mucus-producing goblet-like cells and immune cells that trigger the inflammatory response. Over the past years, the most common gut cell model mimicking the intestinal barrier have been characterized by the use of single intestinal epithelial cell lines as Caco-2, mostly for particles toxicity analysis (20), drugs absorption and metabolism studies (34). The system has been improved over the years with the inclusion of an immune cell line, commonly human or mice monocytes or macrophages cell lines, allowing to simulate or evaluate several inflammatory processes (19, 21, 22). The 3C strategy, even if technically challenging, allows to overcome the simplistic issues derived from the single-cell or two-cells approaches (35). Moreover, it includes a z-axis, enhancing

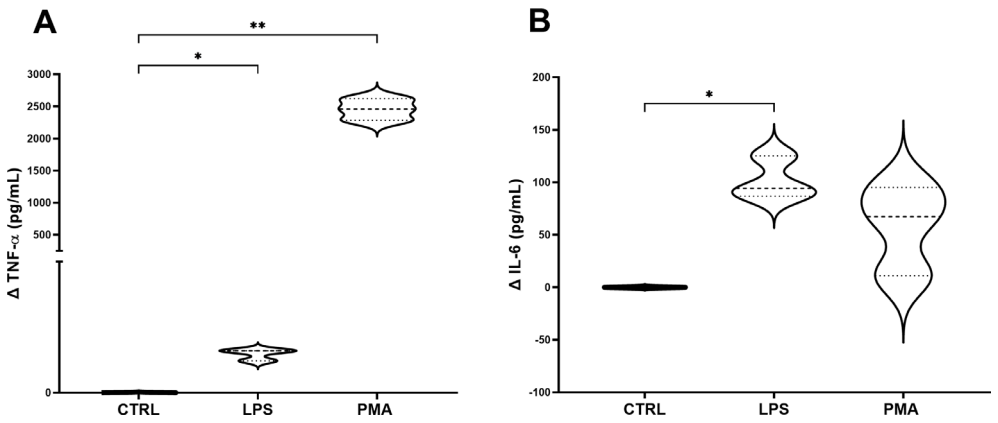

FIGURE 4
Concentration of TNF-α **(A)** and IL-6 **(B)** in the basolateral supernatant of the 3C model. Graphs show the delta values of TNF-α and IL-6 for each experimental group: non-stimulated 3C, 3C stimulated with LPS (100 ng/mL) and 3C stimulated with PMA (100 nM). CTRL: non-stimulated THP-1; PMA, phorbol-12-myristate-13-acetate; LPS, lipopolysaccharide. N=4. *p<0.05; **p<0.01, with respect to the CTRL group (one-way ANOVA, Dunnett's multiple comparisons test).

performance and showing cost-benefits and overall efficiency similar to 3D models, supporting the use of this model based on specific experimental requirements (36, 37).

As a first step, the intestinal epithelial barrier has been stablished by co-culturing the Caco-2 and HT29-MTX-E12 cells on Transwell inserts for up to 21 days, and assessed every 7 days (7, 14, 21 days) prior to the 3C assembly. Even if Caco-2 monolayers are a simple, cost-effective and rapid, reproducible tool to replicate the intestinal epithelial barrier, their use alone may cause an underestimation of some absorption processes, probably due to the lack of variety in the cell population with important roles (38). For instance, goblet cells – here represented by the HT29-MTX-E12 cell line – are the second most abundant population of cells in the intestinal epithelium, responsible for the mucus secretion that forms a layer covering the mucosal surface and acting as a physical barrier (39). Although Caco-2 and the mucus-producing goblet-like cells HT29-MTX-E12 co-culture should overcome some of the absorption problems associated, the main challenge described is the leak, since the co-culture may exhibit lower TEER values when increasing the HT29 cells proportion (40). To overcome this issue, in this study a 9:1 ratio (Caco-2: HT29-MTX-E12) has been used, simulating the proximal part of the intestine and ensuring a proper barrier permeability and mucus production, as supported by several researchers (41–46). Calculated TEER data were consistent with previously published data (40, 47), demonstrating that cells were correctly differentiated and the barrier was stable and intact.

To select the best inflammatory baseline conditions, the induction of a mild-inflammatory status by using multiple stressors at different concentrations has been attempted. A mild-inflammation has been preferred, instead of a high-inflammatory

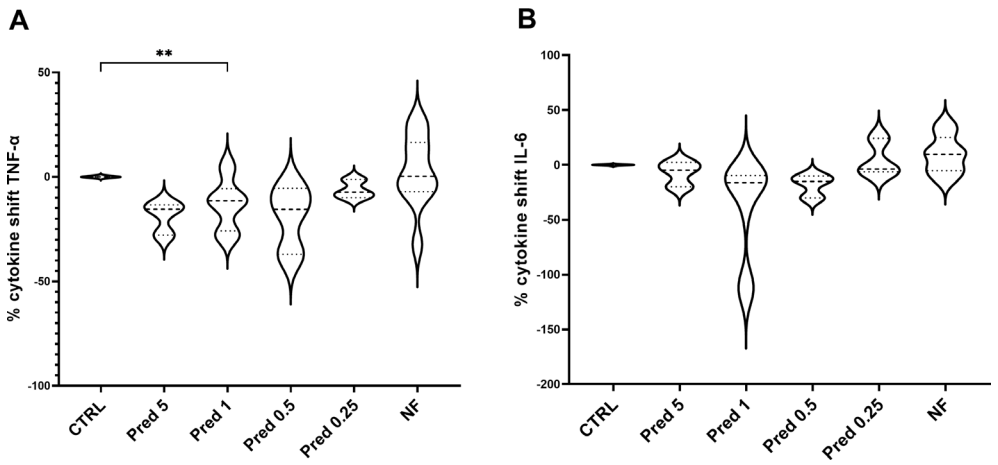

FIGURE 5
Dose-concentration of TNF-α **(A)** and IL-6 **(B)** following prednisolone and NF treatment. Graphs show the delta values of TNF-α and IL-6 for each experimental group: CTRL; prednisolone 5 μM, prednisolone 1 μM, prednisolone 0.5 μM, prednisolone 0.25 μM; digesta no food (NF) at 100 μL per mL. CTRL: PMA-stimulated THP-1; PMA, phorbol-12-myristate-13-acetate; N=3. **p<0.01, with respect to the CTRL group (one-way ANOVA, Dunnett's multiple comparisons test).

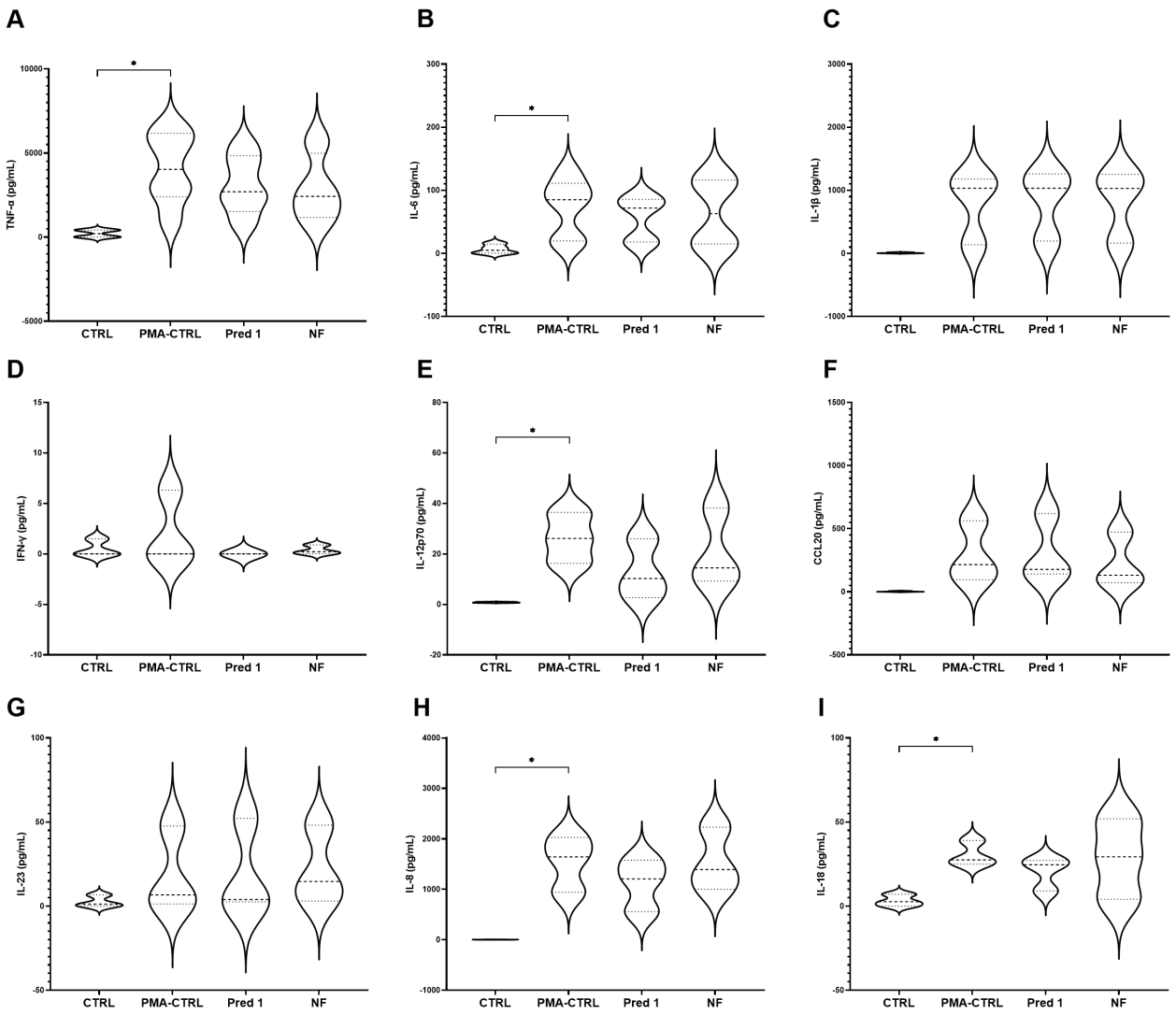

FIGURE 6
Cytokines production by the 3C model. Cytokines TNF-α **(A)**, IL-6 **(B)**, IL-1β **(C)**, IFN-γ **(D)**, IL-12p70 **(E)**, CCL20 **(F)**, IL-23 **(G)**, IL-8 **(H)**, IL-18 **(I)** production and comparison with ad without PMA stimulation. Graphs show the absolute concentration values for each experimental group: CTRL; prednisolone 5 μM, prednisolone 1 μM, prednisolone 0.5 μM, prednisolone 0.25 μM; digesta no food (NF) at 100 μL per mL. CTRL: non-stimulated THP-1; PMA-CTRL: 3C model stimulated with 100 nM PMA; Pred1: prednisolone 1 μM; NF, no-food digesta. PMA, phorbol-12-myristate-13-acetate. n=5 for TNF-α and IL-6; n=3 for the rest of the cytokines. *p<0.05, with respect to the CTRL group (one-way ANOVA, Dunnett's multiple comparisons test).

status, to induce a cytokine response able to be potentially modulated with the subsequent addition of food digesta thanks to their bioactive compounds. A first screening performed directly on THP-1 cells pointed out that 100 nM PMA stands out as the best option to induce a mild inflammatory status, stimulating THP-1 cells versus a macrophage phenotype, enabling their attachment to the surface and their shape modification, but without exceeding in the immune response in terms of TNF-α and IL-6 production. Then, the whole 3C model was assembled and stimulated both with LPS and PMA, at the concentrations previously tested. Supported by previous researchers (19, 48, 49), PMA addition to the basolateral compartment of the model has been selected as the best strategy to stimulate the immune cells and, in this specific environment, the whole intestinal model. PMA has been used at the concentration of 100 nM for 20 hours, inducing the release of a fair concentration of cytokines but reaching values in concordance with a mild-inflamed intestine, without reaching values that correlate with IBDs (50, 51), that may be reverted with a proper anti-inflammatory drug or food digesta. In fact, prednisolone has been used as an anti-inflammatory drug, frequently used for the treatment of IBDs such as Crohn disease thanks to its potential to normalize the intestinal permeability (52, 53). A glucocorticoid as prednisolone has been preferred instead of a non-steroidal anti-inflammatory drug due to their well-ascertained harmful effects on intestinal and gastric epithelial integrity (54, 55).

The extent and rate of nutrients absorption within the gastrointestinal tract, mainly by intestinal epithelial cells, depends on the digestion of the macronutrients and the generated products, with a considerable impact for the human physiological health (56). A key aspect of this study is the testing of food digesta instead of

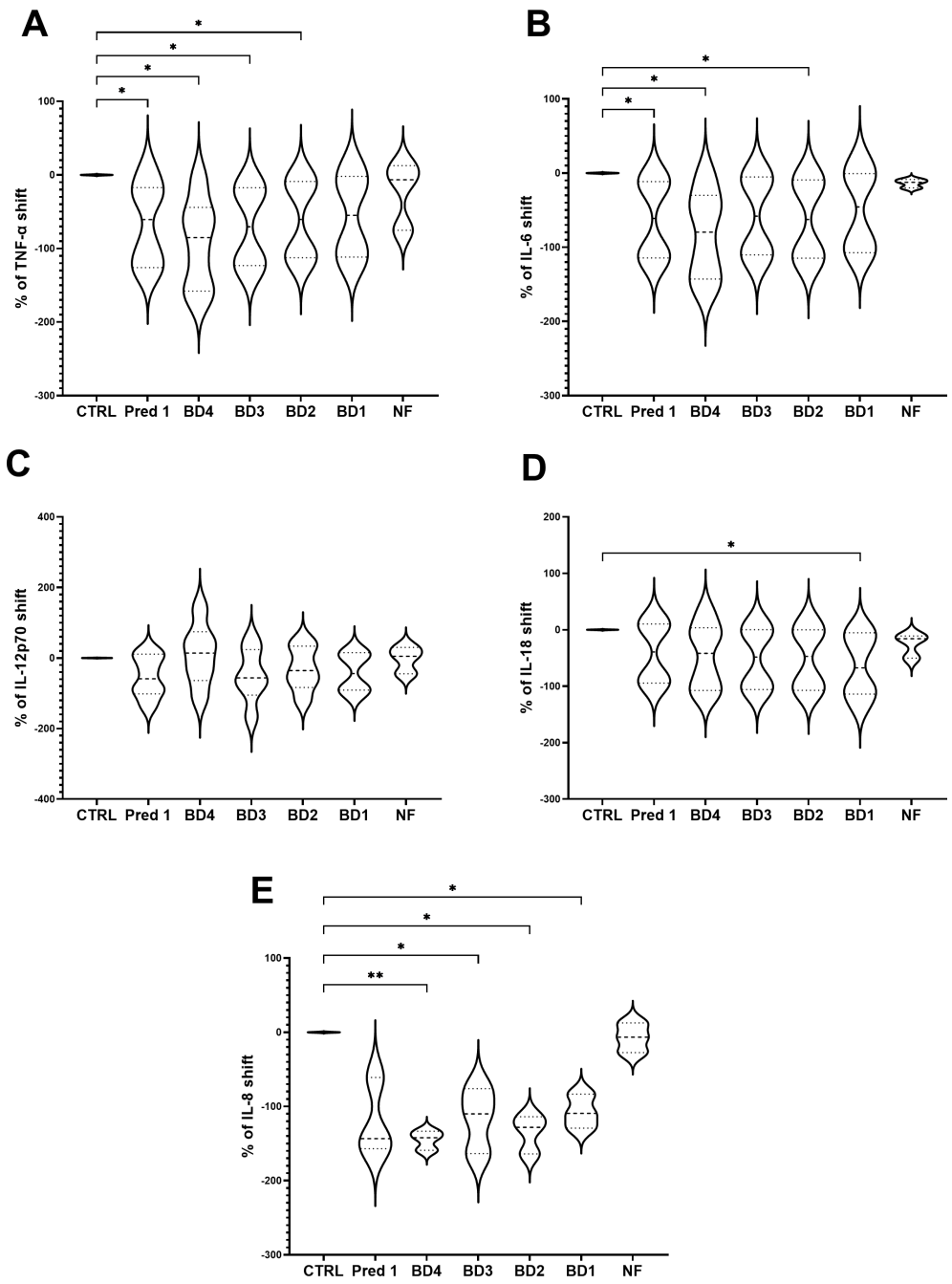

FIGURE 7
Cytokines shift following BD treatments. Graph shows the TNF-α **(A)**, IL-6 **(B)**, IL-12p70 **(C)**, IL-18 **(D)** and IL-8 **(E)** shifts following BD treatments to the PMA-stimulated 3C model. Results are expressed as cytokine shift with respect to the control group. Pred1: prednisolone 1μM; BD, broccoli digesta; NF, digesta no-food; PMA, phorbol-12-myristate-13-acetate. n=5. *p<0.05, **p<0.01, with respect to the control group (ANOVA with Geisser-Greenhouse correction and uncorrected Fisher's LSD).

classical food extracts, commonly used *in vitro* for food research. Indeed, a great number of research articles in this field is based on the study of a single component extracted (using water or organic solvents) or diluted in a standard solution (usually a commercial buffer) or even lyophilized, disregarding the rest of the potential components in real food. For this reason, static and dynamic INFOGEST digestion models (32) have acquired an increased importance to study the gastrointestinal events related to the assumption of several types of foods and beverages, including fish, meat, vegetables, cereals, dairy, and other protein and lipid sources commonly consumed. Even though the complex dynamic processes naturally occurring *in vivo* and the digestion variations among the population groups (infants, adults, elderlies) are not exactly reproducible *in vitro*, this method represents a relatively simple, inexpensive and rapid tool to produce a digesta fluid mimicking the real digestive sample facing the apical membrane of the gut bowel. As a first analysis, the potential effects of the digesta solution with no food but containing all the enzymes needed for the digesta

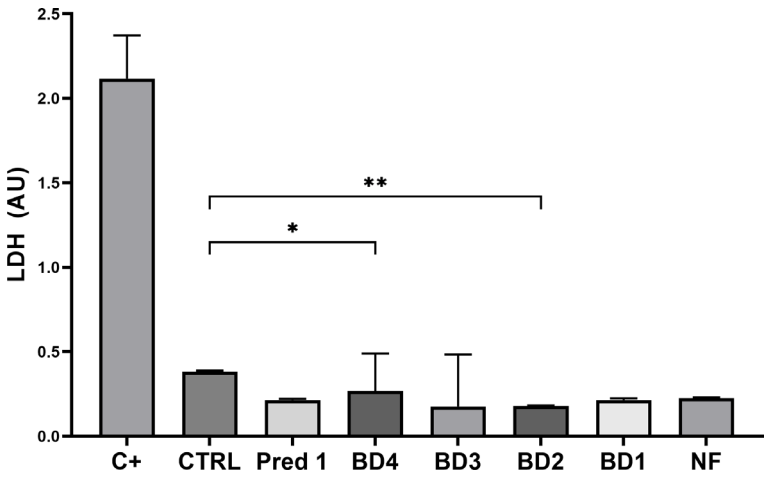

FIGURE 8
Quantification of cell lysis. Graph shows the concentration of LDH released by the intestinal epithelial cells from the apical compartment, compared to the control group. C+, positive control treated with 0.1% Triton x100; CTRL, control group; Pred1, prednisolone 1 μM; BD, broccoli digesta; NF, digesta no-food. LDH is expressed as arbitrary units (AU) following optical density measurement by spectrophotometry. Data are represented as Mean ± SD; n= 3 independent biological experiments; every independent experiment is the result of at least 4 technical replicates. *p<0.05; **p<0.01, with respect to the CTRL group (ANOVA, Friedman test).

process was tested on the model, finding no differences in terms of TNF-α and IL-6 production.

To test the 3C model response to foods, and in particular the pro-/anti-inflammatory potential of foods, a BD was selected. Broccoli has been selected due to the benefits associated with its consumption. Several clinical trials have been conducted to evaluate its effects on human and other animals' health (57–59), using either broccoli sprouts, powder supplementations or seed extracts (60, 61). Broccoli belongs to the cruciferous vegetables (CVs) of the Brassicaceae family, which have been widely studied for their anti-tumoral properties. Broccoli are a good source of vitamins, as C, E and K, as well as of bioactive compounds, including, as soluble and insoluble fibers, quercetin and kaempferol glycosides of flavonoids and a high content of glucosinolates, as glucoraphanin (4-methylsulphinylbutyl glucosinolate) and glucobrassicin (3-indolylmethyl glucosinolate). Among the hydrolysis byproducts known as isothiocyanates (ITC) (62–64) sulforaphane (SFN, 1-isothiocyanato-4-methylsulfinylbutane) stands out as the bioactive responsible for the anti-tumorigenic and anti-oxidant properties attributed to the CVs (60). SFN is a bioactive food component notably abundant especially in young broccoli sprouts, able to cause cell cycle arrest and apoptosis of cancer cells (65). Despite some limitations in its formation due to myrosinase enzyme activity as well as gut microbiota metabolism, *in vivo* studies have

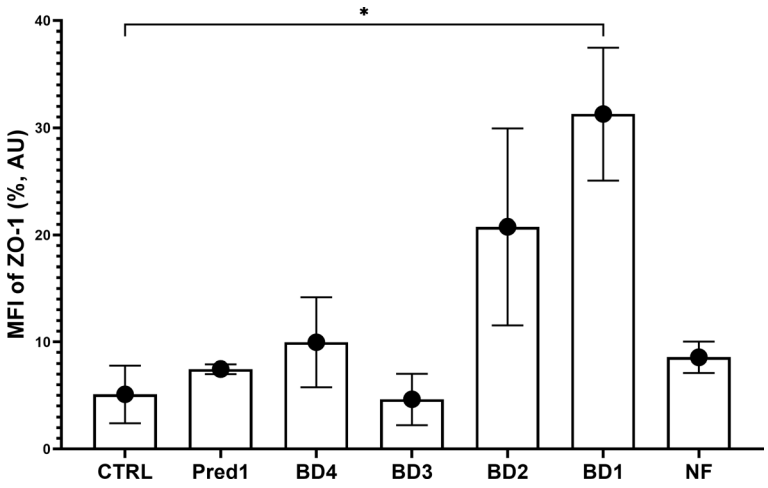

FIGURE 9
ZO-1 expression on the intestinal barrier. Graph shows the median fluorescence intensity of ZO-1 protein on the intestinal epithelial cells from each experimental group, compared to the control group. MFI, median fluorescence intensity; AU, arbitrary units; CTRL, control group; Pred1, prednisolone 1 μM; BD, broccoli digesta; NF, digesta no-food. Data are represented as Mean ± SD; n=3 independent experiments; *p<0.05 with respect to the CTRL group (Welch's ANOVA tests, Dunnett's T3 multiple comparisons test).

demonstrated how SFN reduces inflammatory markers and attenuate lipid peroxidation and oxidative stress in patients suffering from diabetes, improving fasting blood glucose levels and stabilizing insulin response (60, 66). *In vitro*, SFN inactivates the nuclear factor κβ (NF-kB) (67), which in turn downregulates the expression of pro-inflammatory cytokines production (68), attenuating the inflammatory response. Moreover, a recent study has shown that sulforaphane is able to change the growth of bacteria found in the gastrointestinal microbiota, altering some metabolites and producing anti-inflammatory molecules (69).

BD effects on the 3C have been evaluated in terms of cytotoxicity, intestinal barrier permeability and cytokine production. Cytokine analysis after BD treatments has confirmed the potential anti-inflammatory effects attributed to broccoli sprouts by several researchers (67, 68). In detail, BD strongly reduced the production of TNF-α, IL-6 and IL-8 from THP-1 cells after 4 hours of digesta treatment to the apical compartment of the system, in comparison with the control group and obtaining similar results to prednisolone. A reduction of pro-inflammatory cytokines has been described previously by other Authors, finding a downregulation of the release of TNF-α and IL-6 from LPS-stimulated human peripheral blood mononuclear cells (70) after treatments with extracts from broccoli sprouts, while Guo et al. found a reduction in IL-8 concentration after the treatment with an aqueous extract from broccoli seed in patients suffering from atrophic gastritis (71). Similar effects were described by Bessler and Djaldetti, attributing to SFN the ability to exert a concentration-dependent inhibitory effect on pro-inflammatory cytokines as TNF-α and IL-6 by PMBCs co-cultured with colon carcinoma cells (72). Regarding IL-18, a decreased concentration was found when treating with BD at the lowest concentration. IL-18 is released by monocytes to enhance intestinal inflammation upon NLRP3 inflammasome activation by Toll-like receptor 2 (TLR2), activated in turn by high-fat diets (73). IL-18 is implicated in several autoimmune diseases, as intestinal bowel diseases; however, its role in health and diseases is still not clear, with a growing number of studies supporting a protective role for IL-18 (74).

Through the last decades, individual factors as sex, age, body mass index (BMI), physical activity, smoke and certain dietary habits have been associated with the increase or decrease of specific cytokines. Although with controversial results (75), dietary patterns with high intakes of red meats, fried foods or processed ones have been generally associated with an increase of pro-inflammatory cytokines as TNF-α, IL-6 and IL-8, while diets rich in fruits and vegetables, with a high content of micronutrients, fiber and other bioactive components, i.e. polyphenols and glucosinolates, have been mostly associated with a decrease of pro-inflammatory cytokines and an increase of anti-inflammatory markers (76, 77).

As stated, BD treatments have been evaluated also in terms of cytotoxicity. LDH quantification assay has been performed to confirm the absence of toxicity for any of the concentrations used, using an indirect assay that measures, in a rapid and not expensive way, cell lysis without manipulating or damaging the cells (78). As observed, BD do not alter cells viability even at the higher concentrations.

Finally, to evaluate the barrier integrity and permeability after broccoli digesta treatments, the tight junction scaffolding protein zonula occludens-1 (ZO-1) was analyzed by flow cytometry by recovering the intestinal epithelial cells from the inserts after the experiments on the whole 3C model. ZO-1 is a member of the tight junctions system responsible for the cross-linking of its transmembrane proteins (as claudin and occludin) with the actin cytoskeleton (79). ZO-1 expression is downregulated in human and experimental inflammatory bowel disease, compromising mucosal repair and thus promoting disease progression (80). The results obtained in this study show an increase in ZO-1 protein in cells treated with the lowest BD concentration (BD1), highlighting the importance of the dose to achieve a desirable effect and the need for cellular markers to stablish an objective pro-/anti-inflammatory role for food digesta.

5 Conclusions

A reliable and promising 3C model to evaluate the pro-anti/inflammatory properties of digested foods after a process of *in vitro* digestion, mimicking a mild-inflammatory status, has been developed. Broccoli digesta was shown to modulate the release of pro-inflammatory cytokines and the tight junctions of the intestinal barrier by increasing the expression of the protein ZO-1. Although further digested foods should be tested and several additional cytokines may be investigated, the 3C model might be utilized for screening a wide array of food digesta to characterize the pro/anti-inflammatory effect of single foods, contributing to unravel the role of diet in modulating chronic inflammation.

Data availability statement

The raw data supporting the conclusions of this article will be made available by the authors, without undue reservation.

Ethics statement

Ethical approval was not required for the studies on humans in accordance with the local legislation and institutional requirements because only commercially available established cell lines were used.

Author contributions

MR-S: Conceptualization, Data curation, Formal Analysis, Funding acquisition, Investigation, Methodology, Project administration, Resources, Software, Supervision, Validation, Visualization, Writing – original draft, Writing – review & editing. CB-T: Data curation, Investigation, Methodology, Visualization, Writing – review & editing. VD: Conceptualization, Formal Analysis, Investigation, Methodology, Validation, Writing – review & editing. EC: Formal Analysis, Investigation, Methodology, Visualization, Writing – review & editing. AK: Conceptualization, Formal Analysis, Methodology, Supervision, Validation, Writing – review & editing. RS: Methodology, Resources, Validation, Writing –

review & editing. MS: Conceptualization, Formal Analysis, Funding acquisition, Project administration, Resources, Supervision, Validation, Writing – review & editing. DA: Conceptualization, Funding acquisition, Project administration, Resources, Supervision, Validation, Writing – review & editing.

Funding

The author(s) declare financial support was received for the research, authorship, and/or publication of this article. This research was funded by the European Union – Next Generation EU. Project Code: ECS00000041; Project CUP: C43C22000380007; Project Title: Innovation, digitalization and sustainability for the diffused economy in Central Italy – VITALITY. The IUF is funded by the federal and state governments – the Ministry of Culture and Science of North Rhine-Westphalia (MKW) and the Federal Ministry of Education and Research (BMBF).

Acknowledgments

Authors gratefully acknowledge Prof. Cristian Del Bo', from the *Università degli Studi di Milano*, for his help regarding Caco-2 and THP-1 cell lines.

Conflict of interest

The authors declare that the research was conducted in the absence of any commercial or financial relationships that could be construed as a potential conflict of interest.

The author(s) declared that they were an editorial board member of Frontiers, at the time of submission. This had no impact on the peer review process and the final decision.

Generative AI statement

The author(s) declare that no Generative AI was used in the creation of this manuscript.

Publisher's note

References

1. Abbafati C, Abbas KM, Abbasi-Kangevari M, Abd-Allah F, Abdelalim A, Abdollahi M, et al. Global burden of 87 risk factors in 204 countries and territories, 1990–2019: a systematic analysis for the Global Burden of Disease Study 2019. *Lancet*. (2020) 396:1223–49. doi: 10.1016/S0140-6736(20)30752-2

2. Afshin A, Sur PJ, Fay KA, Cornaby L, Ferrara G, Salama JS, et al. Health effects of dietary risks in 195 countries, 1990–2017: a systematic analysis for the Global Burden of Disease Study 2017. *Lancet*. (2019) 393:1958–72. doi: 10.1016/S0140-6736(19)30041-8

3. Hotamisligil GS. Inflammation, metaflammation and immunometabolic disorders. *Nature*. (2017) 542:177–85. doi: 10.1038/NATURE21363

4. Adolph TE, Meyer M, Schwärzler J, Mayr L, Grabherr F, Tilg H. The metabolic nature of inflammatory bowel diseases. *Nat Rev Gastroenterol Hepatol*. (2022) 19:753–67. doi: 10.1038/S41575-022-00658-Y

5. Gonçalves P, Magro F, Martel F. Metabolic inflammation in inflammatory bowel disease: crosstalk between adipose tissue and bowel. *Inflammation Bowel Dis*. (2015) 21:453–67. doi: 10.1097/MIB.0000000000000209

6. Bernardo D, Marin AC, Fernández-Tomé S, Montalban-Arques A, Carrasco A, Tristán E, et al. Human intestinal pro-inflammatory CD11chighCCR2+CX3CR1+ macrophages, but not their tolerogenic CD11c–CCR2–CX3CR1– counterparts, are expanded in inflammatory bowel disease. *Mucosal Immunol*. (2018) 11:1114–26. doi: 10.1038/S41385-018-0030-7

7. Michaels M, Madsen KL. Immunometabolism and microbial metabolites at the gut barrier: Lessons for therapeutic intervention in inflammatory bowel disease. *Mucosal Immunol*. (2023) 16:72–85. doi: 10.1016/J.MUCIMM.2022.11.001

8. Levy RL, Linde JA, Feld KA, Crowell MD, Jeffery RW. The association of gastrointestinal symptoms with weight, diet, and exercise in weight-loss program participants. *Clin Gastroenterol Hepatol*. (2005) 3:992–6. doi: 10.1016/S1542-3565(05)00696-8

9. John BJ, Irukulla S, Abulafi AM, Kumar D, Mendall MA. Systematic review: adipose tissue, obesity and gastrointestinal diseases. *Aliment Pharmacol Ther*. (2006) 23:1511–23. doi: 10.1111/J.1365-2036.2006.02915.X

10. Verdugo-Meza A, Ye J, Dadlani H, Ghosh S, Gibson DL. Connecting the dots between inflammatory bowel disease and metabolic syndrome: A focus on gut-derived metabolites. *Nutrients*. (2020) 12(5):1434. doi: 10.3390/NU12051434

11. Lopez-Candales A, Burgos PMH, Hernandez-Suarez DF, Harris D. Linking chronic inflammation with cardiovascular disease: from normal aging to the metabolic syndrome. *J Nat Sci*. (2017) 3(4):e341.

12. Itsiopoulos C, Mayr HL, Thomas CJ. The anti-inflammatory effects of a Mediterranean diet: a review. *Curr Opin Clin Nutr Metab Care*. (2022) 25:415–22. doi: 10.1097/MCO.0000000000000872

13. Galland L. Diet and inflammation. *Nutr Clin Pract*. (2010) 25:634–40. doi: 10.1177/0884533610385703

14. Rees K, Takeda A, Martin N, Ellis L, Wijesekara D, Vepa A, et al. Mediterranean-style diet for the primary and secondary prevention of cardiovascular disease. *Cochrane Database Syst Rev*. (2019) 2019(3):CD009825. doi: 10.1002/14651858.CD009825.pub3

15. Dinu M, Pagliai G, Angelino D, Rosi A, Dall'Asta M, Bresciani L, et al. Effects of popular diets on anthropometric and cardiometabolic parameters: an umbrella review of meta-analyses of randomized controlled trials. *Adv Nutr*. (2020) 11:815–33. doi: 10.1093/ADVANCES/NMAA006

16. Ding X, Hu X, Chen Y, Xie J, Ying M, Wang Y, et al. Differentiated Caco-2 cell models in food-intestine interaction study: Current applications and future trends. *Trends Food Sci Technol*. (2021) 107:455–65. doi: 10.1016/J.TIFS.2020.11.015

17. Zhang R, Zhang Q, Ma LQ, Cui X. Effects of food constituents on absorption and bioaccessibility of dietary synthetic phenolic antioxidant by caco-2 cells. *J Agric Food Chem*. (2020) 68:4670–7. doi: 10.1021/ACS.JAFC.9B07315/SUPPL_FILE/JF9B07315_SI_001.PDF

18. Costa J, Ahluwalia A. Advances and current challenges in intestinal *in vitro* model engineering: A digest. *Front Bioeng Biotechnol*. (2019) 7:144. doi: 10.3389/FBIOE.2019.00144

19. Kämpfer AAM, Urbán P, Gioria S, Kanase N, Stone V, Kinsner-Ovaskainen A. Development of an *in vitro* co-culture model to mimic the human intestine in healthy and diseased state. *Toxicol In Vitro*. (2017) 45:31–43. doi: 10.1016/J.TIV.2017.08.011

20. Paul MB, Schlief M, Daher H, Braeuning A, Sieg H, Böhmert L. A human Caco-2-based co-culture model of the inflamed intestinal mucosa for particle toxicity studies. *In Vitro Models*. (2023) 2:43–64. doi: 10.1007/S44164-023-00047-Y

21. Belaid M, Javorovic J, Pastorin G, Vllasaliu D. Development of an *in vitro* co-culture model using Caco-2 and J774A.1 cells to mimic intestinal inflammation. *Eur J Pharmaceutics Biopharmaceutics*. (2024) 197:114243. doi: 10.1016/J.EJPB.2024.114243

22. Marzorati M, Van den Abbeele P, Verstrepen L, De Medts J, Ekmay RD. The response of a leaky gut cell culture model (Caco-2/THP-1 co-culture) to administration of alternative protein sources. *Nutraceuticals*. (2023) 3:175–84. doi: 10.3390/NUTRACEUTICALS3010013

23. Le NPK, Altenburger MJ, Lamy E. Development of an inflammation-triggered *in vitro* "Leaky gut" Model using caco-2/HT29-MTX-E12 combined with macrophage-like THP-1 cells or primary human-derived macrophages. *Int J Mol Sci*. (2023) 24:7427. doi: 10.3390/IJMS24087427/S1

24. Kämpfer AAM, Busch M, Büttner V, Bredeck G, Stahlmecke B, Hellack B, et al. Model complexity as determining factor for *in vitro* nanosafety studies: effects of silver and titanium dioxide nanomaterials in intestinal models. *Small*. (2021) 17:2004223. doi: 10.1002/SMLL.202004223

25. Marescotti D, Lo Sasso G, Guerrera D, Renggli K, Ruiz Castro PA, Piault R, et al. Development of an advanced multicellular intestinal model for assessing immunomodulatory properties of anti-inflammatory compounds. *Front Pharmacol*. (2021) 12:639716. doi: 10.3389/FPHAR.2021.639716

26. Kämpfer AAM, Shah U-K, Chu SL, Busch M, Büttner V, He R, et al. Interlaboratory comparison of an intestinal triple culture to confirm transferability and reproducibility. *In Vitro Models*. (2022) 2:89–97. doi: 10.1007/S44164-022-00025-W

27. Busch M, Kämpfer AAM, Schins RPF. An inverted *in vitro* triple culture model of the healthy and inflamed intestine: Adverse effects of polyethylene particles. *Chemosphere*. (2021) 284:131345. doi: 10.1016/J.CHEMOSPHERE.2021.131345

28. Glei M, Matuschek M, Steiner C, Böhm V, Persin C, Pool-Zobel BL. Initial *in vitro* toxicity testing of functional foods rich in catechins and anthocyanins in human cells. *Toxicol Vitro*. (2003) 17:723–9. doi: 10.1016/S0887-2333(03)00099-7

29. Iftikhar M, Iftikhar A, Zhang H, Gong L, Wang J. Transport, metabolism and remedial potential of functional food extracts (FFEs) in Caco-2 cells monolayer: A review. *Food Res Int*. (2020) 136:109240. doi: 10.1016/J.FOODRES.2020.109240

30. Ponce-de-León-Rodríguez-M-del C, Guyot JP, Laurent-Babot C. Intestinal *in vitro* cell culture models and their potential to study the effect of food components on intestinal inflammation. *Crit Rev Food Sci Nutr*. (2019) 59:3648–66. doi: 10.1080/10408398.2018.1506734

31. A.O.A.C. Official methods of analysis, in: *Association of Official Analytical Chemist* (1990). Washington DC: References - Scientific Research Publishing. Available online at: https://www.scirp.org/reference/ReferencesPapers?ReferenceID=1929875 (Accessed May 29, 2024).

32. Brodkorb A, Egger L, Alminger M, Alvito P, Assunção R, Ballance S, et al. INFOGEST static *in vitro* simulation of gastrointestinal food digestion. *Nat Protoc*. (2019) 14:991–1014. doi: 10.1038/S41596-018-0119-1

33. Chen G, Xie M, Wan P, Chen D, Ye H, Chen L, et al. Digestion under saliva, simulated gastric and small intestinal conditions and fermentation *in vitro* by human intestinal microbiota of polysaccharides from Fuzhuan brick tea. *Food Chem*. (2017) 244:331-9. doi: 10.1016/j.foodchem.2017.10.074

34. Fedi A, Vitale C, Ponschin G, Ayehunie S, Fato M, Scaglione S. *In vitro* models replicating the human intestinal epithelium for absorption and metabolism studies: A systematic review. *J Controlled Release*. (2021) 335:247–68. doi: 10.1016/J.JCONREL.2021.05.028

35. Haddad MJ, Sztupecki W, Delayre-Orthez C, Rhazi L, Barbezier N, Depeint F, et al. Complexification of *in vitro* models of intestinal barriers, A true challenge for a more accurate alternative approach. *Int J Mol Sci*. (2023) 24(4):3595. doi: 10.3390/IJMS24043595

36. Liu Y, Chen YG. 2D- and 3D-based intestinal stem cell cultures for personalized medicine. *Cells*. (2018) 7:225. doi: 10.3390/CELLS7120225

37. Roh TT, Chen Y, Paul HT, Guo C, Kaplan DL. 3D bioengineered tissue model of the large intestine to study inflammatory bowel disease. *Biomaterials*. (2019) 225:119517. doi: 10.1016/J.BIOMATERIALS.2019.119517

38. Bischoff SC, Barbara G, Buurman W, Ockhuizen T, Schulzke JD, Serino M, et al. Intestinal permeability - a new target for disease prevention and therapy. *BMC Gastroenterol*. (2014) 14:1–25. doi: 10.1186/S12876-014-0189-7/TABLES/8

39. Johansson MEV, Sjövall H, Hansson GC. The gastrointestinal mucus system in health and disease. *Nat Rev Gastroenterol Hepatol*. (2013) 10:352–61. doi: 10.1038/nrgastro.2013.35

40. Cheng Y, Watanabe C, Ando Y, Kitaoka S, Egawa Y, Takashima T, et al. Caco-2 cell sheet partially laminated with HT29-MTX cells as a novel *in vitro* model of gut epithelium drug permeability. *Pharmaceutics*. (2023) 15:2338. doi: 10.3390/PHARMACEUTICS15092338

41. Pan F, Han L, Zhang Y, Yu Y, Liu J. Optimization of Caco-2 and HT29 co-culture *in vitro* cell models for permeability studies. *Int J Food Sci Nutr*. (2015) 66:680–5. doi: 10.3109/09637486.2015.1077792

42. Mahler GJ, Shuler ML, Glahn RP. Characterization of Caco-2 and HT29-MTX cocultures in an *in vitro* digestion/cell culture model used to predict iron bioavailability. *J Nutr Biochem*. (2009) 20:494–502. doi: 10.1016/J.JNUTBIO.2008.05.006

43. Jochems PGM, Garssen J, Van Keulen AM, Masereeuw R, Jeurink PV. Evaluating human intestinal cell lines for studying dietary protein absorption. *Nutrients*. (2018) 10:322. doi: 10.3390/NU10030322

44. Huang X, Gao Y, Li S, Wu C, Wang J, Zheng N. Modulation of mucin (MUC2, MUC5AC and MUC5B) mRNA expression and protein production and secretion in caco-2/HT29-MTX co-cultures following exposure to individual and combined aflatoxin M1 and ochratoxin A. *Toxins (Basel)*. (2019) 11:132. doi: 10.3390/TOXINS11020132

45. Busch M, Ramachandran H, Wahle T, Rossi A, Schins RPF. Investigating the role of the NLRP3 inflammasome pathway in acute intestinal inflammation: use of THP-1 knockout cell lines in an advanced triple culture model. *Front Immunol*. (2022) 13:898039/BIBTEX. doi: 10.3389/FIMMU.2022.898039/BIBTEX

46. Bredeck G, Kämpfer AAM, Sofranko A, Wahle T, Büttner V, Albrecht C, et al. Ingested engineered nanomaterials affect the expression of mucin genes—an *in vitro-in vivo* comparison. *Nanomaterials*. (2021) 11:2621. doi: 10.3390/NANO11102621/S1

47. Béduneau A, Tempesta C, Fimbel S, Pellequer Y, Jannin V, Demarne F, et al. A tunable Caco-2/HT29-MTX co-culture model mimicking variable permeabilities of the human intestine obtained by an original seeding procedure. *Eur J Pharmaceutics Biopharmaceutics*. (2014) 87:290–8. doi: 10.1016/J.EJPB.2014.03.017

48. Genin M, Clement F, Fattaccioli A, Raes M, Michiels C. M1 and M2 macrophages derived from THP-1 cells differentially modulate the response of cancer cells to etoposide. *BMC Cancer*. (2015) 15:1–14. doi: 10.1186/S12885-015-1546-9/FIGURES/10

49. Tedesco S, De Majo F, Kim J, Trenti A, Trevisi L, Fadini GP, et al. Convenience versus biological significance: are PMA-differentiated THP-1 cells a reliable substitute for blood-derived macrophages when studying *in vitro* polarization? *Front Pharmacol*. (2018) 9:71. doi: 10.3389/FPHAR.2018.00071

50. Singh UP, Singh NP, Murphy EA, Price RL, Fayad R, Nagarkatti M, et al. Chemokine and cytokine levels in inflammatory bowel disease patients. *Cytokine*. (2015) 77:44. doi: 10.1016/J.CYTO.2015.10.008

51. Al Qteishat A, Kirov K, Bokov D. The profile of the key pro-inflammatory cytokines in the serum of patients with CD and their association with the disease severity and activity. *BMC Gastroenterol*. (2022) 22:1–8. doi: 10.1186/S12876-022-02562-W/FIGURES/5

52. Boivin MA, Ye D, Kennedy JC, Al-Sadi R, Shepela C, Ma TY. Mechanism of glucocorticoid regulation of the intestinal tight junction barrier. *Am J Physiol Gastrointest Liver Physiol*. (2007) 292(2):G590-8. doi: 10.1152/AJPGI.00252.2006

53. Xu P, Elizalde M, Masclee A, Pierik M, Jonkers D. Corticosteroid enhances epithelial barrier function in intestinal organoids derived from patients with Crohn's disease. *J Mol Med (Berl)*. (2021) 99:805–15. doi: 10.1007/S00109-021-02045-7

54. d'Angelo M, Brandolini L, Catanesi M, Castelli V, Giorgio C, Alfonsetti M, et al. Differential effects of nonsteroidal anti-inflammatory drugs in an *in vitro* model of human leaky gut. *Cells*. (2023) 12:728. doi: 10.3390/CELLS12050728/S1

55. Zhang M, Xia F, Xia S, Zhou W, Zhang Y, Han X, et al. NSAID-associated small intestinal injury: an overview from animal model development to pathogenesis, treatment, and prevention. *Front Pharmacol*. (2022) 13:818877. doi: 10.3389/FPHAR.2022.818877

56. Zhou H, Tan Y, McClements DJ. Applications of the INFOGEST *in vitro* digestion model to foods: A review. *Annu Rev Food Sci Technol*. (2023) 14:135–56. doi: 10.1146/ANNUREV-FOOD-060721-012235/CITE/REFWORKS

57. Riso P, Vendrame S, Del Bo' C, Martini D, Martinetti A, Seregni E, et al. Effect of 10-day broccoli consumption on inflammatory status of young healthy smokers. *Int J Food Sci Nutr*. (2014) 65:106–11. doi: 10.3109/09637486.2013.830084

58. López-Chillón MT, Carazo-Díaz C, Prieto-Merino D, Zafrilla P, Moreno DA, Villaño D. Effects of long-term consumption of broccoli sprouts on inflammatory markers in overweight subjects. *Clin Nutr*. (2019) 38:745–52. doi: 10.1016/J.CLNU.2018.03.006

59. Marino M, Martini D, Venturi S, Tucci M, Porrini M, Riso P, et al. An overview of registered clinical trials on glucosinolates and human health: the current situation. *Front Nutr*. (2021) 8:730906. doi: 10.3389/FNUT.2021.730906

60. Mirmiran P, Bahadoran Z, Hosseinpanah F, Keyzad A, Azizi F. Effects of broccoli sprout with high sulforaphane concentration on inflammatory markers in type 2 diabetic patients: A randomized double-blind placebo-controlled clinical trial. *J Funct Foods*. (2012) 4:837–41. doi: 10.1016/J.JFF.2012.05.012

61. Fields NJ, Palmer KR, Rolnik DL, Yo J, Nold MF, Giles ML, et al. CO-sprout—A pilot double-blinded placebo-controlled randomised trial of broccoli sprout powder supplementation for pregnant women with COVID-19 on the duration of COVID-19-associated symptoms: study protocol. *Nutrients*. (2023) 15:3980. doi: 10.3390/NU15183980

62. Jeffery EH, Araya M. Physiological effects of broccoli consumption. *Phytochem Rev*. (2009) 8:283–98. doi: 10.1007/S11101-008-9106-4

63. Wu QJ, Xie L, Zheng W, Vogtmann E, Li HL, Yang G, et al. Cruciferous vegetables consumption and the risk of female lung cancer: a prospective study and a meta-analysis. *Ann Oncol*. (2013) 24:1918. doi: 10.1093/ANNONC/MDT119

64. Angelino D, Jeffery E. Glucosinolate hydrolysis and bioavailability of resulting isothiocyanates: Focus on glucoraphanin. *J Funct Foods*. (2014) 7:67–76. doi: 10.1016/J.JFF.2013.09.029

65. Su X, Jiang X, Meng L, Dong X, Shen Y, Xin Y. Anticancer activity of sulforaphane: the epigenetic mechanisms and the nrf2 signaling pathway. *Oxid Med Cell Longev*. (2018) 2018:5438179. doi: 10.1155/2018/5438179

66. Bahadoran Z, Mirmiran P, Hosseinpanah F, Hedayati M, Hosseinpour-Niazi S, Azizi F. Broccoli sprouts reduce oxidative stress in type 2 diabetes: A randomized double-blind clinical trial. *Eur J Clin Nutr*. (2011) 65:972–7. doi: 10.1038/ejcn.2011.59

67. Heiss E, Herhaus C, Klimo K, Bartsch H, Gerhäuser C. Nuclear factor κB is a molecular target for sulforaphane-mediated anti-inflammatory mechanisms. *J Biol*

Chem. (2001) 276:32008–15. doi: 10.1074/JBC.M104794200/ASSET/F291A24C-DA93-41A9-BF8D-43809A678B7E/MAIN.ASSETS/GR12.JPG

68. Ritz SA, Wan J, Diaz-Sanchez D. Sulforaphane-stimulated phase II enzyme induction inhibits cytokine production by airway epithelial cells stimulated with diesel extract. *Am J Physiol Lung Cell Mol Physiol*. (2007) 292:33–9. doi: 10.1152/AJPLUNG.00170.2006/ASSET/IMAGES/LARGE/ZH50010647190005.JPEG

69. Marshall SA, Young RB, Lewis JM, Rutten EL, Gould J, Barlow CK, et al. The broccoli-derived antioxidant sulforaphane changes the growth of gastrointestinal microbiota, allowing for the production of anti-inflammatory metabolites. *J Funct Foods*. (2023) 107:105645. doi: 10.1016/J.JFF.2023.105645

70. Olszewska MA, Granica S, Kolodziejczyk-Czepas J, Magiera A, Czerwinska ME, Nowak P, et al. Variability of sinapic acid derivatives during germination and their contribution to antioxidant and anti-inflammatory effects of broccoli sprouts on human plasma and human peripheral blood mononuclear cells. *Food Funct*. (2020) 11:7231–44. doi: 10.1039/D0FO01387K

71. Guo K, Wang L, Mahe J, Li L, Jiao S, Wang H, et al. Effect of aqueous extract of seed of broccoli on inflammatory cytokines and Helicobacter pylori infection: a randomized, double-blind, controlled trial in patients without atrophic gastritis. *Inflammopharmacology*. (2022) 30:1659–68. doi: 10.1007/S10787-022-01030-X

72. Bessler H, Djaldetti M. Broccoli and human health: immunomodulatory effect of sulforaphane in a model of colon cancer. *Int J Food Sci Nutr*. (2018) 69:946–53. doi: 10.1080/09637486.2018.1439901

73. Dang Y, Ma C, Chen K, Chen Y, Jiang M, Hu K, et al. The effects of a high-fat diet on inflammatory bowel disease. *Biomolecules*. (2023) 13:905. doi: 10.3390/BIOM13060905

74. Dinarello CA, Novick D, Kim S, Kaplanski G. Interleukin-18 and IL-18 binding protein. *Front Immunol*. (2013) 4:289/BIBTEX. doi: 10.3389/FIMMU.2013.00289/BIBTEX

75. D'Esposito V, Di Tolla MF, Lecce M, Cavalli F, Libutti M, Misso S, et al. Lifestyle and dietary habits affect plasma levels of specific cytokines in healthy subjects. *Front Nutr*. (2022) 9:913176/FULL. doi: 10.3389/FNUT.2022.913176/FULL

76. Hosseini B, Berthon BS, Saedisomeolia A, Starkey MR, Collison A, Wark PAB, et al. Effects of fruit and vegetable consumption on inflammatory biomarkers and immune cell populations: a systematic literature review and meta-analysis. *Am J Clin Nutr*. (2018) 108:136–55. doi: 10.1093/AJCN/NQY082

77. Deledda A, Annunziata G, Tenore GC, Palmas V, Manzin A, Velluzzi F. Diet-derived antioxidants and their role in inflammation, obesity and gut microbiota modulation. *Antioxidants*. (2021) 10:708. doi: 10.3390/ANTIOX10050708

78. Smith SM, Wunder MB, Norris DA, Shellman YG. A simple protocol for using a LDH-based cytotoxicity assay to assess the effects of death and growth inhibition at the same time. *PloS One*. (2011) 6:e26908. doi: 10.1371/JOURNAL.PONE.0026908

79. Veres-Székely A, Szász C, Pap D, Szebeni B, Bokrossy P, Vannay Á. Zonulin as a potential therapeutic target in microbiota-gut-brain axis disorders: encouraging results and emerging questions. *Int J Mol Sci*. (2023) 24:7548. doi: 10.3390/IJMS24087548

80. Kuo WT, Zuo L, Odenwald MA, Madha S, Singh G, Gurniak CB, et al. The tight junction protein ZO-1 is dispensable for barrier function but critical for effective mucosal repair. *Gastroenterology*. (2021) 161:1924–39. doi: 10.1053/J.GASTRO.2021.08.047

frontiers | Frontiers in Nutrition

TYPE Conceptual Analysis
PUBLISHED 12 February 2025
DOI 10.3389/fnut.2025.1508767

OPEN ACCESS

EDITED BY
Helena Sá,
Unidade Local de Saúde de Coimbra, Portugal

REVIEWED BY
Michael Kogut,
United States Department of Agriculture, United States
Naheed Aryaeian,
Iran University of Medical Sciences, Iran
Heather Shannon Smallwood,
University of Tennessee Health Sciences Center, United States

*CORRESPONDENCE
Edmund K. LeGrand
✉ elegrand@utk.edu;
✉ edmundlegrand@gmail.com

RECEIVED 09 October 2024
ACCEPTED 31 January 2025
PUBLISHED 12 February 2025

CITATION
LeGrand EK (2025) Beyond nutritional immunity: immune-stressing challenges basic paradigms of immunometabolism and immunology.
Front. Nutr. 12:1508767.
doi: 10.3389/fnut.2025.1508767

Beyond nutritional immunity: immune-stressing challenges basic paradigms of immunometabolism and immunology

Edmund K. LeGrand*

Biomedical and Diagnostic Sciences, College of Veterinary Medicine, University of Tennessee, Knoxville, TN, United States

Pathogens have the well-known advantage of rapid evolution due to short generation times and large populations. However, pathogens have the rarely noted disadvantage of the vulnerability to stress involved in proliferation as well as being localized. Presented here are numerous new paradigms in immunology, and especially immunometabolism, which are derived from examining how hosts capitalize on pathogen vulnerabilities to stress. Universally, proliferation requires both resources and synthesis, which are vulnerable to resource-limiting stress and damaging/noxious stress, respectively. Pathogens are particularly vulnerable to stress at the time when they are most threatening—when they are proliferating. Since immune cells actively controlling pathogens (effector cells) typically do not proliferate at infected sites, there is a "stress vulnerability gap" wherein proliferating pathogens are more vulnerable to any type of stress than are the attacking effector cells. Hosts actively stress vulnerable proliferating pathogens by restricting resources (resource-limiting stress) and generating noxious waste products (damaging/disruptive stress) in a fundamental defense here-in termed "immune-stressing." While nutritional immunity emphasizes denying pathogens micronutrients, immune-stressing extends the concept to restricting all resources, especially glucose and oxygen, coupled with the generation of noxious metabolic products such as lactic acid, reactive oxygen species (ROS), and heat to further harm or stress the pathogens. At present much of the field of immunometabolism centers on how nutrition and metabolism regulate immune function, a central feature being the inefficient use of glucose via aerobic glycolysis (with much lactate/lactic acid production) by effector immune cells. In contrast, immune-stressing emphasizes how the immune system uses nutrition and metabolism to control infections. Immune-stressing addresses effector cell glycolysis *at the infected site* by noting that the high uptake of glucose linked with high output of lactic acid is an ideal double-pronged stressor targeting proliferating pathogens. Once the basic vulnerability of pathogen proliferation is recognized, numerous other paradigms of immunometabolism, and immunology as a whole, are challenged.

KEYWORDS

immunometabolism, nutritional immunity, host-pathogen interactions, glycolysis, glucose, lactic acid, heat, oxidative burst

1 Introduction

This conceptual analysis explores the logical consequences of a fundamental principle, that the process of proliferation, requiring resources and synthesis, is vulnerable to stress from limitation of resources (nutrients, including oxygen) and from disruptive or damaging stress caused by noxious agents. In host-pathogen conflicts there are well-known advantages that pathogens have because of rapid proliferation and large population size permitting rapid evolution, most notably in antibiotic resistance, even within an individual host. However, only rarely noted are the pathogen disadvantages of generally being localized, hence safely permitting application of intense stress by the host, and of having to proliferate (1, 2). This neglect is puzzling since the logical consequences explored here provide crucial insights that challenge or provide numerous new paradigms of immunometabolism and even immunology. Table 1 lists 12 such novel concepts. Most of the analysis will address immunometabolism and its foundations as they relate to the advantages of effector cells *in direct conflict with pathogens,* which are vulnerable due to their localization and proliferation.

Although there has long been interest in the broad intersection of nutrition and metabolism with immune responses, the term "immunometabolism" began being used only in the past decade (3, 4). Immunometabolism has come to emphasize that metabolic processes and the nutritional microenvironment regulate immune cells, especially effector cells whose function is to control pathogens (5–11). Pathogens can be either extracellular (including tumor cells as endogenous pathogens) or intracellular. Infected host cells manipulated by their intracellular pathogens are themselves pathogens and are treated as such by the immune system. The pathogens considered in this conceptual analysis are those that proliferate at the infected (or tumor) site, notably bacteria, protozoa, fungi, viruses, and tumor cells. Specifically excluded are metazoan parasites not proliferating in the tissues where they may occur. Although the function of the immune system is to control pathogens, the field of immunometabolism generally fails to consider pathogens except as competitors of immune cells for nutrients. Nutrient-hungry pathogens are considered a problem since very low levels of resources or very high levels of metabolic wastes impair effector cells' functionality. In other words, in the standard view the effector cells and pathogens are nearly equally matched in terms of resource depletion. However, here it is argued that overlooking the vulnerability of proliferation to stress by localized pathogens (2) has led the field of immunometabolism astray by focusing on metabolic control of immune responses rather than on the immune system's core function of controlling pathogens.

A central theme of immunometabolism is effector cells' enhanced use of glucose for ATP production through aerobic glycolysis (with high lactate production) rather than relying predominantly on mitochondrial OXPHOS. While long recognized for neutrophils (12, 13) and monocyte-macrophages (M1 macrophages) (14), this glycolytic preference and high nutrient uptake, particularly of glucose and glutamine (15), has been found to extend to essentially all immune cells that are involved in directly controlling pathogens. Effector cells' relative preference for glycolysis extends beyond neutrophils and M1 macrophages to include dendritic cells, effector T cells (cytotoxic and helper), natural killer cells, B lymphocytes (3), and even to platelets activated for clotting (16), which helps control pathogens (17, 18). This glycolytic preference, even in the presence of oxygen, occurs not only during cell proliferation and synthesis at distant low-stress sites, but also during activation for migrating toward and confronting the pathogens at infected sites. This confrontation with the pathogens is the phase of effector cell life history focused on in this conceptual analysis. The preference for glycolysis *at infected sites* is not intuitive since aerobic glycolysis generates only 2 ATPs per glucose molecule, while exporting most of the energy value of glucose as lactate/lactic acid, rather than generating the additional 36 ATPs theoretically possible from OXPHOS. Besides this apparent wastefulness of glucose, the large nutrient uptake by activated effector cells is often interpreted as indicating high nutrient needs for the apparently high costs of fighting pathogens (19, 20).

The interpretation of these and other experimental findings has become paradigmatic in immunometabolism. In contrast, this paper describes the host defense strategy of "immune-stressing"—actively making the infected site stressful to preferentially harm the more vulnerable proliferating pathogens. This strategy provides a simple

TABLE 1 Paradigms derived from immune-stressing (i.e., stressing vulnerable localized proliferating pathogens by restricting resources and generating noxious waste products).

1. Effector immune cells actively create much of the stressful conditions at infected sites. Since this preferentially harms the proliferating pathogens, creating this non-specific stress is one of the key functions of effector cells (2).
2. Effector cells typically do not proliferate at infected sites because it is too stressful. Were they to proliferate there, they would lose their advantage of using stress to preferentially harm the pathogens (2).
3. Nutritional immunity, the restriction of micronutrients to pathogens, is overshadowed by "extended" nutritional immunity, the restriction of all nutrients, including oxygen, to the pathogens (2).
4. The restricted nutrients can be converted to noxious products, acting as damaging stressors to harm the more vulnerable pathogens (2).
5. High uptake of glucose and glutamine by effector cells *at infected sites* does not reflect the functional needs of the cells, instead functioning to deprive pathogens of nutrients (2).
6. The metabolic needs of effector cells *when confronting pathogens* cannot be determined by uptake of resources/nutrients or output of metabolic products (any more than the metabolic needs of adipose cells can be determined by measuring lipid uptake).
7. The enhancement of glycolysis of effector cells not only depletes glucose, but also generates noxious acidity from lactic acid (2).
8. Acetic acid, found in very high concentrations at infected sites (55), is likely another host-generated noxious stressor.
9. Oxygen is actively depleted from infected sites and is converted to ROS as neutrophils move toward inflamed sites (56). (Oxygen depletion impairs pathogens' ability to oxidize lipids, amino acids, lactate, and acetate for fuel).
10. Localized heat generated from the oxidative burst is likely to be the main source of heat stress applied to pathogens, with the systemic heat of fever a lesser contributor (2, 29).
11. The oxidative burst harms pathogens not only by ROS (a noxious product), but also by oxygen depletion (a resource) and local heat generation (a noxious product).
12. Immunometabolism should emphasize how the immune system uses metabolism to control pathogens, in addition to emphasizing how metabolism controls the immune system.

and logical evolutionary-based alternative interpretation of many experimental findings, thereby challenging many of the standard principles of immunometabolism. Most notable are the need to consider the pathogen vulnerabilities to metabolic stress, to reconsider the function of aerobic glycolysis for effector cells confronting pathogens, and to recognize that the oxidative burst at the effector cell surface serves to harm pathogens by not only generating noxious reactive oxygen species (ROS), but also by depleting oxygen and by generating noxious localized heat, a long-ignored metabolic product.

2 Fundamentals of immune-stressing

Immune-stressing is an innate host defense strategy of applying stress (harm or possible harm), which preferentially affects proliferating pathogens more than the non-proliferating host cells (2). It is a fundamental principle relating to stress of any kind, and it has relevance beyond host-pathogen interactions to include cancer therapy, military strategy, international relations, finance, and more.

2.1 Universally, proliferation is especially vulnerable to stress

Proliferation requires resources, both for cellular components/materials and for fuel/energy. Resource-limiting stress is typically of slow onset. Proliferation also requires synthesis, which entails the precise manipulation of materials, usually to make more complex structures. Synthesis is vulnerable to damage or disruption from noxious stressors, often of rapid onset. That proliferation requires resources is a simple arithmetic principle. That synthesis is especially vulnerable can be viewed as a variant of the second law of thermodynamics, that systems tend toward disorder. Consequently, it takes effort to create ordered structures and even more effort in the face of disruptive or damaging conditions.

The universality of the principle is exemplified in the building of a house (2). It requires a complete set of materials along with labor (energy), thus being subject to resource-limiting stress. The process of handling and assembling the building materials (synthesis) requires low stress (hence predictable) conditions. However, the wind stress of a hurricane makes it very difficult to handle the materials and to assemble them properly. Additionally, an unfinished house is especially prone to damaging wind gusts and water damage unless extra effort is taken to secure this intermediate structure. This fundamental vulnerability of proliferation to stress applies to cellular processes in both hosts and pathogens.

In terms applicable to infections, the proliferation of an infective inoculum of a thousand bacteria to become a million requires at least a 1,000-fold increase in resources. The 1,000-fold population increase also requires essentially this much proliferation over about 10 generations ($10^3 \approx 2^{10}$), each replication involving the delicate synthesis of precisely constructed molecules of nucleic acids and innumerable proteins and their highly choreographed interactions.

2.2 Infections start out localized

The localization of pathogens allows the host to apply much more intense stress than would be safe to apply diffusely. Extreme localization within phagolysosomes allows for especially intense application of stressors such as ROS, severe pH changes, very low or high metal ion concentrations (21), and presumably heat (22, 23), each of which would be lethal to the host if applied systemically. Essentially the same stressors of less intensity occur extracellularly at the infected sites. Systemically, similar stressors of much lower intensity occur as part of the acute phase response (24), permitting distant host cells to participate in pathogen control by supporting the stress gradient as well as mildly increasing the stress levels for pathogens that escape localization (2).

2.3 Pathogens typically must proliferate to be pathogenic

In contrast to most pathogens (including tumor cells and infected cells producing pathogens), most host tissues have limited immediate needs for proliferation. Although effector cells are essential at infected sites, they proliferate at distant low-stress locations, notably bone marrow and lymphoid tissues. It is notable that M1 (monocyte-derived) macrophages typically do not proliferate locally at infected sites, while M2 (tissue resident) macrophages involved in controlling metazoan parasites and promoting tissue repair do proliferate locally (25). It is argued that it is no coincidence that effector cells typically do not proliferate at infected sites because it is too stressful there, and that infected sites are stressful in part because (as proposed by immune-stressing) a function of effector cells is to actively create stress there (2).

2.4 The "stress vulnerability gap"

The "stress vulnerability gap" is the difference in relative vulnerability between local proliferating pathogens and the local host cells, particularly the effector cells. The host can capitalize on the stress vulnerability gap by increasing the localized stress, which can involve resource-limiting stress and/or damaging/noxious stress. Since much of the stress is actively host-induced as an immune function (2), it is not surprising that effector cells evolved to function best in somewhat stressful conditions, as noted for decreased oxygen (26), increased acidity (27, 28), and heat (29). Most cancer therapy is based on the increased vulnerability of proliferation to stress, while also taking advantage of localization of the tumor to permit applying more intense stress where feasible (with excision being the epitome of intense therapeutic stress).

As noted, metazoan parasites in tissues typically do not proliferate locally and thus are not subject to this stress vulnerability gap. Metazoan parasites are typically controlled with Type 2 immune responses, with eosinophils as specialized effector cells and with fibroblast proliferation and collagen synthesis. Especially interesting are the exceptions to the generalizations that (a) infections tend to start out localized, (b) that pathogens need to proliferate to cause disease, and (c) that most host cells have relatively limited need to proliferate at infected sites, since the exceptions often reveal evidence of the pathogen-host evolutionary arms race, as briefly addressed below. Indeed, many medically important infections involve exceptions to these generalizations where the host cannot take advantage of the stress vulnerability gap.

2.5 Pathogens have defenses against stress

There are four universal strategies for responding to stress:

(1) Ignore the stress. Assume the stress is inconsequential or will soon pass.
(2) Actively oppose or neutralize the stress.
(3) Reduce metabolism / go dormant until the stress passes.
(4) Leave to seek less stressful conditions elsewhere.

1) Immune-stressing, i.e., capitalizing on the stress vulnerability gap, is primarily aimed at pathogens using the first strategy—ignoring the stress and continuing with growth and synthesis as before. Immune-stressing is most effective against proliferating pathogens, which are the most dangerous.
2) The second strategic response is taken by many medically important pathogens, having evolved ways of actively opposing and neutralizing the stress. This stress-neutralization can involve utilizing different metabolic pathways or countering the potentially stressful host defenses such as resource restriction, ROS, acidity, or heat. Nevertheless, the pathogens' necessity of actively opposing host-induced stress entails extra costs compared to not experiencing any stress at all.
3) The strategy of reducing metabolic activity is an effective defense against both resource-limiting stress and damaging/noxious stress. Indeed, dormant pathogens are particularly difficult to eliminate, with bacterial spores and latent viruses being extreme examples.
4) The fourth response to stress is to seek less stressful conditions. This involves avoiding being localized or actively fleeing locally stressful conditions in search of better conditions for proliferation. The host defense strategy of immune-stressing recognizes that both the pathogens and the localized stressors will spread out unless contained. Containment involves not just keeping the pathogens from accessing new resources, but also confining the pathogens along with the stressful conditions. Containment of the stressful conditions also reduces self-harm to nearby tissues.

An additional pathogen defense against host-induced stress is to have a population with individuals predisposed toward each of the four responses to stress. Not only does this bet-hedging occur between individuals, but also within each individual there is likely some degree of bet-hedging in the predispositions among the four basic responses to stress, reflected in the relative degree of gene transcription relevant to each response. This array of strategies for responding to stress complicates pathogen control.

Pathogens may evolve to minimize the stress vulnerability gap by seeking to infect delicate or critical host organs too costly for the host to substantially self-stress (e.g., brain, heart, eyes, bone marrow). Pathogen evolution to infect non-localizable tissues such as blood would also minimize the stress vulnerability gap. An example of a host counter offense would be to try to localize the blood together with immune defenses, as occurs in the spleen. In turn, a pathogen counter defense to this would be to minimize passage of infected RBCs in the spleen, as by adhering to capillaries in the delicate and vital brain, a strategy used by *Plasmodium falciparum* in humans and *Babesia bovis* in cattle (30).

2.6 It is not always feasible or even possible to kill every pathogen

As noted, it is relatively easy to kill localized, vulnerable proliferating pathogens that ignore the host-induced stress. Thus, immune-stressing can promptly help reduce the immediate threat. However, resistant pathogens that take the strategies of dormancy and/or actively opposing the stress may lead to chronic infection. This detente with non-proliferating pathogens entails the long-term costs of vigilance, including chronic inflammation, as well as the risk of recrudescence.

Because of the harm of inflammation (self-stressing), it should be expected that immune responses would be finely tuned to recognize when to shift from inflammation to the low-stress conditions conducive to repair that involve host cell proliferation and matrix synthesis. The value of this fine-tuning is reflected in the immunology literature, where nearly as much attention is given to anti-inflammatory immune suppression to prevent self-harm as is given to pro-inflammatory pathogen control. Indeed, much of the current focus of immunometabolism centers on limiting immune responses via metabolic regulation of effector function.

3 Beyond nutritional immunity

Nutritional immunity is the well-accepted host defense that restricts access of pathogens to critical metal ions, primarily iron, zinc, and manganese, presumably by compartmentalization of the pathogens and/or the nutrients (21, 31, 32). This restriction occurs most intensely at the phagolysosome, but it even occurs systemically as part of the acute-phase response. Some researchers have extended this concept of nutritional stressing to include restriction of certain amino acids, notably arginine (33, 34), tryptophan (3, 35, 36), and of deoxynucleotide triphosphates for making DNA, as well as glucose for energy (36). The host can also direct toxic concentrations of the same metal ions against pathogens (21, 36, 37), perhaps by suddenly dumping toxic amounts on especially susceptible nutrient-deprived pathogens. At present, nutritional immunity seems to be a side branch of immunometabolism that is outside of the paradigms built around metabolic regulation of immune cell function.

Immune-stressing is the extension of nutritional immunity taken to its logical conclusion (Figure 1). All resources needed by pathogens, especially glucose and oxygen, should be restricted. Additionally, where feasible, those resources should be converted to noxious or damaging stressors. For glucose the main noxious stressor is lactic acid (38–41), while the noxious "waste" products of oxygen are ROS and heat. Once one recognizes the utility of stress preferentially applied to the pathogens, many of the conundrums in immunometabolism vanish. Therein, immune-stressing (encompassing and extending nutritional immunity) becomes the main trunk of immunometabolism, and metabolism's key role in effector cell-pathogen interactions can be seen as controlling pathogens rather than controlling the immune response.

4 Caveats on activation phases

Immune-stressing as a strategy depends on effector cells' own stress-vulnerable activities of proliferation and post-proliferative

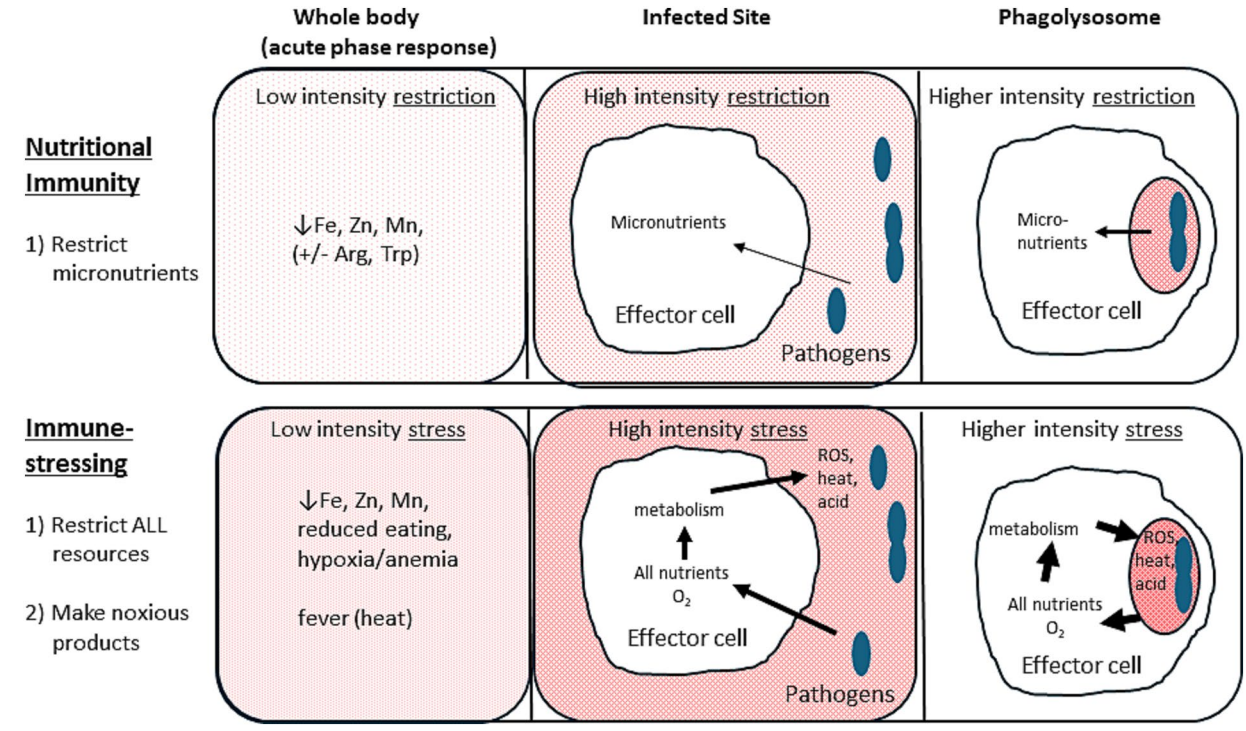

FIGURE 1
Nutritional immunity versus immune-stressing. Nutritional immunity (top portions) restricts micronutrients from pathogens. Immune-stressing (bottom portions) restricts all resources, including oxygen, and converts them to noxious metabolic products to further stress the pathogens. Arrows indicate the host-induced flow of resources and/or metabolic products to impair the pathogens. Arrow width and background shading intensity denote the relative degree of stress applied to the pathogens. Note that the more localized the pathogens (e.g., in the phagolysosomes) the more intense the stress that the host can safely apply.

synthesis being completed *prior to* confronting the proliferating pathogens. Only simple priming (e.g., loading the weapon, rather than making the weapon) should be needed (42). Notable is that phagocyte NADPH oxidase has pre-synthesized components for generating ROS via the oxidative/respiratory burst that are kept separate until needed (43).

However, in much of the immunometabolism literature the distinction between activation for proliferation versus activation for effector function has not been made, such as with the assertions of high nutritional needs of effector cells for proliferation, synthesis, *and effector function*. This overlooks the basic vulnerability of proliferation. Another reason for the failure to make the distinction between effector cells' proliferation (including post-proliferative synthesis) versus effector function is that both phases use enhanced or relatively increased aerobic glycolysis over OXPHOS and do indeed take up large amounts of resources. However, immune-stressing does not address the Warburg effect, the preferential use of aerobic glycolysis by rapidly proliferating cancer and effector cells, since the potential functions of aerobic glycolysis during proliferation (44–48) versus aerobic glycolysis while attacking pathogens are completely different. Immune-stressing applies to and emphasizes non-proliferating effector cells taking in large amounts of resources to keep them from the pathogens and converting resources to noxious waste, as occurs with glycolysis. The use of "Warburg" or "Warburg-like" for the glycolysis of effector cells confronting pathogens only adds to the confusion, as does the unqualified use of "effector cell activation."

5 Specific resources and metabolic products

Immune-stressing potentially applies to all resources needed by pathogens as well as to all non-specific stressors generated by effector cells. These resources are virtually identical for host cells and pathogens, and currently a major theme in immunometabolism is that pathogens harm effector cells by competing for the same resources. Resources can be materials for cellular components (micronutrients, such as metal ions and vitamins, and macronutrients), or resources can be fuels for energy, such as macronutrients and oxygen. Table 2 lists potential resources and related noxious products and how they may play a role in immune-stressing. In this section special attention is given to glucose, glutamine, and oxygen as resources, and to lactic acid, ROS, heat, and acetate as stressful metabolic products.

5.1 Glucose, glutamine and lactic acid

Glucose is the primary nutrient source for energy, and it has a central role in biosynthesis. Glutamine can also be an important energy source and plays a key role in nitrogen metabolism. The high rates of glycolysis and glutaminolysis by effector cells activated to attack pathogens present a conundrum, as stated by Curi, et al. (15):

> *"The lymphocytes under study are not rapidly dividing, but possess the potential for cell division, the macrophages are terminally*

TABLE 2 Resources as cellular components and fuels and their potentially noxious products.

Resources: cellular components	Potentially noxious products
Metal ions (e.g., Fe, Zn, Mn)	High concentrations can be toxic
Other minerals[1]	?
Vitamins[1]	?
Carbohydrates (esp. glucose)	Acids (lactic[2], likely acetic[2])
Amino acids	? (Ammonia?)
Glutamine	Ammonia?
Arginine	Nitric oxide
Tryptophan	Picolinic acid
Lipids	Antimicrobial lipids[2]? Acetic acid[2]?
Nucleic acids	?

Resources: fuels/energy	Potentially noxious products
Oxygen	ROS, heat
Carbohydrates (esp. glucose)	Acids (lactic[2], likely acetic[2])
Amino acids[2]	? (Ammonia?)
Glutamine	Ammonia?
Arginine	Nitric oxide
Tryptophan	Picolinic acid
Lipids[2]	Antimicrobial lipids[2]? Acetic acid[2]?

[1]Not known to be specifically withheld from pathogens.
[2]Restricted use as fuel without oxygen.
See text for discussion and references.

> *differentiated, and the neutrophils have a lifespan of approximately 10 h. Hence any hypothesis must explain high rates of fuel utilization in cells with widely different characteristics."*

The explanation for the nutritional inefficiency that was developed by these authors was termed "branched-point sensitivity"—having large amounts of glucose and glutamine and their intermediates priming the numerous metabolic pathways to be ready for a sudden (i.e., unforeseen) metabolic response (49). More recent explanations for the high uptake of nutrients upon activation *to confront pathogens* are simply that the high costs are evidence that confronting pathogens must be metabolically costly. Glucose use via glycolysis, despite its inefficiency and wastefulness, is often considered preferential to OXPHOS because glycolysis produces ATP much faster than does OXPHOS (3, 45). These explanations presuppose that the metabolic needs of effector cells carrying out their sole function of controlling pathogens are unexpected and sudden. It has been noted that ATP production via glycolysis requires less cellular machinery than reliance on OXPHOS and hence is actually efficient if there is an abundance of glucose (45)—definitely not the case at infected sites. Others have proposed that glycolysis spares oxygen for use in generating antimicrobial ROS in the oxidative burst (50), a point to be addressed subsequently.

In sharp contrast, immune-stressing notes that effector cells use aerobic glycolysis because: (1) it is actively wasteful (~18x more wasteful than OXPHOS) to deprive proliferating pathogens of glucose, and (2) the lactate/lactic acid generated is a noxious waste product causing damaging stress (38–41), particularly to the more vulnerable pathogens. Note that the substantial energy value of lactate/lactic acid is not lost to the host since distant well-oxygenated tissues can use it for fuel. Speed of ATP generation is not important since the effector cells are not suddenly surprised by having to attack pathogens—that *is* their function. If energy were so critical, their OXPHOS pathways would presumably also have been well developed. Instead, evidence suggests that confronting pathogens is much less energetically costly than is typically assumed. It has been calculated that remarkably little energy is needed for cell motility (51), as would be needed for migrating toward pathogens. Furthermore, studies evaluating neutrophil energetics failed to find substantial increases in glucose uptake or lactate production immediately before or during phagocytosis, with researchers concluding that "*it seems safe to conclude that the rate of formation of ATP from carbohydrates is not increased during phagocytosis* (13)."

While the large amounts of glucose taken in by effector cells confronting pathogens are converted to and released as noxious lactate/lactic acid, the large amounts of glutamine taken up apparently in excess of their needs are converted to glutamate, aspartate, alanine, and lactate (15, 49). Besides "branched-point sensitivity" (52), other explanations for high glutamine uptake are based on the importance of maintaining the Krebs cycle for biosynthesis (though irrelevant at the infected site) and immune signaling (53, 54) and for generating noxious nitric oxide via arginine synthesis (3). In contrast, immune-stressing proposes that high glutamine uptake by effector cells actively depletes a major nutrient for pathogens, and also that the metabolic products should be put to good use. Conversion of glutamine (having two nitrogen atoms) to other amino acids yields ammonia. If used effectively for host-defense, speculatively the alkaline ammonia could protect effector cells from their own acids, and/or it could be very locally directed against the pathogens which are likely vulnerably primed to defend against acidosis.

5.2 Oxygen

With immunometabolism's emphasis on high glucose usage via glycolysis by effector cells at infected sites, oxygen takes on a relatively minor role. Of course, oxygen is well recognized to be needed in the oxidative (or respiratory) burst by neutrophils and M1 macrophages to generate ROS to help kill pathogens. The oxidative burst serves not only to generate toxic ROS as a pathogen-damaging stressor, but it also depletes oxygen, thus serving as a resource-restricting stressor. Oxygen depletion at infected sites means that pathogens' energy needs are mostly limited to glycolysis and fermentation, thus impairing their use of lactate, acetate (55), lipids, and amino acids for energy. An experimental finding strongly supporting immune-stressing as a strategy is that neutrophils (having few mitochondria) actively deplete oxygen from the tissues as they migrate toward the infected site (56). This, plus the finding that this oxygen is converted to noxious ROS, fits exactly with the predictions of immune-stressing—resource depletion coupled with noxious waste generation.

5.3 Heat

Immune-stressing proposes that resources to be kept from pathogens, such as oxygen and oxidizable fuels, should be converted

to noxious or disruptive stressors, such as heat. Heat is *the* ignored metabolic product in immunometabolism, although the heat of fever is important in immunology. It noteworthy that fever is a *systemic* host-induced defense involving the slight core temperature increase of 1-4°C (38–41°C from 37°C in humans) (57). However, lethal temperatures for mammalian cells, and presumably most pathogens that infect them, are around 45°C given enough time, with even a single degree or two above this greatly increasing the kill rate (58). Of course, a key point of this conceptual analysis is that the synthesis involved in proliferation is particularly susceptible to damaging stressors such as heat. As suggested in the section on pathogen defenses against immune-stressing, dormant pathogens and/or those opposing heat stress via the heat shock response should be much more heat-tolerant.

Fever, like all systemic stressors of the acute phase response, must necessarily be only mildly stressful compared to the more intense stress that can be safely applied locally at the infected site, and especially ultra-locally within the phagolysosome (Figure 1) (2). Strangely, the benefits and sources of intense localized heat have only rarely been considered (2, 29). Since substantial heat is generated by the oxidative burst via phagocyte NADPH oxidase (22, 23), it has been argued that the systemic heat of fever functions to raise the ambient temperature to aid this intensely localized heat produced at the surface of pathogens (29). While these temperatures have never been measured, substantial highly localized heat is also generated in OXPHOS, with mitochondrial temperatures of 50°C detected using heat-sensitive dyes (59). Recent work has confirmed that mitochondrial temperatures are adapted to be as much as 15°C higher than core body temperatures (60), meaning that much higher temperatures than previously recognized can be locally generated by oxidation. Interestingly, mitochondria have been shown to be recruited to macrophage phagosomes to help kill bacteria by augmenting ROS generation (61), though the associated heat was not mentioned (or considered?).

Heat as a damaging/noxious stressor can be synergistic with other damaging stressors such as acidity and ROS (62) as well as with iron restriction (63). The standard view of the oxidative burst is that the entire antimicrobial effect comes from ROS, ignoring not only oxygen depletion but also the extremely localized heat generation. The oxidative burst also releases arachidonic acid, which causes lipid peroxidative damage to bacteria (64), whose effects are likely enhanced by synergy with this heat.

5.4 Acetate/acetic acid

It was recently found that infections and inflammatory conditions can increase acetate concentrations 5x above normal (1 mM) in the blood (65) and 100x above normal at inflamed foci (55). The rising local acetate levels were found to help control infections early on by stimulating effector lymphocyte function, while later the high acetate concentrations became immunosuppressive. The authors described specific mechanisms by which acetate functions as a context-sensitive metabolite to control infection and also to limit inflammatory damage (55). The source of the acetate was not determined.

In immune-stressing this important finding of acetate abundance at inflamed sites is readily interpreted as a noxious metabolic product, comparable to and complementary with lactic acid. Such high local acetate/acetic acid concentrations (100 mM) can be inhibitory or lethal to bacteria (66, 67). Growth inhibitory activity of acetate against *Pseudomonas* was found to be synergistic with low pH, with substantial inhibition at 20 mM at pH 6 (68). Acetate at 12.5 mM for 24 h killed half of the neoplastic thymocytes tested, while lacking apparent cytotoxicity in normal thymocytes (69) (which presumably were not actively proliferating). Like lactate/lactic acid, acetate's toxicity is due to its high local concentration; and its use for energy at infected sites is likely limited by local hypoxia, while still being readily usable as fuel by distant host cells. The 5x increase in blood acetate levels is in line with other systemic stresses of the acute phase response—they are necessarily much milder than the local stresses, but they enhance the gradient of the stress in addition to making conditions somewhat less favorable for the proliferation of pathogens which have escaped the intense local stresses (2). The enhanced effector cell functionality of slightly increased acetate concentrations (55) parallels that of other stressful metabolic conditions such as slight hypoxia, acidity, and even heat, where it is reasonable that effector cells evolved to function best in their expected working conditions, the somewhat stressful conditions that they themselves have created (29). It will be interesting to determine the metabolic sources of the high acetate concentrations at inflamed sites and the cells responsible (presumably the effector cells themselves).

6 Glycogen storage

6.1 A test of paradigms

Given the importance of glucose at infected sites, it is not surprising that effector cells store glucose as glycogen and bring it with them as they attack the pathogens (70–72). However, the standard paradigm of immunometabolism differs from immune-stressing in a testable prediction. The standard paradigm notes that glucose is so important for effector cells' function that they should store as much glucose (as glycogen) as practical and carry it with them to the infected site (73). Although not stated, the implication is that effector cells should fill up with glycogen while still in the blood where glucose is plentiful, rather than relying on taking up diminishing amounts of glucose upon approaching the infected site.

Immune-stressing, as a strategy, emphasizes that glucose is especially important for the proliferating pathogens, but only somewhat important to the non-proliferating effector immune cells' metabolic needs. Therefore, the effector cells should deplete as much glucose from the tissues as practical and store it away as glycogen. This extra glucose brought into the infected site, which tends to be used last (13), can also be converted later to additional lactic acid as noxious waste to further stress the pathogens. Importantly, the effector cells should *not* fill up with stored glucose (glycogen) while in the blood. Rather, they should vigorously take up glucose as they migrate to the infected site to create a zone of locally increasing stress to harm the more vulnerable pathogens. This means that while late arriving effector cells may not become replete with glycogen, they will still be helping deplete the glucose that the pathogens especially need.

6.2 Experimental results

It has been shown that effector cells, most notably neutrophils, take up glucose for storage as glycogen predominantly *after* they leave

the blood and are migrating to the infected site (70–72). This finding is counter to that implied by the standard paradigm, but it is in line with immune-stressing which proposes that glycogen storage in route to the infected site allows for even greater stress (less glucose and more lactic acid) to be directed against the pathogens.

7 Metabolism and immunosuppression

Effector cells lose functionality when exposed to especially stressful conditions, primarily low glucose (74), but also other nutrient deficiencies and extreme hypoxia (56, 75) and acidity (76). In these very stressful conditions, immunosuppression with reliance on OXPHOS takes over and leads to tissue repair. Bacterial fermentation products such as short chain fatty acids, as would develop in stressful oxygen-depleted sites, can also be immunosuppressive (77, 78).

Resource depletion and waste buildup at infected sites are typically viewed in immunometabolism (and immunology in general) as the expected byproduct of the struggle for resources between immune cells and pathogens. In this view it is the vulnerability of effector cells to increasing stress that largely allows metabolism to regulate or control effector cell responses. In contrast, immune-stressing considers this stressful environment not as a simple byproduct of the metabolism of conflicting pathogens and host cells, but as an active host defense to preferentially harm the more vulnerable proliferating pathogens. The increasing stresses at infected sites are seen as cues to induce the switch from damaging pro-inflammatory conditions to anti-inflammatory and tissue repair conditions, either because the pathogens have been controlled or because they must be tolerated as a chronic infection.

A major concern in immunometabolism is that the microenvironment around many cancers is immunosuppressive due to the tumor cells outcompeting effector cells for resources and accumulation of noxious wastes. Not only are effector cells functionally impaired, but the surrounding immune cells are immunosuppressive and may actively promote tumor growth (9, 73, 74, 79–81). The inability of effector cells to control these tumors has been considered an immune dysregulation, and much of the emphasis in immunometabolism is directed at correcting this metabolic dysfunction (79, 82).

An alternative interpretation presented here is that a large enough assemblage of tumor cells, having already evaded immune control, can create stressful enough local conditions that effector cells misinterpret the situation as needing more immune suppression. A similar condition likely occurs with several infectious diseases such as cryptococcosis and lepromatous leprosy (83, 84), where early immune evasion or underlying immunosuppression allows accumulation of a large pathogen mass (the organisms themselves or infected macrophages), which then can cause metabolically stressful conditions that enhance the immunosuppression. Rather than being seen as immune dysregulation or dysfunction, this metabolic stress that enhances prior immune evasion can be seen as a pathogen subversion of the typically effective strategy of immune-stressing.

8 Discussion

The concept of immune-stressing offers a simple, yet powerful, explanation for almost any puzzle involving the depletion of nutrients at infected sites, as well as for the metabolism of those nutrients into noxious products to be directed against the more vulnerable localized proliferating pathogens. Not only does immune-stressing apply to the central conundrums of effector cells' high glucose and glutamine uptake and inefficient glucose use via aerobic glycolysis with lactic acid production *while in conflict with pathogens*, but it emphasizes the value of oxygen depletion and the use of localized heat as host defenses. Immune-stressing thereby greatly expands the protective value of the oxidative burst beyond simply ROS production. Immune-stressing is compatible with the finding of neutrophil secretory granules having glutaminase (85) and arginase I, which likely act to deplete the phagolysosomes of these amino acids to stress the pathogens (33, 34). Arginine can also be depleted to produce toxic nitric oxide, and tryptophan is well known to be depleted by effector cells (3). Picolinic acid, a secondary metabolite of tryptophan, has antimicrobial activity (86). Lipid metabolism by effector cells at infected sites should also be reconsidered in light of immune-stressing. For example, there is high uptake of lipid by neutrophils moving from the blood toward infected sites (70), and there is prominent synthesis of fatty acids from citrate stored in LPS-stimulated macrophages and other effector cells (3). Immune-stressing would interpret these findings as attempts to remove nutrients from the pathogens, and where feasible to convert them to toxic byproducts such as antimicrobial lipids (87, 88) or acetate, whose metabolic source at inflamed sites is yet undetermined (55).

While the potential scope of immunometabolism is vast, covering all interactions of nutrition, metabolism, and immunology from the systemic to the subcellular levels, unfortunately immunometabolism as a distinct term became applied much more narrowly to the metabolism of immune cells. Surprisingly, the immune system's use of metabolism for control of pathogens is seldom mentioned (2, 36). Since the basic function of the immune system is to control pathogens, it is proposed that effector cells evolved to account for not only their own metabolic needs, but especially the metabolic needs of the even more vulnerable proliferating pathogens. For most non-storage cells it would seem obvious that high nutrient uptake reflects high metabolic needs and therefore these needs must be nutritionally costly. However, this is not true for effector cells actively confronting pathogens because of the genetic conflict with the pathogens. In immune-stressing the high nutrient uptake is to deprive the pathogens and to subject them to the noxious "waste" products. Understanding the acute phase response and its myriad systemic metabolic changes during infections (e.g., metal ion restriction, heat/fever, anorexia) requires recognition of the pathogens' vulnerability to these metabolic changes (2). Likewise at the cellular level, the pathogens' metabolic needs must be considered to understand the metabolism of the local immune response. It is argued that the current narrow field of immunometabolism has been led astray by emphasizing control of immune responses rather than the basic function of the immune system in controlling pathogens. By ignoring the vulnerability of pathogen proliferation to stress, the use of glycolysis and the high uptake of glucose and glutamine by effector cells has been misinterpreted. In contrast, the immune-stressing concept emphasizes that proliferating pathogens that are localized are especially vulnerable to even completely non-specific stress. Recognition of this auxiliary function of effector cells to apply stress to pathogens has profound implications, many of which suggest new paradigms for interpreting metabolic findings relating to effector immune function. It is proposed

that immunometabolism should be the study of how the immune system uses nutrition and metabolism to help control pathogens and to help assess metabolic cues for guiding the appropriateness of the response.

This conceptual analysis emphasizing how immune cells use metabolism to control pathogens leads to numerous research questions, some of which would never have been considered worthwhile or even recognized for addressing. For instance, what other resources (particularly micro- and macronutrients beyond those addressed earlier) are also actively restricted by the infected host? More interestingly, how can each of the restricted resources be converted to damaging/noxious stressors to harm the more vulnerable pathogens? Specifically, is the ammonia derived from glutaminolysis put to good use by effector immune cells to capitalize on the stress vulnerability gap, and if so, how? Which cells are responsible for the noxious concentrations of acetate/acetic acid at infected sites; which nutrients are metabolized to the acetate/acetic acid; and are the relative concentrations of lactate/lactic acid and acetate/acetic acid at infected sites adjusted by the effector cells to maximize the stress vulnerability gap? Are the lipids and lipid precursors which are actively taken up by effector cells that approach infected sites metabolized to create noxious waste (e.g., acetic acid, antimicrobial lipids)? What degree of hypoxia is needed at infected sites to effectively bar pathogens from oxidizing nutrients for energy (e.g., lactate, acetate, lipids, and amino acids)? A glaring need is to determine the actual temperatures to which pathogens are exposed, particularly the surface of phagocytized pathogens exposed to the oxidative burst. Exactly how hot is it directly at the site of ROS generation, recognizing that the surface of a furnace is markedly hotter than the house it is heating? And what are the actual nutrient needs and energy costs of effector immune cells as they confront pathogens, recognizing that their resource uptake at infected sites is not a reliable indicator of their own metabolic needs?

Exploration of the vulnerabilities of pathogens to localization and proliferation, contrasting with their well-recognized advantages of rapid evolution, challenges or creates numerous basic paradigms of immunometabolism and even immunology. New paradigms lead to new insights and generate questions and findings never even imagined. So it is with immune-stressing.

Author contributions

EL: Writing – original draft, Writing – review & editing.

Funding

The author(s) declare that no financial support was received for the research, authorship, and/or publication of this article.

Conflict of interest

The author declares that the research was conducted in the absence of any commercial or financial relationships that could be construed as a potential conflict of interest.

Generative AI statement

The author declares that no Generative AI was used in the creation of this manuscript.

Publisher's note

References

1. LeGrand EK, Alcock J. Turning up the heat: immune brinksmanship in the acute-phase response. *Q Rev Biol*. (2012) 87:3–18. doi: 10.1086/663946

2. LeGrand EK, Day JD. Self-harm to preferentially harm the pathogens within: non-specific stressors in innate immunity. *Proc Biol Sci*. (1828) 2016:20160266. doi: 10.1098/rspb.2016.0266

3. O'Neill LAJ, Kishton RJ, Rathmell J. A guide to immunometabolism for immunologists. *Nat Rev Immunol*. (2016) 16:553–65. doi: 10.1038/nri.2016.70

4. Rathmell JC. Metabolism and autophagy in the immune system: immunometabolism comes of age. *Immunol Rev*. (2012) 249:5–13. doi: 10.1111/j.1600-065X.2012.01158.x

5. Mogilenko DA, Sergushichev A, Artyomov MN. Systems immunology approaches to metabolism. *Annu Rev Immunol*. (2023) 41:317–42. doi: 10.1146/annurev-immunol-101220-031513

6. Purohit V, Wagner A, Yosef N, Kuchroo VK. Systems-based approaches to study immunometabolism. *Cell Mol Immunol*. (2022) 19:409–20. doi: 10.1038/s41423-021-00783-9

7. Van den Bossche J, Saraber DL. Metabolic regulation of macrophages in tissues. *Cell Immunol*. (2018) 330:54–9. doi: 10.1016/j.cellimm.2018.01.009

8. Ketelhuth DFJ, Lutgens E, Back M, Binder CJ, Van den Bossche J, Daniel C, et al. Immunometabolism and atherosclerosis: perspectives and clinical significance: a position paper from the working group on atherosclerosis and vascular biology of the European society of cardiology. *Cardiovasc Res*. (2019) 115:1385–92. doi: 10.1093/cvr/cvz166

9. Buck MD, Sowell RT, Kaech SM, Pearce EL. Metabolic instruction of immunity. *Cell*. (2017) 169:570–86. doi: 10.1016/j.cell.2017.04.004

10. Dussold C, Zilinger K, Turunen J, Heimberger AB, Miska J. Modulation of macrophage metabolism as an emerging immunotherapy strategy for cancer. *J Clin Invest*. (2024) 134:5445. doi: 10.1172/JCI175445

11. Verheijen FWM, Tran TNM, Chang JC, Broere F, Zaal EA, Berkers CR. Deciphering metabolic crosstalk in context: lessons from inflammatory diseases. *Mol Oncol*. (2024) 18:1759–76. doi: 10.1002/1878-0261.13588

12. Sbarra AJ, Karnovsky ML. Biochemical basis of phagocytosis. 1. Metabolic changes during the ingestion of particles by polymorphonuclear leukocytes. *J Biol Chem*. (1959) 234:1355–62. doi: 10.1016/S0021-9258(18)70011-2

13. Borregaard N, Herlin T. Energy-metabolism of human neutrophils during phagocytosis. *J Clin Invest*. (1982) 70:550–7. doi: 10.1172/JCI110647

14. Newsholme P, Curi R, Gordon S, Newsholme EA. Metabolism of glucose, glutamine, long-chain fatty acids and ketone bodies by murine macrophages. *Biochem J*. (1986) 239:121–5. doi: 10.1042/bj2390121

15. Curi R, Newsholme P, Pithon-Curi TC, Pires-de-Melo M, Garcia C, Homem-de-Bittencourt PI, et al. Metabolic fate of glutamine in lymphocytes, macrophages and neutrophils. *Braz J Med Biol Res*. (1999) 32:15–21. doi: 10.1590/S0100-879X1999000100002

16. Aibibula M, Naseem KM, Sturmey RG. Glucose metabolism and metabolic flexibility in blood platelets. *J Thromb Haemost*. (2018) 16:2300–14. doi: 10.1111/jth.14274

17. Engelmann B, Massberg S. Thrombosis as an intravascular effector of innate immunity. *Nat Rev Immunol*. (2013) 13:34–45. doi: 10.1038/nri3345

18. Saadi S, Wrenshall LE, Platt JL. Regional manifestations and control of the immune system. *FASEB J*. (2002) 16:849–56. doi: 10.1096/fj.01-0690hyp

19. Lochmiller RL, Deerenberg C. Trade-offs in evolutionary immunology: just what is the cost of immunity? *Oikos*. (2000) 88:87–98. doi: 10.1034/j.1600-0706.2000.880110.x

20. Walls J, Sinclair L, Finlay D. Nutrient sensing, signal transduction and immune responses. *Semin Immunol*. (2016) 28:396–407. doi: 10.1016/j.smim.2016.09.001

21. Murdoch CC, Skaar EP. Nutritional immunity: the battle for nutrient metals at the host–pathogen interface. *Nat Rev Microbiol*. (2022) 20:657–70. doi: 10.1038/s41579-022-00745-6

22. Ljunggren L, Monti M, Rialdi G. A comparison of the calorimetric analysis of granulocyte activation by flow and batch systems. *Thermochim Acta*. (1992) 207:23–8. doi: 10.1016/0040-6031(92)80120-L

23. Tan AM, Huang YQ, Qu SS. Determination of the respiratory burst of polymorphonuclear leukocytes by microcalorimetry. *J Biochem Biophys Methods*. (1998) 37:91–4. doi: 10.1016/S0165-022X(98)00015-3

24. Gabay C, Kushner I. Acute-phase proteins and other systemic responses to inflammation. *N Engl J Med*. (1999) 340:448–54. doi: 10.1056/NEJM199902113400607

25. Jenkins SJ, Ruckerl D, Cook PC, Jones LH, Finkelman FD, van Rooijen N, et al. Local macrophage proliferation, rather than recruitment from the blood, is a signature of TH2 inflammation. *Science*. (2011) 332:1284–8. doi: 10.1126/science.1204351

26. Walmsley SR, Chilvers ER, Whyte MK. Hypoxia. Hypoxia, hypoxia inducible factor and myeloid cell function. *Arthritis Res Ther*. (2009) 11:219. doi: 10.1186/ar2632

27. Zhang J, Koh J, Lu J, Thiel S, Leong BSH, Sethi S, et al. Local inflammation induces complement crosstalk which amplifies the antimicrobial response. *PLoS Pathog*. (2009) 5:e1000282. doi: 10.1371/journal.ppat.1000282

28. Martinez D, Vermeulen M, Trevani A, Ceballos A, Sabatte J, Gamberale R, et al. Extracellular acidosis induces neutrophil activation by a mechanism dependent on activation of phosphatidylinositol 3-kinase/Akt and ERK pathways. *J Immunol*. (2006) 176:1163–71. doi: 10.4049/jimmunol.176.2.1163

29. Wrotek S, LeGrand EK, Dzialuk A, Alcock J. Let fever do its job the meaning of fever in the pandemic era. *Evol Med Public Health*. (2021) 9:26–35. doi: 10.1093/emph/eoaa044

30. Hakimi H, Yamagishi J, Kawazu SI, Asada M. Advances in understanding red blood cell modifications by Babesia. *PLoS Pathog*. (2022) 18:e1010770. doi: 10.1371/journal.ppat.1010770

31. Kehl-Fie TE, Skaar EP. Nutritional immunity beyond iron: a role for manganese and zinc. *Curr Opin Chem Biol*. (2010) 14:218–24. doi: 10.1016/j.cbpa.2009.11.008

32. Weinberg ED. Iron availability and infection. *Biochim Biophys Acta*. (2009) 1790:600–5. doi: 10.1016/j.bbagen.2008.07.002

33. Munder M, Mollinedo F, Calafat J, Canchado J, Gil-Lamaignere C, Fuentes JM, et al. Arginase I is constitutively expressed in human granulocytes and participates in fungicidal activity. *Blood*. (2005) 105:2549–56. doi: 10.1182/blood-2004-07-2521

34. Rubin-Bejerano I, Fraser I, Grisafi P, Fink GR. Phagocytosis by neutrophils induces an amino acid deprivation response in Saccharomyces cerevisiae and *Candida albicans*. *Proc Natl Acad Sci USA*. (2003) 100:11007–12. doi: 10.1073/pnas.1834481100

35. Murray HW, Szuro-Sudol A, Wellner D, Oca MJ, Granger AM, Libby DM, et al. Role of tryptophan degradation in respiratory burst-independent antimicrobial activity of gamma interferon-stimulated human macrophages. *Infect Immun*. (1989) 57:845–9. doi: 10.1128/iai.57.3.845-849.1989

36. Kreimendahl S, Pernas L. Metabolic immunity against microbes. *Trends Cell Biol*. (2024) 34:496–508. doi: 10.1016/j.tcb.2023.10.013

37. Botella H, Peyron P, Levillain F, Poincloux R, Poquet Y, Brandli I, et al. Mycobacterial p(1)-type ATPases mediate resistance to zinc poisoning in human macrophages. *Cell Host Microbe*. (2011) 10:248–59. doi: 10.1016/j.chom.2011.08.006

38. Alakomi HL, Skyttä E, Saarela M, Mattila-Sandholm T, Latva-Kala K, Helander IM. Lactic acid permeabilizes gram-negative bacteria by disrupting the outer membrane. *Appl Environ Microbiol*. (2000) 66:2001–5. doi: 10.1128/AEM.66.5.2001-2005.2000

39. Webster KA, Discher DJ, Kaiser S, Hernandez O, Sato B, Bishopric NH. Hypoxia-activated apoptosis of cardiac myocytes requires reoxygenation or a pH shift and is independent of p53. *J Clin Invest*. (1999) 104:239–52. doi: 10.1172/JCI5871

40. Goldman SA, Pulsinelli WA, Clarke WY, Kraig RP, Plum F. The effects of extracellular acidosis on neurons and glia in vitro. *J Cereb Blood Flow Metab*. (1989) 9:471–7. doi: 10.1038/jcbfm.1989.70

41. Gatenby RA, Gawlinski ET, Gmitro AF, Kaylor B, Gillies RJ. Acid-mediated tumor invasion: a multidisciplinary study. *Cancer Res*. (2006) 66:5216–23. doi: 10.1158/0008-5472.CAN-05-4193

42. Hallett MB, Lloyds D. Neutrophil priming: the cellular signals that say 'amber' but not 'green'. *Immunol Today*. (1995) 16:264–8. doi: 10.1016/0167-5699(95)80178-2

43. Bokoch GM, Zhao T. Regulation of the phagocyte NADPH oxidase by Rac GTPase. *Antioxid Redox Signal*. (2006) 8:1533–48. doi: 10.1089/ars.2006.8.1533

44. Luengo A, Li Z, Gui DY, Sullivan LB, Zagorulya M, Do BT, et al. Increased demand for NAD(+) relative to ATP drives aerobic glycolysis. *Mol Cell*. (2021) 81:691–707.e6. doi: 10.1016/j.molcel.2020.12.012

45. Kukurugya MA, Rosset S, Titov DV. The Warburg effect is the result of faster ATP production by glycolysis than respiration. *Proc Natl Acad Sci USA*. (2024) 121:e2409509121. doi: 10.1073/pnas.2409509121

46. Wang Y, Stancliffe E, Fowle-Grider R, Wang R, Wang C, Schwaiger-Haber M, et al. Saturation of the mitochondrial NADH shuttles drives aerobic glycolysis in proliferating cells. *Mol Cell*. (2022) 82:3270–83.e9. doi: 10.1016/j.molcel.2022.07.007

47. Brand KA, Hermfisse U. Aerobic glycolysis by proliferating cells: a protective strategy against reactive oxygen species. *FASEB J*. (1997) 11:388–95. doi: 10.1096/fasebj.11.5.9141507

48. Chen Z, Odstrcil EA, Tu BP, McKnight SL. Restriction of DNA replication to the reductive phase of the metabolic cycle protects genome integrity. *Science*. (2007) 316:1916–9. doi: 10.1126/science.1140958

49. Newsholme EA, Calder PC. The proposed role of glutamine in some cells of the immune system and speculative consequences for the whole animal. *Nutrition*. (1997) 13:728–30. doi: 10.1016/S0899-9007(97)83034-1

50. Gleeson LE, Sheedy FJ. Metabolic reprogramming & inflammation: fuelling the host response to pathogens. *Semin Immunol*. (2016) 28:450–68. doi: 10.1016/j.smim.2016.10.007

51. Flamholz A, Phillips R, Milo R. The quantified cell. *Mol Biol Cell*. (2014) 25:3497–500. doi: 10.1091/mbc.e14-09-1347

52. Newsholme EA. The possible role of glutamine in some cells of the immune system and the possible consequence for the whole animal. *Experientia*. (1996) 52:455–9. doi: 10.1007/BF01919315

53. Kelly B, O'Neill LAJ. Metabolic reprogramming in macrophages and dendritic cells in innate immunity. *Cell Res*. (2015) 25:771–84. doi: 10.1038/cr.2015.68

54. Curi R, Mende RS, de Campos Crispin LA, Norata GD, Sampaio SC, Newsholme P. A past and present overview of macrophage metabolism and functional outcomes. *Clin Sci*. (2017) 131:1329–42. doi: 10.1042/CS20170220

55. Balmer ML, Ma EH, Thompson AJ, Epple R, Unterstab G, Lötscher J, et al. Memory CD8(+) T cells balance pro- and anti-inflammatory activity by reprogramming cellular acetate handling at sites of infection. *Cell Metab*. (2020) 32:457–67.e5. doi: 10.1016/j.cmet.2020.07.004

56. Campbell EL, Bruyninckx WJ, Kelly CJ, Glover LE, McNamee EN, Bowers BE, et al. Transmigrating neutrophils shape the mucosal microenvironment through localized oxygen depletion to influence resolution of inflammation. *Immunity*. (2014) 40:66–77. doi: 10.1016/j.immuni.2013.11.020

57. Evans SS, Repasky EA, Fisher DT. Fever and the thermal regulation of immunity: the immune system feels the heat. *Nat Rev Immunol*. (2015) 15:335–49. doi: 10.1038/nri3843

58. Hildebrandt B, Wust P, Ahlers O, Dieing A, Sreenivasa G, Kerner T, et al. The cellular and molecular basis of hyperthermia. *Crit Rev Oncol Hematol*. (2002) 43:33–56. doi: 10.1016/S1040-8428(01)00179-2

59. Chretien D, Benit P, Ha H-H, Keipert S, El-Khoury R, Chang Y-T, et al. Mitochondria are physiologically maintained at close to 50 degrees C. *PLoS Biol*. (2018) 16:e2003992. doi: 10.1371/journal.pbio.2003992

60. Terzioglu M, Veeroja K, Montonen T, Ihalainen TOSalminen TS, Bénit P, et al. Mitochondrial temperature homeostasis resists external metabolic stresses. *eLife*. (2023) 12:RP89232. doi: 10.7554/eLife.89232.3

61. West AP, Brodsky IE, Rahner C, Woo DK, Erdjument-Bromage H, Tempst P, et al. TLR signalling augments macrophage bactericidal activity through mitochondrial ROS. *Nature*. (2011) 472:476–80. doi: 10.1038/nature09973

62. Dewhirst MW, Lee CT, Ashcraft KA. The future of biology in driving the field of hyperthermia. *Int J Hyperth*. (2016) 32:4–13. doi: 10.3109/02656736.2015.1091093

63. Kluger MJ, Rothenburg BA. Fever and reduced iron: their interaction as a host defense response to bacterial infection. *Science*. (1979) 203:374–6. doi: 10.1126/science.760197

64. Beavers WN, Monteith AJ, Amarnath V, Mernaugh RL, Roberts LJ 2nd, Chazin WJ, et al. Arachidonic acid kills *Staphylococcus aureus* through a lipid peroxidation mechanism. *MBio*. (2019) 10:19. doi: 10.1128/mBio.01333-19

65. Balmer ML, Ma EH, Bantug GR, Grählert J, Pfister S, Glatter T, et al. Memory CD8(+) T cells require increased concentrations of acetate induced by stress for optimal function. *Immunity*. (2016) 44:1312–24. doi: 10.1016/j.immuni.2016.03.016

66. Lasko DR, Zamboni N, Sauer U. Bacterial response to acetate challenge: a comparison of tolerance among species. *Appl Microbiol Biotechnol*. (2000) 54:243–7. doi: 10.1007/s002530000339

67. Trček J, Mira NP, Jarboe LR. Adaptation and tolerance of bacteria against acetic acid. *Appl Microbiol Biotechnol*. (2015) 99:6215–29. doi: 10.1007/s00253-015-6762-3

68. Bushell FML, Tonner PD, Jabbari S, Schmid AK, Lund PA. Synergistic impacts of organic acids and pH on growth of *Pseudomonas aeruginosa*: a comparison of parametric and Bayesian non-parametric methods to model growth. *Front Microbiol*. (2019) 9:3196. doi: 10.3389/fmicb.2018.03196

69. Pandey SK, Yadav S, Goel Y, Singh SM. Cytotoxic action of acetate on tumor cells of thymic origin: role of MCT-1, pH homeostasis and altered cell survival regulation. *Biochimie*. (2019) 157:1–9. doi: 10.1016/j.biochi.2018.10.022

70. Robinson JM, Karnovsky ML, Karnovsky MJ. Glycogen accumulation in polymorphonuclear leukocytes, and other intracellular alterations that occur during inflammation. *J Cell Biol*. (1982) 95:933–42. doi: 10.1083/jcb.95.3.933

71. Afonso A, Macedo PM, Ellis AE, Silva MT. Glycogen granules in resting and inflammatory rainbow trout phagocytes - an ultrastructural study. *Dis Aquat Org*. (2000) 42:101–10. doi: 10.3354/dao042101

72. Weisdorf DJ, Craddock PR, Jacob HS. Granulocytes utilize different energy sources for movement and phagocytosis. *Inflammation*. (1982) 6:245–56. doi: 10.1007/BF00916406

73. Kedia-Mehta N, Finlay DK. Competition for nutrients and its role in controlling immune responses. *Nat Commun*. (2019) 10:2123. doi: 10.1038/s41467-019-10015-4

74. Pearce EL, Poffenberger MC, Chang CH, Jones RG. Fueling immunity: insights into metabolism and lymphocyte function. *Science*. (2013) 342:1242454. doi: 10.1126/science.1242454

75. Noman MZ, Hasmim M, Messai Y, Terry S, Kieda C, Janji B, et al. Hypoxia: a key player in antitumor immune response. A review in the theme: cellular responses to hypoxia. *Am J Physiol Cell Physiol*. (2015) 309:C569–79. doi: 10.1152/ajpcell.00207.2015

76. Zhang Y-X, Zhao Y-Y, Shen J, Sun X, Liu Y, Liu H, et al. Nanoenabled modulation of acidic tumor microenvironment reverses anergy of infiltrating T cells and potentiates anti-PD-1 therapy. *Nano Lett*. (2019) 19:2774–83. doi: 10.1021/acs.nanolett.8b04296

77. Ciarlo E, Heinonen T, Herderschee J, Fenwick C, Mombelli M, Le Roy D, et al. Impact of the microbial derived short chain fatty acid propionate on host susceptibility to bacterial and fungal infections in vivo. *Sci Rep*. (2016) 6:37944. doi: 10.1038/srep37944

78. Sumbria D, Berber E, Rouse BT. Supplementing the diet with sodium propionate suppresses the severity of viral immuno-inflammatory lesions. *J Virol*. (2021) 95:20. doi: 10.1128/JVI.02056-20

79. Leone RD, Powell JD. Metabolism of immune cells in cancer. *Nat Rev Cancer*. (2020) 20:516–31. doi: 10.1038/s41568-020-0273-y

80. Gemta LF, Siska PJ, Nelson ME, Gao X, Liu X, Locasale JW, et al. Impaired enolase 1 glycolytic activity restrains effector functions of tumor-infiltrating CD8(+) T cells. *Sci Immunol*. (2019) 4:9520. doi: 10.1126/sciimmunol.aap9520

81. Singer K, Cheng W-C, Kreutz M, Ho P-C, Siska PJ. Immunometabolism in cancer at a glance. *Dis Model Mech*. (2018) 11:34272. doi: 10.1242/dmm.034272

82. Huldani H, Malviya J, Rodrigues P, Hjazi A, Deorari MM, Al-Hetty HRAK, et al. Discovering the strength of immunometabolism in cancer therapy: employing metabolic pathways to enhance immune responses. *Cell Biochem Funct*. (2024) 42:e3934. doi: 10.1002/cbf.3934

83. Yang C, Huang Y, Zhou Y, Zang X, Deng H, Liu Y, et al. Cryptococcus escapes host immunity: what do we know? *Front Cell Infect Microbiol*. (2022) 12:1041036. doi: 10.3389/fcimb.2022.1041036

84. de Sousa JR, Sotto MN, Simões Quaresma JA. Leprosy as a complex infection: breakdown of the Th1 and Th2 immune paradigm in the immunopathogenesis of the disease. *Front Immunol*. (2017) 8:1635. doi: 10.3389/fimmu.2017.01635

85. Castell L, Vance C, Abbott R, Marquez J, Eggleton P. Granule localization of glutaminase in human neutrophils and the consequence of glutamine utilization for neutrophil activity. *J Biol Chem*. (2004) 279:13305–10. doi: 10.1074/jbc.M309520200

86. Oladipo IC, Adeoye IO, Onawumi OOE. Antimicrobial activity of picolinic acid. *Elixir Appl Chem*. (2013) 58:14759–61.

87. Yoon BK, Jackman JA, Valle-González ER, Cho NJ. Antibacterial free fatty acids and monoglycerides: biological activities, experimental testing, and therapeutic applications. *Int J Mol Sci*. (2018) 19:1114. doi: 10.3390/ijms19041114

88. Khovidhunkit W, Kim M-S, Memon RA, Shigenaga JK, Moser AH, Feingold KR, et al. Effects of infection and inflammation on lipid and lipoprotein metabolism: mechanisms and consequences to the host. *J Lipid Res*. (2004) 45:1169–96. doi: 10.1194/jlr.R300019-JLR200

frontiers | Frontiers in Immunology

TYPE Original Research
PUBLISHED 28 February 2025
DOI 10.3389/fimmu.2025.1512293

OPEN ACCESS

EDITED BY
Helena Sá,
Unidade Local de Saúde de Coimbra, Portugal

REVIEWED BY
Liyun He,
Sun Yat-sen University Cancer Center (SYSUCC), China
Ziying Wu,
Central South University, China

*CORRESPONDENCE
Yanchun Ding
yanchunding0880@163.com
Xia Li
lixia416@163.com

†These authors have contributed equally to this work

RECEIVED 16 October 2024
ACCEPTED 11 February 2025
PUBLISHED 28 February 2025

CITATION
Ma R, Zhang C, Liu J, Ren J, Huang H, Wang G, Ding Y and Li X (2025) Associations of magnesium depletion score with the incidence and mortality of osteoarthritis: a nationwide study.
Front. Immunol. 16:1512293.
doi: 10.3389/fimmu.2025.1512293

Associations of magnesium depletion score with the incidence and mortality of osteoarthritis: a nationwide study

Ruicong Ma[1†], Cheng Zhang[2†], Jiaqing Liu[2], Jinyi Ren[2], Huina Huang[2], Guan Wang[2], Yanchun Ding[1*] and Xia Li[2*]

[1]Department of Cardiology, The Second Hospital of Dalian Medical University, Dalian, Liaoning, China, [2]Department of Immunology, College of Basic Medical Science, Dalian Medical University, Dalian, Liaoning, China

Background: Magnesium is an essential immune nutrient for the body, and recent studies have found that it plays an important role in osteoarthritis (OA). Magnesium depletion score(MDS) is a new method for evaluating the magnesium status of the body. Our objective is to explore the association between MDS and the incidence of OA, as well as the relationship between MDS and mortality in patients with OA.

Methods: Eligible participants were obtained from NHANES from 2005 to 2018. Logistic regression models were employed to evaluate the link between MDS and the incidence of OA. Cox regression models were employed to evaluate the link between MDS and mortality among OA patients. In addition, restricted cubic spline was utilized to explore the correlation between MDS and the incidence of OA, as well as the relationship between MDS and mortality in patients with OA. Subgroup analysis were adopted in order to ensure the credibility of the results in different subgroups, including age, gender, race, education level, BMI, smoking, diabetes and hypertension.

Results: 19,394 individuals qualified for analysis, including 3,256 OA patients. After excluding missing follow-up data, 630 all-cause deaths and 172 cardiovascular deaths (CVDs) were observed in 3,250 OA patients. The individuals with OA had higher levels of MDS. In the logistic regression model, MDS was positively related to OA (MDS≥3 vs. MDS=0, OR =1.83 (1.46-2.30, P<0.001)). Besides, a positive association was observed between MDS and all-cause mortality [MDS≥3 vs. MDS=0, HR =2.56 (1.49-4.41, P<0.001)] and CVDs [MDS≥3 vs. MDS=0, HR =3.00 (1.13-7.98, P=0.01)] in cox regression models. In addition, a 1-unit rise in MDS was significantly linked to an increased risk of mortality. Restricted cubic spline indicated a positive relationship between MDS and incidence and mortality of OA. Subgroup analysis demonstrated that the results are stable in different subgroups.

10.3389/fimmu.2025.1512293

Conclusions: MDS is positively correlated with the incidence and mortality of OA. Optimizing the nutritional status of magnesium may bring benefits to OA patients.

KEYWORDS

osteoarthritis, NHANES, magnesium depletion score, all-cause mortality, cardiovascular mortality

Introduction

Osteoarthritis(OA) is a degenerative condition of the joints marked by stiffness, pain, and deformities (1). OA is particularly prevalent among middle-aged and elderly populations, affecting approximately 595 million people worldwide (2). OA affects about 14% of American adults. In addition, it is the second leading cause of labor loss, second only to cardiovascular disease. OA causes medical expenses and other economic losses of up to about $125 billion annually (3). Patients with OA might face an increased risk of mortality in comparison to the overall population (4–6). Although the prevention and surgical treatment measures have been effectively implemented, the incidence and mortality of OA are still difficult to control.

Recently, some studies have found that mineral elements are crucial in the development of OA (7, 8). Magnesium is one of the most important and abundant trace elements in cells. It is an auxiliary factor in enzymatic reactions (9). Furthermore, many metabolic reactions in the human body, including the production of ATP and the maintenance of normal mitochondrial function, rely on the participation of magnesium (10). Magnesium supplementation can reduce joint cartilage damage, apoptosis, and promote chondrocyte generation (11, 12). Moreover, administering intra-articular magnesium injections can help reduce pain in both OA rats and patients (13, 14). Therefore, magnesium plays an important role in OA.The National Institutes of Health (NIH) in the United States pointed out that assessing magnesium levels in the body is very difficult due to the fact that most magnesium remains in tissues or cells. The detection of serum magnesium in clinical practice is not accurate (15). Due to the lack of an effective method for evaluating the magnesium status of the body at present, the significance of magnesium deficiency in OA has been largely neglected.

The magnesium depletion score (MDS) serves as an effective instrument for evaluating the body's magnesium levels. An increase in MDS indicates severe magnesium deficiency in the individual. Fan et al. found that MDS has greater value in evaluating the magnesium status of the body compared with serum magnesium. Furthermore, high MDS may indicate an inflammatory state which is linked to increased long-term mortality in individuals (16). In addition, other studies also revealed that an elevation in MDS is related to an increased risk of abdominal aortic calcification, cardiovascular disease and diabetes retinopathy (17–19). Nonetheless, the relationship between MDS and the incidence and mortality of OA remains ambiguous. Therefore, our objective is to explore the association between MDS and the incidence of OA, as well as the relationship between MDS and mortality in patients with OA.

Materials and methods

Data source and study population

Data for this research were sourced from the National Health and Nutrition Examination Survey (NHANES) database (www.cdc.gov/nchs/nhanes.com).

Part I: The inclusion criteria are as follows: The participants from NHANES between 2005 and 2018. The exclusion criteria are as follows: participants younger than 40 years, participants without OA information and those missing data on MDS.

Part II: Based on Part I, we have developed inclusion and exclusion criteria. The inclusion criteria are as follows: participants with OA. The exclusion criteria are as follows: those missing data on follow-up information.

The assessment of MDS

The MDS calculation comprised the consolidation of four separate scores: (1) the use of diuretics at present received 1 point; (2) using a proton pump inhibitor (PPI) also earned 1 point; (3) an estimated glomerular filtration rate (eGFR) ranging from 60 mL/min/1.73 m^2 to less than 90 mL/min/1.73 m^2 was assigned 1 point, whereas an eGFR below 60 mL/min/1.73 m^2 received 2 points; (4) heavy alcohol consumption (defined as more than 1 drink per day for women and over 2 drinks per day for men) was allocated 1 point (18).

Covariates

Demographic information encompasses age, gender, ethnicity, education levels, body mass index (BMI) and poverty income ratio (≤1.30, 1.31–3.49 and ≥3.50). Physical activity data was obtained through a questionnaire survey. Laboratory tests include total

cholesterol (TC) (mmol/L), glycated hemoglobin (HbA1c) (%), calcium (mmol/L) and phosphorus (mmol/L). Dietary factors (magnesium intake, calcium intake, phosphorus intake, vitamin D intake), smoking status and comorbidities (hypertension and diabetes) are also included. Dietary data is sourced from a dietary recall survey. Oxidative stress is closely related to the occurrence and development of OA. Antioxidant diet may be an easily accepted treatment strategy. Based on previously published articles on OA, we also calculated the composite dietary antioxidant index (CDAI). It comprises a composite score of six dietary antioxidants: vitamins A, C, and E, as well as selenium, zinc, and carotenoids (20). The criteria for diagnosing hypertension include: SBP ≥ 140 mmHg or DBP ≥ 90 mmHg and the patients using antihypertensive medications (21). The criteria used for diagnosing diabetes include: doctor diagnosis as diabetes, HbA1c ≥ 6.5%, fasting glucose ≥ 7.0mmol/L, random blood glucose ≥ 11.1mmol/L, 2h OGTT blood glucose ≥ 11.1mmol/L, or the administration of diabetes medications and insulin therapy (22).

Mortality

The mortality statistics were connected up to December 31, 2019 (https://www.cdc.gov/nchs/data-linkage/mortality.htm). Outcomes were divided into categories of all-cause deaths and CVDs. Death causes were classified according to ICD-10 codes, with CVDs specifically identified using codes 100-109, 111, 113, and 120-151 (23).

Statistical analysis

NHANES is conducted in a complex multi-stage sampling design. Moreover, NHANES is conducted in two-year cycles and includes a representative sample of the U.S. population. Standard error of mean (SEM) reflects the representativeness of sample mean to population mean. Weighted percentages can better represent the overall population. Therefore, SEM and weighted percentage might be more appropriate. Initially, continuous variables were represented as means corresponding standard error of the mean (mean ± SEM) and categorical variables were presented as means [95% confidence intervals (CI)]. The differences between the two groups were compared using chi-square tests and independent-sample t tests. P values < 0.05 were recognized statistically significant. The purpose of regression analysis is to observe the degree of correlation between the dependent variable and the independent variable after adjusting for various confounding factors. To examine the relationship between MDS and the incidence of OA, weighted logistic regression analyses were conducted. Three models were developed: unadjusted, Model I, and Model II. Model I was adjusted for age, sex, and race. Model II was adjusted for age, sex, ethnicity, education levels, BMI, smoking, HbA1c, TC, hypertension, DM, calcium, phosphorus, phosphorus intake, calcium intake, magnesium intake, CDAI, vitamin D intake, physical activity and poverty income ratio. The restricted cubic spline(RCS) curve can more vividly observe the relationship between the dependent variable and the independent variable. RCS analysis was employed to investigate the link between MDS and the incidence of OA. The purpose of subgroup analysis is to divide the study population into different groups based on certain characteristics (such as age, gender, comorbidities, etc.) to observe whether experimental variables have different effects in these different groups. Additionally, subgroup analysis was conducted to determine if the relationship between MDS and the incidence of OA remained consistent across various groups. These subgroups include age, gender, race, education level, BMI, smoking, diabetes and hypertension.

Additionally, weighted Kaplan-Meier curves and log-rank tests were utilized to examine the cumulative survival differences among different MDS groups. Cox regression analysis was carried out to investigate the link between MDS and mortality with OA. The variables included in the model are consistent with cox regression analysis model. Similarly, RCS was employed to investigate the relationship between MDS and mortality. Additionally, subgroup analysis was performed to further verify the robustness of the findings.

Besides, sensitivity analysis was also used to further validate our results. In many studies, weighted and unweighted results may be inconsistent. Consequently, we conducted unweighted Cox regression to carry out sensitivity analysis. Additionally, we also excluded OA patients who died within two years to further analyze the link between MDS and mortality.

Results

The link between MDS and OA

The participants from NHANES between 2005 and 2018 (n = 70,190), we eliminated subjects younger than 40 years (n = 43,908), subjects without OA information (n = 3,211), those missing data on magnesium depletion score (n = 3,677). Consequently, the cross-sectional analysis sample comprised 19,394 participants. Detailed information of the screening process is shown in Figure 1. 19,394 adults were screened for this cross-sectional study, including 3,256 OA patients. The clinical baseline characteristics of non-OA and OA participants are presented in Table 1, including age, gender, ethnicity, educational levels, BMI, HbA1c, TC, calcium, phosphorus, phosphorus intake, calcium intake and magnesium intake, smoking, hypertension, diabetes. Individuals in the OA group tend to be older (63.57 ± 0.26vs.55.72 ± 0.16), with a higher likelihood of being female (64.85%vs.49.09%), white (84.05% vs.70.77%), and former smokers (51.32%vs.46.28%), as well as a greater proportion of those who have hypertension (64.06%vs.45.73%), and diabetes (23.56%vs.18.01%)(P<0.001). We also found differences between laboratory examination measurements (HbA1c, TC, serum calcium and phosphorus) and dietary factors (phosphorus intake, calcium intake and magnesium intake) (P < 0.001). Supplementary Table S1 presents the baseline characteristics of the participants categorized by their MDS levels. Compared with the MDS=0 group, patients in the MDS≥3 group were older (68.65 ± 0.35vs.50.61 ± 0.17), had higher BMI (30.77 ±

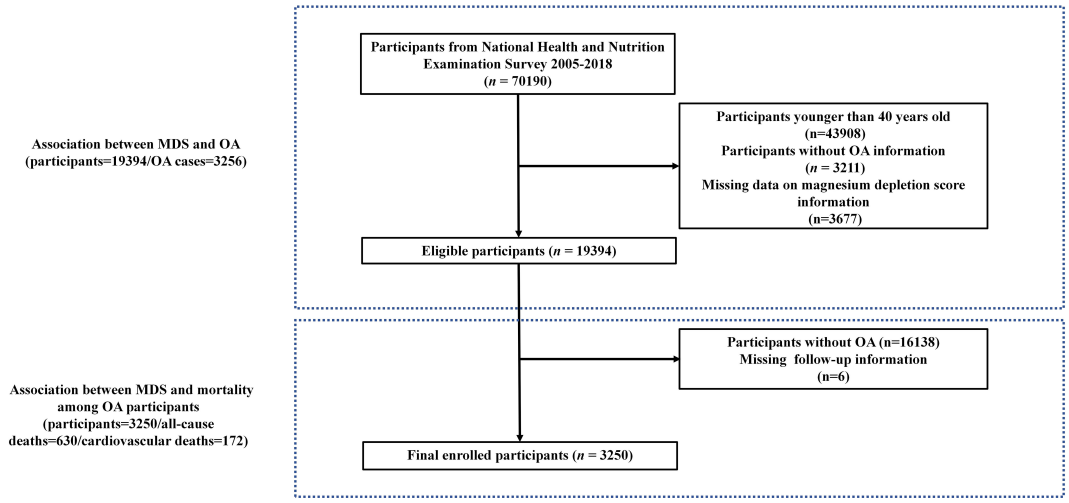

FIGURE 1
The flow chart of participant selection.

TABLE 1 Clinical characteristics of study population.

Variables	Overall	Non-OA	OA	*P* value
Age, %	57.22±0.16	55.72±0.16	63.57±0.26	<0.001
Sex, %				<0.001
Female	52.09(49.33,54.84)	49.09(48.24,49.94)	64.85(62.94,66.76)	
Male	47.91(45.24,50.58)	50.91(50.06,51.76)	35.15(33.24,37.06)	
Race/ethnicity, %				<0.001
White	73.30(67.44,79.15)	70.77(68.23,73.31)	84.05(82.10,86.01)	
Black	9.46(8.46,10.45)	10.25(8.90,11.60)	6.10(4.99, 7.22)	
Mexican	6.32(5.34, 7.30)	7.21(5.99,8.42)	2.56(1.88,3.24)	
Others	10.92(9.95,11.89)	11.78(10.58,12.98)	7.29(6.14, 8.43)	
Education levels, %				<0.001
Less than high school	15.36(14.15,16.57)	16.14(14.94,17.34)	12.09(10.58,13.60)	
High school or equivalent	23.53(21.75,25.31)	23.61(22.43,24.80)	23.21(21.04,25.38)	
College or above	61.07(57.35,64.78)	60.24(58.40,62.09)	64.70(62.21,67.19)	
BMI, kg/m2	29.30±0.08	28.95±0.09	30.77±0.20	<0.001
HbA1c, %	5.78±0.01	5.77±0.01	5.84±0.02	<0.001
TC, mmol/L	5.17±0.01	5.19±0.01	5.13±0.02	0.02
Serum calcium, mmol/L	2.35±0.00	2.35±0.00	2.36±0.00	0.01
Serum phosphorus, mmol/L	1.20±0.00	1.19±0.00	1.22±0.00	<0.001
Magnesium intake, mg	305.46±1.92	308.01±2.17	294.60±3.46	0.001
Calcium intake, mg	940.36±7.09	946.58± 7.56	913.88±14.47	0.03
Phosphorus intake, mg	1360.89±7.11	1375.73± 7.83	1297.79±15.98	<0.001
Vitmain D intake,mcg	4.67±0.07	4.70±0.08	4.55±0.13	0.28
CDAI	0.75(0.62,0.87)	0.77(0.63,0.91)	0.65(0.45,0.85)	0.33

(Continued)

TABLE 1 Continued

Variables	Overall	Non-OA	OA	*P* value
Physical activity, %				0.08
No	53.00(50.22,55.78)	52.55(50.92,54.18)	54.90(52.44,57.36)	
Yes	47.00(43.81,50.19)	47.45(45.82,49.08)	45.10(42.64,47.56)	
Poverty income ratio, %				0.19
≤1.30	15.50(14.27,16.72)	16.89(15.51,18.27)	15.40(13.69,17.10)	
1.31–3.49	32.27(30.15,34.39)	34.25(32.70,35.81)	35.96(33.56,38.35)	
≥3.50	45.55(42.00,49.10)	48.86(46.61,51.10)	48.65(45.43,51.87)	
Smoking, %				<0.001
No	52.74(50.02,55.46)	53.72(52.45,54.99)	48.68(46.05,51.31)	
Yes	47.22(44.19,50.26)	46.28(45.01,47.55)	51.32(48.69,53.95)	
Hypertension, %				<0.001
No	50.78(47.70,53.85)	54.27(52.93,55.62)	35.94(33.52,38.36)	
Yes	49.22(46.55,51.88)	45.73(44.38,47.07)	64.06(61.64,66.48)	
DM, %				<0.001
No	80.86(76.34,85.39)	81.99(81.10,82.88)	76.44(74.54,78.33)	
Yes	19.05(17.92,20.19)	18.01(17.12,18.90)	23.56(21.67,25.46)	

Continuous data were presented as the mean±SEM, category data were presented as the proportion and 95% confidence interval. SEM, Standard Error of the Mean; BMI, body mass index; HbA1c, glycosylated hemoglobin; MDS, Magnesium depletion score; TC, total cholesterol; CDAI, composite dietary antioxidant index; DM, diabetes mellitus.

TABLE 2 MDS and its components among non-OA group and OA group.

Variables	Overall	Non-OA	OA	*P* value
MDS	1.09±0.01	1.01±0.01	1.47±0.02	<0.001
Diuretic use				<0.001
No	83.69(79.12,88.25)	85.86(85.04,86.69)	74.44(72.35,76.52)	
Yes	16.31(15.21,17.41)	14.14(13.31,14.96)	25.56(23.48,27.65)	
PPI use				<0.001
No	88.22(83.70,92.74)	90.58(89.88,91.29)	78.18(76.49,79.88)	
Yes	11.78(10.74,12.82)	9.42(8.71,10.12)	21.82(20.12,23.51)	
Heavy drinking				0.01
No	83.77(79.25,88.28)	83.26(82.16,84.37)	85.89(84.17,87.61)	
Yes	16.23(14.93,17.54)	16.74(15.63,17.84)	14.11(12.39,15.83)	
EGFR scores				<0.001
0	45.15(42.83,47.47)	48.44(47.02,49.86)	31.17(29.13,33.21)	
1	44.75(41.82,47.69)	42.91(41.66,44.15)	52.61(50.45,54.77)	
2	10.10(9.32,10.87)	8.66(8.07, 9.25)	16.22(14.73,17.72)	

Data were presented as the mean±SEM. SEM, Standard Error of the Mean; MDS, Magnesium depletion score; OA,osteoarthritis; PPI, proton pump inhibitor; eGFR, estimated glomerular filtration rate.

10.3389/fimmu.2025.1512293

TABLE 3 Weighted logistic regression analysis on the association between MDS and OA.

	Non-adjusted model		Model I		Model II	
	OR [95% CI]	*P* value	OR [95% CI]	*P* value	OR [95% CI]	*P* value
Continuous MDS	1.59(1.52,1.66)	<0.001	1.25(1.19,1.32)	<0.001	1.22(1.14,1.30)	<0.001
MDS=0	Reference	–	Reference	–	Reference	–
MDS=1	1.76(1.52,2.04)	<0.001	1.28(1.08,1.50)	0.004	1.19(0.98,1.43)	0.07
MDS=2	2.79(2.39,3.26)	<0.001	1.61(1.34,1.94)	<0.001	1.48(1.19,1.85)	<0.001
MDS≥3	4.35(3.72,5.09)	<0.001	2.02(1.67,2.44)	<0.001	1.83(1.46,2.30)	<0.001

Data are presented as OR (95% CI). Model I adjusted for age, sex and race/ethnicity. Model II adjusted for age, sex, race/ethnicity, education levels, BMI, smoking, HbA1c, TC, hypertension, DM, calcium, phosphorus, phosphorus intake, calcium intake, magnesium intake, CDAI, vitmain D intake, physical activity and poverty income ratio. MDS, Magnesium depletion score; OA, osteoarthritis.

0.22vs.29.25 ± 0.12), HbA1c (6.01 ± 0.03vs.5.77 ± 0.02), and had a larger proportion of smoking (51.09%vs.44.55%), hypertension (86.64%vs.33.39%) and diabetes (34.11%vs.16.04%). We can also find that the incidence of OA gradually increases with the increase of MDS. In addition, patients in the OA group have a higher level of MDS (1.47 ± 0.02vs.1.01 ± 0.01). We found that OA patients had higher use of diuretics (25.56%vs.14.14%) and PPIs (21.82% vs.9.42%), as well as lower eGFR (Table 2), which are components of MDS.

Additionally, a positive correlation was presented between MDS and the incidence of OA with an OR of 1.22 (95%CI: 1.14-1.30) in logistic regression analysis (Table 3). Compared with the group with MDS=0, the group with MDS≥3 has a higher incidence of OA (OR = 1.83, 95%CI: 1.46-2.30) in Model II. The use of unweighted multiple analysis as a sensitivity analysis also confirmed this result (Supplementary Table S3).

Figure 2 showed a non-linear positive link between MDS and the incidence of OA (p for overall < 0.001, p for non-linear = 0.04). Moreover, in various subgroups such as age, sex, smoking, and DM, positive relationships were observed between MDS and the incidence of OA (Supplementary Figure S1).

Subgroup analysis showed that the results were significant and stable. This relationship is slightly weakened in elderly people over 60 years old but still statistically significant (*P*<0.001) (Figure 3).

The link between MDS and mortality among OA individuals

Second, we excluded individuals without OA (n = 16,138) and those missing data on follow-up information (n = 6). Consequently, the sample comprised 3,250 participants. A total of 630 deaths from all causes and 172 fatalities due to CVDs were recorded until December 31, 2019 (Figure 1). 3,250 participants were involved in the cohort study, including 630 all-cause deaths and 172 CVDs. As illustrated in Supplementary Table S2, the data were categorized into four groups based on MDS levels. In comparison to the MDS≥3 group, individuals in the MDS=0 category exhibit a greater

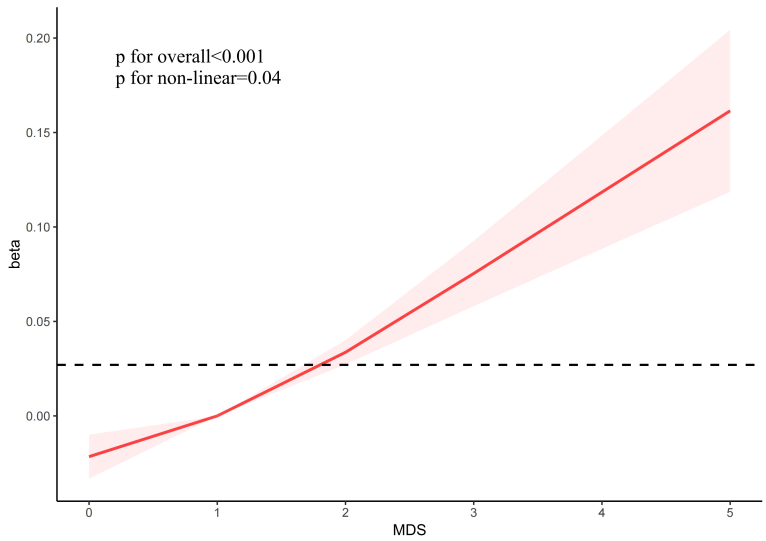

FIGURE 2
The correlation between MDS and the incidence of OA.

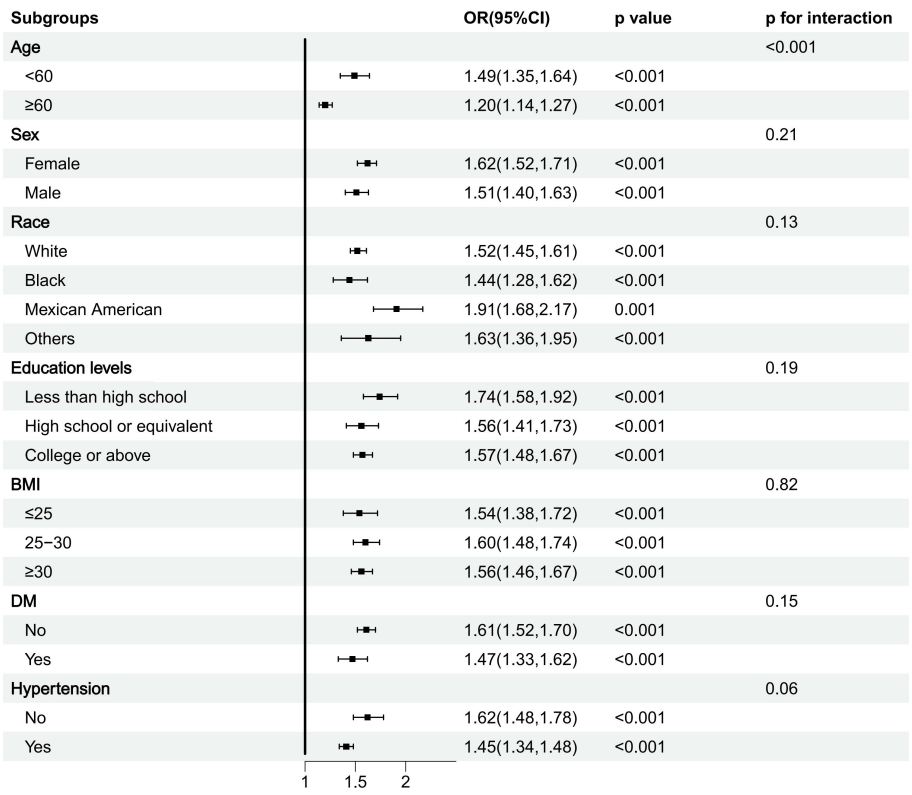

FIGURE 3
Subgroup analysis of MDS with the incidence of OA.

percentage of all-cause mortality (30.46%vs.6.79%) and CVDs (9.65% vs.1.93%) (P<0.001). Individuals in the MDS≥3 cohort tend to be older (70.29 ± 0.51vs.55.77 ± 0.46) and have a higher likelihood of being female (74.09%vs.66.60%) and white (88.20%vs.74.72%), as well as a greater prevalence of hypertension (89.00%vs.46.98%) and diabetes (35.96%vs.21.18%) (P<0.001). The differences were also found between laboratory examination measurements (HbA1c, TC and phosphorus) and dietary factors (phosphorus intake, calcium intake and magnesium intake) (P < 0.001).

Weighted Kaplan-Meier curves along with log-rank tests were employed to analyze the differences in cumulative survival across various MDS groups. The group with MDS≥3 has the highest all-cause mortality rate. The group with MDS=1 or MDS=2 has a moderate survival rate, while the group with MDS=0 have the highest survival rate (long-rank P<0.001) (Figure 4A). Similar death patterns are also reflected in CVDs (Figure 4B).

A positive association was observed between MDS and all-cause mortality with an HR of 1.44 (95%CI:1.27-1.62) (Table 4) and

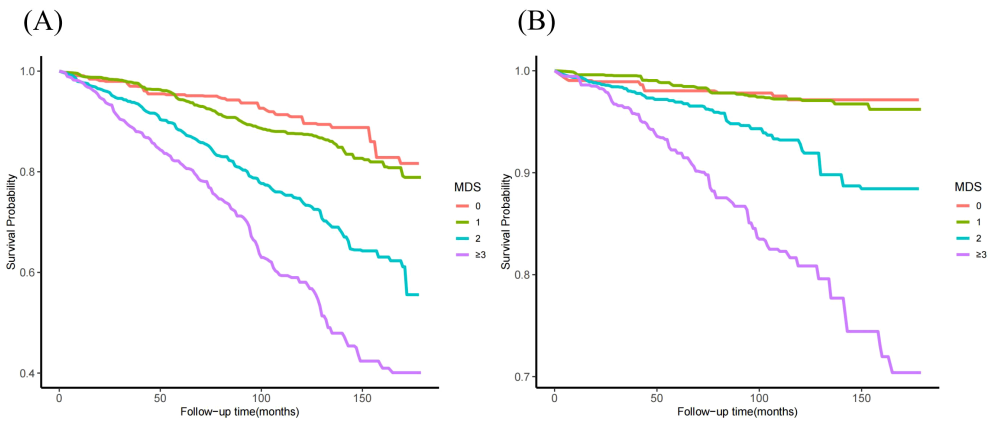

FIGURE 4
Kaplan-Meier survival analysis curves for mortality in different MDS groups. **(A)** all-cause mortality; **(B)** cardiovascular mortality.

TABLE 4 Cox regression analysis on the association between MDS and all-cause mortality.

	Non-adjusted model		Model I		Model II	
	HR [95% CI]	*P* value	HR [95% CI]	*P* value	HR [95% CI]	*P* value
Continuous MDS	1.69(1.54,1.85)	<0.001	1.48(1.35,1.61)	<0.001	1.44(1.27,1.62)	<0.001
MDS=0	Reference	–	Reference	–	Reference	–
MDS=1	1.28(0.77,2.13)	0.35	0.92(0.56,1.51)	0.75	0.98(0.51,1.86)	0.95
MDS=2	2.89(1.84,4.51)	<0.001	1.82(1.18,2.82)	0.01	1.71(1.13,2.95)	0.03
MDS≥3	5.05(3.16,8.05)	<0.001	2.81(1.81,4.38)	<0.001	2.56(1.49,4.41)	<0.001

Data are presented as HR (95% CI). Model I adjusted for age, sex and race/ethnicity. Model II adjusted for age, sex, race/ethnicity, education levels, BMI, smoking, HbA1c, TC, hypertension, DM, calcium, phosphorus, phosphorus intake, calcium intake, magnesium intake, CDAI, vitmain D, physical activity and poverty income ratio. MDS, Magnesium depletion score; OA, osteoarthritis.

cardiovascular mortality with an HR of 1.64 (95%CI: 1.33-2.02) (Table 5) in adjusted cox regression analysis. Besides, MDS was also positively related to all-cause mortality [MDS≥3 vs. MDS=0, HR =2.56 (1.49-4.41, *P*<0.001)] and CVDs [MDS≥3 vs. MDS=0, HR =3.00 (1.13-7.98, *P*=0.01)] as a categorical variable. Sensitivity analysis also confirmed this finding after excluding OA patients who died within two years (Supplementary Table S4).

Figure 5 showed a linear positive correlation between MDS and all-cause mortality (p for overall < 0.001, p for non-linear = 0.783) and CVDs (*P* for overall < 0.001, *P* for non-linear = 0.092) among OA individuals.

Subgroup analysis indicated that the results were significant and stable in most subgroups. Notably, this relationship was only significant in individuals aged 60 and above in the age subgroup (*P*<0.001) (Supplementary Figure S2).

Discussion

Our study indicates a positive correlation between MDS and the incidence of OA among US middle aged and elderly people. Subgroup analysis indicated that the results were significant and stable in most subgroups. Moreover, there was a positive correlation between MDS and the mortality of OA.

Magnesium plays an important role in inflammatory diseases and has good anti-inflammatory effects. Research has found that giving mice a high magnesium diet can reduce levels of inflammatory factors (IL-1β, TNF-α and IL-6) in the body, alleviate joint inflammation and joint damage. Mechanistically, magnesium increases the number of $Foxp3^{+}$Treg cells in an IL-10-dependent manner mediated by gut microbiota (24). The latest research has also found that magnesium can effectively reduce or even reverse the degeneration of cartilage tissue. Magnesium can enhance the proliferation and chondrogenic differentiation of bone marrow mesenchymal stem cells, and has the potential to promote joint cartilage regeneration. In addition, magnesium can also inhibit programmed cell death of chondrocytes, thereby protecting joint cartilage. For osteoclasts, magnesium can inhibit their generation and bone degradation functions (25). Therefore, magnesium has significant potential in the treatment of arthritis. The evaluation of MDS may have significant implications in OA.

In clinical practice, serum magnesium was often used to assess magnesium status. A study involving 2855 patients revealed that serum magnesium concentration was negatively linked to the incidence of imaging knee OA (26). Similarly, a meta-analysis showed that elevated serum magnesium levels correlate with a reduced incidence of OA, but this relationship is significantly affected by serum magnesium concentration (27). The possible

TABLE 5 Cox regression analysis on the association between MDS and cardiovascular mortality.

	Non-adjusted model		Model I		Model II	
	HR [95% CI]	*P* value	HR [95% CI]	*P* value	HR [95% CI]	*P* value
Continuous MDS	1.98(1.63,2.41)	<0.001	1.76(1.46,2.13)	<0.001	1.64(1.33, 2.02)	<0.001
MDS=0	Reference					
MDS=1	0.91(0.29, 2.80)	0.86	0.61(0.21,1.83)	0.38	0.68(0.22, 2.10)	0.51
MDS=2	2.53(0.89, 7.21)	0.08	1.53(0.57,4.13)	0.40	1.34(0.48, 3.73)	0.57
MDS≥3	6.43(2.28,18.08)	<0.001	3.47(1.35,8.95)	0.01	3.00(1.13, 7.98)	0.01

Data are presented as HR (95% CI). Model I adjusted for age, sex and race/ethnicity. Model II adjusted for age, sex, race/ethnicity, education levels, BMI, smoking, HbA1c, TC, hypertension, DM, calcium, phosphorus, phosphorus intake, calcium intake, magnesium intake, CDAI, vitmain D intake, physical activity and poverty income ratio. MDS, Magnesium depletion score; OA, osteoarthritis.

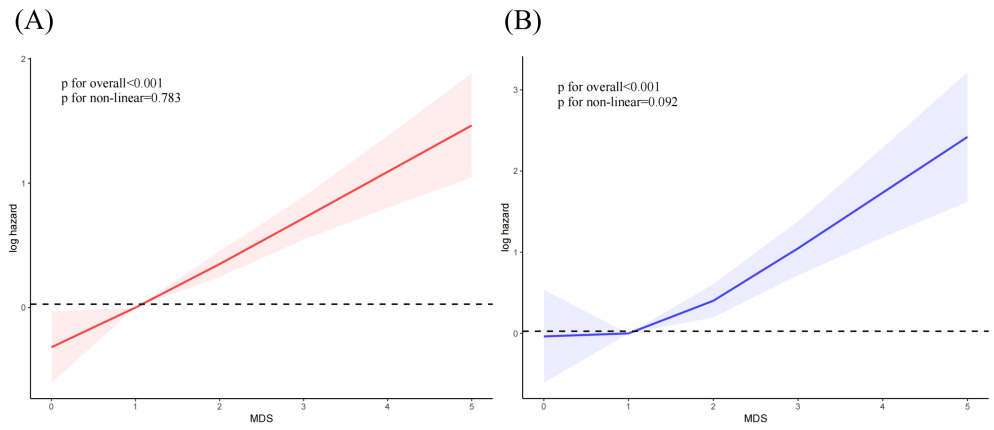

FIGURE 5
The correlation between MDS and mortality among OA individuals. **(A)** all-cause mortality; **(B)** cardiovascular mortality.

reason is that serum magnesium may not comprehensively reflect the magnesium status of the body. Especially in cases of chronic magnesium deficiency, serum magnesium may still remain at normal levels due to the body's compensation (28, 29). While serum magnesium is utilized in clinical practice, a clear correlation has yet to be established between serum magnesium concentrations and systemic magnesium levels or the concentrations found in particular tissues. In addition, the serum contain only holds 0.3% of the body's total magnesium, and most of the rest remain in the organization (30). The National Institutes of Health (NIH) in the United States has pointed out that assessing magnesium levels is difficult due to the fact that most magnesium is present in cells or bones. When determining magnesium deficiency, this may lead to misleading blood test results. More than 80% of serum magnesium undergoes filtration and reabsorption in the kidneys. MDS incorporates pathophysiological factors influencing the renal reabsorption capability. Research has found that compared to serum magnesium, MDS has greater value in predicting the body's magnesium status (16). Furthermore, the four risk factors included in MDS (current use of diuretics and PPIs, heavy alcohol consumption, and kidney function) are easily assessable in clinical practice.

Evaluating urinary magnesium offers an additional approach for determining the body's magnesium levels, but it is easily influenced by diet, medication, and kidney disease (31). And for people with limited mobility, monitoring 24-hour urinary magnesium is difficult to widely implement (32). The evaluation of magnesium tolerance is considered the benchmark for determining the magnesium levels within the body. However, its application is severely limited due to the complexity of its operation and its unsuitability for patients with renal dysfunction (33). MDS is a practical tool for assessing the magnesium status of the body (16). Therefore, exploring its relationship with diseases may provide important guidance for clinical practice.

Magnesium deficiency is very common in middle-aged and elderly populations, with reasons including insufficient magnesium intake and increased excretion caused by various medications (34). In the cross-sectional study, our study found that this relationship between MDS and the incidence of OA is slightly weakened in elderly people over 60 years old but still statistically significant (P<0.001). We consider that the difference in magnesium deficiency levels between non-OA and OA patients in the elderly population may gradually narrow. This may be one of the possible reasons for the occurrence of this result. Additionally, this link between MDS and mortality was only significant in individuals aged 60 and above in the cohort study. Elderly OA patients often have multiple comorbidities and a higher proportion of diuretic use, often accompanied by renal dysfunction. This may partially explain the significant relationship between MDS and all-cause mortality in elderly OA patients. Therefore, in OA patients over 60 years old, MDS may be a better tool for assessing prognosis. Furthermore, we also observed that MDS is significantly associated with the incidence of OA and the death of OA patients in the subgroups of hypertension and diabetes (P<0.001). However, no significant interaction was observed between the two subgroups. This shows that the effect of magnesium deficiency on OA is not affected by hypertension and diabetes.

MDS consists of four elements that influence renal reabsorption: alcohol intake, the usage of diuretics, the use of PPIs, and kidney function (16). PPI mainly causes magnesium deficiency in the body by affecting the intestinal reabsorption of magnesium (35). Some patients who use PPIs in clinical practice may experience hypomagnesemia, but this phenomenon can be alleviated by supplementing magnesium or discontinuing medication. Recent studies have shown that the use of PPIs may accelerate the progression of OA (36), possibly through drug-induced magnesium deficiency, which is consistent with our research findings. Alcohol is deemed crucial for magnesium excretion. The mechanism may be that excessive alcohol use cause renal tubular damage, resulting in an increase in urinary magnesium (37). Magnesium deficiency may trigger systemic inflammatory reactions and promote the production of inflammatory mediators by chondrocytes and synovial cells, ultimately damaging the synthesis of articular cartilage (38). Omeprazole is a classic proton pump inhibitor. Omeprazole may cause an increase in segmental pH value in the small intestine after inhibiting gastric acid secretion, leading to a

decrease in Mg^{2+} dissolution and reabsorption (39). Another presumed mechanism for the diminished absorption of magnesium by intestinal epithelial cells involves the PPIs-induced inhibition of transient receptor potential melastatin-6 (TRPM6) and TRPM7 channels. These factors lead to magnesium deficiency, which triggers joint inflammation and promotes the progression of OA (40). The kidneys are the most important organ for magnesium reabsorption, and the body's magnesium balance depends on the involvement of the kidneys (41). Many diuretics also act on the renal tubules and inhibit magnesium reabsorption (42). For example, thiazide diuretics can act on the renal tubules, significantly reducing the reabsorption of magnesium in the body and serum magnesium concentration, indirectly inducing joint inflammation and the occurrence of OA (43).

In addition, we found that the use of diuretics and decreased renal function are risk factors for mortality in OA patients. Previous studies have shown that renal dysfunction is an independent risk factor for mortality (44). Besides, middle-aged and elderly people are often accompanied by other diseases, including cardiovascular disease, hypertension, diabetes, etc. It is understandable that those who take diuretics face an increased risk of mortality.

Despite the advantage of NHANES large sample research, our study still has some limitations. First, we cannot identify a causal association due to the type of cross-sectional study. Second, the results from the study mainly apply to the American population. Third, while the study utilizes MDS, the reliance on indirect markers (diuretic and PPI use) may not fully capture magnesium deficiency. we are unable to compare their advantages and disadvantages due to the lack of serum magnesium and urinary magnesium. Large prospective studies are needed in the future to further validate the role of MDS in evaluating magnesium deficiency. Finally, there may still be other confounding factors affecting the results although many variables are included.

Conclusion

MDS is positively correlated with the incidence and mortality of OA. Optimizing the nutritional status of magnesium may bring benefits to OA patients.

Data availability statement

Publicly available datasets were analyzed in this study. This data can be found here: https://www.cdc.gov/nchs/nhanes/.

Ethics statement

The data is accessible to the public (found in the NHANES database), therefore there is no need for an ethical approval statement or informed consent for the study.

Author contributions

RM: Writing – original draft. CZ: Writing – original draft. JL: Data curation, Methodology, Writing – original draft. JR: Data curation, Writing – original draft. HH: Data curation, Writing – original draft. GW: Writing – review & editing. YD: Writing – review & editing. XL: Writing – review & editing.

Funding

The author(s) declare financial support was received for the research, authorship, and/or publication of this article. This work was supported by grants from Dalian Medical University Interdisciplinary Research Cooperation Project Team Funding (JCHZ2023010).

Conflict of interest

The authors declare that the research was conducted in the absence of any commercial or financial relationships that could be construed as a potential conflict of interest.

Generative AI statement

The author(s) declare that no Generative AI was used in the creation of this manuscript.

Publisher's note

Supplementary material

The Supplementary Material for this article can be found online at: https://www.frontiersin.org/articles/10.3389/fimmu.2025.1512293/full#supplementary-material

SUPPLEMENTARY FIGURE 1
The correlation between MDS and the incidence of OA in different subgroups. **(A)** Age; **(B)** Sex; **(C)** Smoke; **(D)** DM.

SUPPLEMENTARY FIGURE 2
Subgroup analysis of MDS with mortality among OA individuals. **(A)** all-cause mortality; **(B)** cardiovascular mortality.

References

1. Castagno S, Birch M, van der Schaar M, McCaskie A. Predicting rapid progression in knee osteoarthritis: a novel and interpretable automated machine learning approach, with specific focus on young patients and early disease. *Ann Rheum Dis*. (2024), ard–2024-225872. doi: 10.1136/ard-2024-225872

2. GBD 2021 Osteoarthritis Collaborators. Global, regional, and national burden of osteoarthritis, 1990-2020 and projections to 2050: a systematic analysis for the global burden of disease study 2021. *Lancet Rheumatol*. (2023) 5(9):e508–22. doi: 10.1016/S2665-9913(23)00163-7

3. Chen N, Fong DYT, Wong JYH. Health and economic outcomes associated with musculoskeletal disorders attributable to high body mass index in 192 countries and territories in 2019. *JAMA Netw Open*. (2023) 6(1):e2250674. doi: 10.1001/jamanetworkopen.2022.50674

4. Losina E, Walensky RP, Reichmann WM, Holt HL, Gerlovin H, Solomon DH, et al. Impact of obesity and knee osteoarthritis on morbidity and mortality in older americans. *Ann Intern Med*. (2011) 154(4):217–26. doi: 10.7326/0003-4819-154-4-201102150-00001

5. Mendy A, Park J, Vieira ER. Osteoarthritis and risk of mortality in the USA: a population-based cohort study. *Int J Epidemiol.*. (2018) 47(6):1821–9. doi: 10.1093/ije/dyy187

6. Barbour KE, Lui LY, Nevitt MC, Murphy LB, Helmick CG, Theis KA, et al. Hip osteoarthritis and the risk of all-cause and disease-specific mortality in older women: A population-based cohort study. *Arthritis Rheumatol*. (2015) 67(7):1798–805. doi: 10.1002/art.39113

7. Zhou J, Liu C, Sun Y, Francis M, Ryu MS, Grider A, et al. Genetically predicted circulating levels of copper and zinc are associated with osteoarthritis but not with rheumatoid arthritis. *Osteoarthritis Cartilage.*. (2021) 29(7):1029–35. doi: 10.1016/j.joca.2021.02.564

8. Yao H, Xu J, Wang J, Zhang Y, Zheng N, Yue J, et al. Combination of magnesium ions and vitamin c alleviates synovitis and osteophyte formation in osteoarthritis of mice. *Bioact Mater*. (2020) 6(5):1341–52. doi: 10.1016/j.bioactmat.2020.10.016

9. Bravo M, Simón J, González-Recio I, Martinez-Cruz LA, Goikoetxea-Usandizaga N, Martínez-Chantar ML. Magnesium and liver metabolism through the lifespan. *Adv Nutr*. (2023) 14(4):739–51. doi: 10.1016/j.advnut.2023.05.009

10. Volpe SL. Magnesium in disease prevention and overall health. *Adv Nutr*. (2013) 4(3):378S–83S. doi: 10.3945/an.112.003483

11. Li Y, Yue J, Yang C. Unraveling the role of mg(++) in osteoarthritis. *Life Sci*. (2016) 147:24–9. doi: 10.1016/j.lfs.2016.01.029

12. Kuang X, Chiou J, Lo K, Wen C. Magnesium in joint health and osteoarthritis. *Nutr Res*. (2021) 90:24–35. doi: 10.1016/j.nutres.2021.03.002

13. Yao H, Xu JK, Zheng NY, Wang JL, Mok SW, Lee YW, et al. Intra-articular injection of magnesium chloride attenuates osteoarthritis progression in rats. *Osteoarthritis Cartilage.*. (2019) 27(12):1811–21. doi: 10.1016/j.joca.2019.08.007

14. He Y, He H, Li X, Lei G, Xie D, Wang Y. Intra-articular magnesium plus bupivacaine is the most effective and safe postoperative analgesic option following knee arthroscopy: A network meta-analysis. *Arthroscopy*. (2022) 38(10):2897–2908.e18. doi: 10.1016/j.arthro.2022.03.013

15. Zhou Z, Yao X. The kidney reabsorption-related magnesium depletion score is associated with cardiovascular disease and longitudinal mortality in diabetic kidney disease patients. *Diabetol Metab Syndr*. (2025) 17(1):38. doi: 10.1186/s13098-025-01598-8

16. Fan L, Zhu X, Rosanoff A, Costello RB, Yu C, Ness R, et al. Magnesium depletion score (MDS) predicts risk of systemic inflammation and cardiovascular mortality among US adults. *J Nutr*. (2021) 151(8):2226–35. doi: 10.1093/jn/nxab138

17. Lu J, Li H, Wang S. The kidney reabsorption-related magnesium depletion score is associated with increased likelihood of abdominal aortic calcification among US adults. *Nephrol Dial Transplant.*. (2023) 38(6):1421–9. doi: 10.1093/ndt/gfac218

18. Ye L, Zhang C, Duan Q, Shao Y, Zhou J. Association of magnesium depletion score with cardiovascular disease and its association with longitudinal mortality in patients with cardiovascular disease. *J Am Heart Assoc*. (2023) 12(18):e030077. doi: 10.1161/JAHA.123.030077

19. Chen Y, Xiang X, Wu Y, Han S, Huang Z, Wu M. Magnesium depletion score predicts diabetic retinopathy risk among diabetes: Findings from NHANES 2005-2018. *Biol Trace Elem Res*. (2023) 201(6):2750–6. doi: 10.1007/s12011-022-03384-3

20. Jiang W, Li J, Li H. Association between the composite dietary antioxidant index and all-cause mortality in individuals with osteoarthritis *via* NHANES data. *Sci Rep*. (2024) 14(1):30387. doi: 10.1038/s41598-024-81871-4

21. Zheng X, Zou P, Zeng C, Liu J, He Y. Increased levels of urine volatile organic compounds are associated with hypertension risk. *J Hypertens*. (2025) 43(1):136–44. doi: 10.1097/HJH.0000000000003878

22. Song J, Ma R, Yin L. Associations between estimated glucose disposal rate and arterial stiffness and mortality among US adults with non-alcoholic fatty liver disease. *Front Endocrinol (Lausanne).*. (2024) 15:1398265. doi: 10.3389/fendo.2024.1398265

23. Chang Q, Zhu Y, Liu Z, Cheng J, Liang H, Lin F, et al. Replacement of sedentary behavior with various physical activities and the risk of all-cause and cause-specific mortality. *BMC Med*. (2024) 22(1):385. doi: 10.1186/s12916-024-03599-2

24. Laragione T, Harris C, Azizgolshani N, Beeton C, Bongers G, Gulko PS. Magnesium increases numbers of Foxp3+ treg cells and reduces arthritis severity and joint damage in an IL-10-dependent manner mediated by the intestinal microbiome. *EBioMedicine*. (2023) 92:104603. doi: 10.1016/j.ebiom.2023.104603

25. Zheng L, Zhao S, Li Y, Xu J, Yan W, Guo B, et al. Engineered MgO nanoparticles for cartilage-bone synergistic therapy. *Sci Adv*. (2024) 10(10):eadk6084. doi: 10.1126/sciadv.adk6084

26. Zeng C, Wei J, Li H, Yang T, Zhang FJ, Pan D, et al. Relationship between serum magnesium concentration and radiographic knee osteoarthritis. *J Rheumatol*. (2015) 42(7):1231–6. doi: 10.3899/jrheum.141414

27. Wu Z, Yang J, Liu J, Lian K. The relationship between magnesium and osteoarthritis of knee: A MOOSE guided systematic review and meta-analysis. *Med (Baltimore).*. (2019) 98(45):e17774. doi: 10.1097/MD.0000000000017774

28. Adomako EA, Yu ASL. Magnesium disorders: Core curriculum 2024. *Am J Kidney Dis*. (2024) 83(6):803–15. doi: 10.1053/j.ajkd.2023.10.017

29. Fiorentini D, Cappadone C, Farruggia G, Prata C. Magnesium: Biochemistry, nutrition, detection, and social impact of diseases linked to its deficiency. *Nutrients*. (2021) 13(4):1136. doi: 10.3390/nu13041136

30. Jomova K, Makova M, Alomar SY, Alwasel SH, Nepovimova E, Kuca K, et al. Essential metals in health and disease. *Chem Biol Interact*. (2022) 367:110173. doi: 10.1016/j.cbi.2022.110173

31. Abbasi S, Mohebbi M, Mousavi Vahed SH, Dadgar Moghaddam M, Afiat M, Nematy M, et al. Comparison of magnesium status using 24-h urine magnesium content and magnesium fraction excretion in PCOS with non-PCOS control women: a cross-sectional study. *Biol Trace Elem Res*. (2023) 201(12):5601–6. doi: 10.1007/s12011-023-03626-y

32. Lo Piano F, Corsonello A, Corica F. Magnesium and elderly patient: the explored paths and the ones to be explored: a review. *Magnes Res*. (2019) 32(1):1–15. doi: 10.1684/mrh.2019.0453

33. Costello R, Rosanoff A, Nielsen F, West C. Perspective: Call for re-evaluation of the tolerable upper intake level for magnesium supplementation in adults. *Adv Nutr*. (2023) 14(5):973–82. doi: 10.1016/j.advnut.2023.06.008

34. Dominguez LJ, Veronese N, Barbagallo M. Magnesium and the hallmarks of aging. *Nutrients*. (2024) 16(4):496. doi: 10.3390/nu16040496

35. Chamniansawat S, Suksridechacin N, Thongon N. Current opinion on the regulation of small intestinal magnesium absorption. *World J Gastroenterol*. (2023) 29(2):332–42. doi: 10.3748/wjg.v29.i2.332

36. Zeng C, Neogi T, Chan AT, Wei J, Misra D, Lu N, et al. Proton pump inhibitor therapy and risk of knee replacement surgery: a general population-based cohort study. *Osteoarthritis Cartilage.*. (2022) 30(4):559–69. doi: 10.1016/j.joca.2021.12.010

37. Rivlin RS. Magnesium deficiency and alcohol intake: mechanisms, clinical significance and possible relation to cancer development (a review). *J Am Coll Nutr*. (1994) 13(5):416–23. doi: 10.1080/07315724.1994.10718430

38. Xu H, Kang JH, Choi SE, Park DJ, Kweon SS, Lee YH, et al. Increased alcohol intake is associated with radiographic severity of knee and hand osteoarthritis in men. *Sci Rep*. (2024) 14(1):12648. doi: 10.1038/s41598-024-63559-x

39. Gommers LMM, Hoenderop JGJ, de Baaij JHF. Mechanisms of proton pump inhibitor-induced hypomagnesemia. *Acta Physiol (Oxf).*. (2022) 235(4):e13846. doi: 10.1111/apha.13846

40. Cao S, Wei Y, Yue Y, Li G, Wang H, Lin J, et al. Omeprazole and risk of osteoarthritis: insights from a mendelian randomization study in the UK biobank. *J Transl Med*. (2024) 22(1):504. doi: 10.1186/s12967-024-05255-y

41. de Baaij JH, Hoenderop JG, Bindels RJ. Magnesium in man: implications for health and disease. *Physiol Rev*. (2015) 95(1):1–46. doi: 10.1152/physrev.00012.2014

42. Katopodis P, Karteris E, Katopodis KP. Pathophysiology of drug-induced hypomagnesaemia. *Drug Saf.*. (2020) 43(9):867–80. doi: 10.1007/s40264-020-00947-y

43. Wei J, Neogi T, Terkeltaub R, Fenves AZ, Zeng C, Misra D, et al. Thiazide diuretics and risk of knee replacement surgery among patients with knee osteoarthritis: a general population-based cohort study. *Osteoarthritis Cartilage.*. (2019) 27(10):1454–61. doi: 10.1016/j.joca.2019.05.020

44. Schlackow I, Simons C, Oke J, Feakins B, O'Callaghan CA, Hobbs FDR, et al. Long-term health outcomes of people with reduced kidney function in the UK: A modelling study using population health data. *PloS Med*. (2020) 17(12):e1003478. doi: 10.1371/journal.pmed.1003478

frontiers | Frontiers in Nutrition

TYPE Brief Research Report
PUBLISHED 17 March 2025
DOI 10.3389/fnut.2025.1533734

OPEN ACCESS

EDITED BY
Helena Sá,
Unidade Local de Saúde de Coimbra, Portugal

REVIEWED BY
Luz-Ma.-Adriana Balderas-Peña,
Instituto Mexicano del Seguro Social, Mexico
Davide Leardini,
University of Bologna, Italy

*CORRESPONDENCE
Bhavika Rishi
✉ bhavz83@gmai.com
Aroonima Misra
✉ dr.aroo.2402@gmail.com

†These authors share first authorship

RECEIVED 24 November 2024
ACCEPTED 19 February 2025
PUBLISHED 17 March 2025

CITATION
Singh A, Kushwaha N, Srishwan R, Zaman S, George NG, Kamal R, Swain SK, Kaur M, Siraj F, Sharma S, Noor B, Prabhakar P, Rishi B and Misra A (2025) Evaluating the efficacy and impact of neutropenic diet in pediatric hematology patients: a longitudinal cohort study on adherence, clinical outcomes, and socioeconomic factors. *Front. Nutr.* 12:1533734. doi: 10.3389/fnut.2025.1533734

Evaluating the efficacy and impact of neutropenic diet in pediatric hematology patients: a longitudinal cohort study on adherence, clinical outcomes, and socioeconomic factors

Amitabh Singh[1†], Neetu Kushwaha[2†], Raja Srishwan[3], Shamsuz Zaman[4], Noreen Grace George[2], Raj Kamal[2], Sandeep Kumar Swain[2], Manpreet Kaur[2], Fouzia Siraj[2,5], Saurabh Sharma[2,6], Baseer Noor[2], Prashant Prabhakar[1], Bhavika Rishi[2*] and Aroonima Misra[2*]

[1]Vardhman Mahavir Medical College and Safdarjung Hospital, New Delhi, India, [2]ICMR-National Institute of Child Health and Development Research, New Delhi, India, [3]ICMR-National Institute of Nutrition, Hyderabad, India, [4]ICMR-National Institute of Cancer Prevention and Research, Noida, India, [5]ICMR-Centre for Cancer Pathology, New Delhi, India, [6]Indian Council of Medical Research (ICMR), New Delhi, India

Background and aim: A neutropenic diet aims to reduce hospitalizations from febrile neutropenia and sepsis in pediatric hematology patients during chemotherapy. This study aimed to evaluate its effectiveness in improving mortality, morbidity, and overall outcomes while considering limitations, adherence rates, and its impact on hospital admissions and culture positivity.

Method: A prospective 18-month observational study was conducted on pediatric hematology patients in a pediatric department at a tertiary care center. Using a baseline questionnaire at the introduction of a neutropenic diet, the study assessed the clinical history, diagnosis, clinicopathological parameters, dietary recommendations, and socio-demographic data of the patients. Patients were followed up for up to 1 year to evaluate diet adherence, outcomes, mortality, and morbidity, as indicated by hospital admissions for febrile neutropenia.

Results: An analysis involving 100 patients was conducted to assess adherence to a neutropenic diet and its ramifications on clinical outcomes over a period of 18 months. Initial follow-up data were accessible for 83 patients, revealing an adherence rate of 66%, which subsequently declined to 57% following a 6-month interval. Patients were categorized as compliant or non-compliant, but no correlation was found between adherence and febrile admissions, sepsis, hospitalizations, or mortality. Among compliant patients, 62% showed sepsis signs, though only 19% had positive blood cultures in the whole study group. Non-adherence was linked to demographic factors such as large family size, financial constraints, and limited resources. The neutropenic diet showed minimal impact on morbidity and mortality.

Conclusion: Our study does not support the strict adherence to the neutropenic diet, as there is no evidence of reduced infections and the dietary adherence also imposes an undue financial burden on patients. Instead, focusing on the

safe acquisition of food, food processing, and proper hand cleanliness will probably provide superior protection against infection.

KEYWORDS

neutropenic diet, leukemia, febrile neutropenia, pediatric patients, adherence, socio-economic factors

Introduction

Childhood cancers have high mortality & morbidity owing to factors that are genetic, idiopathic, disease pathogenesis related and those due to to chemotherapy related toxicity (1, 2). The prevalence of morbidity and mortality in hemato-proliferative disorders is often attributed to febrile neutropenia which is the most common sequel of chemotherapy-induced toxicity (3). Therefore, numerous studies have been conducted to improve the various factors that contribute to morbidity and mortality. A neutropenic diet (also called a low microbial diet) is a clinically recommended special diet on permissible food items and is believed to reduce the risk of infection in cancer patients and patients with compromised immune systems (4). This diet eliminates raw produce, soft cheeses, fast food, and other potentially contaminated foods, thus reducing the risk of infections. The clinical practice of a neutropenic diet for cancer patients remains controversial, despite its lack of scientific evidence, as it is still followed in the majority of cancer centers for preventing neutropenia-related infections during chemotherapy (2, 5–7). There is a paucity of empirical evidence regarding the efficacy of this dietary regimen in hematological disorders prevalent in the Indian population, with limited studies assessing its role in preventing sepsis, chemotherapy-induced febrile neutropenia, and its impact on long-term mortality and morbidity in these patients (4).

The efficacy of the neutropenic diet in mitigating the incidence of infections among patients undergoing chemotherapy remains debated in the Indian population. Theoretically, in a setting such as tropical countries like India, which have a high burden of bacterial and infectious agents due to elevated humidity and environmental conditions, a neutropenic diet could be anticipated to significantly reduce morbidity, even if not mortality. Research has identified Gram-negative bacteria, such as *Pseudomonas aeruginosa*, *Escherichia coli*, *Klebsiella*, and *Proteus*, in various foods, especially salads, fresh vegetables, and cold meats. In addition, *Aspergillus*, a potentially deadly fungus for those with extended neutropenia, has been identified in food, water, and ice (6). However, the recent oncology practice worldwide has seen a shift from strict dietary adherence to relaxation of such adherence considering the studies on these diets and the overall marginal resultant improvement in morbidity (8, 9).

There are limited studies in India to validate or refute this hypothesis. Therefore, we conducted a study to determine the impact of a neutropenic diet on a cohort of patients undergoing chemotherapy for acute lymphoblastic leukemia (ALL), acute myeloid leukemia (AML), and other hematology disorders, and we analyzed the correlation between adherence to the neutropenic diet and morbidity outcomes. Thus, the goal of this mixed-methods study was to assess the neutropenic diet intervention in pediatric cancer patients with their clinical outcomes and admission related to febrile neutropenia and clinicopathological parameters, in order to support clinical and nutritional strategies that may improve the chemotherapy patients' quality of life (2). Our study also aimed to assess the feasibility of implementing a neutropenic diet, particularly in hematological malignancies, where the effectiveness of dietary intervention is established, but socioeconomic barriers often hinder adherence.

Abbreviations: AML, acute myeloid leukemia; ALL, acute lymphoblastic leukemia; B-ALL, B-cell acute lymphoid leukemia; T-ALL, T-cell acute lymphoid leukemia; Hb, hemoglobin; TLC, total leucocyte count; LFT, liver function test; KFT, kidney function test; ANC, absolute neutrophil count; MRSA, methicillin-resistant Staphylococcus aureus; HIC, high-income countries; ITP, immune thrombocytopenia; LCH, Langerhans cell histiocytosis.

Methods

Study design and patients

The study was conducted at the Indian Council of Medical Research (ICMR)-National Institute of Child Health & Development Research (NICHDR), New Delhi. Pediatric patients under the age of 13 years who were admitted to the pediatric ward at Vardhman Mahavir Medical College (VMMC) and Safdarjung Hospital for chemotherapy treatment of hematological malignancies were included in the study. The child's age, medical diagnosis, and therapy stage were documented with records for weight, height, hemoglobin level, platelet count, total leukocyte count, absolute neutrophil count, and temperature. Demographic data included age, sex, birth date, admission date, patient's and mother's physiological status, and examination date. In addition, parental income, employment status, and educational background of parents were collected. The baseline data included medical history (diagnosis and its date, surgeries, etc.), neutropenic infection history, and prior dietary adherence.

Samples and qualitative data were collected from the first day of chemotherapy. The blood samples were taken for various tests including hemoglobin (Hb), absolute neutrophil count, platelet count, total leucocyte count (TLC), liver function test (LFT), kidney function test (KFT), and blood culture. Patient data were recorded at the time of admission as well as at the start of chemotherapy and the initiation of a neutropenic diet and then subsequently at 6 months and/or upon hospital admission due to any disease-related morbidity, whichever transpired first. The second follow-up assessment was conducted 1 year subsequent to the initiation of therapy and the neutropenic diet.

Diet intervention at the start of chemotherapy

The investigator explained the details of the diet to the patients and their parents through the guidelines, answering any queries. The

details of the diet to be followed and also the dietary intervention and its precautions are described in Supplementary Table 9. On the first day of the chemotherapy cycle, patients were instructed to start their diet, until the chemotherapy ended. Patients on a neutropenic diet were instructed to avoid leftover foods, fresh fruits, and raw vegetables. The baseline data of all 100 patients were collected at the time of initiation of the neutropenic diet and admission at Vardhman Mahavir Medical College, Safdarjung Hospital. The first follow-up of all the patients was done after 6 weeks, and the second follow-up was done after 3 months from the date of initiation of the neutropenic diet wherever feasible. In addition, in the case of hospital admission, data were collected for the follow-up questionnaire to inquire about the adherence to neutropenic diet and the correlated clinicopathological results for sepsis and related admission.

The principal investigator evaluated hospital admission history, physical examination, and laboratory results to determine the diagnosis, including chemotherapy, and non-neutropenic and neutropenic infections. The lead investigator obtained a complete history from parents of hospitalized patients with neutropenic infections and documented all tests and results including systemic laboratory examinations and culture reports from blood. Patients' blood counts were monitored throughout the treatment until neutrophil recovery, indicated by an absolute neutrophil count (ANC), with fever detected and hospitalization if found.

The following data were collected at the time of baseline and follow-up: adherence to diet, reasons for non-compliance, and details about the diet such as intake of leftover foods, packaged foods, vegetarian or non-vegetarian foods, fresh fruits, and raw vegetables. Then, similar data were recorded at the time of the first follow-up and second follow-up. The questionnaire (see Supplementary Table 5) was based on the guidelines (see Supplementary Table 9) of the neutropenic diet, and the data were collected telephonically or at the time of admission or during OPD visits of all the patients. The 24-h diet recall approach was used to assess diet tenacity, with weekly interviews with parents to assess their child's adherence to the recommended food intake.

Neutropenic infection was chosen as the primary outcome, and it was defined as febrile neutropenia, requiring hospital admission, broad-spectrum antibiotic treatment, and an oral temperature of 38°C or above. Secondary outcomes included documented infections such as pneumonia or positive blood, urine, stool, or sputum cultures. The correlation with adherence to the neutropenic diet was determined for these patients. In addition, the following data were collected from the record files of the patients: ANC count, Hb level, blood culture report, incidence of hospital admission due to febrile neutropenia, and other investigations, as mentioned in Supplementary Tables 1, 2.

Statistical analysis for calculation of the risk ratio between the compliant and non-compliant groups

The statistical analysis of the study was conducted using Jamovi-open statistics software (Version: 2.3.28, Solid). A *p*-value less than 0.05 was the threshold for statistical significance. The study was conducted using the logarithmic risk ratio as the measure of final outcomes. The data were fitted with a random-effects statistical model. We evaluated the level of heterogeneity (tau^2) using the constrained maximum-likelihood estimator. In addition to the tau^2 estimate, the Q-test for heterogeneity and the I^2 statistic were also provided. If any degree of heterogeneity was observed (i.e., $tau^2 > 0$ irrespective of the Q-test findings), a prediction interval for the actual effects was also given. The utilization of studentized residuals and Cook's distance aided in the examination of potential outliers and/or influential studies within the model's context. Studies exhibiting a studentized residual in excess of the $100 \times (1–0.05/ (2 \times k))$th percentile of a regular normal distribution are regarded as possible outliers. This is determined by applying a Bonferroni correction with a two-sided alpha of 0.05 to the k studies included in the meta-analysis (10, 11).

Results

General characteristics of the study population

Out of 100 patients recruited for the study, the second follow-up data were available for 74 patients and the first follow-up data were available for 26 patients recruited at a later part of the study. Our tertiary care setup included a team of senior and junior hemato-oncologists, junior and senior doctors, nurse staff, and supporting staff. Supplementary Table 1 provides the characteristics of the pediatric children at our hospital. Among the 100 pediatric hematology patients, we observed a slight male predominance in hemato-proliferative disorders, with a higher proportion of males (61%) (see Supplementary Tables 1, 3). The reasons for this predominance may include tertiary referral bias and a greater likelihood of a male child receiving medical attention because of socioeconomic factors in India (12). The median age of patients was 5.32 years. The majority of patients were in the age group of 0–5 years (48%) followed by 5–10 years old (31%). The most common type of leukemia in this population was B-ALL (55%) followed by T-ALL (13%) (Supplementary Tables 1, 3). The results of this demography distribution were similar to those reported in previous studies (7, 9, 13, 14). The study also found that literacy could also be a potential confounding factor for the implementation of a neutropenic diet in daily practice, which plays a major role in understanding the importance of a neutropenic diet in leukemia. The compliance was better in the group where both parents were literate than in the group where either or none was literate (with 38% being primary passed and 24% illiterate) (15, 16). The majority of children treated were underweight. Supplementary Table 4 provides the details of the social demographics of the study population.

Presenting symptoms and clinicopathological data of patients

Supplementary Table 2 provides details of the clinical presentation of the study population at baseline. The majority of hematology patients were diagnosed with hepatosplenomegaly (63%), hepatomegaly (16%), splenomegaly (2%), hydronephrosis (1%), and lymphadenopathy (64%). Out of 100 patients, almost all of them experienced fever, the majority (75%) had pallor, followed by abdominal pain, easy bruises, bleeding, and vomiting during admission.

Neutropenic infection

In our study, 91% of patients often developed neutropenic infections and vomiting, believed to be the side effects of chemotherapy, during the entire study period and follow-ups (Supplementary Figure 3). Patients reported experiencing fever (97%), vomiting (25%), and diarrhea (38%) at the time of admission due to febrile neutropenia. We found that 19% of patients showed positive blood culture and 91% of patients had sepsis (Supplementary Table 2). All of these were unrelated to neutropenic diet adherence and were randomly distributed in both adherent and non-adherent groups. One patient had oral candidiasis with *E. coli* sepsis and MRSA sepsis. Another patient had *Acinetobacter* sepsis. One patient had febrile neutropenia with *Klebsiella* sepsis. The majority of the patients on a neutropenic diet showed normal blood cultures, but neutropenic infections also occurred in some individuals (17, 18). There was a lack of laboratory evidence supporting the diagnosis of sepsis, as the majority of cultures obtained from patients admitted with febrile neutropenia yielded negative results. This phenomenon is corroborated by additional research indicating the occurrence of culture-negative sepsis among individuals undergoing chemotherapy (15, 17, 18).

This study found no difference in mortality, indicating that diet does not play a significant role in reducing infection and mortality in oncology treatment patients (Supplementary Figure 4), when comparing those who followed the diet with those who did not. Out of 100 patients, 26 were deceased (18 male and 8 female), while 74 were alive. The causes of death were pancytopenia and sepsis with infection and chemotherapy-induced toxicity. Out of 100 patients, the compliant group had a 27% mortality rate, compared to 23% in the non-compliant group. Of the 66% who were compliant, 18% died. The non-compliance group comprised 34% of patients, of which 8% died. Supplementary Figure 4 shows the mortality rate at a 1-year follow-up period and shows that there were no differences in mortality rates in compliant (27.3%) versus non-compliant patients (23.5%), with an overall mortality rate of 26.0%. There was a complete absence of any correlation observed between the likelihood of survival rates and the strict adherence to a neutropenic diet. This lack of correlation was also evident with equal incidence of sepsis in both groups. The underlying reasons could primarily be attributed to the presence of multiple variables and outcome measures that are associated with these patients. These patients are usually immunocompromised and hence prone to infection because of disease and chemotherapy. Furthermore, it is important to note that sepsis is not directly attributed to the dietary restrictions imposed by the neutropenic diet (9, 10).

Conformation of diet tenacity

The total study population was divided into two groups based on adherence to dietary interventions: compliant and non-compliant (Supplementary Table 8). The compliant group consisted of 66%, strictly following a neutropenic diet, and the non-compliant group consisted of 34%. Almost everyone (99%) avoided leftover foods, 86% ate boiled egg and non-vegetarian food, 14% avoided poultry, and no patients (0%) consumed fresh fruits and raw vegetables (Supplementary Table 11). In the initial survey, 17% of the participants could not be followed up, whereas in the subsequent survey, this percentage was reduced to 10%. The majority of the parents followed neutropenic diet guidelines, but patients had difficulties with food restrictions. The observed log risk ratio ranged from −0.34 to 0.23 in the adverse medical condition population of both the compliant and non-compliant groups, while it was observed to be in the range of −0.89 to 0.08 in the non-adverse medical condition population of both the groups with the majority of estimates being positive (60%). The detailed log risk ratio and the estimated average log risk ratio, based on the random-effects model, were analyzed (Supplementary Figures 1A,B, 2A,B and Supplementary Tables 6, 7), and we observed no significant difference ($p < 0.05$) in both compliant and non-compliant groups for adverse and non-adverse medical conditions (z = 0.5359 and $p = 0.5920$ for adverse medical condition; and z = −0.1944 and $p = 0.8458$ for non-adverse medical condition) (Supplementary Tables 6, 7). According to the Q-test, there was no significant amount of heterogeneity in the true outcomes in the adverse medical condition population (Q(4) = 2.6168, $p = 0.6239$, $tau^2 = 0.0000$, $I^2 = 0.0000\%$). A similar line of outcome was observed in the non-adverse medical condition population with the Q-test (Q(4) = 3.2983, $p = 0.5092$, $tau^2 = 0.0053$, $I^2 = 8.4224\%$) (Supplementary Tables 6, 7). The log risk ratios and meta-analysis data are provided in Supplementary material 2 and Supplementary Tables 6, 7. The major reasons for non-compliance were logistic issues related to a large family (6%), lack of resources (4%), financial issues (4%), perceived lack of advantage (2%), not following doctors' advice (1%), and lost to follow-up, those that were not reachable on the telephone and did not attend the follow-up (17%). Fresh fruits (excluding bananas) and raw vegetables were strictly avoided by the patients. Some parents avoided fast food, struggled to provide dry fruits due to low income, and substituted supplementary protein foods for eggs or non-vegetarian options. The majority of parents provided fresh homemade food, while a few patients consumed leftovers.

Among the 100 pediatric hematology patients studied, 66 patients were classified as compliant/adherent to dietary interventions, while 34 were non-compliant/non-adherent. The median age of compliant patients (4.32 years) was lower than that of non-compliant patients (6.67 years). Gender distribution showed that out of 61 male patients, 44 were compliant, while 17 were non-compliant. Among 39 female patients, there was an equal distribution with 22 being compliant and 17 non-compliant. Regarding disease distribution, B-ALL was the most common diagnosis (55 patients), with 35 patients in the compliant group and 20 in the non-compliant group. This was followed by T-ALL (13 patients; 10 compliant, 3 non-compliant), AML (9 patients; 6 compliant, 3 non-compliant), aplastic anemia (6 patients; 3 in each group), and Ewing sarcoma (2 patients; both compliant). The primary outcome measures of neutropenic infections during chemotherapy showed that 91 patients developed sepsis, with a higher proportion in the compliant group (62 patients) than in the non-compliant group (29 patients). Blood culture results revealed 19 positive cases (11 compliant, 8 non-compliant) and 81 negative cases (55 compliant, 26 non-compliant). The mortality data showed that out of 26 deaths, 18 were males (13 compliant, 5 non-compliant) and 8 were females (5 compliant, 3 non-compliant). The total mortality rate appeared to be similar between compliant (18 deaths) and non-compliant (8 deaths) groups when adjusted for group size. Regarding dietary interventions, nearly all patients (99 out of 100) were advised to avoid leftovers, with similar adherence rates

between groups. All patients (100) were instructed to avoid fresh fruits and raw vegetables. A smaller subset of patients (14) were advised to avoid poultry (9 compliant, 5 non-compliant) and boiled eggs and non-vegetarian food (11 compliant, 4 non-compliant). The data suggest that while compliance with dietary restrictions was observed in approximately two-thirds of the patients, the incidence of neutropenic infections and positive blood cultures remained proportional between compliant and non-compliant groups when adjusted for group size. This raises interesting questions about the direct impact of dietary compliance on infection prevention in pediatric hematology and oncology patients, though other factors such as age, underlying disease, and treatment protocols may have influenced these outcomes (Supplementary Table 8).

Discussion

The current study aimed to evaluate the impact of adherence to a neutropenic diet on morbidity, especially the frequency of hospital admissions, duration of stay. and mortality, among pediatric patients undergoing chemotherapy for ALL, AML, and other hemato-proliferative disorders. As reported in other studies, despite the theoretical benefits of reducing infection risk in patients with compromised immune function, our findings indicate that adherence to a neutropenic diet does not significantly impact the incidence of neutropenic infections or overall survival outcomes (19). There was no significant difference in morbidity and mortality between the compliant and non-compliant groups over a period of 1-year follow-up. The neutropenic diet, a norm for conventional chemotherapy for over two decades, exhibits variability in necessity, implementation, understanding, and impact on outcomes (2). The clinical significance of a neutropenic diet on pediatric hematology patients is related to the length of time needed for diet instruction, the information included in that education regarding food limitations, and the difficulty in following dietary restrictions when experiencing chemotherapeutic side effects (7).

Patient demographics and compliance

The study cohort consisted of 100 pediatric hematology patients with a male predominance (61%), which is consistent with the existing literature (20, 21) suggesting a higher incidence of childhood cancer in males for all genetically predisposed cancers and genetic abnormalities being more common in males for unknown reasons (20, 21). It could also be potentially due to socioeconomic factors in India that influence healthcare-seeking behavior (22). The majority of patients were under the age of 10, with a peak between 0 and 5 years as expected with the published literature, with B-ALL being the prevalent diagnosis, reflecting typical disease demographics (23, 24). Fever, pallor, abdominal pain, swelling, vomiting, and diarrhea were the prevalent signs and symptoms. The male/female ratio was 1.6:1, indicating male dominance in the population. We found that compliance with the neutropenic diet was relatively high (66%), though logistical, financial, and resource-related challenges contributed to non-compliance in 34% of the cases. Interestingly, dietary compliance was notably better among children with literate parents than those with illiterate parents, emphasizing the role of parental education in health-related behavior.

In our study, 38% of mothers had completed primary education, and 24% were illiterate (Supplementary Table 4), highlighting the impact of parental education on the wellbeing of children with leukemia. Research indicates that educated parents are well-equipped to understand leukemia, chemotherapy, and its associated side effects, enabling them to provide more effective care and support (23, 25). This comprehensive understanding facilitates improved communication with healthcare providers, better management of treatment-related challenges, and reduced stress for both parents and children. Consequently, the quality of life for children is significantly enhanced when parents possess formal education, compared to relying solely on informal information sources (25).

Diet adherence and infection outcomes

The primary outcome of the study was the incidence of neutropenic infections, defined by febrile neutropenia requiring hospital admission and broad-spectrum antibiotic treatment. The secondary outcomes included documented infections such as pneumonia and positive cultures. Although 91% of patients experienced neutropenic infections during the study, there was no clinical evidence of a major difference in infection rates between patients adherent and non-adherent to the neutropenic diet. Moreover, the types of infections, including sepsis and febrile neutropenia, were distributed randomly between both groups. In our setting, patients usually reported late, and this is a major reason for such a high incidence of sepsis-related symptoms. Sepsis was defined according to the standard definition as suspected or proven infection caused by any pathogen or clinical syndrome associated with a high probability of infection along with any two of the following four signs: fever >38.5°C, tachycardia, tachypnoea as per age-defined cutoffs, and neutropenia. Severe sepsis was defined as sepsis with organ dysfunction, hypoperfusion, or hypotension. Blood culture was positive in 19% of cases, and the details of growth are shown in the chart. One patient had polymicrobial sepsis in the form of oral candidiasis with laboratory examination showing the growth of *E. coli* and MRSA in the blood (Supplementary Figure 3).

Morbidity, mortality, and clinical implications

In terms of clinical outcomes, the overall mortality rate was 26%, with minimal difference between the compliant (27.3%) and non-compliant (23.5%) groups (Supplementary Tables 6, 7 and Supplementary Figure 4). The primary causes of death were pancytopenia, sepsis, and chemotherapy-induced toxicity, underscoring the multifactorial nature of mortality in pediatric hematology and oncology patients. These results indicate that adherence to a neutropenic diet does not significantly reduce morbidity or mortality in pediatric hematology and oncology patients undergoing chemotherapy. Several studies including randomized controlled trials and systematic reviews have highlighted the futile effects of a neutropenic diet. However,

those are mostly set in high-income countries (HIC) where the pathogen burden is less and incidences of febrile admissions due to sepsis are also low (26). In our study, about 66% followed neutropenic diet, though full compliance was not seen. The mortality rates did not vary between the compliant and non-compliant groups. In fact, the compliant group showed slightly higher mortality rates (2, 19, 27, 28). Nutrition and childhood cancer are closely linked, with malnutrition increasing the infection risk, altering medication metabolism, and limiting treatment effectiveness. A study reported that concerns about cancer outcomes, survival rates, treatment tolerance, and quality of life were identified mainly in children lacking sufficient nutrition (29). The presence of malnutrition is correlated with reduced rates of survival and heightened levels of toxicity resulting from chemotherapy treatment (23). As in any pediatric cohort in Indian tertiary care centers, we had a similar incidence of malnutrition (more than half, 54%) as per Revised IAP 2015 Growth Charts (30). The attribution of the confounding effect of malnutrition in sepsis in overall outcomes of leukemia needs a thorough investigation which is beyond the scope of this study.

Microbiological findings and diet correlation

Blood cultures and other systemic laboratory examinations indicated that infections such as *E. coli*, MRSA, and *Klebsiella* sepsis were not specifically associated with diet adherence, highlighting that factors other than dietary intake play a predominant role in infection risk among these patients. Our findings align with other studies (15, 31) reporting high rates of culture-negative sepsis in chemotherapy patients, further suggesting that neutropenic infections are largely influenced by chemotherapy-induced immunosuppression rather than dietary factors (Supplementary Table 2). Several studies conducted in Western countries have identified common pathogens such as *Campylobacter coli*, *Bacillus cereus*, *Salmonella Typhimurium*, *Aeromonas hydrophila*, and *Staphylococcus aureus*, which were found in blood and respiratory, intestinal, and urinary sites (27, 32, 33). In addition, food-associated infections (FAIs) were notably prevalent in home environments compared to hospital settings, with studies indicating a 64% occurrence in homes versus 18% in hospitals. This variance underscores the paramount importance of domestic sanitation practices in the mitigation of foodborne illnesses (34, 35). The frequency of culture positivity in the aforementioned studies demonstrated considerable heterogeneity, ranging from 0.2 to 30%; nonetheless, it revealed analogous characteristics among both adherent and non-adherent cohorts.

The home environment serves as a crucial locus for FAIs, attributable to heterogeneous hygiene practices and the existence of varied bacterial populations. Inadequate hygienic practices, such as insufficient hand washing and improper food handling, exacerbate the elevated prevalence of FAIs in domestic environments. Conversely, healthcare facilities generally implement more rigorous hygiene protocols, thereby diminishing the occurrence of such infections. Although the incidence of FAIs is markedly elevated in domestic settings, the comparability in culture positivity rates between adherent and non-adherent groups indicates that additional factors such as environmental conditions and the adaptability of pathogens may also exert influence. This highlights the necessity for comprehensive strategies that simultaneously address individual behaviors and systemic food safety frameworks (36).

Reasons for non-compliance

Non-compliance with the neutropenic diet was observed in 34% of the patients, primarily due to logistical challenges, financial constraints, and a lack of perceived benefits. Large family sizes made it difficult for parents to adhere strictly to dietary guidelines, especially in resource-limited settings. Financial issues also played a significant role, as some families struggled to afford the recommended foods, particularly high-protein options such as eggs or non-vegetarian items. In addition, some parents did not perceive any clear advantages to following the diet, leading to reduced motivation for strict adherence. Cultural preferences and accessibility issues further contributed to the challenges of maintaining diet compliance. Other challenges reported in the Western countries were different from those observed in our study, such as unpleasant olfactory sensations, inadequate food presentation, hospitalization, separation from family, and social pressure. Other challenges that have been reported mainly in high-income countries include complaints about dietary limits—particularly for pediatric hematology patients, who were denied desirable foods such as fast food, street foods, and fresh fruits—lengthy hospitalizations, emotional distress, disruptions to daily routines, yearning for social milieu, and dissatisfaction with meals that contribute to diminished appetite among pediatric patients (9, 16).

The study is constrained by its observational design, coupled with the relatively small sample size, factors that may significantly influence the extent to which our findings can be generalized to broader contexts beyond our study. In addition, the reliance on self-reported dietary adherence and parental recall introduces potential biases that could affect the accuracy and reliability of compliance data. The inherent limitations in our study are further compounded by factors such as a relatively brief enrollment period, generalized inclusion criteria, a limited sample size, an array of multifactorial influences, seasonal fluctuations in the availability of foodstuffs, and the notably low accuracy associated with patients' self-reported compliance over designated intervals of 6 and 12 weeks. As a result, future research should prioritize large-scale randomized controlled trials to better establish the role and effectiveness of dietary interventions in pediatric hematology and oncology patients. In addition, it would be prudent to investigate a wider array of preventive strategies, such as the implementation of enhanced infection control mechanisms and the administration of targeted antimicrobial prophylaxis, as these may yield considerable benefits for this particularly vulnerable population of patients. There is an urgent need for further research aimed at improving the treatment outcomes associated with neutropenia, as this condition poses significant challenges in the context of

oncological care. A thorough review of the existing literature indicates a pronounced deficiency in empirical evidence regarding the utilization, feasibility, and overall efficacy of the neutropenic diet specifically in pediatric patients diagnosed with neutropenia, who are actively undergoing oncological treatment.

Conclusion

Our study data do not support the use of the neutropenic diet. Moreover, there is no standardization and recommended diet when it comes to neutropenic diet as it varies between geographic regions based on the availability of food and dietary habits. The absence of a clear link between diet and infection underscores that neutropenic infections are primarily driven by the compromised immune function inherent to chemotherapy, rather than dietary practices alone.

Data availability statement

The original contributions presented in the study are included in the article/Supplementary material, further inquiries can be directed to the corresponding authors.

Ethics statement

The studies involving humans were approved by IEC clearance was obtained from Vardhaman Mahavir Medical College & Safdarjung Hospital, with reference number IEC/VMMC/Thesis/2019-10/207. The studies were conducted in accordance with the local legislation and institutional requirements. Written informed consent for participation in this study was provided by the participants' legal guardians/next of kin.

Author contributions

AS: Writing – review & editing. NK: Writing – review & editing, Writing – original draft. RS: Writing – review & editing, Writing – original draft. SZ: Writing – review & editing. NG: Writing – review & editing. RK: Writing – review & editing. SSw: Writing – review & editing, Formal analysis, Methodology, Visualization. MK: Writing – review & editing. FS: Methodology, Formal analysis, Visualization, Writing – review & editing. SSh: Data curation, Methodology, Funding acquisition, Visualization, Writing – review & editing. BN: Writing – review & editing. PP: Writing – review & editing. BR: Writing – review & editing, Formal analysis, Methodology, Supervision. AM: Conceptualization, Formal analysis, Investigation, Methodology, Project administration, Supervision, Validation, Visualization, Writing – original draft, Writing – review & editing.

Funding

The author(s) declare that no financial support was received for the research and/or publication of this article.

Acknowledgments

ICMR-National Institute of Child Health and Development Research, New Delhi, India, is acknowledged for aiding with infrastructure and study requirements.

Conflict of interest

The authors declare that the research was conducted in the absence of any commercial or financial relationships that could be construed as a potential conflict of interest.

Generative AI statement

The authors declare that no Gen AI was used in the creation of this manuscript.

Publisher's note

Supplementary material

The Supplementary material for this article can be found online at: https://www.frontiersin.org/articles/10.3389/fnut.2025.1533734/full#supplementary-material

References

1. Ricci AM, Emeny RT, Bagley PJ, Blunt HB, Butow ME, Morgan A, et al. Causes of childhood cancer: a review of the recent literature: part I—childhood factors. *Cancers*. (2024) 16:1297. doi: 10.3390/cancers16071297

2. Arnhold APC, Araujo HGS, Cruz AF, Toffolo MCF, Mauricio SF. Use of neutropenic diet in the nutritional care of pediatric cancer patients with neutropenia: a scoping review. *J Pediatr*. (2024) 100:132–42. doi: 10.1016/j.jped.2023.07.009

3. Ceken S, Gedik H, Iskender G, Demirelli M, Mert D, Yapar Toros G, et al. Evaluation of risk factors for mortality in febrile neutropenia. *J Infect Dev Ctries*. (2020) 14:886–92. doi: 10.3855/jidc.12520

4. Fox N, Freifeld AG. The neutropenic diet reviewed: moving toward a safe food handling approach. *Oncology (Williston Park)*. (2012) 26:572–5.

5. Moody K, Charlson ME, Finlay J. The neutropenic diet: What's the evidence? *J Pediatr Hematol Oncol*. (2002) 24:717–21. doi: 10.1097/00043426-200212000-00007

6. Jubelirer SJ. The benefit of the neutropenic diet: fact or fiction? *Oncologist*. (2011) 16:704–7. doi: 10.1634/theoncologist.2011-0001

7. DeMille D, Deming P, Lupinacci P, Jacobs LA. The effect of the neutropenic diet in the outpatient setting: a pilot study. *Oncol Nurs Forum*. (2006) 33:337–43. doi: 10.1188/ONF.06.337-343

8. Bälter K, Möller E, Fondell E. The effect of dietary guidelines on cancer risk and mortality. *Curr Opin Oncol*. (2012) 24:90–102. doi: 10.1097/CCO.0b013e32834e0531

9. Moody K, Finlay J, Mancuso C, Charlson M. Feasibility and safety of a pilot randomized trial of infection rate: neutropenic diet versus standard food safety guidelines. *J Pediatr Hematol Oncol*. (2006) 28:126–33. doi: 10.1097/01.mph.0000210412.33630.fb

10. Ma Y, Lu X, Liu H. Neutropenic diet cannot reduce the risk of infection and mortality in oncology patients with neutropenia. *Front Oncol*. (2022) 12:836371. doi: 10.3389/fonc.2022.836371

11. Viechtbauer W. Conducting meta-analyses in R with the metafor package. *J Stat Softw*. (2010) 36:1–48. doi: 10.18637/jss.v036.i03

12. Marcotte EL, Schraw JM, Desrosiers TA, Nembhard WN, Langlois PH, Canfield MA, et al. Male sex and the risk of childhood cancer: the mediating effect of birth defects. *JNCI Cancer Spectr*. (2020) 4. doi: 10.1093/jncics/pkaa052

13. Lassiter M, Schneider SM. A pilot study comparing the neutropenic diet to a non-neutropenic diet in the allogeneic hematopoietic stem cell transplantation population. *Clin J Oncol Nurs*. (2015) 19:273–8. doi: 10.1188/15.CJON.19-03AP

14. Trifilio S, Helenowski I, Giel M, Gobel B, Pi J, Greenberg D, et al. Questioning the role of a neutropenic diet following hematopoetic stem cell transplantation. *Biol Blood Marrow Transplant*. (2012) 18:1385–90. doi: 10.1016/j.bbmt.2012.02.015

15. Hazwani TR, Kazzaz YM, Alsugheir S, Aldelaijan S, Alsugheir F, Alali H, et al. Association between culture-negative versus culture-positive sepsis and outcomes of patients admitted to the pediatric intensive care unit. *Cureus*. (2020) 12:e9981. doi: 10.7759/cureus.9981

16. Arpaci T, Toruner EK, Altay N. Assessment of nutritional problems in pediatric patients with cancer and the information needs of their parents: a parental perspective. *Asia Pac J Oncol Nurs*. (2018) 5:231–6. doi: 10.4103/apjon.apjon_78_17

17. Wehrenberg K, Mitchell M, Thompson N. The diagnostic and therapeutic challenges of culture negative sepsis. *Curr Treat Options Pediatr*. (2024) 10:52–63. doi: 10.1007/s40746-024-00293-6

18. Baker AH, Leland SB, Freiman E, Herigon JC, Eisenberg MA. Characteristics and outcomes of culture-positive and culture-negative pediatric sepsis. *J Pediatr*. (2023) 263:113718. doi: 10.1016/j.jpeds.2023.113718

19. Moody KM, Baker RA, Santizo RO, Olmez I, Spies JM, Buthmann A, et al. A randomized trial of the effectiveness of the neutropenic diet versus food safety guidelines on infection rate in pediatric oncology patients. *Pediatr Blood Cancer*. (2018) 65

20. Jackson N, Menon BS, Zarina W, Zawawi N, Naing NN. Why is acute leukemia more common in males? A possible sex-determined risk linked to the ABO blood group genes. *Ann Hematol*. (1999) 78:233–6. doi: 10.1007/s002770050507

21. Singh SK, Lupo PJ, Scheurer ME, Saxena A, Kennedy AE, Ibrahimou B, et al. A childhood acute lymphoblastic leukemia genome-wide association study identifies novel sex-specific risk variants. *Medicine (Baltimore)*. (2016) 95:e5300. doi: 10.1097/MD.0000000000005300

22. Williams LA, Richardson M, Marcotte EL, Poynter JN, Spector LG. Sex ratio among childhood cancers by single year of age. *Pediatr Blood Cancer*. (2019) 66:e27620. doi: 10.1002/pbc.27620

23. Totadri S, Radhakrishnan V, Atreya H, Shenoy P, Ganesan P, Ganesan T, et al. Dietary perceptions and beliefs among families with children undergoing therapy for cancer. *Pediatr Hematol Oncol J*. (2017) 2:25–8. doi: 10.1016/j.phoj.2017.06.004

24. Inaba H, Greaves M, Mullighan CG. Acute lymphoblastic leukaemia. *Lancet*. (2013) 381:1943–55. doi: 10.1016/S0140-6736(12)62187-4

25. Hashemi F, Asadi N, Beheshtipour N, Karimi M. The impact of educating parents of leukemic children on the patients' quality of life. *Iran Red Crescent Med J*. (2011) 13:550–5.

26. Ball S, Brown TJ, Das A, Khera R, Khanna S, Gupta A. Effect of neutropenic diet on infection rates in Cancer patients with neutropenia: a meta-analysis of randomized controlled trials. *Am J Clin Oncol*. (2019) 42:270–4. doi: 10.1097/COC.0000000000000514

27. Arora RS, Arora B. Acute leukemia in children: a review of the current Indian data. *South Asian J Cancer*. (2016) 5:155–60. doi: 10.4103/2278-330X.187591

28. Radhakrishnan V, Lagudu PBB, Gangopadhyay D, Vijaykumar V, Rajaraman S, Perumal Kalaiyarasi J, et al. Neutropenic versus regular diet for acute leukaemia induction chemotherapy: randomised controlled trial. *BMJ Support Palliat Care*. (2022) 12:421–30. doi: 10.1136/spcare-2022-003833

29. Lovell AL, Laughton S, Wood A, Pugh G. Nutrition screening, assessment, and intervention practices for children with cancer in Aotearoa, New Zealand. *Nutrition*. (2023) 116:112218. doi: 10.1016/j.nut.2023.112218

30. Premkumar S, Venkatramanan P, Dhivyalakshmi J, Gayathri T. Comparison of nutrition status as assessed by revised IAP 2015 growth charts and CDC 2000 growth charts in lower socioeconomic class school children. *Indian J Pediatr*. (2019) 86:1136–8. doi: 10.1007/s12098-019-03036-w

31. Hanzelina H, Widnyana AANKP, Windiani IGAT, Karyana IPG, Ariawati NK, Mahalini DS. Malnutrition as risk factor for febrile neutropenia in children with acute lymphoblastic leukemia. Open access Macedonian. *J Med Sci*. (2022) 10:681–5. doi: 10.3889/oamjms.2022.8448

32. Heng MS, Barbon Gauro J, Yaxley A, Thomas J. Does a neutropenic diet reduce adverse outcomes in patients undergoing chemotherapy? *Eur J Cancer Care (Engl)*. (2020) 29:e13155. doi: 10.1111/ecc.13155

33. Jakob CEM, Classen AY, Stecher M, Engert A, Freund M, Hamprecht A, et al. Association between the dietary regimen and infection-related complications in neutropenic high-risk patients with cancer. *Eur J Cancer*. (2021) 155:281–90. doi: 10.1016/j.ejca.2021.06.054

34. Toenges R, Greinix H, Lawitschka A, Halter J, Baumgartner A, Simon A, et al. Current practice in nutrition after allogeneic hematopoietic stem cell transplantation - results from a survey among hematopoietic stem cell transplant centers. *Clin Nutr*. (2021) 40:1571–7. doi: 10.1016/j.clnu.2021.02.030

35. Matteucci S, De Pasquale G, Pastore M, Morenghi E, Pipitone V, Soekeland F, et al. Low-bacterial diet in cancer patients: a systematic review. *Nutrients*. (2023) 15. doi: 10.3390/nu15143171

36. Carstens CK, Salazar JK, Sharma SV, Chan W, Darkoh C. Evaluation of the kitchen microbiome and food safety behaviors of predominantly low-income families. *Front Microbiol*. (2022) 13. doi: 10.3389/fmicb.2022.987925

frontiers | Frontiers in Nutrition

TYPE Original Research
PUBLISHED 19 March 2025
DOI 10.3389/fnut.2025.1561235

OPEN ACCESS

EDITED BY
Sofia Viana,
University of Coimbra, Portugal

REVIEWED BY
Sourish Bhattacharya,
Central Salt and Marine Chemicals Research Institute (CSIR), India
Susana Rocha,
University of Porto, Portugal

*CORRESPONDENCE
Tao Lin
✉ kidney1234@163.com
Yunjin Bai
✉ Baiyunjin@163.com

†These authors have contributed equally to this work

RECEIVED 15 January 2025
ACCEPTED 03 March 2025
PUBLISHED 19 March 2025

CITATION
Xiao Y, Yang Y, Gao S, Zhang H, Wang J, Lin T and Bai Y (2025) Dietary index for gut microbiota, a novel protective factor for the prevalence of chronic kidney diseases in the adults: insight from NHANES 2007–2018. *Front. Nutr.* 12:1561235. doi: 10.3389/fnut.2025.1561235

Dietary index for gut microbiota, a novel protective factor for the prevalence of chronic kidney diseases in the adults: insight from NHANES 2007–2018

Yunfei Xiao[1,2†], Yaqing Yang[3†], Shunyu Gao[1], Hao Zhang[1,2], Jia Wang[1], Tao Lin[1,2*] and Yunjin Bai[1*]

[1]Department of Urology, Institute of Urology, West China Hospital, Sichuan University, Chengdu, China, [2]Organ Transplantation Center, West China Hospital, Sichuan University, Chengdu, Sichuan, China, [3]Department of Respiratory and Critical Care Medicine, West China Hospital, Sichuan University, Chengdu, China

Introduction: This study explore the association between the dietary index for gut microbiota (DI-GM) and the prevalence of chronic kidney disease (CKD).

Method: A cross-sectional study of participants aged ≥20 years using the data drawn from NHANES (2007–2018). DI-GM is comprised 14 dietary components (10 beneficial and 4 unfavorable). CKD diagnosis based on urine albumin-to-creatinine ratio (uACR) and estimated glomerular filtration rate (eGFR). Logistic regression models were employed to evaluate the relationship between DI-GM and CKD while controlling for various covariates. Additionally, a spline smooth analysis was performed. Subgroup and interaction analyses were conducted to investigate whether any factors modified this relationship.

Results: A total of 28,843 participants were eligible for the study, of whom 5,461 were diagnosed with CKD, while 23,382 were not. Patients with CKD exhibited significantly lower DI-GM scores compared to healthy individuals. A negative association between DI-GM and the prevalence of CKD was observed across all models, with the relationship being more pronounced in individuals with DI-GM scores greater than 5 compared to those with scores ≤3. Beneficial components, such as dietary fiber, whole grains, and coffee, were identified as protective factors. Moreover, sex make an effect on this relationship, with stronger effects noted in women.

Conclusion: Higher DI-GM scores correlate with reduced CKD prevalence, and the effect appears to be more pronounced in women than in men. These findings suggest that enhancing gut health through diet may serve as a viable strategy for the prevention and management of CKD, with particular attention to sex-based differences in prevention.

KEYWORDS

chronic kidney diseases, dietary index for gut microbiota, metabolism, cross-section, association

1 Introduction

Chronic kidney disease (CKD) is a long-term condition characterized by progressive renal dysfunction, leading to impaired filtration and waste elimination. CKD frequently progresses to complications such as cardiovascular disease, anemia, and bone disorders, and may ultimately necessitate dialysis or transplantation. Globally, CKD affects over 850 million people and is projected to become the fifth leading cause of death by 2040 (1). The primary risk factors for CKD include diabetes, hypertension, obesity, and aging (2). Recent studies have highlighted the role of gut dysbiosis in CKD, as it exacerbates systemic inflammation, promotes insulin resistance, and generates uremic toxins like indoxyl sulfate and p-cresyl sulfate (3, 4). These toxins contribute to further kidney damage and cardiovascular complications, highlighting the connection between gut health and CKD progression (5, 6). Consequently, the gut microbiome is increasingly recognized as a potential therapeutic target in the management of CKD.

The dietary index for gut microbiota (DI-GM) is a novel metric designed to assess the impact of diet on the diversity of gut microbiota. This comprehensive index was developed through a review of 106 articles that investigated the association between diet and gut microbiota in adults. The DI-GM encompasses 14 dietary components, with beneficial components such as fermented dairy, whole grains, fiber, and specific fruits and vegetables, and unfavorable components like red and processed meats, refined grains, and high-fat diets (7, 8). This index serves as a standardized tool for evaluating dietary patterns that promote or hinder gut microbiota health. Research indicates that diet affecting gut microbiota diversity can influence systemic health, particularly concerning metabolic conditions such as diabetes and cardiovascular diseases (9, 10). Given the established roles of metabolic disturbances and gut dysbiosis in kidney disease, understanding whether DI-GM correlates with CKD prevalence is essential for developing dietary interventions aimed at preserving renal function. Despite the growing body of evidence linking diet, gut microbiota, and chronic diseases, there is a notable scarcity of research exploring the relationship between DI-GM and CKD. This study aims to investigate the association between the DI-GM and the prevalence of CKD, hypothesizing that higher DI-GM scores, indicative of a gut-friendly diet, are associated with a lower prevalence of CKD. The urgency of this research is emphasized by the global rise in CKD incidence, which is significantly influenced by lifestyle factors, including poor dietary habits and metabolic health. By examining this relationship within a cross-sectional adult population, the study aims to provide insights into how dietary strategies targeting gut microbiota may help mitigate the risk and progression of CKD.

2 Method

2.1 Study design and population

The data utilized in this research was obtained from the National Health and Nutrition Examination Survey (NHANES) database, which covers the period from 2007 to 2018. NHANES is a comprehensive, nationally representative survey designed to investigate the dietary patterns and health of individuals residing in the United States. Data were collected through structured interviews, physical evaluations, and laboratory tests, employing a multistage probability sampling technique. The primary objective is to accurately represent the demographics of the U.S. population, with stringent measures implemented during the data collection process to ensure the confidentiality and privacy of participants. The initial sample, collected over six consecutive cycles, comprised 59,842 individuals. First, individuals under 20 years of age were excluded from the sample (n = 34,770). Next, pregnant individuals were also removed (n = 372). Additionally, individuals with missing information regarding CKD diagnoses (n = 3,468) and DI-GM (n = 2,087) were excluded. Ultimately, 28,843 adults were included in the analysis, as detailed in Supplementary Figure S1.

All NHANES study protocols received approval from the Ethics Review Committee of the NCHS, and informed consent was obtained from all participants.

2.2 The dietary index for gut microbiota

The DI-GM is a literature-based index developed to assess dietary patterns that influence gut microbiota composition (7). It encompasses a set of dietary components that either positively or negatively impact gut microbial diversity. This index was constructed using dietary recall data and consists of 14 food components, categorized into beneficial and unfavorable groups based on their effects on gut microbiota diversity (Supplementary Table S1) (8). Beneficial components include foods such as fermented dairy, whole grains, fiber, soybean, broccoli, avocados, cranberries, chickpeas, coffee, and green tea, all of which have been shown to promote a healthier gut microbiome. Conversely, red meat, processed meats, refined grains, and high-fat diets (defined as ≥40% of total energy from fat) are classified as unfavorable due to their association with dysbiosis. For beneficial food components, a score of 1 is assigned when intake meets or exceeds the sex-specific median, indicating sufficient consumption. If intake falls below this threshold, a score of 0 is assigned. For unfavorable components, the scoring is reversed: a score of 1 is assigned if intake is below the median or under 40% of daily energy for high-fat diets, while a score of 0 is given. The total DI-GM score ranges from 0 to 14, with higher scores indicating diets that are more supportive of gut microbiota health. Participants are categorized into four subgroups based on the total score: (1) 0–3 points, (2) 4 points, (3) 5 points, and (4) ≥6 points.

2.3 Diagnosis of chronic kidney diseases

In this study, CKD was diagnosed based on the patient's urine albumin-to-creatinine ratio (uACR) and estimated glomerular filtration rate (eGFR) (11). The uACR was categorized into three levels: A1 (<30 mg/g), A2 (30–300 mg/g), and A3 (>300 mg/g), while the eGFR was classified into six levels: G1 (≥90 mL/min/1.73 m^2), G2 (60–89 mL/min/1.73 m^2), G3a (45–59 mL/min/1.73 m^2), G3b (30–44 mL/min/1.73 m^2), G4 (15–29 mL/min/1.73 m^2), and G5 (<15 mL/min/1.73 m^2). Based on the combination of uACR and eGFR, CKD prognosis was stratified into four risk categories: (1) Low Risk: uACR <30 mg/g (A1) with eGFR ≥60 mL/min/1.73 m^2 (G1 or G2), indicating minimal risk of kidney damage; (2) Moderate Risk: uACR <30 mg/g (A1) with eGFR 45–59 mL/min/1.73 m^2 (G3a), or uACR 30–300 mg/g (A2) with eGFR ≥60 mL/min/1.73 m^2, suggesting a moderate risk of kidney damage; (3) High Risk: uACR <30 mg/g (A1) with eGFR 30–44 mL/min/1.73 m^2 (G3b), or uACR 30–300 mg/g (A2) with eGFR 45–59 mL/min/1.73 m^2, or uACR >300 mg/g (A3) with eGFR ≥60 mL/min/1.73 m^2,

indicating significant kidney damage; (4) Very High Risk: eGFR <30 mL/min/1.73 m^2, or uACR >30 mg/g with eGFR 30–59 mL/min/1.73 m^2, indicating severe kidney damage and a poor prognosis. This stratification facilitates a precise assessment of CKD prognosis, confirming a diagnosis of CKD ('yes') for moderate or higher risk categories.

2.4 Covariates

The continuous variables included age, poverty income ratio (PIR, a ratio of family income to poverty threshold), and body mass index (BMI). The categorical variables encompassed sex, race, education, marital status, smoking status (never, former, or current), alcohol consumption (never, former, or current), diabetes, cardiovascular diseases (CVD), hypertension (HBP), cancer, vigorous activity, and moderate activity (all classified as yes/no). Specifically, age was categorized into the intervals of 20–34, 35–49, 50–64, and ≥ 65 years, while racial categories included Mexican American, other Hispanic, Non-Hispanic Black, non-Hispanic White, and other races. Participants were classified based on BMI into the following groups: <25, ≥25 & <30, and ≥ 30 kg/m^2.

2.5 Statistical analysis

The baseline characteristics of all participants were presented using means ± standard deviations (SD) and proportions. Specifically, continuous variables were evaluated using a linear regression model, while categorical variables were analyzed using chi-square tests. To identify independent risk factors associated with CKD, logistic regression analyses were conducted. Participants were categorized into four groups based on the DI-GM, and three logistic regression models were developed to investigate the relationship between DI-GM and CKD. Furthermore, to assess the association between the components of DI-GM and the prevalence of CKD among adults, three additional logistic regression models were employed. In the unadjusted model, no variables were modified. The minimally adjusted model controlled for age, sex, race, PIR, BMI, marital status, and education. The fully adjusted model further included smoking habits, alcohol consumption, HBP, diabetes, CVD, cancer, vigorous activity, and moderate activity. Additionally, spline smoothing using a generalized additive model (GAM) was performed to illustrate whether a linear relationship between DI-GM and CKD present in the fully adjusted model. To further investigate whether any factors could influence the association between these two variables, interaction and subgroup analyses were conducted.

Moreover, sensitivity analyses of multivariable logistic regression were performed. The DI-GM was based on dietary information collected from a day-two recall. All statistical analyses were conducted using R version 4.2.2 (the R Foundation)[1] and EmpowerStats (X&Y Solutions, Inc.).[2] A *p*-value of less than 0.05 was considered statistically significant.

1 http://www.R-project.org

2 http://www.empowerstats.com

3 Results

3.1 Baseline characteristics of study participants

A total of 28,843 individuals were enrolled in the NHANES study from 2007 to 2018, among which 5,461 participants were diagnosed with CKD while 23,382 were not. As presented in Table 1, individuals with CKD exhibited a higher unfavorable to gut microbiota score (2.71 ± 1.07) and a lower DI-GM (4.54 ± 1.61) and beneficial to gut microbiota score (1.83 ± 1.32) compared to those without CKD. In comparison to healthy participants, those with CKD were older (63.07 ± 16.15 years), with a significant proportion aged ≥65 years (55.01%), and had a higher BMI (30.27 ± 7.33) with 45.50% classified as obese (≥30 kg/m^2). Additionally, the proportion of females (52.10%), individuals with low education levels (less than college, 44.79%), smokers (49.59%), and those with diabetes (50.25%), HBP (72.77%), CVD (27.63%), and cancer (17.92%) was higher among CKD patients compared to those without. Conversely, participants with CKD had a lower PIR (2.26 ± 1.51 vs. 2.56 ± 1.64) and were less likely to be in non-single living situations (married/living with a partner, 53.98%), engage in moderate physical activity (29.88%), vigorous activity (13.50%), and consume alcohol (81.95%) when compared to healthy individuals. Regarding the components of the DI-GM, we observed that the scores for components beneficial to gut microbiota, such as avocado, broccoli, chickpeas, cranberries, fermented dairy, fiber, green tea, and soybeans, were predominantly lower in CKD patients, while the scores for components unfavorable to gut microbiota, specifically red meat and refined grains, were higher in this group (Supplementary Table S2 and Figure 1).

3.2 Multivariable logistic regression

Table 2 demonstrates a negative association between DI-GM and the prevalence of CKD across all models. In the non-adjusted model, the odds ratio (OR) was 0.964 (95% CI, 0.946 to 0.982), in the minimally-adjusted model, it was 0.919 (95% CI, 0.901 to 0.937), and in the fully-adjusted model, the OR was 0.958 (95% CI, 0.936 to 0.980). Furthermore, individuals with a DI-GM score > 5 exhibited a significantly higher prevalence of CKD compared to those in the ≤3 score group (OR = 0.837, 95% CI, 0.754 to 0.928). Additionally, the P vale of trend test analyses was <0.5 in all three models.

Furthermore, the results showed that beneficial to gut microbiota serves as a protective factor for CKD (OR = 0.923, 95% CI 0.897 to 0.950), with no significant differences observed in the unfavorable to gut microbiota within the fully adjusted model. Additionally, components of beneficial to gut microbiota, such as coffee, fiber, and whole grains, play a crucial role in protecting CKD across the three models (Table 3).

3.3 A smooth spline curve

The results demonstrate a negative linear association between DI-GM and the prevalence of CKD, as illustrated in

10.3389/fnut.2025.1561235

TABLE 1 Characteristics of participants by categories of Chronic kidney diseases: NHANES 2007–2018.*

Variables	All (*n*=28843)	Chronic kidney diseases		*p*-value
		No (*n*=23382)	Yes (*n*=5461)	
DI-GM (mean ± SD)	4.62 ± 1.61	4.64 ± 1.62	4.54 ± 1.61	<0.001
Beneficial to gut microbiota (mean ± SD)	1.99 ± 1.34	2.03 ± 1.34	1.83 ± 1.32	<0.001
Unfavorable to gut microbiota (mean ± SD)	2.63 ± 1.06	2.61 ± 1.06	2.71 ± 1.07	<0.001
Age (years, mean ± SD)	49.97 ± 17.59	46.91 ± 16.47	63.07 ± 16.15	<0.001
20–34 (%)	24.18	28.05	7.62	
35–49 (%)	25.15	28.09	12.58	
50–64 (%)	26.62	27.05	24.79	
≥65 (%)	24.04	16.81	55.01	
PIR (mean ± SD)	2.50 ± 1.62	2.56 ± 1.64	2.26 ± 1.51	<0.001
≤1.3 (%)	32.08	31.33	35.28	
>1.3 and ≤ 3.5 (%)	37.72	36.74	41.95	
>3.5 (%)	30.20	31.93	22.77	
BMI (kg/m^2, mean ± SD)	29.29 ± 6.94	29.07 ± 6.83	30.27 ± 7.33	<0.001
<25 (%)	28.16	29.20	23.61	
≥25 and < 30 (%)	32.95	33.43	30.89	
≥30 (%)	38.89	37.37	45.50	
Sex (%)				0.026
Female	50.74	50.42	52.10	
Male	49.26	49.58	47.90	
Race (%)				<0.001
Mexican American	15.29	15.86	12.87	
Other Hispanic	42.21	41.11	46.90	
Non-Hispanic White	20.71	20.17	23.00	
Non-Hispanic Black	10.52	10.92	8.79	
Other races	11.27	11.94	8.44	
Education (%)				<0.001
Less than 9th grade	10.30	9.21	14.99	
9–11th grade	13.90	13.43	15.91	
High school graduate	22.89	22.54	24.40	
Some college	29.71	30.22	27.54	
College graduate or above	23.19	24.60	17.16	
Marital (%)				<0.001
Married/Living with partner	59.49	60.77	53.98	
Divorced/Separated/Widowed	22.41	19.42	35.21	
Never married	18.10	19.80	10.81	
Vigorous activity (%)				<0.001
No	79.94	78.41	86.50	
Yes	20.06	21.59	13.50	
Moderate activity (%)				<0.001
No	62.67	60.93	70.12	
Yes	37.33	39.07	29.88	
Alcohol (%)				<0.001

(Continued)

TABLE 1 (Continued)

Variables	All (*n*=28843)	Chronic kidney diseases		*p*-value
		No (*n*=23382)	Yes (*n*=5461)	
Never	14.15	13.26	18.05	
Former	15.83	13.71	25.15	
Yes	70.02	73.03	56.80	
Smoke (%)				<0.001
Never	55.44	56.62	50.41	
Former	24.32	22.35	32.77	
Yes	20.23	21.03	16.82	
Diabetes (%)				<0.001
No	71.82	76.98	49.75	
Borderline	8.58	8.59	8.55	
Yes	19.60	14.43	41.70	
HBP (%)				<0.001
No	56.63	63.50	27.23	
Yes	43.37	36.50	72.77	
CVD (%)				<0.001
No	88.69	92.50	72.37	
Yes	11.31	7.50	27.63	
Cancer (%)				<0.001
No	90.31	92.23	82.08	
Yes	9.69	7.77	17.92	

*Mean + SD for continuous variables, and *p* value was calculated by weighted t test. % for categorical variables, and *p* value was calculated by weighted chi-square test. SD, Standard Deviation; BMI, Body Mass Index; PIR, Poverty Income Ratio; CVD, Cardiovascular Disease; HBP, Hypertension; DI-GM, dietary index for gut microbiota.

Supplementary Figure S2. Specifically, the dose–response relationship indicates that higher levels of DI-GM are correlated with a lower prevalence of CKD.

3.4 Subgroup and interaction analysis

Our findings indicate that sex significantly influenced the relationship under investigation (Supplementary Figure S3). Specifically, the stratified analysis revealed notable differences in effects based on sex, with a *p*-value of 0.043 for the interaction, and the association was more pronounced in female. No other significant interactions were observed among the other variables.

3.5 Sensitivity analysis

Based on the dietary information collected on day two for DI-GM, the logistic regression analysis revealed consistent results, demonstrating a negative association between the two (Supplementary Table S3).

4 Discussion

This study utilized NHANES data from 2007 to 2018, encompassing a sample of 28,843 adults, to evaluate the association between DI-GM and the prevalence of CKD. Baseline characteristics of the study population indicated that patients with CKD had a higher median age and a greater proportion of individuals with high BMI, HBP, and diabetes. The results demonstrated a linear negative association between DI-GM and the prevalence of CKD, with sex influencing this relationship. Additionally, higher scores of beneficial to gut microbiota were significantly associated with a lower prevalence of CKD. Furthermore, specific dietary components within the beneficial to gut microbiota, such as dietary fiber, coffee, and whole grains, exhibited potential protective effects against CKD.

The above mentioned results underscore the critical role of healthy intestinal flora in preserving kidney health. Recent research suggests that an imbalance in intestinal flora can lead to increased production of uremic toxins, such as indoxyl sulfate and p-cresol sulfate (12). These toxins are detrimental to renal tubular cells and exacerbate CKD progression by promoting systemic inflammation (13, 14). Studies have shown that CKD patients experience a marked reduction in intestinal flora diversity, with this imbalance closely linked to elevated urinary toxin production (15). Moreover, a high DI-GM dietary pattern, which is abundant in dietary fiber and prebiotics, promotes the production of short-chain fatty acids (SCFAs), such as butyrate. These metabolites have been demonstrated to exert anti-inflammatory effects by inhibiting pro-inflammatory cytokines, including TNF-α and IL-6, and by mitigating oxidative stress (16, 17). Andrade-Oliveira et al. emphasized that butyrate plays a vital regulatory role in the

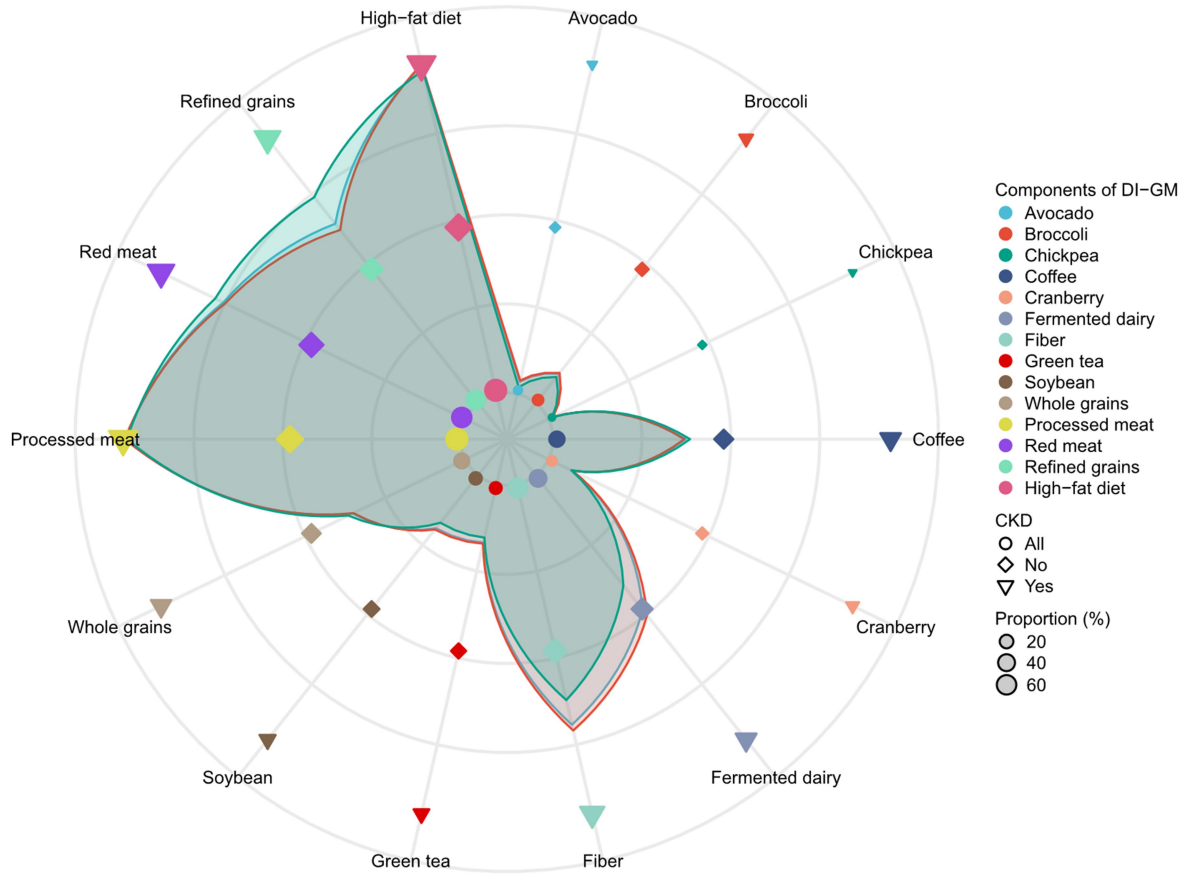

FIGURE 1
The distributions of dietary index for gut microbiota (DI-GM) components by categories of chronic kidney diseases (CKD).

TABLE 2 Association between DI-GM and the prevalence of CKD in the adults.

Variables (%)	Non-adjusted model*		Minimally-adjusted model**		Fully-adjusted model***	
	OR (95%CI)	*p*	OR (95%CI)	*p*	OR (95%CI)	*p*
DI-GM	0.964 (0.946, 0.982)	<0.001	0.919 (0.901, 0.937)	<0.001	0.958 (0.936, 0.980)	<0.001
Category of DI-GM						
≤3	Ref		Ref		Ref	
>3, and ≤ 4	0.912 (0.839, 0.991)	0.030	0.887 (0.810, 0.971)	0.009	0.938 (0.845, 1.042)	0.235
>4, and ≤ 5	0.924 (0.849, 1.006)	0.070	0.848 (0.773, 0.930)	<0.001	0.939 (0.844, 1.044)	0.245
>5	0.863 (0.795, 0.936)	<0.001	0.699 (0.639, 0.764)	<0.001	0.837 (0.754, 0.928)	<0.001
P for trend	0.001		<0.001		0.001	
Beneficial to gut microbiota	0.894 (0.874, 0.915)	<0.001	0.878 (0.857, 0.900)	<0.001	0.923 (0.897, 0.950)	<0.001
Unfavorable to gut microbiota	1.095 (1.064, 1.126)	<0.001	1.002 (0.973, 1.033)	0.876	1.022 (0.987, 1.059)	0.220

CI, confidence interval; OR, odds ratio; CKD, chronic kidney diseases; DI-GM, dietary index for gut microbiota.
*Non-adjusted model adjusts for none.
**Minimally-adjusted model adjusts for age, sex, race, body mass index, race, poverty income ratio, education, marital.
***Fully-adjusted model adjusts for age, sex, body mass index, race, poverty income ratio, education, marital, alcohol, smoke, hypertension, cardiovascular disease, cancer, diabetes, moderate activity, vigorous activity.

gut-kidney axis, particularly in cases of ischemia–reperfusion-induced acute kidney injury, suggesting that SCFA production may help delay disease progression in CKD patients (18). This finding indicates that enhancing DI-GM scores, for instance, through increased dietary fiber intake, could offer renal protection for CKD patients. Clinically, improving the DI-GM score may contribute to

TABLE 3 Association between the components of DI-GM and the prevalence of CKD in the adults.

HEI-2015 Components	Non-adjusted model*		Minimally-adjusted model**		Fully-adjusted model***	
	OR (95%CI)	*p*	OR (95%CI)	*p*	OR (95%CI)	*p*
Beneficial to gut microbiota						
Avocado	0.505 (0.404, 0.631)	<0.001	0.752 (0.589, 0.961)	0.023	0.866 (0.670, 1.119)	0.272
Broccoli	0.855 (0.766, 0.955)	0.006	0.934 (0.822, 1.061)	0.291	1.001 (0.873, 1.148)	0.989
Chickpea	0.751 (0.552, 1.022)	0.068	0.970 (0.670, 1.404)	0.871	0.923 (0.621, 1.373)	0.694
Coffee	1.063 (0.997, 1.133)	0.063	0.844 (0.782, 0.910)	<0.001	0.843 (0.776, 0.915)	<0.001
Cranberry	0.962 (0.847, 1.091)	0.545	1.060 (0.914, 1.229)	0.441	1.087 (0.924, 1.278)	0.315
Fermented dairy	0.689 (0.647, 0.733)	<0.001	0.960 (0.892, 1.033)	0.271	0.949 (0.877, 1.027)	0.191
Fiber	0.754 (0.711, 0.800)	<0.001	0.806 (0.751, 0.864)	<0.001	0.821 (0.761, 0.885)	<0.001
Green tea	0.883 (0.807, 0.965)	0.006	0.922 (0.833, 1.020)	0.114	0.921 (0.827, 1.027)	0.139
Soybean	0.855 (0.785, 0.931)	<0.001	0.927 (0.842, 1.022)	0.129	0.938 (0.845, 1.041)	0.230
Whole grains	1.064 (0.997, 1.135)	0.063	0.880 (0.815, 0.949)	<0.001	0.865 (0.796, 0.939)	<0.001
Unfavorable to gut microbiota						
Processed meat	0.973 (0.909, 1.042)	0.433	0.966 (0.892, 1.046)	0.392	0.986 (0.905, 1.074)	0.743
Red meat	1.111 (1.045, 1.180)	<0.001	0.990 (0.923, 1.062)	0.778	0.993 (0.921, 1.072)	0.864
Fat	0.928 (0.867, 0.993)	0.031	1.008 (0.932, 1.091)	0.840	1.042 (0.957, 1.135)	0.341
Refined grains	1.462 (1.377, 1.552)	<0.001	1.058 (0.987, 1.135)	0.114	1.062 (0.984, 1.145)	0.121

CI, confidence interval; OR, odds ratio.
*Non-adjusted model adjusts for none.
**Minimally-adjusted model adjusts for age, sex, race, body mass index, race, poverty income ratio, education, marital.
***Fully-adjusted model adjusts for age, sex, body mass index, race, poverty income ratio, education, marital, alcohol, smoke, hypertension, cardiovascular disease, cancer, diabetes, moderate activity, vigorous activity.

delaying CKD progression. Future studies should further explore the potential of SCFAs as prognostic biomarkers for CKD and examine the varying protective effects of different types of intestinal flora on CKD.

This study found that sex significantly moderates the relationship between DI-GM and CKD, and a high DI-GM diet offers a more pronounced protective effect against CKD in women, potentially linked to estrogen's role in regulating intestinal flora and barrier function. Gomez et al. highlighted that estrogen enhances the intestinal barrier by upregulating tight junction proteins, such as occludin, which reduces the production of pro-inflammatory uremic toxins and mitigates kidney damage (19, 20). Furthermore, women typically exhibit greater diversity in gut microbiota, which may enhance the benefits derived from a high DI-GM diet (21, 22). In contrast, men often favor high-fat and high-protein diets, which can disrupt bacterial balance and elevate pro-inflammatory bacteria, thereby diminishing the protective effects of DI-GM (23, 24). This study underscores the importance of considering sex differences in the dietary management of CKD patients, particularly for women who may experience greater advantages from a high DI-GM diet. Future personalized strategies should be developed to address these sex-specific dietary needs. Additionally, further research is warranted to elucidate the mechanisms by which estrogen contributes to intestinal barrier integrity and renal protection, thereby providing a more precise foundation for nutritional interventions targeting female CKD patients.

This study also analyzed the role of specific food components in dietary interventions for CKD and found that dietary fiber, coffee, and whole grains significantly contribute to kidney protection. As a prebiotic, dietary fiber promotes the proliferation of beneficial bacteria, such as Bifidobacteria, produces SCFAs, reduces pro-inflammatory factors, and enhances the intestinal environment (25). Research highlighted that dietary fiber intake is significantly associated with slowing the progression of CKD, with its mechanism closely linked to the improvement of bacterial flora diversity and the anti-inflammatory effects of dietary fiber (26). Furthermore, whole grain consumption has been shown to lower levels of chronic inflammatory markers, such as C-reactive protein, while improving metabolic health (27). Antioxidant components, such as polyphenols found in coffee, are also recognized for their protective effects against CKD. Research indicated that moderate coffee intake is associated with a deceleration in the progression of CKD, further corroborating the anti-inflammatory effects of coffee (28–30). This study provides specific guidance for the dietary management of CKD patients, suggesting that increasing the intake of dietary fiber, whole grains, and moderate amounts of coffee may enhance kidney protection. Future research should further explore the specific protective effects of these dietary components on CKD to optimize dietary strategies for renal health.

This study presents both strengths and weaknesses. It utilizes the NHANES large-scale database, which boasts a substantial sample size and broad representativeness, thereby enhancing the feasibility and generalizability of the results. Additionally, the study is noteworthy for being the first to analyze the correlation between DI-GM and CKD, providing a novel reference point for dietary interventions in CKD patients. However, the cross-sectional design of this study presents challenges in establishing

a causal relationship between the two variables. Furthermore, the NHANES database lacks specific data on intestinal flora, which limits further investigation into the role of intestinal microorganisms in the mechanisms underlying CKD. Future research should incorporate longitudinal studies alongside microbiome technologies to elucidate the long-term effects of DI-GM on intestinal flora regulation and the protection of renal function.

5 Conclusion

This study provides compelling evidence that higher DI-GM scores are associated with a reduced prevalence of CKD in adults, with the protective effect being more pronounced in women than in men. Our findings highlight the significant contributions of beneficial dietary components, such as dietary fiber, whole grains, and coffee, which are integral to a gut-healthy diet. These results suggest that enhancing gut health through diet may serve as a viable strategy for the prevention and management of CKD, particularly by focusing on sex-based differences in prevention efforts. Future prospective cohort studies and microbiome analyses are warranted to further elucidate the role of gut microbiota in the progression of CKD and to support the development of more precise, individualized dietary intervention strategies.

Data availability statement

The datasets presented in this study can be found in online repositories. The names of the repository/repositories and accession number(s) can be found at: https://www.cdc.gov/nchs/nhanes/index.htm.

Ethics statement

This study was performed using public data from the National Center for Health Statistics (NCHS) program and the National Health and Nutrition Examination Survey (NHANES). The data have been de-identified and not merged or augmented in a way that has compromised the privacy of the participants. Therefore, the study requires no further approval and follows ethical guidelines.

Author contributions

YFX: Conceptualization, Data curation, Formal analysis, Investigation, Methodology, Resources, Software, Visualization, Writing – original draft, Writing – review & editing. YQY: Data curation, Formal analysis, Investigation, Methodology, Resources, Software, Validation, Visualization, Writing – original draft, Writing – review & editing. SYG: Data curation, Formal analysis, Investigation, Methodology, Resources, Software, Validation, Visualization, Writing – review & editing. HZ: Data curation, Formal analysis, Investigation, Methodology, Resources, Software, Validation, Visualization, Writing – review & editing. JW: Investigation, Resources, Validation, Visualization, Writing – review & editing. TL: Funding acquisition, Investigation, Project administration, Resources, Supervision, Validation, Visualization, Writing – review & editing. YJB: Conceptualization, Investigation, Project administration, Resources, Supervision, Visualization, Writing – review & editing.

Funding

The author(s) declare that financial support was received for the research and/or publication of this article. This work was supported by the National Natural Science Foundation of China (82370753).

Conflict of interest

The authors declare that the research was conducted in the absence of any commercial or financial relationships that could be construed as a potential conflict of interest.

Generative AI statement

The authors declare that no Gen AI was used in the creation of this manuscript.

Publisher's note

Supplementary material

The Supplementary material for this article can be found online at: https://www.frontiersin.org/articles/10.3389/fnut.2025.1561235/full#supplementary-material

SUPPLEMENTARY FIGURE S1
Flow diagram of obtaining the final inclusion in the population.

SUPPLEMENTARY FIGURE S2
A spline smoothing demonstrated the linear association between DI-GM and the prevalence of CKD.

SUPPLEMENTARY FIGURE S3
Logistic regression analysis to identify variables that modify the correlation between DI-GM and the prevalence of CKD.

References

1. GBD Chronic Kidney Disease Collaboration. Global, regional, and national burden of chronic kidney disease, 1990-2017: a systematic analysis for the global burden of disease study 2017. *Lancet*. (2020) 395:709–33. doi: 10.1016/S0140-6736(20)30045-3

2. Glassock RJ, Warnock DG, Delanaye P. The global burden of chronic kidney disease: estimates, variability and pitfalls. *Nat Rev Nephrol*. (2017) 13:104–14. doi: 10.1038/nrneph.2016.163

3. Perna AF, Glorieux G, Zacchia M, Trepiccione F, Capolongo G, Vigorito C, et al. The role of the intestinal microbiota in uremic solute accumulation: a focus on sulfur compounds. *J Nephrol*. (2019) 32:733–40. doi: 10.1007/s40620-019-00589-z

4. Li J, Shen Y, Yan K, Wang S, Jiao J, Chi H, et al. The compositional and functional imbalance of the gut microbiota in CKD linked to disease patterns. *J Transl Med*. (2024) 22:773. doi: 10.1186/s12967-024-05578-w

5. Pan L, Yu H, Fu J, Hu J, Xu H, Zhang Z, et al. Berberine ameliorates chronic kidney disease through inhibiting the production of gut-derived uremic toxins in the gut microbiota. *Acta Pharm Sin B*. (2023) 13:1537–53. doi: 10.1016/j.apsb.2022.12.010

6. Yang T, Richards EM, Pepine CJ, Raizada MK. The gut microbiota and the brain-gut-kidney axis in hypertension and chronic kidney disease. *Nat Rev Nephrol*. (2018) 14:442–56. doi: 10.1038/s41581-018-0018-2

7. Kase BE, Liese AD, Zhang J, Murphy EA, Zhao L, Steck SE. The development and evaluation of a literature-based dietary index for gut microbiota. *Nutrients*. (2024) 16:1045. doi: 10.3390/nu16071045

8. Zhang X, Yang Q, Huang J, Lin H, Luo N, Tang H. Association of the newly proposed dietary index for gut microbiota and depression: the mediation effect of phenotypic age and body mass index. *Eur Arch Psychiatry Clin Neurosci*. (2024). doi: 10.1007/s00406-024-01912-x

9. Flint HJ, Duncan SH, Scott KP, Louis P. Links between diet, gut microbiota composition and gut metabolism. *Proc Nutr Soc*. (2015) 74:13–22. doi: 10.1017/S0029665114001463

10. Wang H, Ainiwaer A, Song Y, Qin L, Peng A, Bao H, et al. Perturbed gut microbiome and fecal and serum metabolomes are associated with chronic kidney disease severity. *Microbiome*. (2023) 11:3. doi: 10.1186/s40168-022-01443-4

11. Kidney Disease: Improving Global Outcomes (KDIGO) Glomerular Diseases Work Group. KDIGO 2021 clinical practice guideline for the Management of Glomerular Diseases. *Kidney Int*. (2021) 100:S1–S276. doi: 10.1016/j.kint.2021.05.021

12. Holle J, Kirchner M, Okun J, Bayazit AK, Obrycki L, Canpolat N, et al. Serum indoxyl sulfate concentrations associate with progression of chronic kidney disease in children. *PLoS One*. (2020) 15:e0240446. doi: 10.1371/journal.pone.0240446

13. Wang X, Yang S, Li S, Zhao L, Hao Y, Qin J, et al. Aberrant gut microbiota alters host metabolome and impacts renal failure in humans and rodents. *Gut*. (2020) 69:2131–42. doi: 10.1136/gutjnl-2019-319766

14. Chen Z, Wu S, Zeng Y, Chen Z, Li X, Li J, et al. FuZhengHuaYuJiangZhuTongLuoFang prescription modulates gut microbiota and gut-derived metabolites in UUO rats. *Front Cell Infect Microbiol*. (2022) 12:837205. doi: 10.3389/fcimb.2022.837205

15. Gryp T, De Paepe K, Vanholder R, Kerckhof FM, Van Biesen W, Van de Wiele T, et al. Gut microbiota generation of protein-bound uremic toxins and related metabolites is not altered at different stages of chronic kidney disease. *Kidney Int*. (2020) 97:1230–42. doi: 10.1016/j.kint.2020.01.028

16. Lee J, d'Aigle J, Atadja L, Quaicoe V, Honarpisheh P, Ganesh BP, et al. Gut microbiota-derived short-chain fatty acids promote poststroke recovery in aged mice. *Circ Res*. (2020) 127:453–65. doi: 10.1161/CIRCRESAHA.119.316448

17. Deehan EC, Yang C, Perez-Muñoz ME, Nguyen NK, Cheng CC, Triador L, et al. Precision microbiome modulation with discrete dietary fiber structures directs short-chain fatty acid production. *Cell Host Microbe*. (2020) 27:389–404.e6. doi: 10.1016/j.chom.2020.01.006

18. Andrade-Oliveira V, Amano MT, Correa-Costa M, Castoldi A, Felizardo RJ, de Almeida DC, et al. Gut Bacteria products prevent AKI induced by ischemia-reperfusion. *J Am Soc Nephrol*. (2015) 26:1877–88. doi: 10.1681/ASN.2014030288

19. Acharya KD, Noh HL, Graham ME, Suk S, Friedline RH, Gomez CC, et al. Distinct changes in gut microbiota are associated with estradiol-mediated protection from diet-induced obesity in female mice. *Meta*. (2021) 11:499. doi: 10.3390/metabo11080499

20. Ma Y, Liu T, Li X, Kong A, Xiao R, Xie R, et al. Estrogen receptor β deficiency impairs gut microbiota: a possible mechanism of IBD-induced anxiety-like behavior. *Microbiome*. (2022) 10:160. doi: 10.1186/s40168-022-01356-2

21. Yuan X, Chen R, Zhang Y, Lin X, Yang X. Sexual dimorphism of gut microbiota at different pubertal status. *Microb Cell Factories*. (2020) 19:152. doi: 10.1186/s12934-020-01412-2

22. Baldeon AD, McDonald D, Gonzalez A, Knight R, Holscher HD. Diet quality and the fecal microbiota in adults in the American gut project. *J Nutr*. (2023) 153:2004–15. doi: 10.1016/j.tjnut.2023.02.018

23. Amicis R, Galasso L, Cavallaro R, Mambrini SP, Castelli L, Montaruli A, et al. Sex differences in the relationship between Chronotype and eating behaviour: a focus on binge eating and food addiction. *Nutrients*. (2023) 15:4580. doi: 10.3390/nu15214580

24. Anguah KO, Syed-Abdul MM, Hu Q, Jacome-Sosa M, Heimowitz C, Cox V, et al. Changes in food cravings and eating behavior after a dietary carbohydrate restriction intervention trial. *Nutrients*. (2019) 12:52. doi: 10.3390/nu12010052

25. Spencer CN, McQuade JL, Gopalakrishnan V, McCulloch JA, Vetizou M, Cogdill AP, et al. Dietary fiber and probiotics influence the gut microbiome and melanoma immunotherapy response. *Science*. (2021) 374:1632–40. doi: 10.1126/science.aaz7015

26. Li YJ, Chen X, Kwan TK, Loh YW, Singer J, Liu Y, et al. Dietary Fiber protects against diabetic nephropathy through short-chain fatty acid-mediated activation of G protein-coupled receptors GPR43 and GPR109A. *J Am Soc Nephrol*. (2020) 31:1267–81. doi: 10.1681/ASN.2019101029

27. Mazidi M, Katsiki N, Mikhailidis DP, Banach M. A higher ratio of refined grain to whole grain is associated with a greater likelihood of chronic kidney disease: a population-based study. *Br J Nutr*. (2019) 121:1294–302. doi: 10.1017/S0007114518003124

28. Kennedy OJ, Pirastu N, Poole R, Fallowfield JA, Hayes PC, Grzeszkowiak EJ, et al. Coffee consumption and kidney function: a Mendelian randomization study. *Am J Kidney Dis*. (2020) 75:753–61. doi: 10.1053/j.ajkd.2019.08.025

29. Zhou X, Zhang B, Zhao X, Zhang P, Guo J, Zhuang Y, et al. Coffee leaf tea extracts improve hyperuricemia nephropathy and its associated negative effect in gut microbiota and amino acid metabolism in rats. *J Agric Food Chem*. (2023) 71:17775–87. doi: 10.1021/acs.jafc.3c02797

30. He WJ, Chen J, Razavi AC, Hu EA, Grams ME, Yu B, et al. Metabolites associated with coffee consumption and incident chronic kidney disease. *Clin J Am Soc Nephrol*. (2021) 16:1620–9. doi: 10.2215/CJN.05520421

frontiers | Frontiers in Nutrition

TYPE Original Research
PUBLISHED 21 March 2025
DOI 10.3389/fnut.2025.1564580

OPEN ACCESS

EDITED BY
Sofia Viana,
University of Coimbra, Portugal

REVIEWED BY
Tania Martins-Marques,
University of Coimbra, Portugal
Liliana Santos,
University of Coimbra, Portugal

*CORRESPONDENCE
Ming Cui
✉ mingcui@bjmu.edu.cn

†These authors have contributed equally to this work

RECEIVED 21 January 2025
ACCEPTED 06 March 2025
PUBLISHED 21 March 2025

CITATION
Xu H, Xie P, Liu H, Tian Z, Zhang R and Cui M (2025) The relationship between dietary inflammatory index in adults and coronary heart disease: from NHANES 1999–2018.
Front. Nutr. 12:1564580.
doi: 10.3389/fnut.2025.1564580

The relationship between dietary inflammatory index in adults and coronary heart disease: from NHANES 1999–2018

Hong Xu[1†], Pengxin Xie[2,3†], Hui Liu[2,3], Zhenyu Tian[2,3], Ruitao Zhang[2,3] and Ming Cui[2,3*]

[1]College of Science, Minzu University of China, Beijing, China, [2]Department of Cardiology and Institute of Vascular Medicine, Peking University Third Hospital, Beijing, China, [3]State Key Laboratory of Vascular Homeostasis and Remodeling, Peking University Third Hospital, Beijing, China

Background: Previous studies have shown that pro-inflammatory diets increase the risk of coronary heart disease (CHD) and all-cause mortality. The dietary inflammatory index (DII) is a quantitative measure of dietary inflammation, and its accuracy has been validated by several studies.

Methods: This study included 43,842 participants aged ≥18 years from the National Health and Nutrition Examination Survey (NHANES) 1999–2018. The data of CHD was obtained through a questionnaire survey, and the DII was calculated using 24-h dietary recall data. Generalized linear models and logistic regression were used to determine the mediation factors, and subgroup analyses were conducted to evaluate the interaction between DII and CHD. Mean decrease in Gini (MDG) was used to determine the importance of individual dietary components.

Results: The age of the participants was 49.81 ± 18.10 years, with 20,793 (47.4%) being male. A total of 1,892 (4.3%) participants were diagnosed with CHD, and the median DII score was 1.33 (0.11, 2.40). After adjusting for potential confounders, logistic regression analysis revealed that DII independently associated with CHD [OR: 1.049 (1.012–1.087), $p = 0.008$]. Triglyceride-glucose index, visceral adiposity index, body mass index, waist-to-height ratio, high-density lipoprotein, and glomerular filtration rate (all $p < 0.05$) may mediate the relationship between DII and CHD. Subgroup analyses showed that DII was more sensitive in participants aged <75 years ($p < 0.001$), females ($p = 0.028$), those with low cholesterol levels ($p = 0.004$), and individuals with low Framingham risk scores ($p = 0.005$). MDG analysis indicated that carbohydrate, vitamin C and iron intake have the greatest impact on CHD.

Conclusion: This study suggests that various metabolic and lipid indicators play a mediating role in the relationship between DII and CHD. DII may have a greater adverse impact on traditional low-risk CHD populations.

KEYWORDS

dietary inflammatory index, coronary heart disease, National Health and Nutrition Examination Survey, mediating factors, interaction

1 Introduction

Coronary heart disease (CHD) is characterized by accumulation of lipids and fibrous tissue in the intima of the arterial wall, smooth muscle cell proliferation, and local and systemic inflammatory responses (1). CHD poses a giant threat to health. In the United States, approximately 20.1 million individuals are diagnosed with CHD (2). Despite recent advances in treatment, it remains one of the leading causes of death globally (3). The complex pathophysiological mechanisms of CHD present a significant challenge to improving patient outcomes. Studies have shown that inflammation plays a key role in the onset and progression of CHD (4). It is involved in several stages of atherosclerosis initiation and progression, plaque rupture, ischemia–reperfusion injury, and ventricular remodeling (4).

Healthy dietary habits, such as the Mediterranean diet, high-fiber diets, and plant-based diets, have been shown to be associated with lower systemic inflammation levels. The dietary inflammatory index (DII), first proposed by Cavicchia et al. (5), is used to quantitatively assess the inflammatory potential of diet. The DII is based on 45 different anti-inflammatory and pro-inflammatory food components. A positive DII score indicates a pro-inflammatory effect, while a negative score indicates an anti-inflammatory effect. The higher the score, the more pronounced the pro-inflammatory effect. An increasing body of evidence has described a certain correlation between higher DII and elevated levels of inflammatory markers, such as hypersensitive C-reactive protein (hsCRP), tumor necrosis factor-α (TNF-α) and interleukin-6 (IL-6) (6–8).

Current research suggests that the DII is associated with subclinical atherosclerosis. DII in patients with CHD was significantly higher than in those without CHD (9). A 36-month follow-up study found a positive association between DII and the risk of atherosclerosis-related mortality [HR: 1.36(1.15–1.60)] (10). Additionally, DII was positively associated with all-cause mortality risk in CHD patients, particularly among women (11). However, current studies have not explored the interaction between DII and traditional risk factors, nor have they investigated potential mediating factors between DII and CHD. Due to the inclusion of multiple variables, guiding patients on diet based on DII becomes more complex.

Therefore, this study aims to explore the correlation between DII and CHD, as well as traditional risk factors, further analyze mediating factors and interactions, and rank the importance of dietary components to enhance the practicality in clinical settings.

2 Methods

2.1 Study design and population

The National Health and Nutrition Examination Survey (NHANES) is a research project aimed at assessing the health and nutritional status of United States. The survey used scientific sampling methods and annually collected data from approximately 5,000 individuals from 15 counties, representing the national population. The inclusion criteria for this study were: (1) participants in NHANES surveys from 1999 to 2018; (2) age ≥ 18 years. The exclusion criteria were: (1) missing key variables regarding the presence of CHD; (2) missing dietary data required for the calculation of the DII. Ultimately, 43,842 participants were included in this study. The detailed participant inclusion process was shown in Figure 1. The NHANES

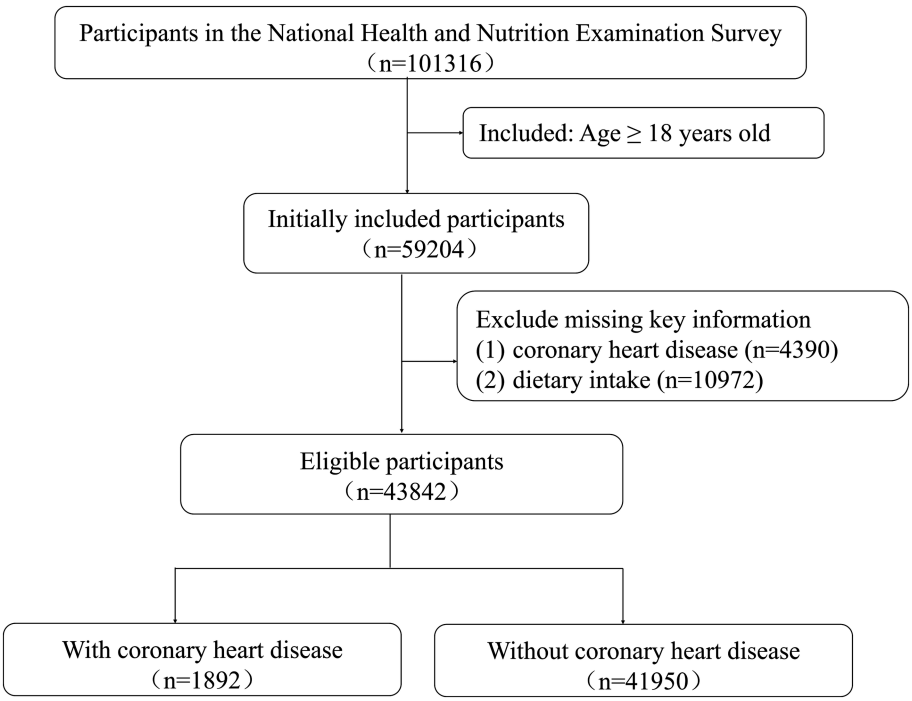

FIGURE 1
Flowchart of the study population.

study was approved by the Institutional Review Board of the National Center for Health Statistics, and all participants provided written informed consent.

2.2 Dietary inflammatory index (DII)

The DII was calculated based on individual dietary components, with dietary data collected through 24-h dietary recall interviews in NHANES. For the 1999–2002, only 1 day's dietary component records were included, and from 2003 to 2018, the average of 2 days of dietary data was used. The two dietary recall data collections were conducted separately: the first was carried out at the Mobile Examination Center, while the second was collected via telephone 3 to 10 days later. This approach helps provide a more comprehensive evaluation of each participant's dietary habits. The calculation of the DII requires 45 dietary components; however, due to limitations in NHANES data collection, this study included 28 dietary components for DII calculation, which are: alcohol, vitamin B12, vitamin B6, β-carotene, caffeine, carbohydrate, cholesterol, energy, total fat, fiber, folic acid, iron, magnesium, monounsaturated fatty acid, niacin, n-3 fatty acid, n-6 fatty acid, protein, polyunsaturated fatty acid, riboflavin, saturated fat, selenium, thiamine, vitamin A, vitamin C, vitamin D, vitamin E, and zinc. Previous studies have shown that using fewer than 30 dietary components for DII calculation does not significantly affect its accuracy (6, 12). Even a DII calculation that incorporates 28 dietary components has a strong predictive ability for high CRP levels [OR 1.10 (1.02–1.19)] (6). The DII calculation formula is as follows:

$$\text{Z score} = \frac{daily\ mean\ intake - global\ daily\ mean\ intake}{standard\ deviation}$$

Convert the *Z*-score to a percentile score and then standardize it

$$\text{Z score}' = \left(\text{Z score percentile score}\right) \times 2 - 1$$

$$\text{DII} = \sum\left(\text{Z score}' \times \text{inflammation effect score}\right)$$

2.3 Outcome definition

The data of CHD was collected from the NHANES interview, where each question was standardized and administered by trained professionals. CHD was defined as "Has a doctor or other health professional ever told you that you had coronary heart disease? (MCQ160C)."

2.4 Covariates

The following variables were extracted from the NHANES: age, sex, race, education level, smoking, hypertension, diabetes, body mass index (BMI), glomerular filtration rate (GFR), total cholesterol, triglycerides, high-density lipoprotein (HDL), low-density lipoprotein (LDL), and hemoglobin A1c. Smoking was defined as having smoked more than 100 cigarettes in one's lifetime. Biochemical parameters were evaluated using a standardized methodology detailed in the NHANES Laboratory/Medical Technologist Procedure Manual (CDC: NHANES Laboratory/Medical Technologists Procedures Manual, Atlanta, GA, CDC, 2001).

The triglyceride-glucose index (TyG) is defined as ln[triglycerides (mg/dL)/fasting glucose (mg/dL)/2]. The Waist-to-Height Ratio (WHtR) is defined as waist circumference (cm)/height (cm). The Framingham score, first proposed in 2008 to assess cardiovascular disease risk, was updated in 2015[1] (13). The formula for the visceral adiposity index (VAI) is as follows:

$$\text{VAI} = \frac{waist\ circumference}{\left(39.68 + 1.88 \times BMI\right)} \times \frac{TG}{1.03} \times \frac{1.31}{HDL}\ \left(\text{Male}\right)$$

$$\text{VAI} = \frac{waist\ circumference}{\left(36.58 + 1.89 \times BMI\right)} \times \frac{TG}{0.81} \times \frac{1.52}{HDL}\ \left(\text{Female}\right)$$

2.5 Statistical methods

Due to the complexity of NHANES sampling, weighted regression models were used with WTDRD1 and WTDR2D as weights. All participants were divided into three groups based on the tertiles of the DII. Normally distributed continuous data were expressed as means ± standard deviations, and differences between the three groups were examined using one-way ANOVA. Non-normally distributed continuous data were expressed as medians (Q1, Q3) and compared using the Kruskal-Wallis H test. For continuous variables, effect sizes were calculated using Cohen's F, and *post hoc* comparisons were performed using the Newman–Keuls method. Categorical data were presented as counts and percentages and were compared using the chi-squared test, with Cramér's V employed to assess effect sizes and calculating pairwise comparisons between pairs of proportions with bonferroni correction for multiple testing. The relationship between DII and traditional cardiovascular risk factors was assessed using restricted cubic splines (RCS). The association between DII and CHD was explored using multivariable logistic regression models, with DII as both continuous and categorical variable to evaluate the robustness of the results.

In exploring the mediating factors in the association between DII and CHD, two models were constructed. The first is the mediator model, using generalized linear models (GLM) to fit the Gaussian distribution (linear regression with an identity link function) between DII and potential mediators, while controlling for potential confounders. The second is the outcome model, which uses both GLM and logistic regression models, incorporating both exposure factors and mediators. To ensure the reliability of the results, Bootstrap resampling was performed 1,000 time (14). Further subgroup analyses were conducted based on age, sex, cholesterol levels, and Framingham

1 https://www.thecalculator.co/health/Framingham-Risk-Score-Calculator-for-Coronary-Heart-Disease-745.html

risk scores to assess whether there are interaction effects between DII and these factors. The mean decrease in Gini (MDG) is a commonly used method for measuring feature importance in random forest models, reflecting the contribution of each dietary component to the model's predictive performance.

Statistical significance was set at $p < 0.05$. All analyses were performed using R version 4.2.0 (R Foundation for Statistical Computing, Vienna, Austria). The analysis mainly used the 'survey', 'plotRCS', 'mediation', and 'randomForest' packages.

3 Results

3.1 Characteristics of the study population

A total of 43,842 participants were included in this study, with a mean age of 49.81 ± 18.10 years, of whom 20,793 (47.4%) were male. Among the participants, 15,310 (34.9%) had hypertension, and 5,289(12.1%) had diabetes. The DII score was 1.33 (0.11, 2.40). Participants were divided into three groups based on the DII tertiles, with 14,614 individuals in each group. Significant differences were observed between the groups in terms of age, sex, race, education level, hypertension, diabetes, CHD, BMI, GFR, total cholesterol and HDL (all $p < 0.05$). The characteristics and effect size data of the three groups were shown in Table 1. Pairwise comparisons between the three groups were performed (Supplementary Table S1). Further comparisons of dietary components between the three groups revealed significant differences across all 28 dietary components included in this study (all $p < 0.001$) (Supplementary Tables S2, S3).

3.2 Association between DII and CHD, and risk factors

After adjusting for age, sex, race, and education level, the relationship between DII, CHD, and common risk factors was analyzed using RCS. The knots between 3 and 7 were tested, and the model with the lowest Akaike information criterion value was selected for the RCS analysis. As shown in Figure 2A, there appears to be a J-shaped curve between DII and CHD, with the risk of CHD increasing at an accelerating rate as DII rises. The results indicated a positive correlation between DII and WHtR, BMI, TyG, and the Framingham score (Figures 2B,D–F). DII was negatively correlated with HDL (Figure 2C).

3.3 The association between DII and CHD

For confounder adjustment, multivariable logistic regression was used to analyze the relationship between DII and CHD. DII was analyzed as a continuous variable. Based on previous literature (15) and the covariates included in this study, Model 1 did not adjust for any covariates; Model 2 adjusted for age, sex, race, and education; Model 3 adjusted for hypertension, diabetes, smoking, BMI, GFR and total cholesterol in addition to the covariates in Model 2. In the unadjusted model, a higher DII was significantly associated with an increased risk of CHD [OR: 1.057 (1.026–1.089), $p < 0.001$]. In Model 2, the association between DII and CHD remained significant [OR: 1.065 (1.031–1.101), $p < 0.001$]. In Model 3, the correlation between DII and CHD continued to exist [OR: 1.049 (1.012–1.087), $p = 0.008$]. When DII was categorized into lower, middle, and higher DII groups, the analysis results remained consistent [OR: 1.095 (1.024–1.171), $p = 0.008$] (Table 2).

3.4 Mediators between DII and CHD

Given the correlation between DII and traditional CHD risk factors, further analysis of the mediators between DII and CHD was conducted after adjusting for age, sex, race, and education level. The average direct effect (ADE) represents the direct effect of DII on the outcome variable without mediation, while the average causal mediation effect (ACME) represents the indirect effect of DII on the outcome variable through mediators. The results indicated that DII indirectly increases the risk of CHD by elevating TyG, VAI, BMI, and WHtR. Additionally, DII was found to increase the risk of CHD by lowering HDL and GFR (Figure 3). However, since this study is cross-sectional, causality still needs to be confirmed through further longitudinal research.

3.5 The impact of DII on CHD in different subgroups

To further explore the role of DII in different populations, subgroup analyses were performed based on age (≥75 years vs. <75 years), sex, cholesterol levels (≥5.2 mmol/L vs. <5.2 mmol/L), and Framingham risk score. After adjusting for sex, race, and education level, the subgroup aged <75 years showed higher sensitivity to DII (p for interaction <0.001). When adjusted for age, race, and education level, a stronger association between DII and CHD was observed in females (p for interaction = 0.028). In the Framingham risk groups, individuals with a 10-year heart disease risk >10% were classified as high-risk (men ≥12 points, women ≥20 points). Further analysis showed that, after adjusting for age, sex, race, and education level, individuals with low cholesterol levels (p for interaction = 0.004) and those in the Framingham low-risk group (p for interaction = 0.005) were more sensitive to DII (Figure 4).

3.6 Contribution of dietary components to CHD

To assess the contribution of dietary components to CHD, we used a random forest model to calculate the MDG for each dietary component. The larger the MDG value, the greater the contribution of that dietary component to the model's performance. The results showed that the top 5 dietary components contributing the most to CHD were carbohydrate, vitamin C, iron, vitamin A and caffeine, while the bottom 3 components were vitamin D, alcohol, and monounsaturated fatty acids (Figure 5).

4 Discussion

This study, which included 43,842 participants from the NHANES between 1999 and 2018, showed the association between the DII and

TABLE 1 The characteristics of participants from the 1999–2018 NHANES.

Variate	Overall (*N* = 43,842)	DII Tertile 1 (*N* = 14,614)	DII Tertile 2 (*N* = 14,614)	DII Tertile 3 (*N* = 14,614)	*p*	Effect size*
Age, years	49.81 ± 18.10	48.66 ± 17.57	49.54 ± 18.14	51.22 ± 18.49	<0.001	0.057
Sex, male	20,793 (47.4%)	8,912 (61.0%)	6,875 (47.0%)	5,006 (34.3%)	<0.001	0.219
Race					<0.001	0.079
Mexican American	7,595 (17.3%)	2,356(16.1%)	2,656 (18.2%)	2,583 (17.7%)		
Other Hispanic	3,455 (7.9%)	978 (6.7%)	1,093 (7.5%)	1,384 (9.5%)		
Non-Hispanic White	20,134 (45.9%)	7,485 (51.2%)	6,729 (46.0%)	5,920 (40.5%)		
Non-Hispanic Black	9,147 (20.9%)	2,488 (17.0%)	2,977 (20.4%)	3,682 (25.2%)		
Other Race	3,511 (8.0%)	1,307 (8.9%)	1,159 (7.9%)	1,045 (7.2%)		
Education level					<0.001	0.138
No high school diploma	4,932 (11.2%)	1,059(7.2%)	1,655 (11.3%)	2,218 (15.2%)		
Some high school	6,399 (14.6%)	1,694 (11.6%)	2072 (14.2%)	2,633 (18.0%)		
High school graduate	10,159 (23.2%)	3,047 (20.8%)	3,414 (23.4%)	3,698 (25.3%)		
Some college/ associate degree	12,556 (28.6%)	4,261 (29.2%)	4,260 (29.2%)	4,035 (27.6%)		
Bachelor's degree or higher	9,747 (22.2%)	4,545 (31.1%)	3,188 (21.8%)	2014 (13.8%)		
Smoking	19,991 (45.6%)	6,639 (45.4%)	6,667 (45.6%)	6,685 (45.7%)	0.859	0.003
Hypertension	15,310 (34.9%)	4,588 (31.4%)	5,002 (34.2%)	5,720 (39.1%)	<0.001	0.068
Diabetes	5,289 (12.1%)	1,421 (9.7%)	1729 (11.8%)	2,139 (14.6%)	<0.001	0.062
CHD	1892 (4.3%)	580 (4.0%)	613 (4.2%)	699 (4.8%)	0.002	0.017
BMI, kg/m^2	29.06 ± 6.79	28.40 ± 6.43	29.15 ± 6.76	29.64 ± 7.12	<0.001	0.076
GFR, mL/ min/1.73 m^2	94.49 ± 24.96	95.85 ± 23.17	94.85 ± 24.94	92.72 ± 26.58	<0.001	0.051
Cholesterol, mmol/L	4.99 (4.32, 5.74)	4.99 (4.32, 5.72)	5.02 (4.34, 5.77)	4.97 (4.29, 5.72)	0.001	0.018
HDL, mmol/L	1.37 ± 0.42	1.38 ± 0.42	1.37 ± 0.42	1.36 ± 0.41	<0.001	0.022
LDL, mmol/L	3.00 ± 0.93	2.98 ± 0.90	3.01 ± 0.95	3.01 ± 0.95	0.073	0.016
HbA1c, %	7.0 (6.1, 8.0)	7.0 (6.1, 7.8)	7.0 (6.2, 7.7)	7.0 (6.1, 8.0)	0.857	0.026
TyG	8.66 ± 0.68	8.62 ± 0.69	8.66 ± 0.68	8.69 ± 0.67	<0.001	0.042
WHtR	0.59 ± 0.10	0.58 ± 0.09	0.59 ± 0.10	0.61 ± 0.10	<0.001	0.12
VAI	0.044 (0.026, 0.077)	0.041 (0.024, 0.074)	0.044 (0.026, 0.076)	0.047 (0.028, 0.081)	<0.001	0.03
Framingham score	12 (5, 16)	11 (4, 15)	12 (5, 16)	13 (6, 17)	<0.001	0.094

*For continuous variables, effect sizes were calculated using Cohen's f, and for categorical variables, effect sizes were calculated using Cramér's V. DII, dietary inflammatory index; CHD, coronary heart disease; BMI: body mass index; GFR, glomerular filtration rate; HDL, high-density lipoprotein; LDL, low-density lipoprotein; TyG, triglyceride-glucose index; WHtR, waist-to-height ratio; VAI, visceral adiposity index.

CHD, and explored the potential mediating factors and interactions. The results showed that: (1) After adjusting for multiple variables, DII remained independently associated with CHD. (2) DII may be associated with CHD through its impact on factors such as TyG, VAI, BMI, WHtR, HDL and GFR. (3) The association between DII and CHD was more sensitive in individuals aged <75 years, females, those with low cholesterol levels, and those in the low-risk Framingham score group. (4) Among the 28 dietary components analyzed in this study, carbohydrate, vitamin C and iron were found to have the greatest association on CHD.

CHD is a chronic inflammatory disease influenced by various factors. The DII is an inflammation indicator based on dietary components, and studies have shown that DII is correlated with multiple inflammatory markers in the body (6–8, 16). Previous research has also confirmed the association between DII and CHD (9). In this study, despite adjusting for age, sex, race, education level,

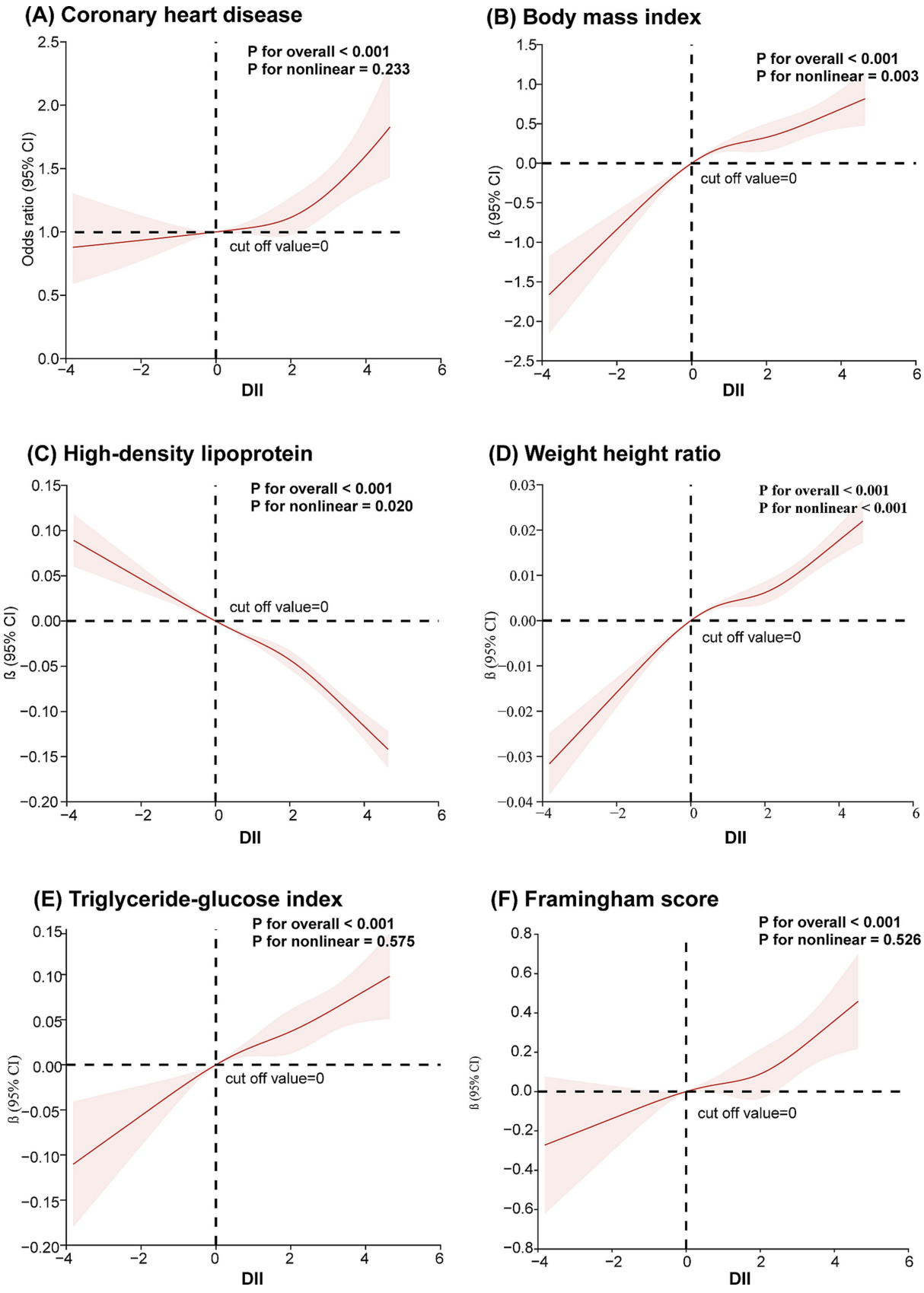

FIGURE 2
Restricted cubic spline analysis of the association between dietary inflammation index and coronary heart disease and its risk factors **(A)** coronary heart disease; **(B)** body mass index; **(C)** high-density lipoprotein; **(D)** waist-to-height ratio; **(E)** triglyceride and glucose index; **(F)** Framingham score. A restricted cubic spline model was calculated after adjusting for age, sex, race and education level.

TABLE 2 The association between DII and CHD in different logistics models.

	DII as a continuous variable[a]			DII as a nominal variable[b]		
	OR	95% CI	*p*	OR	95% CI	*p*
Model 1	1.057	1.026–1.089	< 0.001	1.104	1.043–1.168	< 0.001
Model 2	1.065	1.031–1.101	< 0.001	1.116	1.050–1.188	< 0.001
Model 3	1.049	1.012–1.087	0.008	1.095	1.024–1.171	0.008

Model 1: Crude. Model 2: Adjusted for Model 1, age, sex, race and education. Model 3: Adjusted for Model 2, hypertension, diabetes, smoking, body mass index, glomerular filtration rate, and total cholesterol. OR, odds ratio; CI confidence interval.

[a]OR was examined by per 1-unit increase of DII.

[b]divided into lower, middle, and higher DII groups based on the tertiles of the DII distribution.

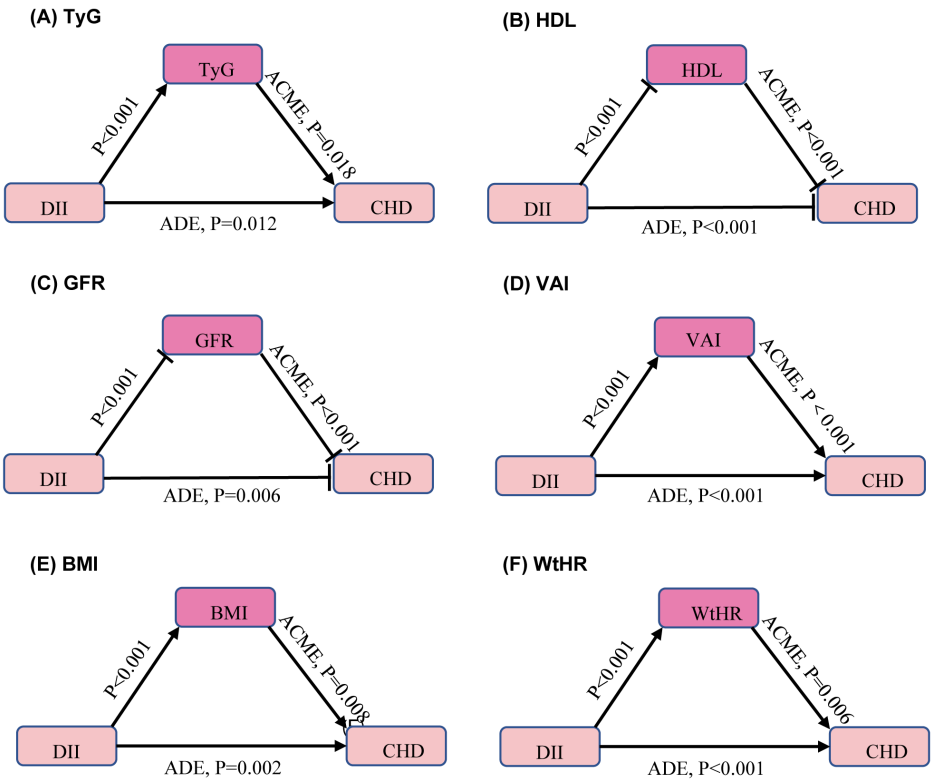

FIGURE 3
Mediators of the association between dietary inflammation index and coronary heart disease. Arrows and rounded heads indicate promotion and inhibition, respectively. The model was calculated after adjusting for age, sex, race and education level. ACME, average causal mediation effects; ADE, average direct effects. TyG, triglyceride-glucose index; HDL, high-density lipoprotein cholesterol; GFR, glomerular filtration rate; VAI, visceral adiposity index; BMI, body mass index; WHtR, waist-to-height ratio. **(A)** TyG, **(B)** HDL, **(C)** GFR, **(D)** VAI, **(E)** BMI, **(F)** WtHR.

and traditional cardiovascular risk factors, DII remained independently associated with CHD. Prior studies showed that higher DII in CHD patients is associated with significantly reduced plaque stability, indicating that anti-inflammatory diets may play an important protective role in the pathogenesis of CHD (17).

In this study, TyG, VAI, BMI, WHtR, HDL, and GFR may serve as mediators in the relationship between DII and CHD. TyG index is a well-established indicator of insulin resistance and has been shown to effectively predict the risk of various cardiovascular diseases, including CHD, atherosclerosis, and stroke (18, 19). Pro-inflammatory diets elevate circulating inflammatory cytokines (e.g., TNF-α, IL-6), which impair insulin signaling in adipose tissue, muscle, and liver. Chronic insulin resistance directly damages vascular endothelial cells and smooth muscle cells, promoting atherosclerotic plaque formation (20). Additionally, excessive reactive oxygen species and harmful glycation products generated by hyperglycemia contribute to chronic inflammation, further amplifying the risk of CHD (21). Shu et al. (22) reported that DII was positively correlated with fasting glucose, fasting insulin, and the homeostasis model assessment of insulin resistance. Furthermore, a cohort study further suggested that the relationship between pro-inflammatory diets and nonfatal cardiovascular diseases was partially mediated by TyG (23).

VAI, BMI, and WHtR are indicators of visceral adiposity and obesity, and they exhibit strong associations with CHD and all-cause mortality (24, 25). Pro-inflammatory diets, such as high-fat diets, activate the pro-inflammatory factor NF-κB by inducing endoplasmic

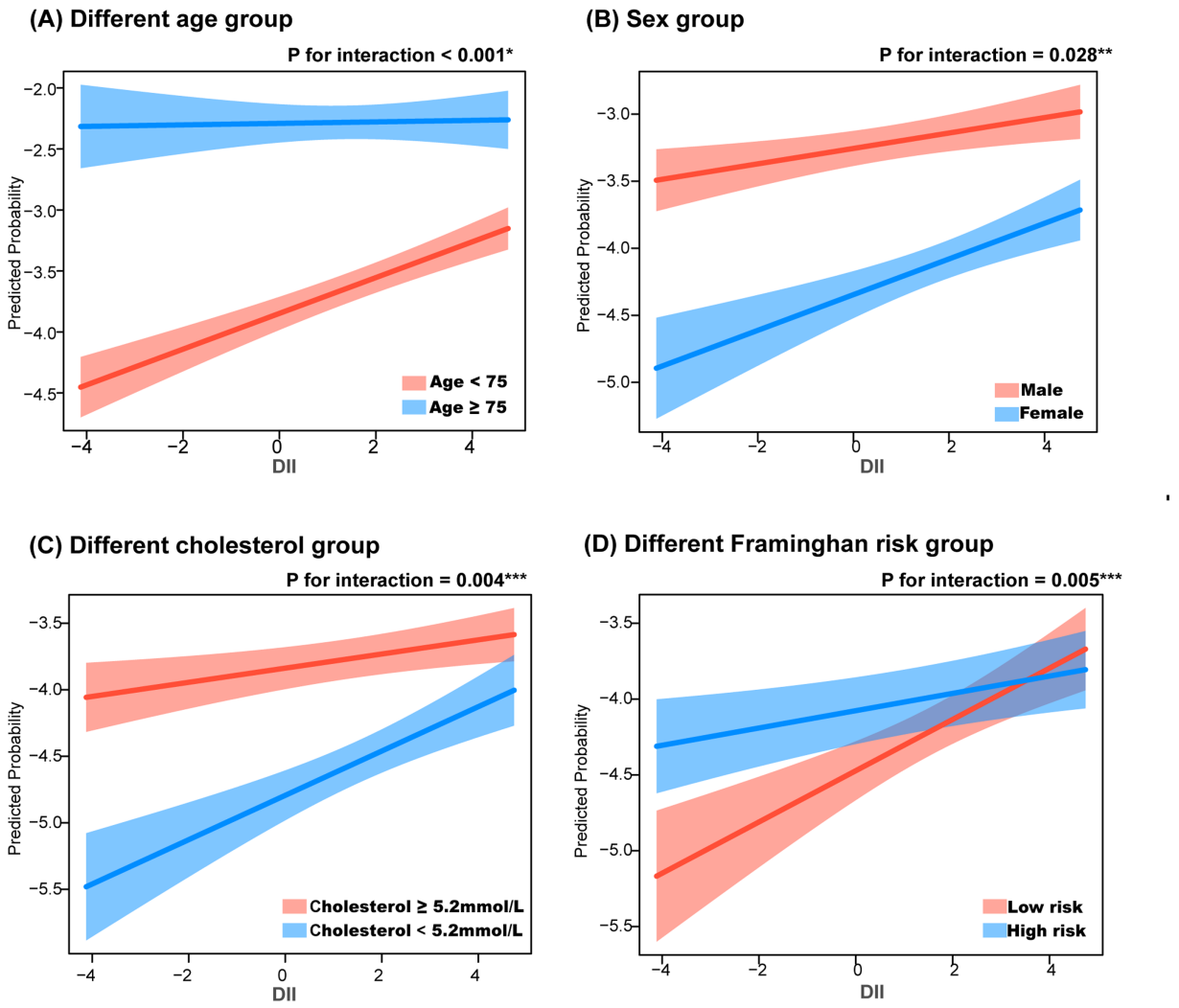

FIGURE 4
Subgroup analysis in the relationship between dietary inflammation index and coronary heart disease. *, adjusting for sex, race and education level; **, adjusting for age, race and education level; ***, adjusting for age, sex, race and education level. **(A)** Different age group, **(B)** Sex group, **(C)** Different cholesterol group, **(D)** Different framinghan risk group.

reticulum (ER) stress and promoting the interaction of TLR4 and TLR2. Oxidative stress in the ER plays a critical role in initiating inflammation and metabolic disorders, further contributing to visceral fat accumulation and obesity (26). Moreover, dietary inflammation levels may influence gut microbiota composition. Anti-inflammatory diets have been shown to lower the proportion of Gram-negative bacteria in the gut, strengthen intestinal barrier function, and reduce endotoxin levels, thereby mitigating metabolic and inflammatory responses (27).

Moreover, pro-inflammatory diets promote inflammatory markers (TNF-α and NF-κB) and oxidative stress markers (elevated NADPH oxidase activity) in the renal cortex, inducing mesangial cell proliferation and the progression of proteinuria, ultimately leading to a decline in GFR (28). Chronic kidney disease is often associated with lipid metabolism disorders, and the accumulation of toxins in the body can directly damage endothelial cells, promote platelet adhesion, and contribute to the formation of atherosclerotic plaques (29). Due to incomplete and methodologically inconsistent CRP/hsCRP measurements in NHANES (1999–2018), CRP was not analyzed as a mediator in this study.

Subgroup analyses were conducted to examine the relationship between DII and CHD across different CHD risk factors, including age, sex, total cholesterol levels, and Framingham risk score, to evaluate the robustness of the findings. This study found that elevated DII may be more strongly associated with CHD in individuals aged <75 years, females, those with low cholesterol levels, and individuals at low risk group according to the Framingham score. A prospective cohort study involving 155,724 participants, with approximately 10 years of follow-up, revealed that poor dietary quality was more strongly associated with cardiovascular disease in women than in men, and DII was also linked to a higher risk of all-cause mortality in female CHD patients (11, 30). From Figure 4D, it can be observed that when DII is at a low level, the CHD risk in the low-risk group is significantly lower compared to the high-risk group. As DII increases,

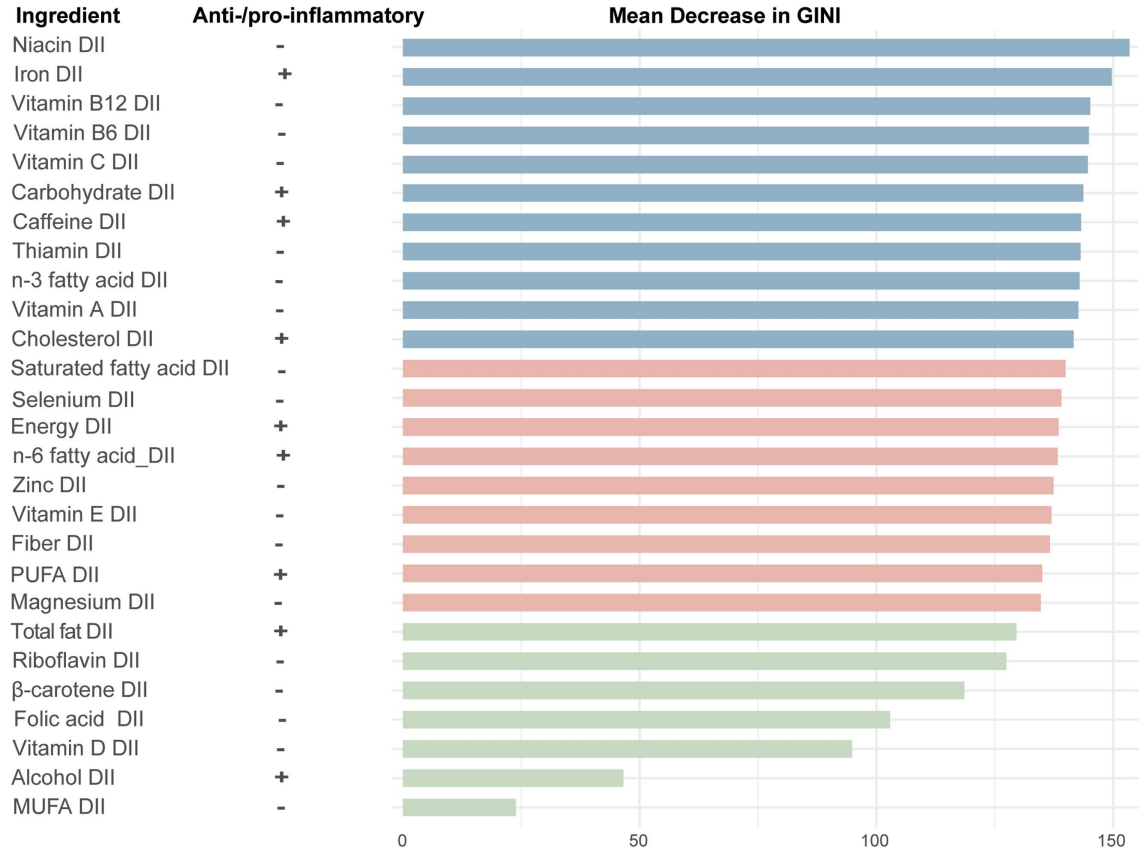

FIGURE 5
The importance ranking of 28 dietary components in the dietary inflammation index for CHD using random forest. +, pro-inflammatory; –, anti-inflammatory; GINI, gini index; PUFA, polyunsaturated fatty acids; MUFA, monounsaturated fatty acids.

the CHD risk in the low-risk group rises rapidly, ultimately approaching that of the high-risk group. This suggests that the impact of DII is more sensitive in the low-risk population than in the high-risk group. One possible explanation is that individuals in the low-risk group lack other strong risk factors, making the inflammatory response triggered by diet more prominent. Additionally, high-risk individuals may have access to more health education and lifestyle interventions, thereby reducing their risk of CHD. Finally, DII may exert a greater effect in the low-risk group through interactions with other metabolic and inflammatory markers. Despite adjusting for general demographic characteristics (sex, age, race, and education level), potential confounding factors may still exist, requiring further validation through prospective cohort studies and mechanistic research.

Calculating the DII requires the collection of 45 different dietary components, which poses a challenge for both doctors and patients in clinical practice. This increases the complexity of assessment due to individual differences, dietary habits, and measurement errors. In this study, we used the random forest method to rank the contribution of dietary components to CHD risk based on their DII. However, this is only a preliminary exploration, and further research is needed to assess its feasibility and accuracy.

Our study found that carbohydrate, vitamin C and iron were the three components with the greatest DII contribution to CHD. Carbohydrates are the primary source of energy in the diet. A study involving over 10,000 participants, followed for more than a decade, found a significant association between carbohydrate intake and major adverse cardiovascular events (HR: 1.35; 95%CI: 1.07–1.71; p-trend = 0.001) (31). Another study from 18 countries showed a non-linear relationship between carbohydrate intake and cardiovascular disease mortality (32). Vitamin C is a well-known antioxidant. A research has shown that the intake of vitamin C is negatively correlated with the carotid intima-media thickness in patients with CHD ($r = -0.113$, $p = 0.001$) (33). Additionally, vitamin C intake is positively correlated with plaque stability in these patients and may exert its effects by reducing IL-6 and TNF-α, thereby inhibiting the inflammatory response in atherosclerosis (34). Iron's DII ranked third in contributing to CHD risk. Iron intake has been positively correlated with CRP levels (p trend = 0.03) (35). A meta-analysis of 6 prospective studies indicated that individuals with higher heme iron intake had a 31% increased risk of CHD (36). This suggests that iron intake, particularly heme iron, may need to be controlled to reduce inflammation.

Interestingly, alcohol, typically considered a risk factor for CHD, ranked second to last in DII contribution. This may be related to the relatively low alcohol intake in the study population compared to the upper limits recommended in current guidelines. In the United States, the recommended alcohol intake limit is 196 g per week for men and

98 g per week for women (37). A J-shaped curve relationship exists between alcohol consumption and CHD (38). Recent research has found that reducing alcohol consumption can help consistently lower cardiovascular disease risk, although a clear threshold for alcohol intake remains undefined (39).

4.1 Limitations

This study has several limitations. First, since NHANES is a cross-sectional survey, this study cannot determine a causal relationship between DII and CHD risk, but only an association between the two. Future studies with longitudinal designs are needed to better evaluate the impact of DII on CHD risk. Second, dietary data were collected using recall methods, which may introduce subjective bias and may not accurately reflect long-term daily dietary intake. However, studies have shown a strong correlation between dietary data obtained through food records and 24-h recalls (40). Moreover, 24-h recall methods have been widely used in dietary intervention trials and national surveys (40). Third, the outcome variable in this study was based on self-reported questionnaires, which are subject to recall bias, information bias, and potential misclassification of exposure. Although NHANES implements multiple measures to minimize recall and information bias during data collection, the possibility of data quality issues remains. Lastly, although we adjusted for potential confounding factors, the influence of other unmeasured confounders on the results cannot be entirely excluded.

5 Conclusion

Higher DII is independently associated with an increased risk of CHD, potentially through pathways involving metabolism, lipid levels, and kidney function. The impact of DII on CHD is more sensitive in individuals with low traditional risk. These findings provide new evidence for the role of dietary interventions in reducing CHD incidence and lay the groundwork for future cohort studies and mechanistic investigations.

Data availability statement

Publicly available datasets were analyzed in this study. This data can be found at: https://wwwn.cdc.gov/nchs/nhanes/.

Ethics statement

The studies involving humans were approved by Institutional Review Board of the National Center for Health Statistics. The studies were conducted in accordance with the local legislation and institutional requirements. The participants provided their written informed consent to participate in this study.

Author contributions

HX: Formal analysis, Software, Writing – review & editing. PX: Data curation, Methodology, Visualization, Writing – original draft. HL: Resources, Supervision, Writing – review & editing. ZT: Methodology, Validation, Writing – review & editing. RZ: Project administration, Writing – review & editing. MC: Conceptualization, Funding acquisition, Investigation, Project administration, Writing – review & editing.

Funding

The author(s) declare that financial support was received for the research and/or publication of this article. This study was funded by the Beijing Research Ward Excellence Clinical Study Program (BRWEP2024W014090201) and the Key Clinical Projects of Peking University Third Hospital (No. 2024003).

Acknowledgments

We thank all participants, researchers and staff in the NHANES study.

Conflict of interest

The authors declare that the research was conducted in the absence of any commercial or financial relationships that could be construed as a potential conflict of interest.

Generative AI statement

The authors declare that no Gen AI was used in the creation of this manuscript.

Publisher's note

Supplementary material

The Supplementary material for this article can be found online at: https://www.frontiersin.org/articles/10.3389/fnut.2025.1564580/full#supplementary-material

References

1. Lechner K, von Schacky C, McKenzie AL, Worm N, Nixdorff U, Lechner B, et al. Lifestyle factors and high-risk atherosclerosis: pathways and mechanisms beyond traditional risk factors. *Eur J Prev Cardiol*. (2020) 27:394–406. doi: 10.1177/2047487319869400

2. Writing Committee M, Virani SS, Newby LK, Arnold SV, Bittner V, Brewer LC, et al. 2023 AHA/ACC/ACCP/ASPC/NLA/PCNA guideline for the management of patients with chronic coronary disease: a report of the American Heart Association/American College of Cardiology Joint Committee on clinical practice guidelines. *J Am Coll Cardiol*. (2023) 82:833–955. doi: 10.1016/j.jacc.2023.04.003

3. Tsao CW, Aday AW, Almarzooq ZI, Alonso A, Beaton AZ, Bittencourt MS, et al. Heart disease and stroke statistics-2022 update: a report from the American Heart Association. *Circulation*. (2022) 145:e153–639. doi: 10.1161/CIR.0000000000001052

4. Punnanithinont N, Kambalapalli S, Iskander B, Ichikawa K, Krishnan S, Lakshmanan S, et al. Anti-inflammatory therapies in atherosclerosis–where are we going? *Curr Atheroscler Rep*. (2024) 27:19. doi: 10.1007/s11883-024-01267-7

5. Cavicchia PP, Steck SE, Hurley TG, Hussey JR, Ma Y, Ockene IS, et al. A new dietary inflammatory index predicts interval changes in serum high-sensitivity C-reactive protein. *J Nutr*. (2009) 139:2365–72. doi: 10.3945/jn.109.114025

6. Shivappa N, Steck SE, Hurley TG, Hussey JR, Ma Y, Ockene IS, et al. A population-based dietary inflammatory index predicts levels of C-reactive protein in the seasonal variation of blood cholesterol study (seasons). *Public Health Nutr*. (2014) 17:1825–33. doi: 10.1017/S1368980013002565

7. Shivappa N, Hebert JR, Rietzschel ER, De Buyzere ML, Langlois M, Debruyne E, et al. Associations between dietary inflammatory index and inflammatory markers in the asklepios study. *Br J Nutr*. (2015) 113:665–71. doi: 10.1017/S000711451400395X

8. Shivappa N, Hebert JR, Marcos A, Diaz LE, Gomez S, Nova E, et al. Association between dietary inflammatory index and inflammatory markers in the Helena study. *Mol Nutr Food Res*. (2017) 61:707. doi: 10.1002/mnfr.201600707

9. Agraib LM, Azab M, Al-Shudifat AE, Allehdan SS, Shivappa N, Hebert JR, et al. Dietary inflammatory index and odds of coronary artery disease in a case-control study from Jordan. *Nutrition*. (2019) 63-64:98–105. doi: 10.1016/j.nut.2018.11.027

10. Bondonno NP, Lewis JR, Blekkenhorst LC, Shivappa N, Woodman RJ, Bondonno CP, et al. Dietary inflammatory index in relation to sub-clinical atherosclerosis and atherosclerotic vascular disease mortality in older women. *Br J Nutr*. (2017) 117:1577–86. doi: 10.1017/S0007114517001520

11. Wang E, Fang C, Zhang J, Wang Y. Association between dietary inflammatory index and all-cause mortality risk in adults with coronary heart disease in the United States. *Sci Rep*. (2024) 14:23998. doi: 10.1038/s41598-024-75381-6

12. Park YM, Choi MK, Lee SS, Shivappa N, Han K, Steck SE, et al. Dietary inflammatory potential and risk of mortality in metabolically healthy and unhealthy phenotypes among overweight and obese adults. *Clin Nutr*. (2019) 38:682–8. doi: 10.1016/j.clnu.2018.04.002

13. D'Agostino RB Sr, Vasan RS, Pencina MJ, Wolf PA, Cobain M, Massaro JM, et al. General cardiovascular risk profile for use in primary care: the Framingham heart study. *Circulation*. (2008) 117:743–53. doi: 10.1161/CIRCULATIONAHA.107.699579

14. Valente MJ, Rijnhart JJM, Smyth HL, Muniz FB, MacKinnon DP. Causal mediation programs in R, Mplus, SAS, SPSS, and Stata. *Struct Equ Modeling*. (2020) 27:975–84. doi: 10.1080/10705511.2020.1777133

15. Wang B, Sun X. Weight-adjusted waist index shows superior detection of coronary artery disease than body mass index in NHANES 1999-2020. *Sci Rep*. (2025) 15:7077. doi: 10.1038/s41598-025-90877-5

16. Smidowicz A, Regula J. Effect of nutritional status and dietary patterns on human serum C-reactive protein and Interleukin-6 concentrations. *Adv Nutr*. (2015) 6:738–47. doi: 10.3945/an.115.009415

17. Zhao Z, Li L, Gao X, Hu G, Liu G, Tao H, et al. High dietary inflammatory index is associated with decreased plaque stability in patients with coronary heart disease. *Nutr Res*. (2023) 119:56–64. doi: 10.1016/j.nutres.2023.08.007

18. Liu X, Tan Z, Huang Y, Zhao H, Liu M, Yu P, et al. Relationship between the triglyceride-glucose index and risk of cardiovascular diseases and mortality in the general population: a systematic review and meta-analysis. *Cardiovasc Diabetol*. (2022) 21:124. doi: 10.1186/s12933-022-01546-0

19. Liu L, Peng J, Wang N, Wu Z, Zhang Y, Cui H, et al. Comparison of seven surrogate insulin resistance indexes for prediction of incident coronary heart disease risk: a 10-year prospective cohort study. *Front Endocrinol (Lausanne)*. (2024) 15:1290226. doi: 10.3389/fendo.2024.1290226

20. Laakso M, Kuusisto J. Insulin resistance and hyperglycaemia in cardiovascular disease development. *Nat Rev Endocrinol*. (2014) 10:293–302. doi: 10.1038/nrendo.2014.29

21. Li JM, Li X, Chan LWC, Hu R, Zheng T, Li H, et al. Lipotoxicity-polarised macrophage-derived exosomes regulate mitochondrial fitness through miro1-mediated mitophagy inhibition and contribute to type 2 diabetes development in mice. *Diabetologia*. (2023) 66:2368–86. doi: 10.1007/s00125-023-05992-7

22. Shu Y, Wu X, Wang J, Ma X, Li H, Xiang Y. Associations of dietary inflammatory index with prediabetes and insulin resistance. *Front Endocrinol (Lausanne)*. (2022) 13:820932. doi: 10.3389/fendo.2022.820932

23. Liu B, Ren X, Tian W. Dietary inflammatory potential and the risk of nonfatal cardiovascular diseases in the China health and nutrition survey. *Nutrition*. (2024) 124:112469. doi: 10.1016/j.nut.2024.112469

24. Luo Y, Zhan X, Liu Y, Chen L, Zhu L, Cai W. Predicted visceral adiposity index in relation to risk of coronary heart disease and all-cause mortality: insights from NHANES. *Front Endocrinol (Lausanne)*. (2023) 14:1296398. doi: 10.3389/fendo.2023.1296398

25. Wang F, Chen Y, Chang Y, Sun G, Sun Y. New anthropometric indices or old ones: Which perform better in estimating cardiovascular risks in Chinese adults. *BMC cardiovasc. disord.* (2018) 18:14. doi: 10.1186/s12872-018-0754-z

26. Sozen E, Ozer NK. Impact of high cholesterol and endoplasmic reticulum stress on metabolic diseases: an updated mini-review. *Redox Biol*. (2017) 12:456–61. doi: 10.1016/j.redox.2017.02.025

27. Xu J, Xie L, Fan R, Shi X, Xu W, Dong K, et al. The role of dietary inflammatory index in metabolic diseases: the associations, mechanisms, and treatments. *Eur J Clin Nutr*. (2024). doi: 10.1038/s41430-024-01525-6

28. Duan Y, Zeng L, Zheng C, Song B, Li F, Kong X, et al. Inflammatory links between high fat diets and diseases. *Front Immunol*. (2018) 9:2649. doi: 10.3389/fimmu.2018.02649

29. Silva RP, Diogenes C. Heart disease and the kidneys. *Contrib Nephrol*. (2021) 199:71–9. doi: 10.1159/000517704

30. Walli-Attaei M, Rosengren A, Rangarajan S, Breet Y, Abdul-Razak S, Sharief WA, et al. Metabolic, behavioural, and psychosocial risk factors and cardiovascular disease in women compared with men in 21 high-income, middle-income, and low-income countries: an analysis of the Pure study. *Lancet*. (2022) 400:811–21. doi: 10.1016/S0140-6736(22)01441-6

31. Lim CGY, Tai ES, van Dam RM. Replacing dietary carbohydrates and refined grains with different alternatives and risk of cardiovascular diseases in a multi-ethnic Asian population. *Am J Clin Nutr*. (2022) 115:854–63. doi: 10.1093/ajcn/nqab403

32. Dehghan M, Mente A, Zhang X, Swaminathan S, Li W, Mohan V, et al. Associations of fats and carbohydrate intake with cardiovascular disease and mortality in 18 countries from five continents (Pure): a prospective cohort study. *Lancet*. (2017) 390:2050–62. doi: 10.1016/S0140-6736(17)32252-3

33. Ramezankhani A, Hadaegh P, Hadaegh F. Association of Novel Dietary and Lifestyle Inflammation Scores with incidence and progression of coronary artery calcification in middle-late adulthood: a longitudinal cohort study. *Nutr J*. (2024) 23:127. doi: 10.1186/s12937-024-01028-x

34. Li L, Zhao Z, Wang Y, Gao X, Liu G, Yu B, et al. Association between dietary intakes and plaque vulnerability measured by optical coherence tomography in patients with coronary heart disease: a mediation analysis of inflammatory factors. *Front Nutr*. (2022) 9:920892. doi: 10.3389/fnut.2022.920892

35. de Oliveira Otto MC, Alonso A, Lee DH, Delclos GL, Jenny NS, Jiang R, et al. Dietary micronutrient intakes are associated with markers of inflammation but not with markers of subclinical atherosclerosis. *J Nutr*. (2011) 141:1508–15. doi: 10.3945/jn.111.138115

36. Yang W, Li B, Dong X, Zhang XQ, Zeng Y, Zhou JL, et al. Is heme Iron intake associated with risk of coronary heart disease? A meta-analysis of prospective studies. *Eur J Nutr*. (2014) 53:395–400. doi: 10.1007/s00394-013-0535-5

37. Kalinowski A, Humphreys K. Governmental standard drink definitions and low-risk alcohol consumption guidelines in 37 countries. *Addiction*. (2016) 111:1293–8. doi: 10.1111/add.13341

38. Biddinger KJ, Emdin CA, Haas ME, Wang M, Hindy G, Ellinor PT, et al. Association of habitual alcohol intake with risk of cardiovascular disease. *JAMA Netw Open*. (2022) 5:e223849. doi: 10.1001/jamanetworkopen.2022.3849

39. Wood AM, Kaptoge S, Butterworth AS, Willeit P, Warnakula S, Bolton T, et al. Risk thresholds for alcohol consumption: combined analysis of individual-participant data for 599 912 current drinkers in 83 prospective studies. *Lancet*. (2018) 391:1513–23. doi: 10.1016/S0140-6736(18)30134-X

40. Satija A, Yu E, Willett WC, Hu FB. Understanding nutritional epidemiology and its role in policy. *Adv Nutr*. (2015) 6:5–18. doi: 10.3945/an.114.007492

frontiers | Frontiers in Nutrition

TYPE Original Research
PUBLISHED 28 April 2025
DOI 10.3389/fnut.2025.1550490

OPEN ACCESS

EDITED BY
Sofia Viana,
University of Coimbra, Portugal

REVIEWED BY
Jani Almeida,
University of Coimbra, Portugal
Jixin Fu,
Weihai Central Hospital, China

*CORRESPONDENCE
Jia Zeng
✉ 2905885860@qq.com
Ran Duan
✉ 1345295687@qq.com

†These authors have contributed equally to this work

RECEIVED 23 December 2024
ACCEPTED 11 March 2025
PUBLISHED 28 April 2025

CITATION
Yao J, Wu P, Li Z, Zhao L, Fu Z, Shi P, Xiong X, Chen X, Yu B, He Y, Feng T, Zeng J and Duan R (2025) Nutritional status and systemic inflammation in COPD: prognostic value of the advanced lung cancer inflammation index.
Front. Nutr. 12:1550490.
doi: 10.3389/fnut.2025.1550490

Nutritional status and systemic inflammation in COPD: prognostic value of the advanced lung cancer inflammation index

Jun Yao[1†], Peng Wu[1†], Zhishu Li[1†], Lingyan Zhao[1†], Ziqiao Fu[1], Ping Shi[1], Xiaomin Xiong[1], Xuping Chen[1], Bin Yu[1], Yan He[1], Tong Feng[2], Jia Zeng[1*] and Ran Duan[3,4*]

[1]Department of Respiratory and Critical Care, Guangyuan Central Hospital, Sichuan, China, [2]Department of Respiratory and Critical Care Medicine, Deyang People's Hospital, Affiliated Hospital of Chengdu College of Medicine, Deyang, China, [3]School of Clinical Medicine, Chengdu Medical College, Chengdu, Xindu, China, [4]Department of Oncology, The First Affiliated Hospital of Chengdu Medical College, Chengdu, China

Background: Chronic Obstructive Pulmonary Disease (COPD) is a leading cause of global mortality, with systemic inflammation and malnutrition playing pivotal roles in its progression and outcomes. The Advanced Lung Cancer Inflammation Index (ALI), which integrates nutritional status and systemic inflammation, may offer potential prognostic value in COPD management.

Objectives: This study aimed to evaluate the relationship between ALI and mortality outcomes in COPD patients, with a specific focus on the interplay between nutrition, inflammation, and their non-linear associations with all-cause and cardiovascular mortality.

Methods: Data were derived from the NHANES (1999–2018) cohort, comprising 47,880 participants, including 1,960 COPD patients. ALI was calculated using body mass index (BMI), serum albumin levels, and the neutrophil-to-lymphocyte ratio (NLR). Survival analyses, including Kaplan–Meier curves, Cox proportional hazards models, and restricted cubic splines, were used to assess the association between ALI and mortality outcomes, exploring non-linear trends and thresholds.

Results: Higher ALI levels were significantly associated with reduced risks of all-cause and cardiovascular mortality in COPD patients. Protective effects plateaued at ALI thresholds (88.32 for all-cause mortality and 89.73 for cardiovascular mortality), with mortality risks reversing at excessively high levels for cardiovascular mortality.

Conclusion: ALI, as a composite marker of nutritional status and systemic inflammation, is a valuable prognostic tool for COPD patients. Its non-linear relationship with mortality underscores the need to optimize nutritional and inflammatory management strategies. These findings emphasize the critical importance of addressing malnutrition and systemic inflammation to improve COPD outcomes. Future research should validate these findings and investigate tailored nutritional interventions and anti-inflammatory treatments.

KEYWORDS

chronic obstructive pulmonary disease, advanced lung cancer inflammation index, all-cause mortality, cardiovascular mortality, National Health and Nutrition Examination Survey

Introduction

Chronic Obstructive Pulmonary Disease (COPD) is a prevalent and debilitating condition characterized by persistent respiratory symptoms and airflow limitation, with a substantial impact on global health. According to the World Health Organization, more than 330 million individuals worldwide are affected by COPD, which is projected to become the third leading cause of mortality by 2030 (1). Identifying modifiable factors that can improve long-term outcomes for COPD patients is crucial to alleviating the disease burden and reducing premature deaths.

Inflammation is a key driver of COPD progression, initiated by exposure to harmful particles such as cigarette smoke, air pollution, and occupational irritants. These stimuli activate epithelial cells and alveolar macrophages in the lungs, leading to the release of pro-inflammatory cytokines, including tumor necrosis factor-alpha (TNF-α), interleukin-6 (IL-6), and interleukin-8 (IL-8) (2). These mediators recruit neutrophils, macrophages, and CD8+ T cells to the airways, resulting in tissue damage, airway remodeling, and impaired mucociliary clearance. However, focusing solely on inflammation without considering the patient's nutritional status may provide an incomplete understanding of its impact on disease progression and outcomes. Serum albumin, a critical marker of nutritional status and systemic inflammation, often declines in COPD patients due to chronic inflammation, oxidative stress, and reduced hepatic synthesis. A recent meta-analysis of 26 studies found that COPD patients have significantly lower serum albumin levels compared to individuals without COPD (3). Additionally, individuals with low body mass index (BMI) frequently experience muscle wasting and reduced respiratory muscle strength, which exacerbate dyspnea and functional limitations. Chronic exposure to smoke can accelerate the aging process, resulting in reduced body weight and pulmonary aging (4). This acceleration may explain the observed strong correlation between low BMI and increased mortality in COPD patients. Furthermore, analyses from the ECLIPSE cohort, which includes patients with GOLD stage 2–4 COPD, suggest that the presence of cachexia is a significant predictor of mortality in COPD (5). Integrating inflammatory and nutritional markers offers a more comprehensive approach to predicting outcomes in COPD patients.

The Advanced Lung Cancer Inflammation Index (ALI), which combines markers of systemic inflammation and nutritional status, has shown promise in predicting outcomes in various conditions, including cancer and cardiovascular diseases (6, 7). Its proven prognostic value suggests it may also serve as a useful tool for assessing long-term prognosis in COPD patients, although its utility in this population remains understudied.

This study aims to provide new insights into the determinants of long-term prognosis in COPD patients by evaluating the role of ALI. By identifying potential intervention strategies, the research seeks to improve quality of life and survival outcomes for individuals living with COPD.

Methods

This study utilized data from the National Health and Nutrition Examination Survey (NHANES), a nationally representative, ongoing cross-sectional survey conducted by the National Center for Health Statistics (NCHS). NHANES combines structured interviews, physical examinations, and laboratory tests to collect comprehensive health and nutritional data from the U.S. population. A multistage, stratified probability sampling method ensures its representativeness.

Study population

The study initially included 101,316 participants from the NHANES 1999–2018 cohort. After excluding 44,207 individuals under 18 years old, 57,109 participants remained. Subsequently, 7,435 participants with missing data on ALI and 1,711 participants with missing data on COPD status were removed, leaving 47,963 participants. Finally, 83 participants with missing survival data were excluded, resulting in a final study population of 47,880 participants for analysis (Figure 1).

COPD diagnosis

COPD was defined using a combination of spirometry results, self-reported medical history, medication usage, and specific risk factors. Participants were classified as having COPD if they met any of the following criteria: (1) a spirometry-based diagnosis, defined as a post-bronchodilator forced expiratory volume in 1 s (FEV_1) to forced vital capacity (FVC) ratio of less than 0.7 ($FEV_1/FVC < 0.7$), with spirometry data limited to tests graded as "A" or "B" for reliability; (2) a self-reported diagnosis, indicated by answering "yes" to either "Have you ever been told by a doctor or other health professional that you had emphysema?" (mcq160g); or (3) a medication-based diagnosis, defined as the current use of COPD-specific medications, including selective phosphodiesterase-4 inhibitors, mast cell stabilizers, leukotriene modifiers, or inhaled corticosteroids, combined with being aged 40 years or older and having a history of smoking or reported chronic bronchitis symptoms.

Pulmonary function testing and assessment of chronic pulmonary symptoms

Pulmonary function was assessed through spirometry performed in the NHANES Mobile Examination Center (MEC) by trained technicians following standardized protocols. Both pre-bronchodilator and post-bronchodilator measurements of FEV_1 and FVC were recorded, with participants inhaling a bronchodilator medication (albuterol) prior to the post-bronchodilator test. The quality and validity of the spirometry data were evaluated according to American Thoracic Society (ATS) guidelines, and only tests graded as "A" (excellent quality) or "B" (good quality) were included in the analysis.

Chronic pulmonary symptoms were assessed through a standardized questionnaire administered during the NHANES interview. Participants were asked the following questions regarding respiratory symptoms:

Frequent cough: "Do you cough on most days for three consecutive months or more during the year?"

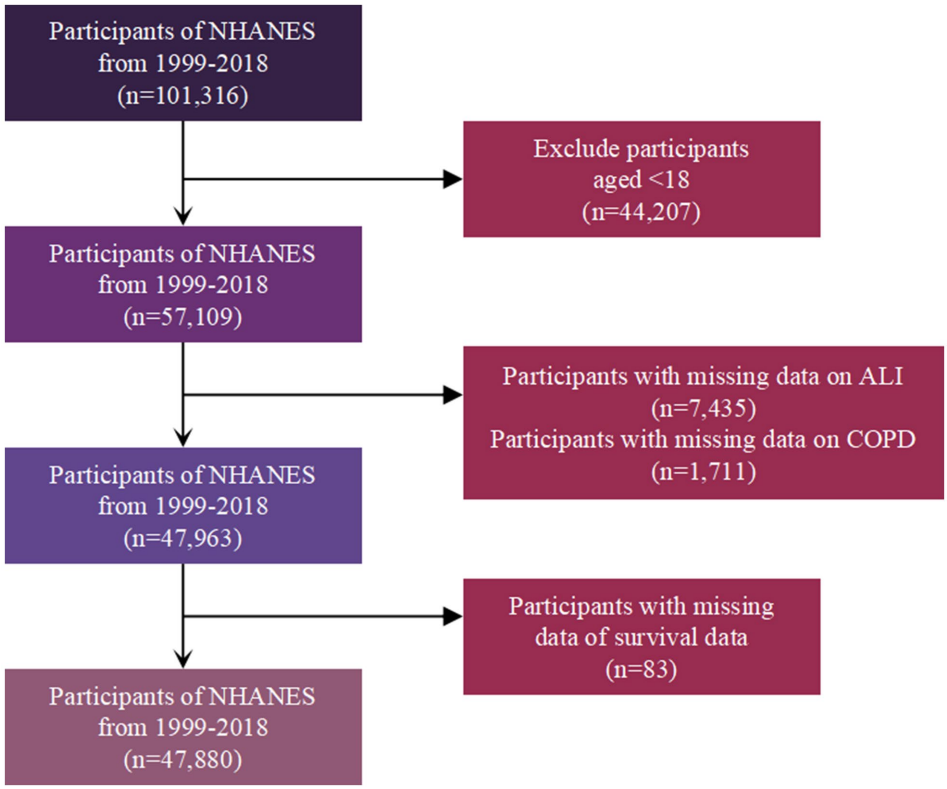

FIGURE 1
Flow chart of study participants.

Frequent phlegm: "Do you bring up phlegm (thick mucus) on most days for three consecutive months or more during the year?"

Past-year wheeze: "Have you had wheezing or whistling in your chest at any time in the past 12 months?"

Assessment of ALI

The ALI was assessed as a composite measure reflecting nutritional status and systemic inflammation. It comprised three components: BMI, serum albumin, and the neutrophil-to-lymphocyte ratio (NLR). The index was calculated using the formula: BMI (kg/m^2) × albumin level (g/dL) ÷ NLR, where NLR was determined by dividing neutrophil counts by lymphocyte counts. BMI was derived from measured height and weight, serum albumin levels were obtained from blood samples, and NLR was calculated from complete blood count data. Higher ALI values indicated better nutritional reserves and lower systemic inflammation. For analysis, ALI was categorized into four groups: Minimal (<44.43), Low (44.43–60.92), Intermediate (60.92–81.9), and High (>81.9).

Mortality outcomes

Mortality outcomes, including all-cause mortality and Cardiovascular disease (CVD)-specific mortality, were determined by linking NHANES participant data to the National Death Index (NDI) records through December 31, 2019. The NDI provides verified and detailed mortality data, including date and cause of death, using standardized codes based on the International Classification of Diseases, 10th Revision (ICD-10). All-cause mortality was defined as death from any cause, while CVD-specific mortality was identified using ICD-10 codes I00–I99. Mortality status and follow-up duration were calculated from the date of NHANES examination to the date of death or the end of the follow-up period.

Covariates definitions

Self-reported sociodemographic characteristics included age (in years), gender (male or female), and race/ethnicity (Mexican American, Non-Hispanic Black, Non-Hispanic White, Other Hispanic, or Other Race, including multiracial individuals). Educational attainment was categorized as less than high school, high school or equivalent, or college and above. The family income-to-poverty ratio (PIR) was used as a measure of socioeconomic status and analyzed as a continuous variable.

Lifestyle factors included smoking status (never, former, or current smoker) and alcohol consumption, categorized as never, former, mild, moderate, or heavy drinker. Physical activity levels were assessed using Metabolic Equivalent of Task (MET) scores, recorded in minutes per week, and dietary quality was evaluated using the Healthy Eating Index-2015 (HEI-2015), where higher scores indicated better adherence to dietary guidelines.

Health-related conditions were determined based on self-reported diagnoses, laboratory tests, or clinical measurements. Diabetes mellitus (DM) was defined by a self-reported diagnosis, current use of insulin or antidiabetic medications, or laboratory findings, including fasting plasma glucose levels ≥7.0 mmol/L (126 mg/dL), glycated

hemoglobin (HbA1c) ≥6.5%, or a 2-h plasma glucose level ≥ 11.1 mmol/L (200 mg/dL) from an oral glucose tolerance test. Hypertension was defined as a self-reported diagnosis, current use of antihypertensive medications, or measured systolic blood pressure ≥ 140 mmHg or diastolic blood pressure ≥ 90 mmHg, based on the average of three standardized blood pressure measurements taken during the NHANES physical examination.

Cancer status was categorized as yes or no based on participants' history of cancer diagnosis. CVD was defined as self-reported diagnosis of any of the following: coronary heart disease, angina, stroke, myocardial infarction, or heart failure.

Statistical analysis

Survey design and weights recommended by NHANES were applied to ensure the national representativeness of the results. Continuous variables were presented as means ± standard error. Categorical variables were reported as counts (percentages). Baseline characteristics among groups were compared using an analysis of variance test for continuous variables and the chi-square (χ^2) test for categorical variables.

The association between ALI with all-cause and CVD mortality was evaluated using Kaplan–Meier survival analysis and Cox proportional hazards regression models. Three models were constructed for the Cox regression analysis: Model 1: Unadjusted crude analysis. Model 2: Adjusted for basic demographic and lifestyle factors (e.g., age, sex, race/ethnicity, marital status, family income, and educational attainment). Model 3: Fully adjusted for all covariates, including comorbidities, e.g., diabetes, hypertension, cancer, CVD, smoking status, alcohol consumption, physical activity (MET scores), and HEI-2015 scores. Because dividing ALI by 10 makes the odds ratio (OR) or hazard ratio (HR) more clinically interpretable, we divided each participant's ALI level by 10 and included them as continuous variables in the multivariate Cox regression analysis.

Subgroup analyses were performed to explore the relationship between ALI and CVD mortality in various populations, such as those stratified by age, gender, smoking status, and comorbidities. Restricted cubic splines were used to investigate potential non-linear relationships between ALI with all-cause and CVD mortality.

Additionally, a propensity score matching (PSM) analysis was conducted to mitigate confounding effects. COPD patients were matched with non-COPD individuals using the nearest neighbor method. The balance of baseline covariates after matching was assessed using standardized mean differences, and Cox regression analysis was repeated in the matched cohort to confirm the robustness of the findings. To reduce the potential for reverse causation, sensitivity analyses excluded participants who died within the first 2 years of follow-up.

A two-sided p-value <0.05 was considered statistically significant for all analyses. All statistical analyses were conducted using R software (version 4.4.1; R Foundation for Statistical Computing, Vienna, Austria).

Results

In this study, we aimed to explore the relationship between the ALI and mortality outcomes in COPD patients. The data analysis focused on how ALI, as a combined measure of nutritional status and systemic inflammation, correlates with all-cause and CVD mortality. To assess these relationships, we utilized Kaplan–Meier survival curves, Cox proportional hazards regression models, and restricted cubic splines to investigate both linear and non-linear associations between ALI and mortality. We present the findings from these analyses in the following subsections, beginning with baseline characteristics and progressing through specific outcomes related to COPD severity, lung function, chronic pulmonary symptoms, and survival analysis.

Baseline characteristics

The baseline characteristics of the study participants are summarized in Table 1. A total of 478,800 participants were included, with an average age of 46.99 years (±16.86). The gender distribution showed 52% males and 48% females. Significant differences were observed across groups in several variables, including age, sex, race/ethnicity, family income-to-poverty ratio, education level, smoking status, and chronic disease prevalence such as diabetes, hypertension, cancer, CVD, and COPD.

ALI and COPD

Table 2 displays the association between ALI and COPD. In the crude model, a lower ALI category was significantly associated with a higher risk of COPD (p for trend = 0.001). After adjusting for age, gender, race, marital status, family income, education, smoking status, alcohol intake, physical activity, HEI-2015 score, and comorbidities (Model 2), this trend was not statistically significant ($p = 0.086$). Compared to the minimal ALI category, the low (OR = 0.81, 95% CI: 0.69–0.95) and intermediate categories (OR = 0.80, 95% CI: 0.69–0.93) were associated with reduced odds of COPD, while the high ALI category showed a weaker but still significant protective effect (OR = 0.85, 95% CI: 0.70–0.98).

ALI and lung function

Supplementary Table S1 examines the relationship between ALI and lung function, measured by FVC and FEV1. In the fully adjusted model (Model 2), no significant association was observed between ALI and either FVC or FEV1. While some improvements in lung function were noted in the intermediate ALI group for FEV1 ($\beta = 54.61$, 95% CI: 14.34–94.87), the overall trend was not consistent or clinically significant.

ALI and chronic pulmonary symptoms

Supplementary Table S2 presents the relationship between ALI and chronic pulmonary symptoms, including frequent cough, frequent phlegm, and past-year wheeze. In the fully adjusted model (Model 2), no significant associations were observed between ALI and these symptoms. While lower ALI categories appeared to show reduced odds for frequent cough and phlegm in the crude and

TABLE 1 Characteristic of study sample.

Characteristic	Overall N = 47880[1]	Minimal N = 12264[1]	Low N = 11323[1]	Intermediate N = 11374[1]	High N =12929[1]	p-value[2]
Age, years	46.99 ± (16.86)	49.85 ± (18.53)	46.82 ± (16.72)	45.93 ± (16.05)	45.34 ± (15.62)	<0.001
Sex						<0.001
Male	24,770 (52%)	6,458 (55%)	5,880 (53%)	5,696 (49%)	6,736 (50%)	
Female	23,110 (48%)	5,806 (45%)	5,433 (47%)	5,678 (51%)	6,193 (50%)	
Race/Ethnicity						<0.001
Mexican American	8,529 (8.2%)	1899 (6.5%)	2,109 (8.0%)	2,276 (9.2%)	2,245 (9.2%)	
Non-Hispanic Black	9,625 (11%)	1,549 (6.3%)	1,597 (7.0%)	2031 (9.1%)	4,448 (20%)	
Non-Hispanic White	21,359 (69%)	6,781 (76%)	5,506 (72%)	4,933 (68%)	4,139 (58%)	
Other Hispanic	3,976 (5.6%)	878 (4.7%)	974 (5.6%)	1,055 (6.3%)	1,069 (5.9%)	
Other Race - Including Multi-Racial	4,391 (6.8%)	1,157 (6.9%)	1,127 (6.8%)	1,079 (7.1%)	1,028 (6.5%)	
Marital						<0.001
Never married	8,246 (17%)	1960 (17%)	1964 (17%)	1907 (17%)	2,415 (18%)	
Married/Living with partner	29,209 (64%)	7,307 (62%)	6,962 (65%)	7,185 (66%)	7,755 (65%)	
Divorced/Widowed/Separated	10,425 (18%)	2,997 (22%)	2,387 (17%)	2,282 (17%)	2,759 (17%)	
Family income poverty ratio	2.99 ± (1.60)	2.96 ± (1.59)	3.04 ± (1.60)	3.06 ± (1.60)	2.92 ± (1.59)	<0.001
Education						<0.001
Less than high school	5,752 (5.9%)	1,423 (5.7%)	1,420 (6.0%)	1,386 (5.9%)	1,523 (6.2%)	
High school or equivalent	18,158 (35%)	4,734 (36%)	4,174 (34%)	4,209 (34%)	5,041 (37%)	
College and above	23,970 (59%)	6,107 (58%)	5,719 (60%)	5,779 (60%)	6,365 (57%)	
Smoking status						<0.001
Former	11,877 (25%)	3,303 (25%)	2,759 (24%)	2,734 (25%)	3,081 (25%)	
Never	26,035 (54%)	6,150 (50%)	6,097 (54%)	6,365 (55%)	7,423 (56%)	
Now	9,968 (21%)	2,811 (25%)	2,457 (22%)	2,275 (20%)	2,425 (19%)	
Drinking status						0.003
Former	7,993 (14%)	2,308 (15%)	1757 (13%)	1808 (13%)	2,120 (14%)	
Mild	9,642 (22%)	2,346 (22%)	2,344 (22%)	2,311 (21%)	2,641 (22%)	
Moderate	16,487 (37%)	4,233 (37%)	3,996 (38%)	3,887 (37%)	4,371 (36%)	
Heavy	6,652 (16%)	1,565 (15%)	1,601 (16%)	1,664 (17%)	1822 (16%)	
Never	7,106 (11%)	1812 (11%)	1,615 (11%)	1704 (12%)	1975 (12%)	

(Continued)

10.3389/fnut.2025.1550490

TABLE 1 (Continued)

Characteristic	Overall N = 47880[1]	Minimal N = 12264[1]	Low N = 11323[1]	Intermediate N = 11374[1]	High N =12929[1]	p-value[2]
MET scores, min/week	3,394.98 ± (5,074.74)	3,180.68 ± (4,868.35)	3,337.21 ± (5,024.44)	3,463.54 ± (5,153.87)	3,598.55 ± (5,235.94)	<0.001
HEI-2015	50.43 ± (13.25)	50.95 ± (13.44)	50.37 ± (13.20)	50.27 ± (13.28)	50.13 ± (13.07)	0.003
Cancer						<0.001
No	43,589 (91%)	10,679 (87%)	10,323 (91%)	10,524 (92%)	12,063 (93%)	
Yes	4,291 (9.3%)	1,585 (13%)	990 (8.9%)	850 (7.9%)	866 (7.3%)	
CVD						<0.001
No	42,648 (91%)	10,435 (88%)	10,097 (92%)	10,297 (93%)	11,819 (93%)	
Yes	5,232 (8.6%)	1829 (12%)	1,216 (8.2%)	1,077 (7.4%)	1,110 (7.2%)	
DM						<0.001
No	39,697 (87%)	10,249 (87%)	9,537 (89%)	9,402 (88%)	10,509 (86%)	
Yes	8,183 (13%)	2015 (13%)	1776 (11%)	1972 (12%)	2,420 (14%)	
Hypertension						<0.001
No	28,004 (63%)	7,179 (63%)	6,868 (66%)	6,750 (64%)	7,207 (60%)	
Yes	19,876 (37%)	5,085 (37%)	4,445 (34%)	4,624 (36%)	5,722 (40%)	
COPD						<0.001
No	45,920 (96%)	11,510 (94%)	10,881 (96%)	10,979 (97%)	12,550 (97%)	
Yes	1960 (3.9%)	754 (5.8%)	432 (3.6%)	395 (3.2%)	379 (3.1%)	

[1]Mean ± error; n (unweighted) (%).

[2]An analysis of variance; Pearson's X^2: Rao & Scott adjustment.

HEI-2015, Healthy Eating Index-2015; MET, Metabolic Equivalent of Task; CVD, cardiovascular disease; DM, diabetes mellitus; COPD, chronic obstructive pulmonary disease.

10.3389/fnut.2025.1550490

TABLE 2 Association between advanced lung cancer inflammation index and COPD.

Outcomes		Crude Model	Model 1	Model 2
		OR (95%CI)	OR (95%CI)	OR (95%CI)
COPD	Continuous	0.95 (0.92, 0.98)	0.98 (0.97, 1.01)	0.99 (0.98, 1.01)
	Categories			
	Minimal	**Ref.**	**Ref.**	**Ref.**
	Low	**0.61 (0.52, 0.70)**	**0.75 (0.65, 0.88)**	**0.81 (0.69, 0.95)**
	Intermediate	**0.54 (0.47, 0.62)**	**0.74 (0.64, 0.86)**	**0.80 (0.69, 0.93)**
	High	**0.52 (0.43, 0.62)**	**0.76 (0.63, 0.91)**	**0.85 (0.70, 0.98)**
	p for trend	0.001	0.004	0.086

Crude Model: no covariates were adjusted. Model 1: Adjusted covariates for model 1 included age, gender, race, marital status, family income level, and educational level. Model 2: Adjusted covariates for model 2 included the covariates for model 1 plus smoking status, alcohol intake, physical activity, and HEI-2015 data, diabetes, hypertension, cancer and cardiovascular disease. Bolded results represent statistically significant associations based on a p-value of less than 0.05. COPD, chronic obstructive pulmonary disease; 95%CI, 95% confidence interval.

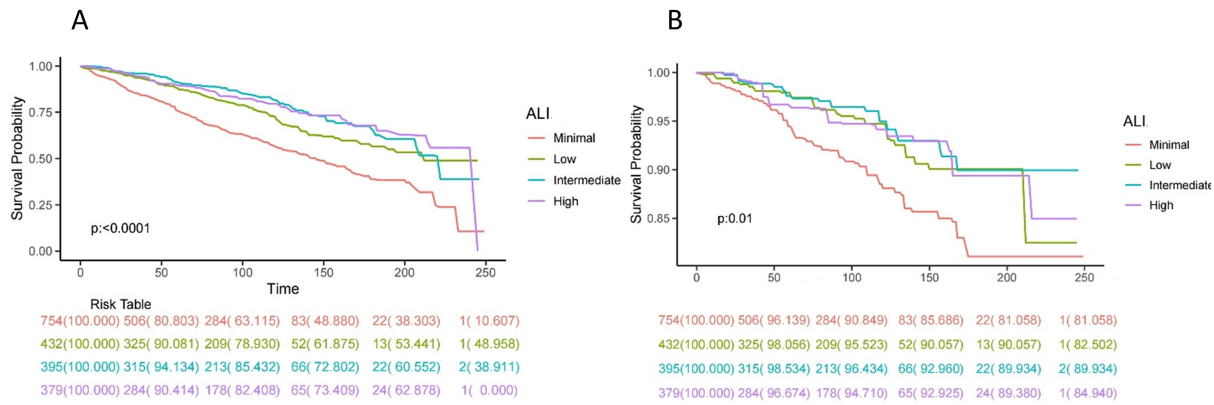

FIGURE 2
Kaplan–Meier survival curves of ALI impact on long-term all-cause **(A)** and CVD **(B)** mortality in patients with COPD (weighted). ALI, advanced lung cancer inflammation index; CVD, cardiovascular disease.

partially adjusted models, the associations diminished after full adjustment.

Kaplan–Meier analysis

Figure 2 presents Kaplan–Meier survival curves for all-cause mortality and CVD mortality across different ALI categories. The curves indicate that higher ALI levels are associated with improved survival, with the most pronounced difference observed for all-cause mortality. Patients in the higher ALI categories exhibit better survival probabilities compared to those in the minimal or low ALI categories. Figure 3 illustrates the time-dependent survival probability S(t) across different ALI levels for two groups: all-cause mortality (A) and cardiovascular disease (CVD) mortality (B) in patients with COPD. The heatmap in panel A (All-Cause Mortality) represents the survival probability over time (x-axis) at varying ALI levels (y-axis), with the color gradient reflecting the S(t) value for each combination of time and ALI. A lower S(t) value indicates a lower survival probability, with the color scale ranging from yellow (higher survival probability, closer to 1) to purple (lower survival probability, closer to 0). For all-cause mortality, the survival probability decreases significantly when ALI levels fall below 50. Similarly, panel B (CVD Mortality) shows the time-dependent survival probability for cardiovascular disease mortality, with the color scale again ranging from yellow (higher survival probability) to purple (lower survival probability). Compared to the all-cause mortality panel, the survival probability for CVD mortality is lower at certain ALI levels, with a significant decrease in survival probability when ALI levels fall below 25.

ALI and mortality

Table 3 examines the relationship between ALI and mortality outcomes, including all-cause and CVD mortality, in patients with COPD. In the fully adjusted model (Model 2), higher ALI categories were significantly associated with lower all-cause mortality. Compared to the minimal ALI category, the low ALI category (HR = 0.68, 95% CI: 0.53–0.87) was associated with a significant reduction in all-cause mortality risk, while the intermediate ALI category (HR = 0.50, 95% CI: 0.38–0.65) exhibited the strongest protective effect. However, in the high ALI category (HR = 0.60, 95% CI: 0.46–0.78), the reduction in mortality risk was slightly less pronounced than in the intermediate

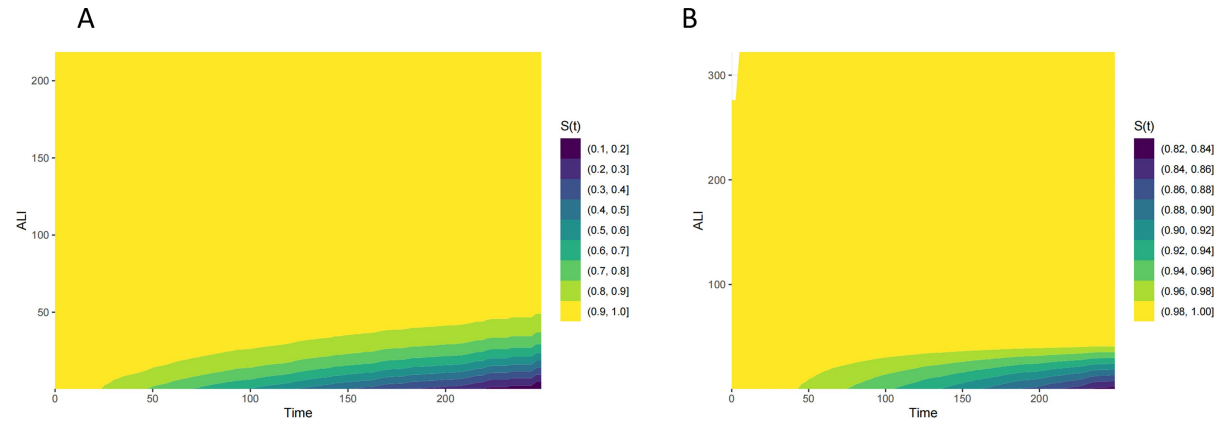

FIGURE 3
Time-dependent survival probability [S(t)] across ALI levels all-cause **(A)** and CVD **(B)** mortality in patients with COPD.

TABLE 3 Relationships of advanced lung cancer inflammation index with all-cause and CVD mortality in patients with COPD.

Outcomes		Crude Model	Model 1	Model 2
		HR (95%CI)	HR (95%CI)	HR (95%CI)
All causes	Continuous	0.93 (0.88, 0.98)	0.97 (0.93, 1.02)	0.97 (0.93, 1.02)
	Categories			
	Minimal	Ref.	Ref.	Ref.
	Low	**0.56 (0.43, 0.73)**	**0.69 (0.54, 0.90)**	**0.68 (0.53, 0.87)**
	Intermediate	**0.41 (0.31, 0.54)**	**0.55 (0.43, 0.71)**	**0.50 (0.38, 0.65)**
	High	**0.41 (0.33, 0.52)**	**0.59 (0.45, 0.78)**	**0.60 (0.46, 0.78)**
	p for trend	0.001	0.001	0.001
CVD	Continuous	0.92 (0.85, 1.01)	0.98 (0.92, 1.05)	0.98 (0.91, 1.05)
	Categories			
	Minimal	Ref.	Ref.	Ref.
	Low	0.55 (0.32, 0.96)	0.69 (0.39, 1.22)	0.68 (0.39, 1.19)
	Intermediate	0.44 (0.24, 0.81)	0.64 (0.34, 1.18)	0.53 (0.28, 1.00)
	High	0.52 (0.29, 0.95)	0.87 (0.46, 1.66)	0.88 (0.44, 1.76)
	p for trend	0.033	0.646	0.593

Crude Model: no covariates were adjusted. Model 1: Adjusted covariates for model 1 included age, gender, race, marital status, family income level, and educational level. Model 2: Adjusted covariates for model 2 included the covariates for model 1 plus smoking status, alcohol intake, physical activity, and HEI-2015 data, diabetes, hypertension, cancer and cardiovascular disease. Bolded results represent statistically significant associations based on a *p*-value of less than 0.05. OR, Odds Ratio; 95%CI, 95% confidence interval.

group. For CVD mortality, however, no significant association was observed in the fully adjusted model.

Tables 4, 5 examine the stratified relationships between ALI and mortality in COPD patients. Table 4 shows that higher ALI levels are consistently associated with a reduced risk of all-cause mortality across most subgroups, including those stratified by age, CVD, diabetes, and cancer, with no significant interactions observed. Table 5, however, reveals that the association between ALI and CVD mortality is less consistent, with significant protective effects observed in some subgroups (e.g., age < 60), but not others. While ALI is a strong predictor of reduced all-cause mortality in COPD patients, its role in reducing CVD mortality is more variable and context-dependent.

Non-linear relationships

Figure 4 showing a clear non-linear association between ALI and both mortality outcomes. The protective effects plateau at higher ALI levels, with a potential increase in mortality risk for very high ALI values. Figure 5 illustrates the sex-stratified relationship between ALI and mortality outcomes in COPD patients. For all-cause mortality, the protective effect of higher ALI levels is consistent across both sexes. For CVD mortality, the relationship is more variable, with clearer protective effects in females than in males.

Tables 6, 7 collectively evaluate the threshold effect of ALI on all-cause and CVD mortality in COPD patients. Table 6 shows that

TABLE 4 Stratified analyses of the relationships of advanced lung cancer inflammation index with all-cause mortality in patients with COPD.

Characteristics	ALI					
	Minimal	Low	Intermediate	High	*P* for trend	*P* for interaction
Age						0.82
<60	Ref	0.58(0.30, 1.12)	0.35(0.19, 0.64)	0.38(0.20, 0.72)	0.02	
≥60	Ref	0.67(0.52, 0.87)	0.50(0.37, 0.67)	0.52(0.38, 0.70)	0.22	
Gender						0.35
Male	Ref	0.69(0.49, 0.98)	0.50(0.34, 0.72)	0.79(0.51, 1.21)	0.02	
Female	Ref	0.69(0.48, 1.00)	0.50(0.33, 0.77)	0.46(0.31, 0.68)	0.02	
Smoke status						0.96
Never	Ref	0.96(0.45, 2.05)	0.73(0.33, 1.62)	0.46(0.24, 0.90)	0.28	
Former	Ref	0.63(0.45, 0.88)	0.49(0.34, 0.71)	0.58(0.39, 0.86)	0.71	
Now	Ref	0.58(0.38, 0.89)	0.40(0.25, 0.62)	0.72(0.44, 1.18)	0.48	
Hypertension						0.94
No	Ref	0.72(0.45, 1.14)	0.54(0.31, 0.94)	0.53(0.31, 0.91)	0.1	
Yes	Ref	0.64(0.48, 0.85)	0.44(0.32, 0.61)	0.47(0.34, 0.65)	<0.001	
DM						0.66
No	Ref	0.61(0.45, 0.83)	0.49(0.36, 0.69)	0.43(0.29, 0.64)	0.06	
Yes	Ref	0.57(0.35, 0.95)	0.43(0.25, 0.74)	0.57(0.39, 0.83)	0.06	
CVD						0.56
No	Ref	0.56(0.40, 0.79)	0.48(0.33, 0.68)	0.42(0.27, 0.65)	0.06	
Yes	Ref	0.72(0.51, 1.02)	0.44(0.29, 0.69)	0.53(0.34, 0.82)	0.74	
Cancer						0.42
No	Ref	0.69(0.52, 0.93)	0.50(0.37, 0.69)	0.45(0.33, 0.62)	<0.0001	
Yes	Ref	0.47(0.30, 0.74)	0.43(0.25, 0.76)	0.53(0.31, 0.92)	0.3	

The adjusted covariates encompassed age, gender, race, marital status, family income level, educational attainment, smoking status, alcohol consumption, physical activity, HEI-2015 scores, as well as the presence of diabetes, hypertension, cancer, and cardiovascular disease, excluding the stratified variables. CVD, cardiovascular disease; DM, diabetes mellitus; COPD, chronic obstructive pulmonary disease.

for all-cause mortality, ALI had a significant protective effect when ALI values were below the threshold of 88.32 (HR per 10-unit increment = 0.842, 95% CI: 0.801–0.884, $p < 0.0001$). However, above this threshold, the association became non-significant (HR = 1.012, 95% CI: 0.999–1.024, $p = 0.062$). Similarly, Table 7 highlights that for CVD mortality, ALI was protective below the threshold of 89.73 (HR per 10-unit increment = 0.82, 95% CI: 0.78–0.86, $p < 0.0001$), but the association reversed above the threshold, becoming positively associated with risk (HR = 1.02, 95% CI: 1.00–1.03, $p = 0.01$).

Sensitivity analyses

Table 8 presents a sensitivity analysis that excludes participants who died within 2 years to address potential reverse causation. The results reaffirm that higher ALI levels are significantly associated with reduced all-cause mortality in COPD patients.

Table 9 indicates significant differences in baseline characteristics between COPD and non-COPD participants before matching, including age, education level, comorbidities (e.g., hypertension, diabetes, and cancer), and smoking status. After PSM, Table 10 and Figure 6 shows that the baseline characteristics were balanced between the two groups, ensuring comparability. Table 11 demonstrates the association between ALI and COPD was similar.

Discussion

Our study reveals that the ALI is significantly associated with both all-cause mortality and CVD mortality in COPD patients, exhibiting a notable non-linear relationship. Higher ALI levels were protective up to specific thresholds (88.32 for all-cause mortality and 89.73 for CVD mortality); however, beyond these thresholds, the protective effect plateaued and became non-significant for all-cause mortality, while reversing for CVD mortality, indicating increased risk. This non-linear trend underscores the intricate balance between inflammation and nutritional status, suggesting that optimizing ALI within an appropriate range can improve outcomes, whereas excessive levels may reflect underlying pathological changes requiring further investigation.

Chronic inflammation in individuals with COPD is primarily driven by the infiltration of inflammatory cells, including neutrophils, macrophages, and lymphocytes, into the small airways (8). This process leads to the degradation of structural cells such as airway epithelial cells, stromal cells, and

TABLE 5 Stratified analyses of the relationships of advanced lung cancer inflammation index with CVD mortality in patients with COPD.

Characteristics	ALI					
	Minimal	Low	Intermediate	High	*P* for trend	*P* for interaction
Age						0.82
<60	Ref	0.58(0.30, 1.12)	0.35(0.19, 0.64)	0.38(0.20, 0.72)	0.02	
≥60	Ref	0.67(0.52, 0.87)	0.50(0.37, 0.67)	0.52(0.38, 0.70)	0.22	
Gender						0.26
Male	Ref	0.60(0.33, 1.10)	0.46(0.21, 0.99)	1.07(0.44, 2.60)	0.05	
Female	Ref	0.75(0.27, 2.07)	0.67(0.23, 1.99)	0.34(0.14, 0.87)	0.45	
Smoke status						0.96
Never	Ref	0.77(0.10, 5.72)	1.00(0.15, 6.82)	0.33(0.11, 1.02)	0.26	
Former	Ref	0.62(0.31, 1.24)	0.62(0.27, 1.46)	0.77(0.34, 1.71)	0.97	
Now	Ref	0.55(0.19, 1.60)	0.31(0.10, 0.95)	0.76(0.20, 2.93)	0.83	
Hypertension						0.99
No	Ref	0.53(0.17, 1.66)	0.29(0.06, 1.41)	0.27(0.11, 0.66)	0.14	
Yes	Ref	0.65(0.36, 1.19)	0.52(0.26, 1.03)	0.82(0.38, 1.77)	0.39	
DM						0.62
No	Ref	0.46(0.22, 0.96)	0.51(0.23, 1.13)	0.70(0.30, 1.64)	0.83	
Yes	Ref	0.62(0.31, 1.25)	0.34(0.12, 0.99)	0.56(0.24, 1.34)	0.11	
CVD						0.69
No	Ref	0.44(0.18, 1.05)	0.54(0.24, 1.20)	0.62(0.22, 1.75)	0.55	
Yes	Ref	0.86(0.44, 1.66)	0.50(0.19, 1.34)	0.87(0.42, 1.79)	0.42	
Cancer						0.11
No	Ref	0.69(0.38, 1.28)	0.57(0.30, 1.07)	0.48(0.25, 0.90)	0.03	
Yes	Ref	0.36(0.11, 1.14)	0.16(0.02, 1.13)	1.02(0.43, 2.41)	0.22	

The adjusted covariates encompassed age, gender, race, marital status, family income level, educational attainment, smoking status, alcohol consumption, physical activity, HEI-2015 scores, as well as the presence of diabetes, hypertension, cancer, and cardiovascular disease, excluding the stratified variables. CVD, cardiovascular disease; DM, diabetes mellitus; COPD, chronic obstructive pulmonary disease.

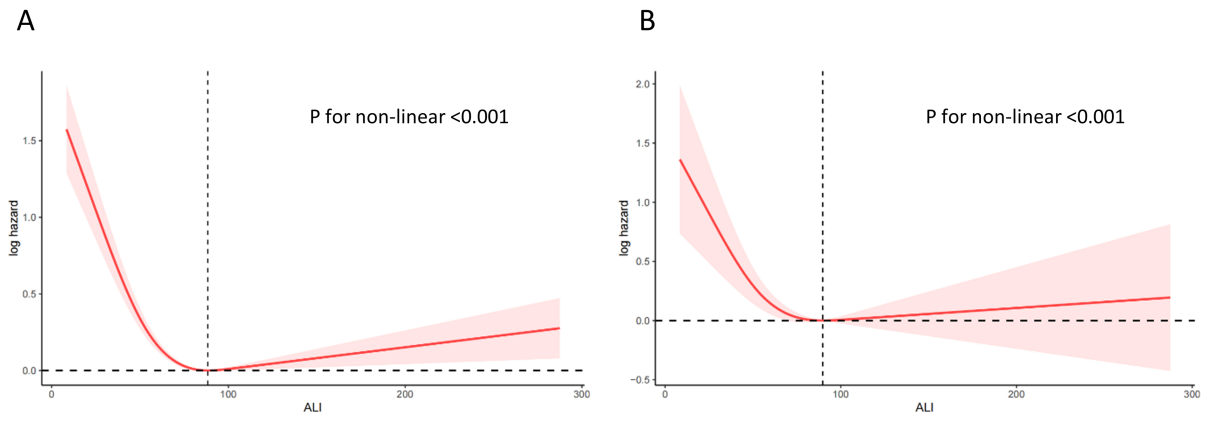

FIGURE 4
Relationship between ALI and all-cause **(A)** and CVD **(B)** mortality in patients with COPD. The solid and red shadow represent the estimated values and their 95% CIs, respectively. ALI, advanced lung cancer inflammation index; CVD, cardiovascular disease.

parenchymal cells. As COPD progresses, airway inflammation intensifies. The NLR in peripheral blood is a well-established biomarker for quantifying systemic inflammation. Previous studies have explored the relationship between NLR and lung function decline, a key indicator of COPD severity and risk (9). These studies emphasize the clinical relevance of NLR as a biomarker, linking it to impaired lung function, increased COPD risk, and specific DNA methylation patterns. Additionally,

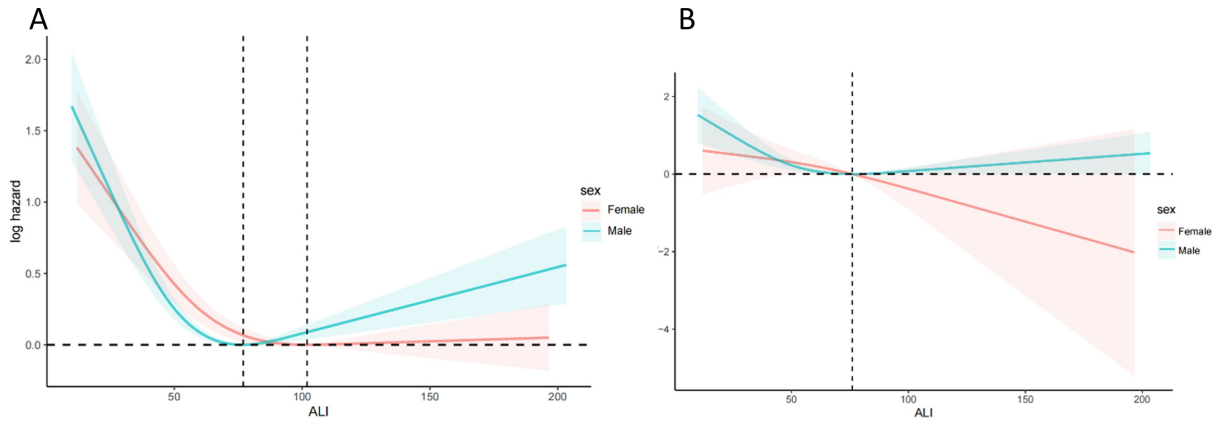

FIGURE 5
Relationship between ALI and all-cause **(A)** and CVD **(B)** mortality in patients with COPD stratified by sex. The solid and red or blue shadow represent the estimated values and their 95% CIs, respectively. ALI, advanced lung cancer inflammation index; CVD, cardiovascular disease.

TABLE 6 Threshold effect analysis of advanced lung cancer inflammation index on all-cause mortality in patients with COPD.

	All-cause mortality	
	Per 10 U increment	*P*
<88.32	0.842(0.801, 0.884)	<0.0001
>88.32	1.012(0.999, 1.024)	0.062

Adjusted covariates included age, gender, race, marital status, family income level, educational level, smoking status, alcohol intake, physical activity, and HEI-2015 data, diabetes, hypertension, cancer and cardiovascular disease.

TABLE 7 Threshold effect analysis advanced lung cancer inflammation index on of CVD mortality in patients with COPD.

	CVD mortality	
	Per 10 U increment	*P*
<89.73	0.82(0.78, 0.86)	<0.0001
>89.73	1.02(1.00, 1.03)	0.01

Adjusted covariates included age, gender, race, marital status, family income level, educational level, smoking status, alcohol intake, physical activity, and HEI-2015 data, diabetes, hypertension, cancer and cardiovascular disease. CVD, cardiovascular disease.

research focusing on patients with COPD has demonstrated the prognostic value of hematologic inflammatory markers, such as NLR, in predicting mortality risk (10). Similarly, the platelet-to-lymphocyte ratio (PLR) has been associated with elevated COPD risk (11). These findings highlight the critical role of inflammation in influencing COPD outcomes and align with the conclusions of our study.

Previous research has predominantly focused on individual inflammatory markers to evaluate the prognosis of patients with COPD. However, this approach lacks the comprehensiveness needed to accurately assess the complex relationship between inflammation and mortality risk in COPD. A critical factor contributing to poor prognosis in COPD patients is the high prevalence of malnutrition within this population. A recent meta-analysis of 26 studies found that COPD patients have significantly lower serum albumin levels compared to individuals without COPD (3), with low serum albumin levels being strongly associated with adverse outcomes (12). Furthermore, a large cohort study of 220,000 Chinese men aged 40–79 years, followed over a 15-year period, reported that a 5 kg/m^2 reduction in Body Mass Index (BMI) was linked to a 31% increase in mortality risk from COPD (13). These findings underscore the importance of simultaneously addressing inflammation and malnutrition in the prognostic evaluation of COPD patients.

The ALI, initially developed as a prognostic marker for survival in non-small cell lung cancer (14), has been applied across various other cancer types, including esophageal, colorectal, pancreatic, and gastric cancers (15–18). Research indicates that cancer survivors with elevated ALI levels and no depressive symptoms face the lowest risks of both all-cause and non-cancer mortality (19). In individuals with type 2 diabetes mellitus (T2DM), elevated ALI levels are strongly associated with reduced risks of all-cause and cardiovascular mortality, particularly among women (20). However, when ALI exceeds a certain threshold, a slight increase in mortality risk may occur. These findings emphasize the importance of weight management and inflammation control in improving the prognosis of individuals with T2DM. Additionally, studies suggest that optimizing ALI levels can significantly reduce cardiovascular mortality in individuals with chronic hypertension, providing valuable insights for managing hypertension-related conditions (21).

The potential biological mechanisms explaining the significantly reduced risk of mortality in individuals with COPD are as follows: Firstly, BMI is a critical indicator of adiposity. Prolonged exposure to cigarette smoke accelerates aging, leading to reduced body weight and premature lung aging (4, 22). This phenomenon may account for the strong association between low BMI and higher COPD-related mortality. A large prospective community cohort study in Japan found that decreased BMI and substantial weight loss were independently associated with an increased risk of COPD mortality (23). Secondly, serum albumin, a protein synthesized by the liver, plays essential roles in the transport and regulation of nutrients, hormones, and medications. Recent studies have shown that reduced serum albumin levels are linked to systemic inflammation activation and an increased risk of malnutrition (24). Additionally, albumin protects tissues from

TABLE 8 Relationships of advanced lung cancer inflammation index with all-cause and CVD mortality in patients with COPD after excluding participants who died within 2 years.

Outcomes		Crude model	Model 1	Model 2
		OR (95%CI)	OR (95%CI)	OR (95%CI)
All-cause	Continuous	**0.93 (0.88, 0.99)**	0.96 (0.91, 1.01)	0.95 (0.90, 1.00)
	Categories			
	Minimal	Ref.	Ref.	Ref.
	Low	**0.61 (0.46, 0.80)**	**0.68 (0.52, 0.89)**	**0.68(0.53, 0.89)**
	Intermediate	**0.44 (0.33, 0.59)**	**0.53 (0.40, 0.71)**	**0.50(0.36, 0.67)**
	High	**0.44 (0.33, 0.59)**	**0.52 (0.38, 0.71)**	**0.52(0.37, 0.71)**
	p for trend	0.001	0.001	0.001
CVD	Continuous	0.92 (0.85, 1.01)	0.99 (0.93, 1.06)	0.98 (0.91, 1.06)
	Categories			
	Minimal	Ref.	Ref.	Ref.
	Low	0.55 (0.32, 0.96)	0.61 (0.32, 1.15)	0.60 (0.32, 1.11)
	Intermediate	0.44 (0.24, 0.81)	0.65 (0.34, 1.27)	0.55 (0.28, 1.09)
	High	0.52 (0.29, 0.95)	0.87 (0.44, 1.72)	0.83 (0.40, 1.76)
	p for trend	0.033	0.756	0.626

inflammatory damage. Thirdly, neutrophils accumulate in the sputum of stable COPD patients with severe disease, unlike those with mild or moderate COPD. This accumulation is associated with elevated expression of macrophage inflammatory protein-1α (MIP-1α) in bronchial epithelial cells (25). As COPD progresses, increased neutrophil levels are observed in the small airways of COPD patients compared to smokers with normal lung function (26). Lymphocytes also contribute to alveolar destruction in COPD. Specifically, CD8+ T cells produce pro-inflammatory cytokines such as IL-2, interferon-γ, and TNFα, which recruit additional inflammatory cells (27, 28). These cells also release perforin and granzyme B, inducing lysis and apoptosis of alveolar epithelial cells and advancing emphysema development (29). In summary, maintaining an appropriate BMI, achieving optimal serum albumin levels, and reducing the NLR can improve ALI scores, thereby supporting a more favorable prognosis in COPD patients.

In this study, we observed that ALI, as a combined measure of inflammation and nutritional status, holds prognostic value in COPD patients. Specifically, lower ALI values are associated with higher risks of COPD, emphasizing the importance of malnutrition and chronic inflammation in this population. Therefore, COPD patients may benefit from interventions aimed at improving nutritional status or reducing inflammation to optimize ALI levels and improve survival outcomes. For patients with very high ALI levels, clinicians should consider the possibility of undiagnosed comorbidities, which may explain the increased mortality risk.

These findings provide new insights for personalized treatment strategies in COPD management. By using ALI as a comprehensive prognostic marker, clinicians can better identify high-risk patients and tailor treatment plans accordingly. For patients with lower ALI levels, nutritional interventions and anti-inflammatory therapies may be prioritized, while those with higher ALI levels may require further assessment of other disease factors. Future research should further validate these thresholds and explore interventions aimed at optimizing ALI, advancing personalized treatment approaches for COPD.

This study has several strengths. First, it utilized data from the NHANES database, which provides a large, nationally representative cohort with comprehensive health and nutrition information, enhancing the generalizability of our findings. Second, by integrating markers of systemic inflammation (neutrophil-to-lymphocyte ratio) and nutritional status (BMI and serum albumin) into the ALI, the study offers a holistic approach to evaluating risk in COPD patients, moving beyond single-biomarker analyses. Third, the use of robust statistical methods, including Kaplan–Meier survival analyses, Cox proportional hazards models, and propensity score matching, strengthens the validity of the results by minimizing potential biases and confounding effects. Finally, the investigation into non-linear relationships between ALI and mortality outcomes provides nuanced insights that can inform clinical risk stratification and personalized interventions.

Despite these strengths, this study also has notable limitations. First, the cross-sectional nature of NHANES data limits the ability to establish causal relationships between ALI and mortality outcomes in COPD patients. Second, ALI relies on serum albumin and BMI, which can be influenced by acute illness or fluid status, potentially confounding its predictive value in chronic conditions like COPD. Third, the study did not include specific inflammatory biomarkers such as C-reactive protein (CRP) or IL-6, which could further refine the understanding of systemic inflammation in this context. Fourth, the thresholds identified for ALI's protective effects may vary across populations and settings, requiring external validation to confirm their clinical applicability. Lastly, residual confounding cannot be entirely ruled out, despite the comprehensive adjustment for covariates, as certain factors such as genetic

10.3389/fnut.2025.1550490

TABLE 9 Basic characteristics of participants before PSM (propensity score matching) analysis.

Characteristic	Overall N = 47880[1]	Normal N = 45920[1]	COPD N= 1960[1]	p-value[2]
Age, years	46.99 ± (16.86)	46.43 ± (16.77)	60.66 ± (12.85)	<0.001
Sex				0.133
Male	24,770 (52%)	23,916 (52%)	854 (49%)	
Female	23,110 (48%)	22,004 (48%)	1,106 (51%)	
Age, years				<0.001
Sex	8,529 (8.2%)	8,420 (8.5%)	109 (1.7%)	
Male	9,625 (11%)	9,304 (11%)	321 (6.9%)	
Female	21,359 (69%)	20,068 (68%)	1,291 (83%)	
Age, years	3,976 (5.6%)	3,864 (5.7%)	112 (2.3%)	
Sex	4,391 (6.8%)	4,264 (6.9%)	127 (6.3%)	
Male				<0.001
Female	8,246 (17%)	8,095 (18%)	151 (6.5%)	
Age, years	29,209 (64%)	28,112 (65%)	1,097 (62%)	
Sex	10,425 (18%)	9,713 (18%)	712 (31%)	
Family income poverty ratio	2.99 ± (1.60)	3.00 ± (1.60)	2.74 ± (1.58)	<0.001
Education				<0.001
Less than high school	5,752 (5.9%)	5,484 (5.8%)	268 (8.3%)	
High school or equivalent	18,158 (35%)	17,302 (35%)	856 (42%)	
College and above	23,970 (59%)	23,134 (59%)	836 (50%)	
Cancer				<0.001
No	43,589 (91%)	42,025 (91%)	1,564 (77%)	
Yes	4,291 (9.3%)	3,895 (8.7%)	396 (23%)	
CVD				<0.001
No	42,648 (91%)	41,325 (92%)	1,323 (72%)	
Yes	5,232 (8.6%)	4,595 (7.8%)	637 (28%)	
DM				<0.001
No	39,697 (87%)	38,311 (88%)	1,386 (76%)	
Yes	8,183 (13%)	7,609 (12%)	574 (24%)	
HEI-2015	50.43 ± (13.25)	50.45 ± (13.25)	49.82 ± (13.29)	0.158
Hypertension				<0.001
No	28,004 (63%)	27,307 (64%)	697 (41%)	
Yes	19,876 (37%)	18,613 (36%)	1,263 (59%)	
MET scores, min/week	3,394.98 ± (5,074.74)	3,383.81 ± (5,085.16)	3,669.99 ± (4,804.11)	<0.001
Smoking status				<0.001
Former	11,877 (25%)	10,922 (24%)	955 (47%)	
Never	26,035 (54%)	25,720 (55%)	315 (17%)	
Now	9,968 (21%)	9,278 (21%)	690 (36%)	
Drinking status				<0.001
Former	7,993 (14%)	7,371 (13%)	622 (28%)	
Mild	9,642 (22%)	9,359 (22%)	283 (16%)	
Moderate	16,487 (37%)	15,799 (37%)	688 (36%)	
Heavy	6,652 (16%)	6,427 (16%)	225 (14%)	
Never	7,106 (11%)	6,964 (12%)	142 (6.4%)	

[1]Mean ± error; n (unweighted) (%).
[2]An analysis of variance; Pearson's X^2: Rao & Scott adjustment.
HEI-2015, Healthy Eating Index-2015; MET, Metabolic Equivalent of Task; CVD, cardiovascular disease; DM, diabetes mellitus; COPD, chronic obstructive pulmonary disease.

10.3389/fnut.2025.1550490

TABLE 10 Basic characteristics of participants after PSM (propensity score matching) analysis.

Characteristic	Overall N = 3,795[1]	Normal N = 1,930[1]	COPD N = 1,865[1]	p-value[2]
Characteristic	60.14 ± (14.24)	59.68 ± (15.48)	60.62 ± (12.83)	0.521
Age, years				0.437
Sex	1,692 (48%)	841 (47%)	851 (49%)	
Male	2,218 (52%)	1,114 (53%)	1,104 (51%)	
Female				0.668
Age, years	212 (1.7%)	103 (1.7%)	109 (1.7%)	
Sex	657 (7.0%)	336 (7.1%)	321 (6.9%)	
Male	2,549 (82%)	1,263 (81%)	1,286 (83%)	
Female	193 (2.3%)	81 (2.2%)	112 (2.3%)	
Age, years	299 (6.9%)	172 (7.4%)	127 (6.4%)	
Sex				0.868
Male	277 (6.5%)	126 (6.5%)	151 (6.5%)	
Female	2,266 (63%)	1,171 (63%)	1,095 (63%)	
Age, years	1,367 (31%)	658 (30%)	709 (31%)	
Sex	2.78 ± (1.54)	2.82 ± (1.50)	2.75 ± (1.58)	0.230
Family income poverty ratio				0.895
Education	553 (8.1%)	287 (7.9%)	266 (8.3%)	
Less than high school	1,678 (42%)	824 (42%)	854 (42%)	
High school or equivalent	1,679 (50%)	844 (50%)	835 (50%)	
College and above	62.55 ± (58.94)	63.10 ± (58.12)	61.99 ± (59.79)	0.072
Cancer				0.381
No	3,080 (78%)	1,519 (79%)	1,561 (77%)	
Yes	830 (22%)	436 (21%)	394 (23%)	
CVD				0.248
No	2,673 (73%)	1,350 (74%)	1,323 (72%)	
Yes	1,237 (27%)	605 (26%)	632 (28%)	
DM				0.797
No	2,768 (76%)	1,383 (76%)	1,385 (76%)	
Yes	1,142 (24%)	572 (24%)	570 (24%)	
HEI-2015	49.68 ± (13.00)	49.51 ± (12.72)	49.85 ± (13.28)	0.542
Hypertension				0.842
No	1,403 (41%)	706 (41%)	697 (41%)	
Yes	2,507 (59%)	1,249 (59%)	1,258 (59%)	
MET scores, min/week	3,812.44 ± (5,648.26)	3,949.50 ± (6,356.79)	3,670.64 ± (4,804.14)	0.022
Smoking status				0.646
Former	1939 (48%)	985 (49%)	954 (47%)	
Never	632 (17%)	317 (16%)	315 (17%)	
Now	1,339 (35%)	653 (35%)	686 (36%)	
Drinking status				0.317
Former	1,227 (26%)	609 (25%)	618 (28%)	
Mild	581 (17%)	298 (18%)	283 (16%)	
Moderate	1,389 (37%)	702 (38%)	687 (36%)	
Heavy	435 (14%)	210 (13%)	225 (14%)	
Never	278 (6.0%)	136 (5.6%)	142 (6.4%)	

[1]Mean ± error; n (unweighted) (%).

[2]An analysis of variance; Pearson's X^2: Rao & Scott adjustment.

HEI-2015, Healthy Eating Index-2015; MET, Metabolic Equivalent of Task; CVD, cardiovascular disease; DM, diabetes mellitus; COPD, chronic obstructive pulmonary disease.

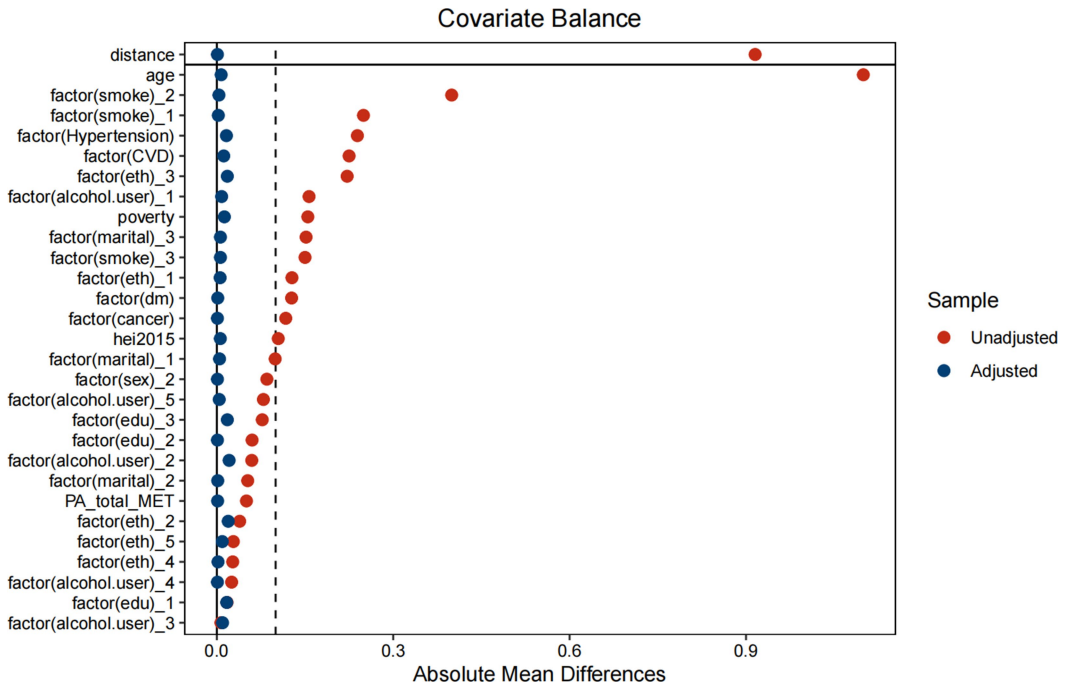

FIGURE 6
Propensity score matching analysis of the standardized mean difference results for the different variables.

TABLE 11 Association between advanced lung cancer inflammation index and COPD after PSM (propensity score matching) analysis.

	OR	95%CI	*p*
Continuous	1.00	0.99, 1.01	0.549
Categories	–	–	–
Minimal	Ref.	Ref.	–
Low	0.74	0.59, 0.93	0.01
Intermediate	0.75	0.61, 0.92	0.03
High	0.86	0.68, 1.08	0.16
p for trend			0.04

Adjusted MET scores, min/week.

predisposition and unmeasured lifestyle variables were not accounted for in the analysis.

Conclusion

This study underscores the importance of the ALI as a prognostic marker in COPD patients, demonstrating its significant association with all-cause and cardiovascular mortality. The non-linear relationship observed suggests that ALI provides protective effects up to specific thresholds (88.32 for all-cause mortality and 89.73 for CVD mortality), beyond which the association weakens or reverses. These findings highlight the need to address both systemic inflammation and nutritional status in COPD management. Future research should validate these thresholds and explore interventions to optimize ALI, paving the way for more personalized and effective treatment strategies.

Data availability statement

Publicly available datasets were analyzed in this study. This data can be found at: The survey data are publicly available on the internet for data users and researchers throughout the world (www.cdc.gov/nchs/nhanes/).

Ethics statement

The ethics review board of the National Center for Health Statistics approved all NHANES protocols. The studies were conducted in accordance with the local legislation and institutional requirements. Written informed consent for participation was not required from the participants or the participants' legal guardians/next of kin in accordance with the national legislation and institutional requirements.

Author contributions

JY: Writing – original draft, Writing – review & editing. PW: Writing – original draft, Writing – review & editing. ZL: Writing – original draft, Writing – review & editing. LZ: Writing – original draft, Writing – review & editing. ZF: Writing – original draft, Writing – review & editing. PS: Writing – original draft, Writing – review & editing. XX: Writing – original draft, Writing – review & editing. XC: Writing – original draft, Writing – review & editing. BY: Writing – original draft, Writing – review & editing. YH: Writing – original draft, Writing – review & editing. TF: Writing – original draft,

Writing – review & editing. JZ: Writing – original draft, Writing – review & editing. RD: Writing – original draft, Writing – review & editing, Methodology.

Funding

The author(s) declare that financial support was received for the research and/or publication of this article. This study was funded by the Medical Research Project/Youth Innovation Project of the Sichuan Medical Association (Grant No. S2024017).

Acknowledgments

Thanks to Jing Zhang (Shanghai Tongren Hospital) for his work on the NHANES database. His outstanding work, nhanesR package and webpage, makes it easier for us to explore the NHANES database.

Conflict of interest

The authors declare that the research was conducted in the absence of any commercial or financial relationships that could be construed as a potential conflict of interest.

Generative AI statement

The authors used GPT-4 for proofreading and editing the paper. After using this tool/service, the authors reviewed and edited the content as needed and take full responsibility for the content of the publication.

Publisher's note

Supplementary material

The Supplementary material for this article can be found online at: https://www.frontiersin.org/articles/10.3389/fnut.2025.1550490/full#supplementary-material

References

1. World Health Organization. Available online at: www.who.int/news-room/fact-sheets/detail/chronic-obstructive-pulmonary-disease-(copd). World Health Organization (Accessed November 06, 2024).

2. Ritchie AI, Wedzicha JA. Definition, causes, pathogenesis, and consequences of chronic obstructive pulmonary disease exacerbations. *Clin Chest Med*. (2020) 41:421–38. doi: 10.1016/j.ccm.2020.06.007

3. Zinellu E, Fois AG, Sotgiu E, Mellino S, Mangoni AA, Carru C, et al. Serum albumin concentrations in stable chronic obstructive pulmonary disease: a systematic review and meta-analysis. *J Clin Med*. (2021) 10:269. doi: 10.3390/jcm10020269

4. Ito K, Barnes PJ. COPD as a disease of accelerated lung aging. *Chest*. (2009) 135:173–80. doi: 10.1378/chest.08-1419

5. McDonald MN, Wouters EFM, Rutten E, Casaburi R, Rennard SI, Lomas DA, et al. It's more than low BMI: prevalence of cachexia and associated mortality in COPD. *Respir Res*. (2019) 20:100. doi: 10.1186/s12931-019-1073-3

6. Song M, Zhang Q, Song C, Liu T, Zhang X, Ruan G, et al. The advanced lung cancer inflammation index is the optimal inflammatory biomarker of overall survival in patients with lung cancer. *J Cachexia Sarcopenia Muscle*. (2022) 13:2504–14. doi: 10.1002/jcsm.13032

7. Fan W, Zhang Y, Liu Y, Ding Z, Si Y, Shi F, et al. Nomograms based on the advanced lung Cancer inflammation index for the prediction of coronary artery disease and calcification. *Clin Appl Thromb Hemost*. (2021) 27:10760296211060455. doi: 10.1177/10760296211060455

8. Richmond BW, Du RH, Han W, Benjamin JT, van der Meer R, Gleaves L, et al. Bacterial-derived neutrophilic inflammation drives lung remodeling in a mouse model of chronic obstructive pulmonary disease. *Am J Respir Cell Mol Biol*. (2018) 58:736–44. doi: 10.1165/rcmb.2017-0329OC

9. Gao X, Coull B, Lin X, Vokonas P, Sparrow D, Hou L, et al. Association of Neutrophil to lymphocyte ratio with pulmonary function in a 30-year longitudinal study of US veterans. *JAMA Netw Open*. (2020) 3:e2010350. doi: 10.1001/jamanetworkopen.2020.10350

10. Hosseninia S, Ghobadi H, Garjani K, Hosseini SAH, Aslani MR. Aggregate index of systemic inflammation (AISI) in admission as a reliable predictor of mortality in COPD patients with COVID-19. *BMC Pulm Med*. (2023) 23:107. doi: 10.1186/s12890-023-02397-5

11. Kumar P, Law S, Sriram KB. Evaluation of platelet lymphocyte ratio and 90-day mortality in patients with acute exacerbation of chronic obstructive pulmonary disease. *J Thorac Dis*. (2017) 9:1509–16. doi: 10.21037/jtd.2017.05.77

12. Ling M, Huiyin L, Shanglin C, Haiming L, Zhanyi D, Shuchun W, et al. Relationship between human serum albumin and in-hospital mortality in critical care patients with chronic obstructive pulmonary disease. *Front Med*. (2023) 10:1109910. doi: 10.3389/fmed.2023.1109910

13. Yang L, Zhou M, Smith M, Yang G, Peto R, Wang J, et al. Body mass index and chronic obstructive pulmonary disease-related mortality: a nationally representative prospective study of 220,000 men in China. *Int J Epidemiol*. (2010) 39:1027–36. doi: 10.1093/ije/dyq051

14. Jafri SH, Shi R, Mills G. Advance lung cancer inflammation index (ALI) at diagnosis is a prognostic marker in patients with metastatic non-small cell lung cancer (NSCLC): a retrospective review. *BMC Cancer*. (2013) 13:158. doi: 10.1186/1471-2407-13-158

15. Feng JF, Huang Y, Chen QX. A new inflammation index is useful for patients with esophageal squamous cell carcinoma. *Onco Targets Ther*. (2014) 7:1811–5. doi: 10.2147/ott.S68084

16. Shibutani M, Maeda K, Nagahara H, Fukuoka T, Matsutani S, Kimura K, et al. The prognostic significance of the advanced lung cancer inflammation index in patients with unresectable metastatic colorectal cancer: a retrospective study. *BMC Cancer*. (2019) 19:241. doi: 10.1186/s12885-019-5468-9

17. Topkan E, Mertsoylu H, Ozdemir Y, Sezer A, Kucuk A, Besen AA, et al. Prognostic usefulness of advanced lung cancer inflammation index in locally-advanced pancreatic carcinoma patients treated with radical Chemoradiotherapy. *Cancer Manag Res*. (2019) 11:8807–15. doi: 10.2147/cmar.S222297

18. Chen H, Zhang F, Luo D, Guo J, Lin Y, Chen S, et al. Advanced lung cancer inflammation index predicts the outcomes of patients with non-metastatic gastric cancer after radical surgical resection. *J Gastrointest Oncol*. (2023) 14:85–96. doi: 10.21037/jgo-22-657

19. Yao J, Chen X, Meng F, Cao H, Shu X. Combined influence of nutritional and inflammatory status and depressive symptoms on mortality among US cancer survivors: findings from the NHANES. *Brain Behav Immun*. (2024) 115:109–17. doi: 10.1016/j.bbi.2023.10.002

20. Chen Y, Guan M, Wang R, Wang X. Relationship between advanced lung cancer inflammation index and long-term all-cause, cardiovascular, and cancer mortality among type 2 diabetes mellitus patients: NHANES, 1999-2018. *Front Endocrinol*. (2023) 14:1298345. doi: 10.3389/fendo.2023.1298345

21. Tu J, Wu B, Xiu J, Deng J, Lin S, Lu J, et al. Advanced lung cancer inflammation index is associated with long-term cardiovascular death in hypertensive patients: national health and nutrition examination study, 1999-2018. *Front Physiol*. (2023) 14:1074672. doi: 10.3389/fphys.2023.1074672

22. Vermeeren MA, Creutzberg EC, Schols AM, Postma DS, Pieters WR, Roldaan AC, et al. Prevalence of nutritional depletion in a large out-patient population of patients with COPD. *Respir Med*. (2006) 100:1349–55. doi: 10.1016/j.rmed.2005.11.023

23. Wada H, Ikeda A, Maruyama K, Yamagishi K, Barnes PJ, Tanigawa T, et al. Low BMI and weight loss aggravate COPD mortality in men, findings from a large prospective cohort: the JACC study. *Sci Rep*. (2021) 11:1531. doi: 10.1038/s41598-020-79860-4

24. Don BR, Kaysen G. Serum albumin: relationship to inflammation and nutrition. *Semin Dial*. (2004) 17:432–7. doi: 10.1111/j.0894-0959.2004.17603.x

25. Hogg JC, Timens W. The pathology of chronic obstructive pulmonary disease. *Annu Rev Pathol*. (2009) 4:435–59. doi: 10.1146/annurev.pathol.4.110807.092145

26. Hogg JC. Pathophysiology of airflow limitation in chronic obstructive pulmonary disease. *Lancet*. (2004) 364:709–21. doi: 10.1016/s0140-6736(04)16900-6

27. Guiedem E, Ikomey GM, Nkenfou C, Walter PE, Mesembe M, Chegou NN, et al. Chronic obstructive pulmonary disease (COPD): neutrophils, macrophages and lymphocytes in patients with anterior tuberculosis compared to tobacco related COPD. *BMC Res Notes*. (2018) 11:192. doi: 10.1186/s13104-018-3309-6

28. Grundy S, Plumb J, Lea S, Kaur M, Ray D, Singh D. Down regulation of T cell receptor expression in COPD pulmonary CD8 cells. *PLoS One*. (2013) 8:e71629. doi: 10.1371/journal.pone.0071629

29. Demedts IK, Demoor T, Bracke KR, Joos GF, Brusselle GG. Role of apoptosis in the pathogenesis of COPD and pulmonary emphysema. *Respir Res*. (2006) 7:53. doi: 10.1186/1465-9921-7-53

frontiers | Frontiers in Nutrition

TYPE Original Research
PUBLISHED 30 April 2025
DOI 10.3389/fnut.2025.1545720

OPEN ACCESS

EDITED BY
Francisco José Pérez-Cano,
University of Barcelona, Spain

REVIEWED BY
Yu Fang,
Affiliated Hospital of Guizhou Medical University, China
Jiyu Ju,
Shandong Second Medical University, China
Zongde Zhang,
Southwest Medical University, China

*CORRESPONDENCE
Jian Song
✉ sjjhm@hotmail.com
Tonghua Wang
✉ wangtonghua420@163.com
Lingzhang Meng
✉ m.lingzhang@hotmail.com

†These authors have contributed equally to this work

RECEIVED 15 December 2024
ACCEPTED 07 April 2025
PUBLISHED 30 April 2025

CITATION
Qin Y, Wang X, Zhang X, Nong L, Hou Q, Chen Y, Li Y, Lin W, Mao X, Wu K, Nong W, Wang T, Meng L and Song J (2025) Retinoic acid modulates peritoneal macrophage function and distribution to enhance antibacterial defense during inflammation. *Front. Nutr.* 12:1545720. doi: 10.3389/fnut.2025.1545720

Retinoic acid modulates peritoneal macrophage function and distribution to enhance antibacterial defense during inflammation

Yujuan Qin[1,2†], Xi Wang[2,3†], Xiamin Zhang[1,4†], Lianting Nong[1,2†], Qiyan Hou[2], Yuhong Chen[1,2], Yuting Li[1,2], Wenxian Lin[2], Xiuli Mao[2], Kezhao Wu[2], Wenqian Nong[2], Tonghua Wang[4]*, Lingzhang Meng[1,2]* and Jian Song[1,2,5]*

[1]Graduate School, Youjiang Medical University for Nationalities, Baise, China, [2]Institute of Cardiovascular Sciences, The People's Hospital of Guangxi Zhuang Autonomous Region & Guangxi Academy of Medical Sciences, Nanning, China, [3]School of Medicine, Guangxi University, Nanning, China, [4]Department of Digestive Diseases, Affiliated Hospital of Youjiang Medical University for Nationalities, Baise, China, [5]Institute of Physiological Chemistry and Pathobiochemistry, University of Münster, Münster, Germany

Background: Peritoneal macrophages, comprising large peritoneal macrophages (LPMs) and small peritoneal macrophages (SPMs), play a vital role in maintaining immune defenses during inflammation. However, the molecular mechanisms governing their responses, particularly the impact of retinoic acid (RA), remain poorly understood. This study aims to elucidate the role of RA in modulating macrophage function, distribution, and immune responses during bacterial infections.

Methods: A murine model of peritonitis was established using *Escherichia coli* expressing a tdTomato fluorescence marker. The effects of RA on macrophage phagocytic capacity, population dynamics, and transcriptomic profiles were assessed using immunofluorescence, flow cytometry, RNA sequencing, and quantitative PCR. Additionally, RA-loaded ZIF-8 nanoparticles were employed to investigate the sustained effects of RA delivery.

Results: RA significantly enhanced macrophage phagocytic activity, delayed functional decline, and promoted the recruitment of SPMs in the peritoneal cavity. Transcriptomic analysis revealed upregulation of leukocyte migration and cell adhesion pathways in RA-treated SPMs. RA treatment also induced distinct gene expression profiles in macrophage subpopulations, reflecting its role in immune modulation. Notably, RA-loaded ZIF-8 nanoparticles prolonged RA retention within macrophages, sustaining its effects.

Conclusion: RA enhances antibacterial defense by modulating macrophage activity, providing new insights into immune regulation. These findings underscore the therapeutic potential of RA and its nanoparticle formulations in managing bacterial infections and inflammation.

KEYWORDS

peritonitis, large peritoneal macrophages, small peritoneal macrophages, retinoic acid, nanoparticles

Introduction

Two distinct subpopulations of macrophages have been identified within the peritoneal cavity. The first is a subpopulation of large peritoneal macrophages (LPMs), which have a large morphology and constitute approximately 90% of peritoneal cavity macrophages (1, 2). The majority of macrophages are LPMs, which express high levels of F4/80 but low levels of MHC-II. This classification is based on the expression of cell markers, specifically CD11b, F4/80, MHCII, and GATA6. The remaining subpopulation is that of the smaller macrophages, which occupy approximately 10% of the peritoneal cavity. The remaining subpopulation comprises a smaller macrophage within the peritoneal cavity, representing approximately 10% of the LPMs. This is the small peritoneal macrophage (SPMs). SPMs express low levels of F4/80, but high levels of MHC-II, and their surface markers are $CD11b^{+}/F4/80^{LOW}/MHCII^{+}/GATA6^{-}$ (1). The LPM is currently the more extensively researched of the two, whereas the SPMs remains relatively understudied (1, 3–5).

The transcription factor GATA6 is indispensable for the sustenance of the LPMs community. It preserves the cellular state in a non-autonomous manner and is induced by retinoic acid (RA), which is produced by the metabolism of vitamin A within the peritoneal cavity (6, 7). RA production is dependent on the metabolic enzymes RALDH1 and RALDH2, the activity of which is essential for RA synthesis. The fact that these enzymes are produced by large omental mesothelial cells and mesenchymal fibroblasts in the peritoneal cavity, which express the transcription factor Wilms' tumor 1 (WT1) (8), and retinoic acid induces and reversibly regulates gene expression of GATA6 and other PMSGs in peritoneal macrophages. Chronic deficiency of vitamin A (retinoic acid precursor) leads to decreased expression of GATA6 in LPMs, triggering an inflammatory response and leading to the disappearance of LPMs. RA selectively affects the function and distribution of LPMs by regulating the expression of the transcription factor GATA6, a signature transcription factor of LPMs involved in the regulation of their gene expression profiles and in the maintenance of an anti-inflammatory phenotype (9). In the presence of RA, GATA6 upregulation was able to enhance the resistance of LPMs to infection and promote cell survival. This fact highlights the central role of the peritoneal microenvironment in RA generation and LPMs population maintenance. On the other hand, it is believed that SPMs are generated as macrophages by recruiting monocytes, which are the predominant cells in the peritoneal cavity as they respond to inflammation (5, 10, 11). Nevertheless, the rationale behind the presence of SPMs in the absence of inflammation and the potential role of retinoic acid in the peritoneal microenvironment in SPM recruitment under steady-state conditions remain uncertain Louwe et al. (12).

In the event of peritoneal cavity inflammation, both macrophage types undergo significant alterations, with the LPM disappearing rapidly in response to the inflammatory stimulus (13). This phenomenon is known as the macrophage disappearance reaction (MDR). The MDR is initiated when the LPMs undertakes bacterial containment by aggregating on the surface of the cavity or by aggregating in fibrous clots (14). A considerable number of LPMs undergo pyroptosis following aggregation and die, thereby rendering local proliferation an inadequate means of recovering the same number of LPMs that existed prior to the aggregation (15). In contrast, SPMs proliferate and become the predominant population in the peritoneal cavity during the inflammatory process (11, 12, 16). It is therefore generally accepted that SPMs are recruited and transformed from blood mononuclear cells. However, the transcriptomic, functional and phenotypic profiles of LPMs and SPMs during peritonitis remain unclear. Furthermore, the series of infectious events caused by peritonitis ultimately results in increased omental fibrosis, which in turn leads to the destruction of $WT1^{+}$ mesothelium and mesenchymal fibroblasts, thereby reforming the peritoneal microenvironment conducive to RA production and the LPMs/SPMs compartment. Therefore, it is of clinical relevance to understand the role of RA for LPMs and SPMs in the inflammatory state.

The aim of this study was to investigate the response of peritoneal macrophages to bacterial attack in the presence of RA and changes in their immune defenses. Retinoic acid, a metabolite of vitamin A, has been shown to play a key role in the regulation of several immune functions. However, its specific effects on macrophage population dynamics and function under conditions of abdominal infection are unclear. To this end, we used pUC19-tdtomato to establish a peritonitis model with transduced bacteria and investigated the effects of RA on phagocytosis and on LPMs and SPMs macrophage populations by quantitative analysis and transcriptome sequencing. Our results suggest that RA may alter the distribution and function of macrophages in the peritoneal cavity by regulating their migration-related genes. At the early stage of infection, RA not only enhanced the phagocytic capacity of macrophages, but also significantly delayed the decline of their phagocytic function. In addition, RA-treated macrophages showed up-regulation of key genes GATA6 and RA-responsive genes, which was accompanied by significant changes in the cell migration-related transcriptome. In particular, changes in key genes related to migration function may play an important role in the dynamics of LPMs and SPMs populations. These findings reveal potential mechanisms of RA in regulating the antimicrobial function of abdominal macrophages. These findings provide important insights into the potential clinical applications of RA in infection control and other inflammatory disease therapies, and future studies may further explore the synergistic effects of RA with conventional anti-infective therapies.

Materials and methods

Mice

All C57BL/6J mice were obtained from the Guangxi Medical University Laboratory Animal Centre, and the animals were housed in the laboratory animal center under specific pathogen-free conditions, with feed and sterile water provided for the animals. The animals were kept using a 12 h light/12 h dark cycle.

Peritonitis model and *E. coli*, RA injection

The experimental design included three different treatment groups to study the dynamic effects of RA and bacterial challenge on peritoneal macrophages:

Bacteria-only group

Mice were injected intraperitoneally with an *Escherichia coli* ER2272 strain harboring the pUC19-tdTomato construct (cultured overnight in LB at 37°C and then resuspended in 0.2 mL PBS to yield 1×10^{7} CFU).

Samples were collected at 30 min, 60 min, and 4 h post-injection to assess baseline kinetics of bacterial uptake and macrophage response.

Only the RA group was injected

Mice were injected intraperitoneally with 200 μL of RA solution (10 μmol/mL). In this group, samples were also collected at 30 min, 60 min, and 4 h post-injection to assess the immediate distribution of RA in the peritoneal cavity and cellular uptake.

RA pretreatment with bacteria group

In another set of experiments, mice were injected once intraperitoneally with RA (200 μL, 10 μmol/mL) 24 h before bacterial challenge. 24 h later, these mice were injected with 1×10^7 CFU *E. coli* Tdtomato in 0.2 mL of PBS. Subsequent samples were taken at the indicated time points for transcriptome sequencing.

Immunofluorescence

The peritoneal mesothelium and greater omentum were excised and immediately embedded in Tissue-Tek O.C.T. compounds (Triangle Biomedical Sciences) and frozen in liquid nitrogen. They were then processed into 15-μm-thick sections. Following fixation in methanol at −20°C for 5 min, the frozen sections were rinsed on three occasions with PBS. Following a 40 min sealing process with PBS/1% BSA at room temperature, the sections were incubated with the antibody at a dilution of 1:1,000 at 4°C overnight. The images were captured using a ZEISS Axiovert 5 microscope.

Flow cytometry

The peritoneal cavity was repeatedly flushed with 5 mL of ice-cold RPMI 1640 basal medium and cells were collected from the peritoneal exudate. Erythrocytes were lysed for antibody staining. All antibodies were incubated with the cells on ice at a 1:200 dilution for 15 min, then washed, resuspended, and analysis on a FACSC anto II (BD Biosciences) using FlowJo software.

Real-time PCR

Peritoneal macrophages were extracted from the peritoneal cavity of mice. After 24 h of adhesion of macrophages to petri dish in complete medium containing 30% FBS, the macrophages were purified by washing away the non-adhesive cells and cultivated in serum-free basal medium supplemented with different drugs. For real-time PCR analysis, RNA was extracted using the TaKaRa RNAiso Plus kit. cDNA was reverse transcribed using Novozymes HiScript IV RT SuperMix for qPCR. Real-time PCR was performed on a QuantStudio5 detection system using SYBR green qPCR Master Mix (Table 1).

TABLE 1 Primers sequence.

Gene	Forward primer	Reverse primer
Apoc2	ctcggttcttcctggctctat	catgctgatcgggtatgtctt
Arg1	atggaagagtcagtgtggtgctg	tcaggagaaaggacacaggttgc
Cd62p	gaacctttgggtacaacagca	ttactgggaaccggaaactct
Cd73	agaaagttcgaggtgtggacat	cttcaggtagcccaggtatttg
Fn1	caagccacagtttctgatattcc	tctgctcctggtttaatgttgtt
Gata6	accatcaccatcacccgacctac	ctctccgacaggtcctccaacag
Icam2	acagctctgaaaaaggacggtct	gcagtattgacaccaccacgatg
Lrg1	agctatggtctcttggcagcatc	aattccaccgacagatggacagt
Rarb	acatgatctacacttgccatcg	tgaaggctccttctttttcttg
Serpinb2	gtgctgaagaagctagggaaaa	gttcacacggaaaggataaagc
Tgfb2	gtctcaacaatggagaaaaatgc	ctggttttcacaaccttgctatc
Thbs1	ggagatggaatcctcaatgaac	aagtgtcccctatgaggtctga
Cd49f	ctgaattcaaatgaagccaaaac	gactaattctgggatgccttttt

Sorting peritoneal macrophages for RNAseq

To compared the effect of 24 h RA treatment on the SPMs and LPMs, we separated the mice into two groups: control and RA treatment. Upon the injection of bacteria containing pUC19-tdTomato, both SPMs and LPMs in the peritoneal cavity can be detected based on the antibody staining and phagocytosis of *E. coli*. SPMs and LPMs from the respective group were isolated from the peritoneal cavity using flow cytometry sorting. Total RNA was extracted from cell pellets using Trizol reagent according to the manufacturer's protocol. The library was constructed using SMART-Seq_V4 Ultra Low Input RNA Kit for Sequencing. High-throughput RNA sequencing was performed using the Illumina NovaSeq Xplus platform, the raw data of which have been uploaded to GEO database.

Bioinformatics analysis

Reference genome and gene model annotation files were directly downloaded from http://ftp.ensembl.org/pub/release-77/gtf/mus_musculus/. The index of the reference genome was built using Bowtie v2.2.3 and paired-end clean reads were aligned to the reference genome using STAR software. The alignment was converted to gene expression raw counts using feature counts and listed as a gene expression matrix, which can be included in the Supplementary data (on request). Prior to differential gene expression analysis, for each sequenced library, the read counts were adjusted by the edge R program package through one scaling normalized factor. Differential expression analysis of two conditions was performed using the DEG Seq R package (1.20.0). GSEA scoring of leukocyte migration was based on the hallmarker gene signature from GO database.

ZIF-8 nanoparticles loaded with RA

Anhydrous ethanol was employed to solubilize 1 mg/mL ZIF-8 nanoparticles and RA individually, and the two were ultimately combined and loaded into the ZIF-8 Nanoparticles at 4°C. The loading amount of nanoparticles was tested for fluorescence intensity using a Thermo Fischer Multiscan Go Reader microplate reader under Alexa Fluor 488.

Statistical analyses

One-way ANOVA and student *t test* were employed for the statistical analyses respectively, with a significance level of $p < 0.05$. The results of all replicate experiments are presented, with values expressed as Mean ± SEM.

Results

In flow cytometry analysis of peritoneal lavage fluid, different peritoneal cell populations were differentiated not only on the basis of their size (SSC), but also on the basis of their expression levels of CD11b and F4/80. These included: peripheral blood-derived monocytes, LPMs, and SPMs (Figure 1A). Large peritoneal macrophages and small peritoneal macrophages were subsequently subdivided on the basis of their expression of Ly6c and MHC II. LPMs were characterized by high expression of F4/80 and low expression of Ly6c, whereas SPMs were characterized by high expression of Ly6c and MHC II (Figure 1B).

To study the impact of RA on the peritoneal macrophages during inflammation, a peritonitis model was established by using the *E. coli* Tdtomato strain. C57BL/6 mice were injected intraperitoneally with 1×10^7 CFU of the *E. coli* Tdtomato strain. The peritoneal mesothelium and the greater omentum were observed to detect the aggregation of bacterial phagocytosis at 60 min post-injection. Also, we photographed the peritoneal mesothelium and the greater omentum after injections of Alexa Fluor 488 labeled RA. The results showed that RA was distributed around the macrophage aggregates in the mesothelium (Figure 2A) and the greater omentum (Figure 2B). After further injection of *E. coli*, clustering of RA, *E. coli* Tdtomato and F4/80 staining was observed in the aggregates, suggesting that RA may influence the local immune response by regulating macrophage migration and aggregation. Notably, cells phagocytosing high concentrations of RA did not completely overlap with cells phagocytosing large amounts of *E. coli*.

To gain further insight into the impact of retinoic acid on peritoneal macrophages in the context of *E. coli* infection, a flow cytometry analysis was conducted based on two treatment groups: one group injected with only *E. coli*, and the other group injected with RA. The majority of F4/80+ macrophages were observed to phagocytose *E. coli* within 30 min. By 60 min, the number of F4/80+ macrophages that had phagocytosed bacteria had decreased substantially, with the majority of these cells disappearing by fourth (Figure 3A). However, the RA group was injected and demonstrated the ability to persist at the fourth hour (Figure 3C), indicating that macrophages phagocytosing RA are more stable in mice compared to macrophages phagocytosing bacteria. This indicates that RA is not rapidly metabolized or cleared. In particular, by the fourth hour, there was a notable decrease in cellular phagocytosis, which may have been attributed to a macrophage disappearance response to the substantial early depletion of macrophages. It was evident that retinoic acid reached its peak effect on macrophage activity at 60 min, after which a decline was observed (Figure 3D). This indicates that retinoic acid exerts a considerable influence on macrophage phagocytosis during the initial stages, although this impact may diminish over time. Additionally, we investigated the impact of RA on bacterial uptake by macrophages. The bacteria were injected 24 h after the administration of RA, and an increase in SPMs of F4/80 cells and a decrease in LPMs of F4/80 cells were observed (Figure 3B). This indicates that the recruitment or activation of macrophages may have been enhanced following RA treatment, resulting in an increased number of macrophages or a greater proportion of specific subpopulations within 24 h (Figure 3A).

To elucidate the mechanism of retinoic acid action in macrophages of different origin, we performed quantitative polymerase chain reaction (qPCR) analysis of key gene expression in peritoneal macrophages (Figure 4A) and bone marrow-derived macrophages (BMDM, Figure 4B) under different treatment conditions. The aim of this experiment was to investigate the regulatory effects of RA on macrophage gene expression and the potential synergistic effects of intraperitoneal lavage fluid as an additional signaling source. The peritoneal macrophages were initially treated with RA and the peritoneal lavage, which served as an additional source of signals. The peritoneal lavage was prepared in a serum-free medium devoid of any vitamin A metabolite. This resulted in a notable induction of Arg1, Fn1, Gata6, and Rarb by RA, while the expression of CD49f, Icam2, Tgfb2, Lrg1, and serpinb2 was all found to be down-regulated. The observed alterations in gene expression suggest that RA may regulate macrophage activity and function by influencing cell adhesion, fibronectin production, intercellular signaling, and other biological pathways. In the peritoneal lavage-treated group, a trend of

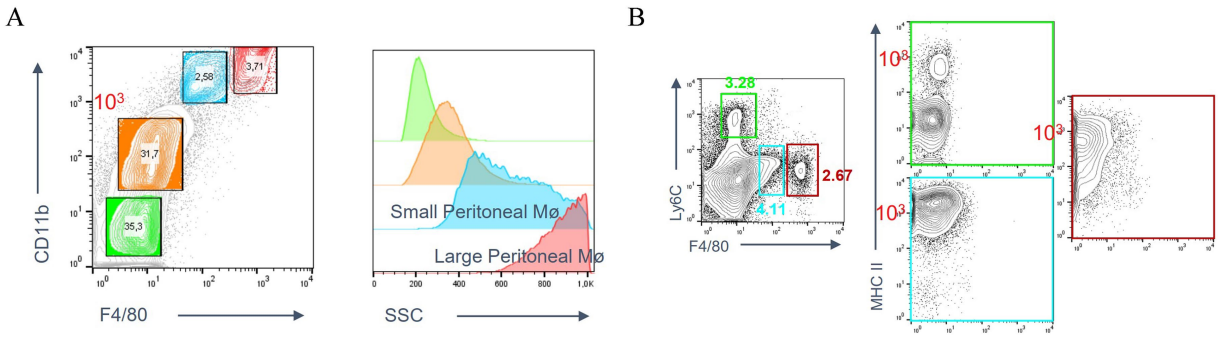

FIGURE 1
Peritoneal macrophage subpopulations. **(A)** Definition of LPMs and SPMs populations based on the expression of CD11b and F4/80 using flow cytometry. **(B)** Expression of by Ly6c and MHC II on LPMs and SPMs.

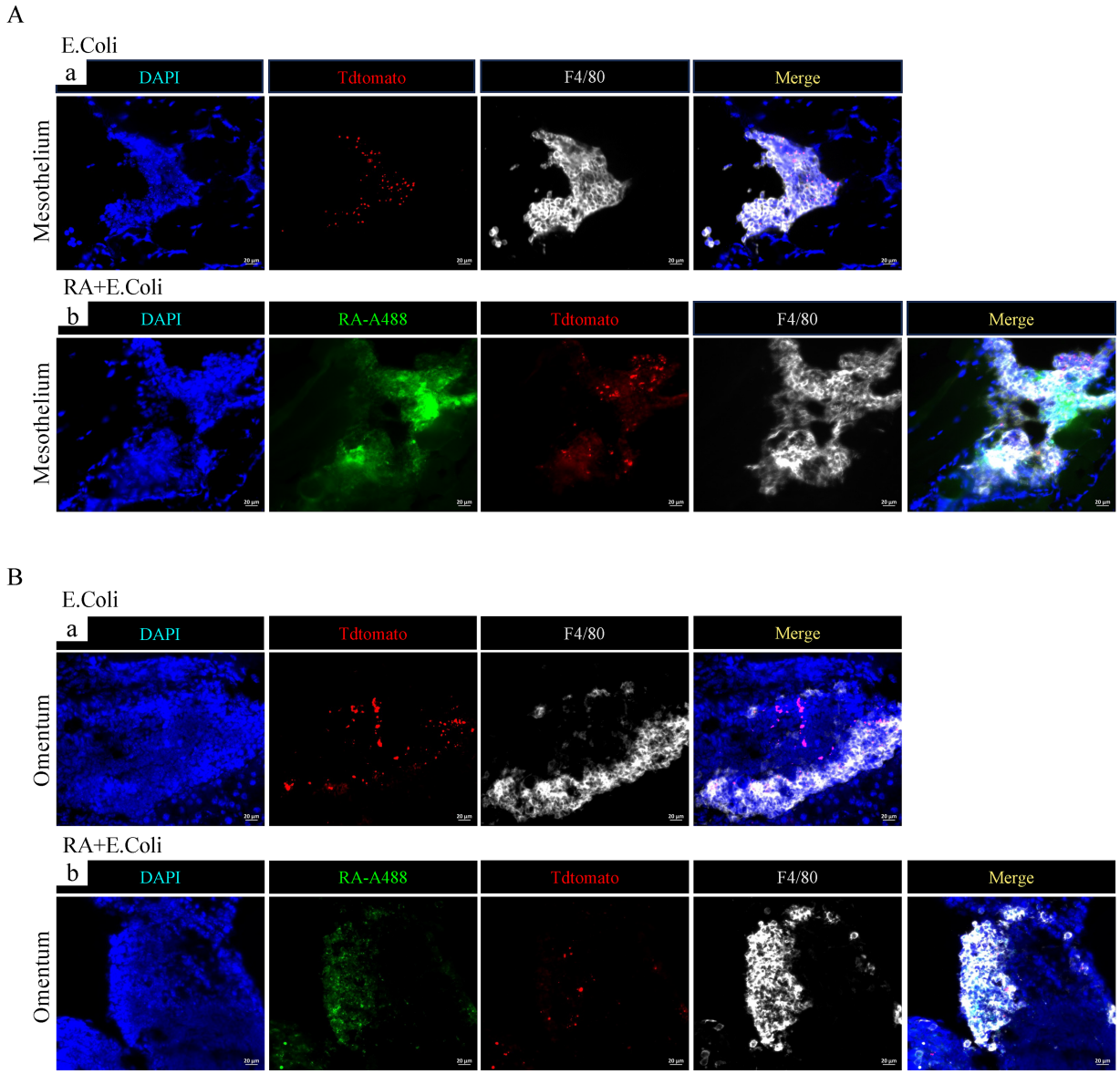

FIGURE 2
Immunofluorescence analysis of phagocytosis of RA and *E. coli* as well as the aggregates of macrophages on the peritoneal mesothelium and the greater omentum. **(A)** Immunofluorescence images of peritoneal mesothelial tissue showing the distribution of F4/80 staining (white), RA (green) and *E. coli* Tdtomato (red). **(B)** Immunofluorescence images of the greater omentum with F4/80 staining, RA and *E. coli* Tdtomato.

up-regulation was observed for Apoc2, Thbs1, Arg1, Cd62p, Tgfb2, and Thbs1. In the peritoneal lavage plus RA-treated group, Apoc2, Cd62p, Arg1, Lrg1, Rarb, and Thbs1 were found to be up-regulated, indicating that the components in the peritoneal lavage may have a coordinating effect, thereby further enhancing the expression of these genes (Figure 4A).

The same cultivation condition were employed to treat bone marrow-derived macrophages, and it was determined that Apoc2, Arg1, Cd62p, Cd73, Rarb, and Thbs1 were induced by RA. In the peritoneal lavage -treated group, an increase in the expression of Apoc2, Arg1, Cd62p, Cd73, Cd49f, Tgfb2, Thbs1, and Rarb was observed, indicating that the components in the peritoneal lavage may have a promotional effect on the expression of these genes in the BMDM (Figure 4B). The different effects of RA on peritoneal macrophages and BMDM may be related to their different origins and differentiation characteristics. LPMs, as peritoneal resident cells, may be more responsive to changes in local signaling molecules, whereas BMDM, due to their origin from myeloid cells, may be sensitive to systemic metabolic signals. These results further highlight the potential role of RA in regulating the function of different macrophage subpopulations.

In this study, SPMs and LPMs from the peritoneal cavity of mice were categorized after RA treatment, and RNA sequencing was performed 24 h post-RA treatment to decipher their genome-wide expression. Prior evidence pointed to a varied set of DEGs between SPM and LPMs concerning gene expression, thereby permitting the annotation of selective traits of either SPMs or LPMs genes. The aim of this study was to see if RA influences SPMs and LPMs functional

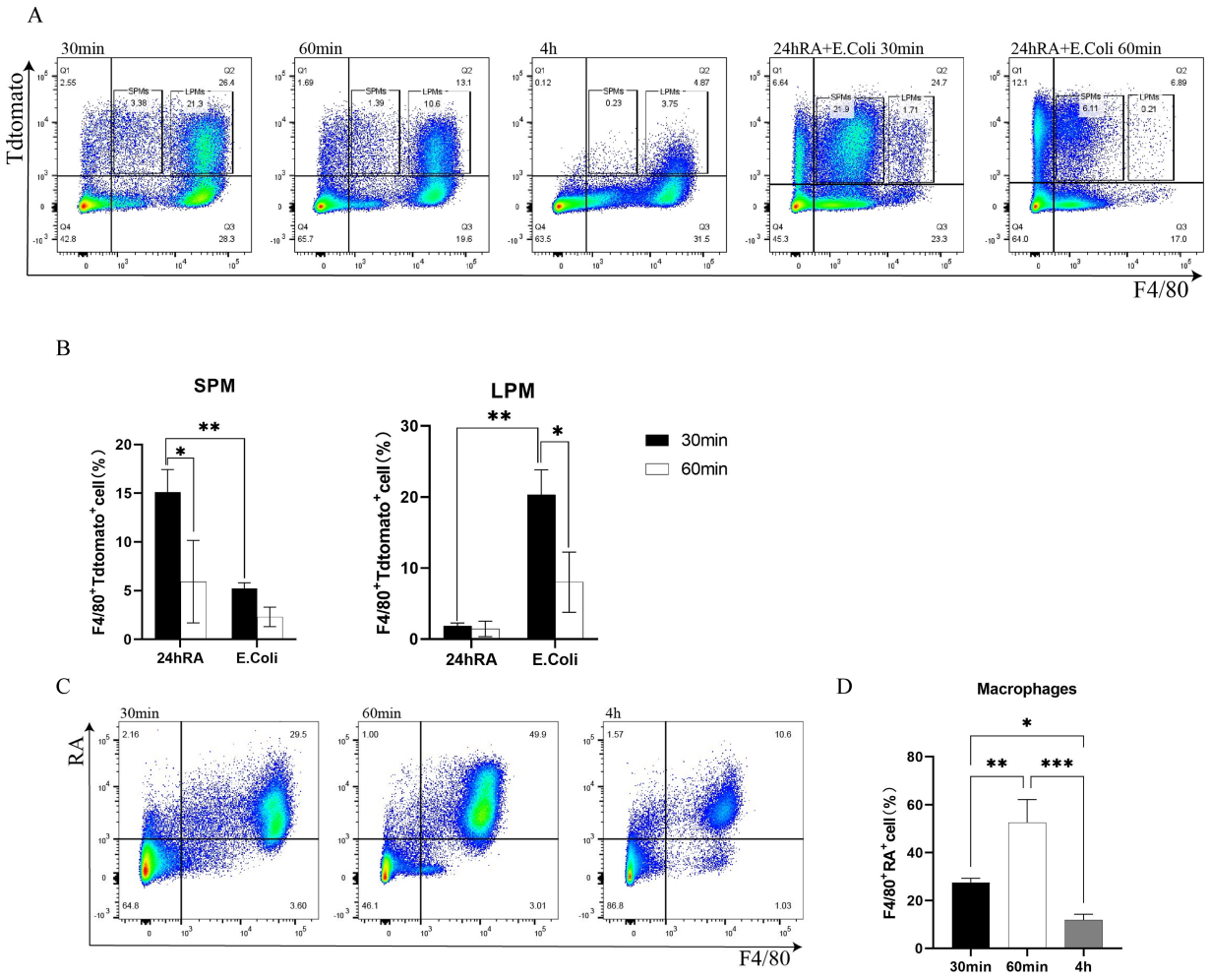

FIGURE 3
Flow cytometric analysis of macrophage phagocytosis of bacteria, RA uptake, and the effect of RA on phagocytosis of bacteria. **(A)** Phagocytosis of SPMs by macrophages in the peritoneal cavity of *Escherichia coli* and after 24 h of RA injection (24 h of RA pretreated group was not sampled after 4 h). **(B)** The ability of macrophages to phagocytose SPMs and LPMs bacteria was calculated separately 24 h after RA injection. Bars are expressed as mean ± SEM (n = 6) and significant differences were tested by t-test. **(C)** Phagocytosis of RA by peritoneal macrophages. **(D)** Quantitative determination of bacterial phagocytosis by macrophages after RA injection. Bar graphs are expressed as mean ± SEM (n = 6) and significant differences were calculated using one-way ANOVA.

activity via the modification of these engaged gene signatures. Post RNA sequencing analysis denoted that SPMs of the treated group maintained higher expression of "SPMs" gene signatures, while LPMs lost their expression of distinctive "LPMs" genes when treated with RA (Figures 5A,B). This indicates that RA seems to have a regulatory effect on the transcriptome which clearly differs between SPM and LPMs. In order to further characterize RA functional effects on SPMs and LPMs, GO analysis was performed. Contrarily, when compared to untreated LPMs, RA-untreated SPMs significantly express GO functions connected to cell migration and adhesion, such as actin-binding, actin filament binding, small GTPase binding, and integrin binding (Figure 5C). The SPMs-associated cell migration functions were effectively enhanced in the RA treated group; in contrast, no significant upregulation was seen within treated LPMs. This suggests RA might drive SPMs distribution and expansion by encouraging cell migration (Figure 5D). GSEA was therefore performed on metadata of leukocyte-targeted migration genes in RA-treated SPMs blood to test this hypothesis. Analysis of the genes showed that SPMs from the RA-treated group had significant enrichment of leukocyte-targeted migration genes when compared to the untreated SPMs (Figures 5E,F). Probably, such functional differences cannot be linked to the ability of macrophages to phagocytize bacteria and might explain rather the changed distribution of SPMs and their expansion under RA conditions. KEGG results showed (Supplementary Figure 2A) that DEGs were mainly involved in Efferocytosis, cytokine–cytokine receptor interaction, Rap1 signaling pathway, Phagosome, NOD−like receptor signaling pathway. In closing, these data suggest that RA has a profound effect on the differentiation genes and functional state characteristics of SPM and LPM by regulating cell migration and adhesion-related genes. To confirm the involvement of SPM, peritoneal macrophages from mice injected with *E. coli* were analyzed for CD44 and CCR2 flow 24 h after RA pretreatment; CD44 was expressed at a high level up to 30 min before the peak time point, followed by a steady decline. In contrast, there were no significant changes in the control (blank) and RA alone treated groups (Supplementary Figure 2B). CCR2 was not significantly different between the two groups. This

10.3389/fnut.2025.1545720

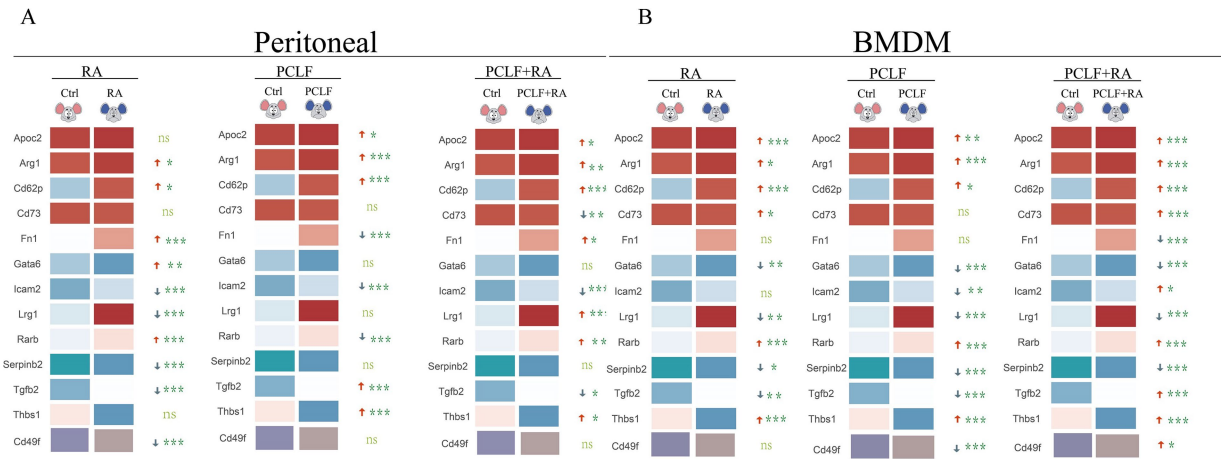

FIGURE 4
Distinct profiles of RA-response genes in peritoneal macrophages and BMDM. **(A)** In peritoneal macrophages, RA treatment significantly up-regulated the expression of Fn1, Gata6, Arg1, and Rarb (*$p < 0.05$). **(B)** In BMDM, RA treatment resulted in the up-regulation of the expression of the indicated genes. However, the trend observed for Rarb and Thbs1 differed from that seen in peritoneal macrophages. All data were subjected to one-way ANOVA for significance analysis, with $n = 6$ for each repeated experiment.

suggests that CD44 expression in macrophages increased at 60 min post-infection after 24 h of RA pretreatment, indicating that RA treatment enhanced the time-dependent expression of adhesion molecules on the macrophage surface.

To improve the sustained loading capacity of retinoic acids in macrophages, we designed a drug-loading system based on ZIF-8 nanoparticles (Figure 6A). ZIF-8 is a stabilized metal–organic framework (MOF) that is widely used in delivery systems for its good biocompatibility and drug-loading capacity (Supplementary Figure 2C). In this study, we loaded RA into ZIF-8 with the aim of prolonging its retention time in macrophages and thus overcoming the limitation of rapid metabolism of RA injected alone (Supplementary Figure 2D). We first verified the phagocytosis of ZIF-8 loaded with RA by peritoneal macrophages through *in vitro* experiments (Figure 6B). The results showed that macrophages were able to effectively phagocytose RA-loaded ZIF-8, and the nanoparticles were uniformly distributed in macrophages. Subsequently, we injected RA-loaded ZIF-8 into the abdominal cavity of mice. *In vivo* experiments showed that RA nanoparticles were still stably present in macrophages 4 h after injection, and the proportion of RA-loaded F4/80-positive macrophages was significantly increased compared with that of RA alone. More importantly, a small residue of RA nanoparticles was still detected in F4/80-positive macrophages 8 h after injection (Figure 6C). This result suggests that RA-loaded ZIF-8 nanoparticles significantly prolonged the presence of RA in macrophages compared with the rapid metabolism or clearance of RA injected alone. In conclusion, this study demonstrates the potential of a ZIF-8-based nanoparticle delivery system in prolonging the duration of RA within macrophages. This strategy provides new ideas for the application of RA in inflammation regulation and lays the foundation for future studies on the role of nanoparticle delivery systems in immunotherapy.

Discussion

Retinoic acid, a known immunomodulator, has been demonstrated to regulate the expression and function of macrophages, playing an integral role in the immune response (6, 7, 17). In this study, we demonstrated the pivotal role of RA in LPMs and *E. coli* infection through the use of immunofluorescence, flow cytometry, and qPCR. It was observed that RA was predominantly distributed in mesothelial and omental tissues and surrounded by F4/80-positive macrophages following the injection of RA (7, 18, 19). This suggests that RA may modulate its antimicrobial capacity by affecting the distribution and function of macrophages in the peritoneal cavity. Furthermore, a 24 h RA injection treatment resulted in a significant prolongation of macrophage phagocytic activity of bacteria, indicating that RA treatment has facilitated bacterial clearance by enhancing the early phagocytic response and rapidly activating macrophage-associated gene expression. In peritoneal macrophages treated with RA, the expression of genes such as Apoc2, Arg1, Cd62p, Lrg1, Rarb, and Thbs1 was highly upregulated. The respective change in expression from these genes would further strengthen the supposed important function of the RA pathway in regard to macrophage metabolism and anti-inflammatory functions (5, 20). In addition, the transcriptome profiles from systematic analysis showed that RA treatment greatly increased the expression of SPMs-identifying genes and was also related to leukocyte migration underlining the importance that RA probably holds in stimulating abdominal immune defense responses through the recruitment of SPMs. With these collective insights, the present major findings uncover how significantly RA controlled phagocytosis by macrophages and altered their numbers and distribution within the peritoneal cavity. Such findings not only broaden the horizon of the understanding of the mechanism of the importance of RA in immunomodulation but also pave the way for new insights and scientific bases for the therapeutic potential of RA in controlling infection.

In the initial stages of bacterial invasion, LPMs rapidly accumulate at the site of infection and eliminate invading pathogens through phagocytosis. However, they are eliminated from the peritoneal fluid when the peritoneum is inflamed (11, 12, 16). Unfortunately, LPMs, while not directly linked to apoptosis, is able to migrate to injured tissues and establish binding interactions. In this aseptic liver injury model, such LPMs migrates

10.3389/fnut.2025.1545720

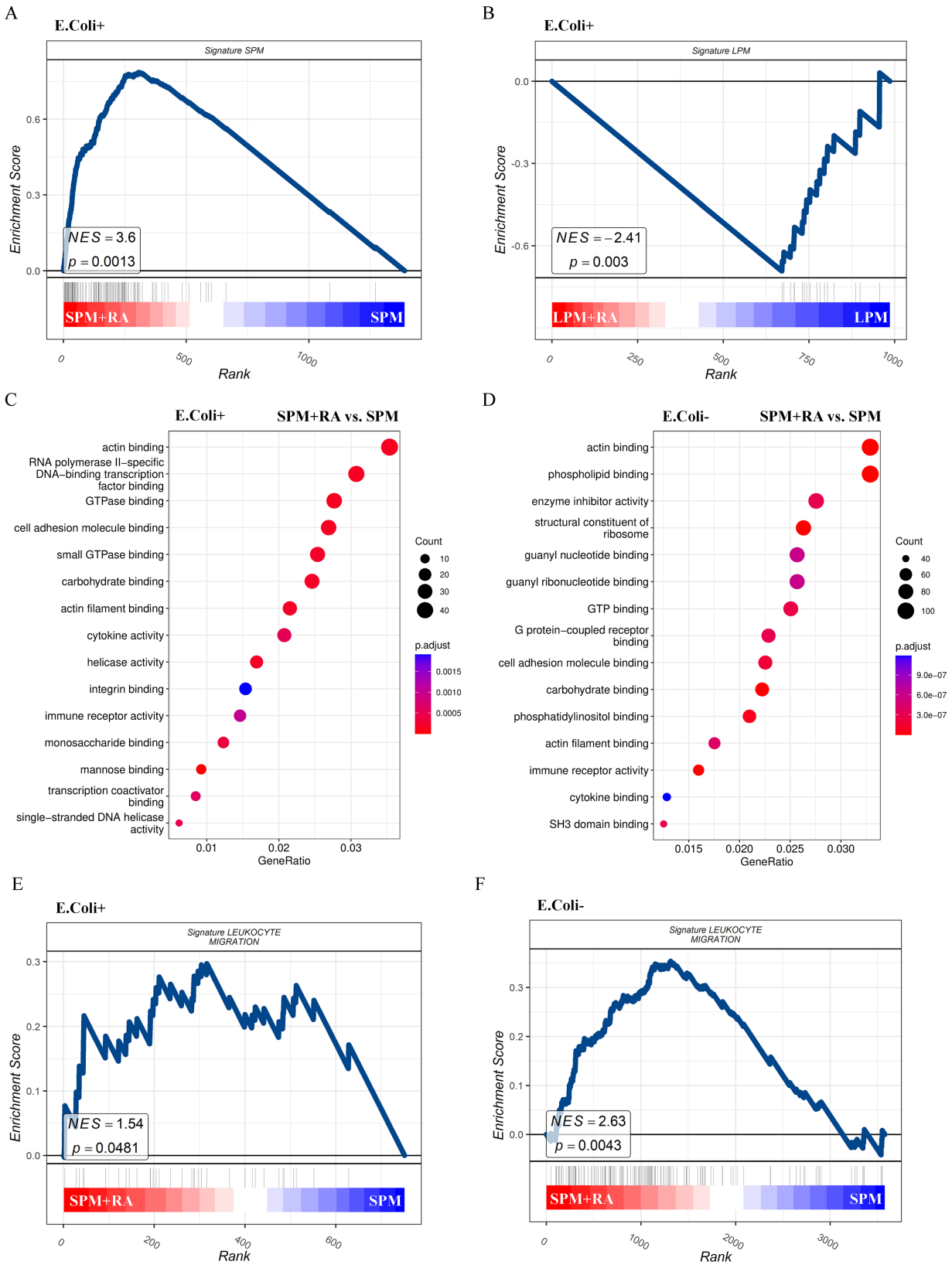

FIGURE 5
RA treatments promote the expression of genes of SPM signature as well as genes relevant to leukocyte migration. Gene set enrichment analysis (GSEA) visualization of gene signatures of SPM in the *E. coli* phagocytosing SPMs **(A)** and LPMs **(B)** treated with or without RA. GO enrichment analysis in the *E. coli* phagocytosing **(C)** or free **(D)** SPMs treated with vs. without RA. GSEA visualization of gene signatures of leukocyte migration in the *E. coli* phagocytosing **(E)** or free **(F)** SPMs treated with or without RA.

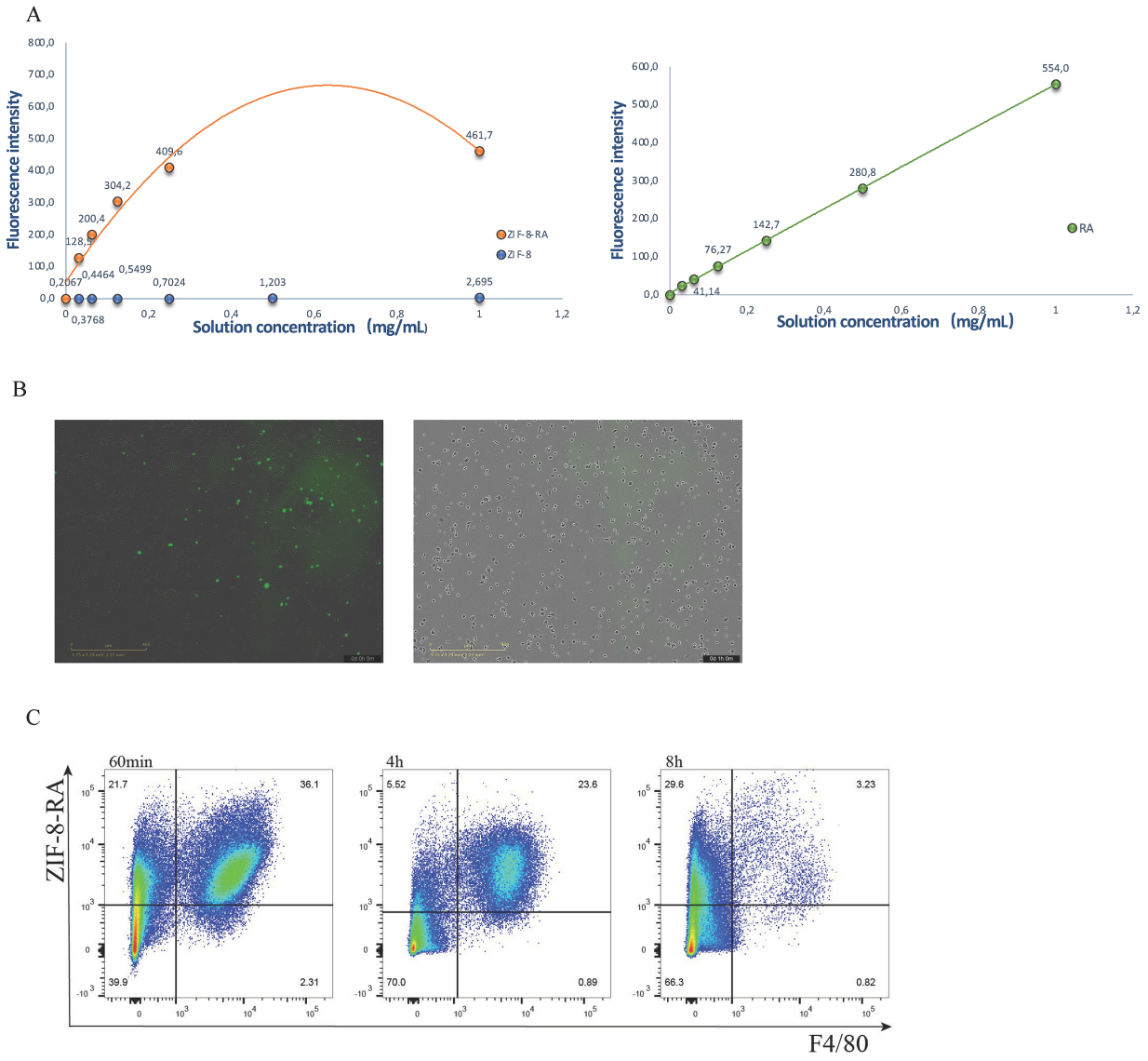

FIGURE 6
Nanoparticles improved the persistence of RA. **(A)** Fluorescence intensity analysis of ZIF-8 nanoparticles loaded with RA. **(B)** Microscopic imaging of RA-loaded ZIF-8 nanoparticles phagocytosed by peritoneal macrophages (left) and empty ZIF-8 (right) in vitro. **(C)** Time course of peritoneal macrophages that uptake ZIF-8 nanoparticles loaded with RA.

to the area of injury, controlling whether the necrotic tissue is bound and thus enhancing the preferred clearance processes. LPMs is one of the mechanisms of defense employed against infection, yet these *E. coli* models or systems in which heparin was injected resulted in increased peritoneal cavity bacterial load in mice (13), with corresponding increases in mortality. Thus, this suggests what could be of potential use in infection management given the fact that there is possible retention or restoration of LPMs function. There is increased resistance to infections with LPMs linked to RA treatment. RA can extend the time for LPMs to remain in peritoneal fluid by modulating their distribution and activity in the early phases of infection and by boosting their phagocytosis and antimicrobial functions. This gives a solid theoretical background for the anticipatory employment of RA in the management and control of inflammatory diseases and infections.

It is proposed that RA may facilitate bacterial clearance by enhancing the early phagocytic response and rapidly activating macrophage-associated gene expression. The modulation of macrophage phagocytosis by RA is consistent with existing literature findings that RA enhances macrophage recognition and clearance of pathogens by regulating the expression of phagocytosis-related genes in the immune response (21). In the RA-treated group of peritoneal macrophages, the upregulation of Arg1 may be associated with the shift of macrophages to an anti-inflammatory phenotype, as evidenced by previous research (22). Furthermore, the up-regulation of Rarb suggests positive feedback regulation of the RA signaling pathway, as observed in other studies (17). In addition, RA has selective effects on small peritoneal macrophages populations. During the early stages of the peritonitis response, when the classical macrophage disappearance response (MDR) leads to LPM depletion, SPMs are recruited to engage in phagocytosis and thus play a key role in maintenance of the

peritoneal inflammatory response. Our study further revealed that increased recruitment of SPMs was associated with significant up-regulation of their characterized genes and showed high scores of leukocyte migration related genes by genomic enrichment analysis (GSEA). Among the KEGG pathways it was shown that in Efferocytosis signaling pathway was the most significantly enriched pathway, mainly associated with genes such as Arg1, Mfge8, Alox15, Cx3cr1, etc. Efferocytosis is a process by which macrophages or other macrophage cells remove apoptotic cells by recognizing and removing them, and it is a key mechanism for maintaining tissue homeostasis and immune balance. Apoptotic cells activate the Efferocytosis pathway by releasing inflammatory factors, which can promote M2 macrophage polarization to inhibit the inflammatory response and achieve efficient, anti-inflammatory clearance. Unlike ordinary phagocytosis, it is highly specific and relies on chemokines such as CXCL1 (binding receptor CX3CR1) to attract macrophages to migrate to the vicinity of apoptotic cells to promote phagocytosis initiation (23, 24). This suggests that RA not only plays an important role in enhancing macrophage phagocytosis, but may also modulate peritoneal inflammatory responses by promoting recruitment and functional enhancement of SPMs. In our flow cytometry, we showed an increase in CD44 expression in early macrophages 24 h after RA pretreatment; however, this appeared to be a transient effect. This suggests that RA could act in an immunomodulatory manner to promote the adhesion and migration of macrophages in early infection phases through the CD44 pathway. The majority of CCR2 expression changes were limited, indicating that RA-escorting macrophage modulation was, temporally speaking, mainly dependent on the CD44 pathway. In conclusion, these findings clarify the final mechanism of RA in the modifications of macrophage functioning and outline the temporal features etiological to the pharmacological effects. With corroboration from long-term observational studies, more data from RA would further increase macrophages' functional status in a more sustained manner.

It was observed that in macrophages treated with RA-loaded ZIF-8 nanoparticles, the nanoparticles were still retained by F4/80-positive cells after 8 h. This is correlated with the feature of ZIF-8 with adjustable sustained release of loaded drugs (25). More interestingly, this prolongation suggests that the nanoparticles not only increased the retention time of RA *in vivo* but may also have altered the dynamic distribution and function of macrophages, which provides new clues for an in-depth study of the role of nanocarriers in immunomodulation.

In conclusion, our data provide a more in-depth theoretical basis for understanding the regulatory role of RA in infection and inflammation, as well as new ideas for developing therapeutic strategies targeting RA. However, it should be noted that this study has certain limitations, On the whole such limitations do not interfere with the scientific value of this study; instead, they should provide a precise path for the improvement of future studies and move the application of RA forward within infection control and immunotherapy. RA has very relevant effects in the regulation of peritoneal macrophage function, and the RA delivery system demonstrated is a promising candidate for prolonging the bioavailability of the active drug. To cite some possible limitations: The investigations performed used a single animal model of peritonitis and an *in vitro* macrophage culture system which somehow do not allow a full representation of the varied pathological mechanisms behind human peritonitis. This study has been quite limited in the evaluation of the respective effect of RA over the long run in regulating innate immune responses during various stages of inflammation, as well as the control spanning over limited time intervals (60 min, 4 h, and 24 h). Besides, the specific distinction of LPMs from SPMs has not yet been finely analyzed nor have we independently assessed the expression of genes representing LPMs and SPMs in qPCR: this will affect our understanding of specific RA regulatory roles across different macro-phage subpopulations. In our ZIF-8 nano-delivery system, retention studies on a longer duration for RA in macrophages have not been performed, and still, we are under an open question about the stability of nanoparticles in complex vivo environments. Future studies are expected to fully optimize the nanoparticle-loaded drug regimen and to evaluate the scope of that treatment in other infection, or inflammation models. After taking into account those limitations, we aim to perform dynamic sequencing on multiple models/time points for single-cell monitoring. We shall further see the in-depth system to realize RA-modulated different macrophage subpopulation modes during peritonitis and allergenic strife. Also, this would further bolster robust nanocarrier delivery systems, and enhance the stability and clinical prospect of RA.

Data availability statement

The datasets presented in this study can be found in online repositories. The names of the repository/repositories and accession number(s) can be found in the article/Supplementary material.

Ethics statement

The animal study was approved by the Animal Ethics Committee of Guangxi Academy of Medical Sciences. The study was conducted in accordance with the local legislation and institutional requirements.

Author contributions

YQ: Investigation, Writing – original draft, Writing – review & editing. XW: Investigation, Writing – original draft, Writing – review & editing. XZ: Investigation, Writing – original draft, Writing – review & editing. LN: Investigation, Writing – original draft, Writing – review & editing. QH: Investigation, Writing – original draft, Writing – review & editing. YC: Investigation, Writing – original draft, Writing – review & editing. YL: Investigation, Writing – original draft, Writing – review & editing. WL: Investigation, Writing – original draft, Writing – review & editing. XM: Investigation, Writing – original draft, Writing – review & editing. KW: Investigation, Writing – original draft, Writing – review & editing. WN: Writing – original draft, Writing – review & editing, Conceptualization, Methodology. TW: Conceptualization, Writing – original draft, Writing – review & editing, Project administration. LM: Conceptualization, Project administration, Writing – original draft, Writing – review & editing, Resources. JS: Conceptualization, Project administration, Resources, Writing – original draft, Writing – review & editing, Data curation, Formal analysis, Funding acquisition, Investigation, Methodology, Software, Supervision, Validation, Visualization.

Funding

The author(s) declare that financial support was received for the research and/or publication of this article. This study would not be possible with the funding from National Natural Science Foundation of China (32360176) and Natural Science Foundation of Guangxi Zhuang Autonomous Region (2023GXNSFAA026241).

Conflict of interest

The authors declare that the research was conducted in the absence of any commercial or financial relationships that could be construed as a potential conflict of interest.

Generative AI statement

The authors declare that no Gen AI was used in the creation of this manuscript.

Publisher's note

All claims expressed in this article are solely those of the authors and do not necessarily represent those of their affiliated organizations, or those of the publisher, the editors and the reviewers. Any product that may be evaluated in this article, or claim that may be made by its manufacturer, is not guaranteed or endorsed by the publisher.

Supplementary material

The Supplementary material for this article can be found online at: https://www.frontiersin.org/articles/10.3389/fnut.2025.1545720/full#supplementary-material

SUPPLEMENTARY FIGURE 1
Immunofluorescence analysis of phagocytosis of RA and *E. coli* and macrophage aggregation on peritoneal mesothelium and greater omentum at different scales. **(A)** Immunofluorescence images of peritoneal mesothelial tissue showing the distribution of F4/80 staining (white), RA (green) and *E. coli* Tdtomato (red). **(B)** Immunofluorescence images of the greater omentum with F4/80 staining, RA and *E. coli* Tdtomato.

SUPPLEMENTARY FIGURE 2
(A) KEGG pathway enrichment analysis of LPM and SPM after RA treatment. **(B)** FACS analysis of CCR2 and CD44 expression in mice after intraperitoneal RA treatment. **(C)** Morphology of ZIF-8 under transmission electron microscope. **(D)** High performance liquid chromatography showed that ZIF-8 was loaded with retinoic acid, and ZIF-8 particles successfully encapsulated retinoic acid in 8 min, and the separation effect was well.

SUPPLEMENTARY FIGURE 3
Integrated technical workflow for RA-related macrophage study.

References

1. Ghosn EE, Cassado AA, Govoni GR, Fukuhara T, Yang Y, Monack DM, et al. Two physically, functionally, and developmentally distinct peritoneal macrophage subsets. *Proc Natl Acad Sci USA*. (2010) 107:2568–73. doi: 10.1073/pnas.0915000107

2. Jin H, Liu K, Tang J, Huang X, Wang H, Zhang Q, et al. Genetic fate-mapping reveals surface accumulation but not deep organ invasion of pleural and peritoneal cavity macrophages following injury. *Nat Commun*. (2021) 12:2863. doi: 10.1038/s41467-021-23197-7

3. Cassado Ados A, D'Imperio Lima MR, Bortoluci KR. Revisiting mouse peritoneal macrophages: heterogeneity, development, and function. *Front Immunol*. (2015) 6:225. doi: 10.3389/fimmu.2015.00225

4. Ginhoux F, Guilliams M. Tissue-resident macrophage ontogeny and homeostasis. *Immunity*. (2016) 44:439–49. doi: 10.1016/j.immuni.2016.02.024

5. Grzywa TM, Sosnowska A, Matryba P, Rydzynska Z, Jasinski M, Nowis D, et al. Myeloid cell-derived arginase in cancer immune response. *Front Immunol*. (2020) 11:938. doi: 10.3389/fimmu.2020.00938

6. Yamada H, Mizuno S, Ross AC, Sugawara I. Retinoic acid therapy attenuates the severity of tuberculosis while altering lymphocyte and macrophage numbers and cytokine expression in rats infected with *Mycobacterium tuberculosis*. *J Nutr*. (2007) 137:2696–700. doi: 10.1093/jn/137.12.2696

7. Hall JA, Grainger JR, Spencer SP, Belkaid Y. The role of retinoic acid in tolerance and immunity. *Immunity*. (2011) 35:13–22. doi: 10.1016/j.immuni.2011.07.002

8. Buechler MB, Kim KW, Onufer EJ, Williams JW, Little CC, Dominguez CX, et al. A stromal niche defined by expression of the transcription factor WT1 mediates programming and homeostasis of cavity-resident macrophages. *Immunity*. (2019) 51:119–130.e5. doi: 10.1016/j.immuni.2019.05.010

9. Morizawa YM, Hirayama Y, Ohno N, Shibata S, Shigetomi E, Sui Y, et al. Reactive astrocytes function as phagocytes after brain ischemia via ABCA1-mediated pathway. *Nat Commun*. (2017) 8:28. doi: 10.1038/s41467-017-00037-1

10. Okabe Y, Medzhitov R. Tissue-specific signals control reversible program of localization and functional polarization of macrophages. *Cell*. (2014) 157:832–44. doi: 10.1016/j.cell.2014.04.016

11. Liu Z, Gu Y, Chakarov S, Bleriot C, Kwok I, Chen X, et al. Fate mapping via Ms4a3-expression history traces monocyte-derived cells. *Cell*. (2019) 178:1509–1525.e19. doi: 10.1016/j.cell.2019.08.009

12. Louwe PA, Badiola Gomez L, Webster H, Perona-Wright G, Bain CC, Forbes SJ, et al. Recruited macrophages that colonize the post-inflammatory peritoneal niche convert into functionally divergent resident cells. *Nat Commun*. (2021) 12:1770. doi: 10.1038/s41467-021-21778-0

13. Vega-Perez A, Villarrubia LH, Godio C, Gutierrez-Gonzalez A, Feo-Lucas L, Ferriz M, et al. Resident macrophage-dependent immune cell scaffolds drive anti-bacterial defense in the peritoneal cavity. *Immunity*. (2021) 54:2578–2594.e5. doi: 10.1016/j.immuni.2021.10.007

14. Zindel J, Peiseler M, Hossain M, Deppermann C, Lee WY, Haenni B, et al. Primordial GATA6 macrophages function as extravascular platelets in sterile injury. *Science*. (2021) 371:eabe0595. doi: 10.1126/science.abe0595

15. Han J, Gallerand A, Erlich EC, Helmink BA, Mair I, Li X, et al. Human serous cavity macrophages and dendritic cells possess counterparts in the mouse with a distinct distribution between species. *Nat Immunol*. (2024) 25:155–65. doi: 10.1038/s41590-023-01688-7

16. Zigmond E, Varol C, Farache J, Elmaliah E, Satpathy AT, Friedlander G, et al. Ly6C hi monocytes in the inflamed colon give rise to proinflammatory effector cells and migratory antigen-presenting cells. *Immunity*. (2012) 37:1076–90. doi: 10.1016/j.immuni.2012.08.026

17. Schonberger K, Obier N, Romero-Mulero MC, Cauchy P, Mess J, Pavlovich PV, et al. Multilayer omics analysis reveals a non-classical retinoic acid signaling axis that regulates hematopoietic stem cell identity. *Cell Stem Cell*. (2022) 29:131–148.e10. doi: 10.1016/j.stem.2021.10.002

18. Liu Y, Hu JN, Luo N, Zhao J, Liu SC, Ma T, et al. The essential involvement of the omentum in the peritoneal defensive mechanisms during intra-abdominal sepsis. *Front Immunol*. (2021) 12:631609. doi: 10.3389/fimmu.2021.631609

19. Zhang N, Czepielewski RS, Jarjour NN, Erlich EC, Esaulova E, Saunders BT, et al. Expression of factor V by resident macrophages boosts host defense in the peritoneal cavity. *J Exp Med*. (2019) 216:1291–300. doi: 10.1084/jem.20182024

20. Paynich ML, Jones-Burrage SE, Knight KL. Exopolysaccharide from *Bacillus subtilis* induces anti-inflammatory M2 macrophages that prevent T cell-mediated disease. *J Immunol*. (2017) 198:2689–98. doi: 10.4049/jimmunol.1601641

21. Cassado Ados A, de Albuquerque JA, Sardinha LR, Buzzo Cde L, Faustino L, Nascimento R, et al. Cellular renewal and improvement of local cell effector activity in peritoneal cavity in response to infectious stimuli. *PLoS One*. (2011) 6:e22141. doi: 10.1371/journal.pone.0022141

22. Cai W, Dai X, Chen J, Zhao J, Xu M, Zhang L, et al. STAT6/Arg1 promotes microglia/macrophage efferocytosis and inflammation resolution in stroke mice. *JCI Insight*. (2019) 4:e131355. doi: 10.1172/jci.insight.131355

23. Feng X, Zhu S, Qiao J, Ji Z, Zhou B, Xu W. CX3CL1 promotes M1 macrophage polarization and osteoclast differentiation through NF-κB signaling pathway in ankylosing spondylitis in vitro. *J Transl Med*. (2023) 21:573. doi: 10.1186/s12967-023-04449-0

24. Zhang S, Weinberg S, DeBerge M, Gainullina A, Schipma M, Kinchen JM, et al. Efferocytosis fuels requirements of fatty acid oxidation and the electron transport chain to polarize macrophages for tissue repair. *Cell Metab*. (2019) 29:443–456.e5. doi: 10.1016/j.cmet.2018.12.004

25. Wang Y, Zeng M, Fan T, Jia M, Yin R, Xue J, et al. Biomimetic ZIF-8 nanoparticles: a novel approach for biomimetic drug delivery systems. *Int J Nanomedicine*. (2024) 19:5523–44. doi: 10.2147/IJN.S462480

Frontiers in Nutrition

Explores what and how we eat in the context of health, sustainability and 21st century food science

A multidisciplinary journal that integrates research on dietary behavior, agronomy and 21st century food science with a focus on human health.

Discover the latest Research Topics

See more →

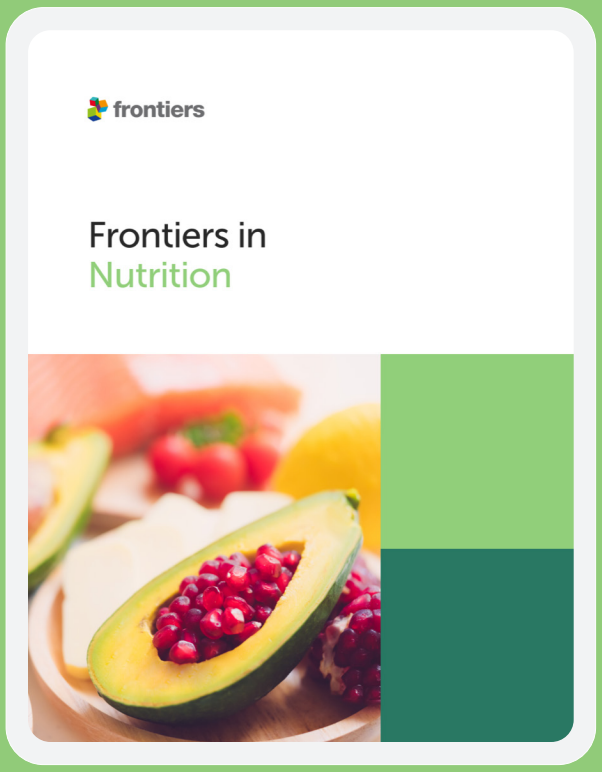

Frontiers

Avenue du Tribunal-Fédéral 34
1005 Lausanne, Switzerland
frontiersin.org

Contact us

+41 (0)21 510 17 00
frontiersin.org/about/contact